A MODULAR POINT-OF-CARE PLATFORM FOR REAL-TIME MONITORING AND TRANSMISSION OF PHYSIOLOGICAL SIGNALS

By

René Harder

Dissertation

Submitted to the Faculty of the

Graduate School of Vanderbilt University

in partial fulfillment of the requirements

for the degree of

DOCTOR OF PHILOSOPHY

in

Electrical Engineering

August 2015

Nashville, Tennessee

Approved:

Alfred B. Bonds, Ph.D.

Julie A. Adams, Ph.D.

Theodore Bapty, Ph.D.

Franz J. Baudenbacher, Ph.D.

André M. Diedrich, M.D., Ph.D.

This dissertation is dedicated:

To my family.

Special gratitude to my mother, Heidemarie Harder,
whose words of encouragement,
push for tenacity and constant love have
supported me throughout my life

ACKNOWLEDGMENTS

First of all, I would like to extend gratitude to my PhD committee, Dr. Alfred B. Bonds, Dr. Julie A. Adams, Dr. Theodore Bapty, Dr. Franz J. Baudenbacher and Dr. André M. Diedrich, for their time, support, and expert advice leading to the successful completion of this dissertation.

I am grateful for the numerous helpful advices and inspiring discussions I had with my advisors, Dr. Franz J. Baudenbacher and Dr. André M. Diedrich. You both helped me succeed as a PhD student, and you taught me to define and approach research as a scientist.

My sincere gratitude goes to Jonathan S. Whitfield which I had the honor to introduce him into the world of mixed signal circuit design. In return, he provided me with dearly needed support during assembly and design of the many prototypes.

I would also like to give my appreciation to Susan S. Eagle, Maciej S. Buchowski, John B. Pietsch, Italo O. Biaggioni, Satish R. Raj, and Regina N. Tyree for their assistance and support related to the clinical studies.

Furthermore, I would like to thank the various institutions and grants that have sponsored my research, including the Bill & Melinda Gates Foundation, National Institute of Health, Vanderbilt Institute for Clinical and Translational Research and Vanderbilt Center for Technology Transfer & Commercialization. Without their extensive support this work would not have been possible.

TABLE OF CONTENTS

LIST OF TABLES

LIST OF FIGURES

DEFINITIONS AND ACRONYMS

ADC:
Analog to Digital Converter

AFE:
Analog Front-End

Ag/AgCl:
Silver / Silver Cloride

API:
Application Programming Interface

APN:
Apple Push Notification Service, a service that sends data from servers to applications on iOS devices.

AV:
Atrioventricular

BAN:
Body Area Network

BIA:
Bioelectrical Impedance Analysis

BIVA:
Bioelectrical Impedance Vector Analysis

BP:
Blood Pressure

CA:
Certification Authority, an entity that issues digital certificates

CMR:
Common Mode Rejection

CMRR:
Common Mode Rejection Ratio

ECG:
Electrocardiogram or Electrocardiography, a noninvasive procedure to measure the surface potential of the electrical activity of the heart over time.

ECG Record:
A static representation of the heart's muscle activity

EDA:
Electrodermal Activity

EKG:
Electrocardiography

EMG:
Electromyography

GCM:
Google Cloud Messaging, a service that sends data from servers to applications on Android devices.

HR:
Heart Rate

ICG:
Impedance Cardiography

LMD:
Local Mobile Device, the mobile device connected to the Main Device. e.g. Smartphone or tablet

LVET:
Left Ventricular Ejection Time

MCU:
Microcontroller Unit

MD:
Main Device, the wireless ECG recording device.

OH:
Orthostatic Hypotension

PBKDF2:
Password-Based Key Derivation Function 2

PEP:
Pre-Ejection Period

PN:
Push Notification, is an Internet based communication style where the request for a given transaction is initiated by the publisher or central server.

POTS:
Postural Orthostatic Tachycardia Syndrome

PPG:
Photoplethysmography, a method to measure volume changes of blood, typically performed on the finger tip, using reflection or transmission of light.

RMD:
Remote Mobile Device, mobile device used to receive and visualize ECG records and messages. e.g. Smartphone or Tablet

SPI:
Serial Programming Interface

SpO2:
Peripheral capillary oxygen saturation

SPS:
Samples per Second

SSL:
Secure Socket Layer, a cryptographic protocols that is designed to provide communication security over the Internet.

Syncope:
A temporary loss of consciousness and posture (fainting)

TLS:
Transport Layer Security, the successor of SSL.

Transport Address:
Also referred to as forwarding address, is an address defined by an organization which redirects an incoming event to multiple or single user within this organization

TVS:
Transient Voltage Suppressor

TWB:
Total Body Water

UART:
Universal Asynchronous Receiver / Transmitter

URS:
User Registration Service, a service which handles user registration and authentication.

WCT:
Wilson's Central Terminal, a virtual reference representing a point source used for unipolar ECG measurements. It is composed of the average of ECG electrodes RA, LA and LL.

CHAPTER I

INTRODUCTION

In 2013 the National Institute of Health conducted a study between comparable high-income countries and came to the conclusion that the United States is among the countries with the highest prevalence for diabetes, heart and lung disease, sexually transmitted infections, infant mortality, injuries, homicides, and disability [1]. This study further found that life expectancy and survival rate in the United States increased significantly over the last century, but at a much slower rate than in any of the peer countries. The life expectancy of an American male is 3.7 years shorter when compared to other high income countries.

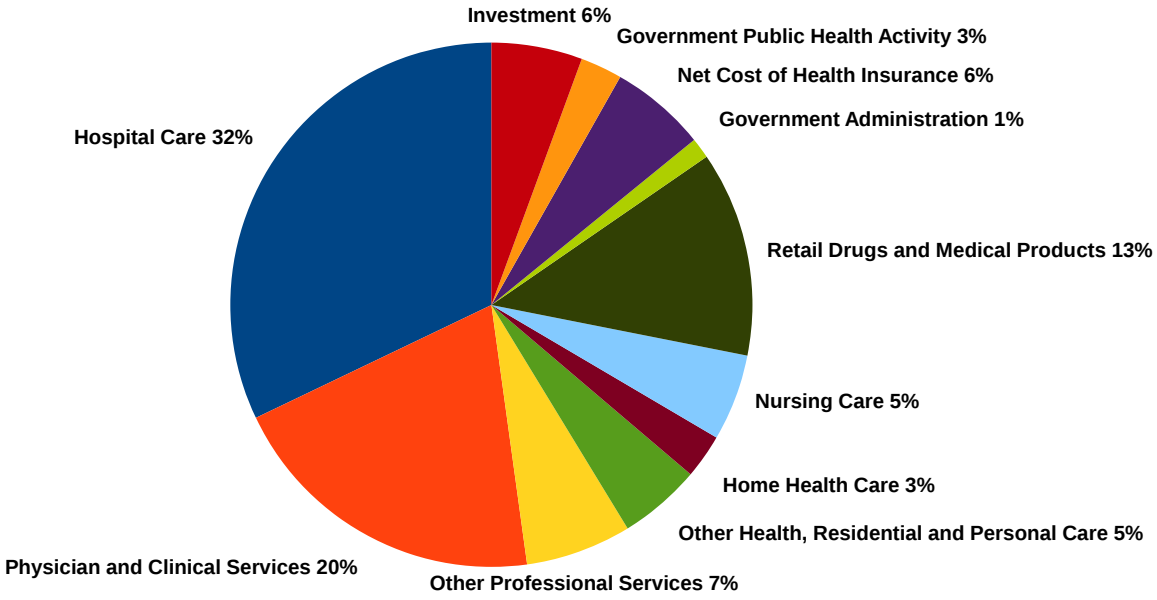

Figure 1: Distribution of US Health Spending for the year 2013 [2].

In the year 2013 healthcare cost rose by 3.6% to a total of $2.9 trillion ($9,255 per person), with more than 50% spent for hospital and clinical services [2], see Figure 1. Traditional healthcare solutions focus on the treatment rather than the prevention of a disease. A steadily aging society and sky rocketing healthcare costs drives the need for a transformation from a reactive and hospital-

driven to a proactive, patient-centered and enabling healthcare. Furthermore, due to increased governmental regulation and adjustment of reimbursement policies, health care providers were asked to not only maintain, but also to reduce costs. To meet this requirement there is a need to limit the in-hospital stay of patients and prevent costly readmissions. One strategy to engage patients and reduce readmission is through a deployment of ambulatory mobile health monitor systems that promote intervention before critical or life threatening conditions occur.

Table 1: Potential biosensors and physiological parameters for mobile applications [3], [4].

Type of Parameter	**Sensor Type**	**Description**
Electrocardiogram (ECG)	Skin electrodes	Electrical activity of the heart.
Oscillometric Blood Pressure	Arm cuff	Is the pressure exerted by the circulating blood onto the walls of the blood vessel
Respiration Rate	Piezoelectric Piezoresistive Thoracic impedance	The number of inhalation-, exhalation cycles per unit time.
Heart Rate	Pulse Oximeter / ECG	The frequency of the completed cardiac cycle.
Cardiac Output	Thoracic impedance	Represents the volume of blood pumped during each cardiac cycle.
Fluid Distribution	Impedance	Indicates the proportion of fluids within different body sections.
Body Composition	Complex Impedance	Represents the different percentages of fat, bone and muscle in human bodies.
Electroencephalogram (EEG)	Skin electrodes	Recording of the electrical activity of the brain.
Oxygen Saturation	Pulse Oximeter	Indicates the oxygenation level of the blood.
Plethysmogram	Pulse Oximeter Impedance Piezo	The volumetric measurement of the blood in a particular organ.
Phonocardiogram	Sound	Recording of heart murmurs generated by vibrations of the heart valves.
Activity Posture	Acceleration	Measurement of position and movement using acceleration forces in 3 dimensional space.

Table 1 lists several clinically relevant ambulatory physiological sensing modalities, which can be integrated into a mobile health monitoring system and their corresponding physiological variables. The measurement of these signals and

their subsequent processing for feature extraction leads to the aggregation of real-time collected physiological parameters, which can give an overall approximation of the individual's health status at any time.

Large medical device manufacturers have not responded to the increasing demand of easy to use and mobile medical devices for professional home and ambulatory use. In an attempt to fill this health monitoring void, several small companies have introduced commercial ECG Holter systems and cardiac monitors that provide multiparameter monitoring, such as biopotential, activity, posture, blood pressure and impedance measurements (Table 2) [5].

Furthermore, recent technological advances have lead to the development of personal fitness monitors, such as FitBit, JawBone, and wearable chest straps [6]–[9]. However, these fitness monitors target the consumer market and focus on the pure acquisition of a limited number of physiological parameters(Table 2), due to size, power and cost constraints. Recent studies have reported variable outcomes depending on the subjects activity and/or device placement [10]–[12]. Hence, consumer fitness devices provide limited use for professional are generally not suited for medical diagnostic.

Table 2 provides an overview of state of the art ambulatory monitoring and personal fitness devices for monitoring multiple physiological variables, such as eclectrocardiogram (ECG), heart rate (HR), heart rate variability (HRV), impedance cardiography (ICG), respiration rate, activity, electrodermal activity (EDA), blood pressure (BP), photoplethmography (PPG), blood oxygen saturation (SpO2) and electromyography (EMG).

Table 2: Comparison of Ambulatory Health Monitors [5]–[9], [13], [14]

Device	Manufacture	ECG / HR	HRV	ICG	Resp. Rate	Activity	EDA	BP	PPG / Sp02	EMG	Time >24h	Wireless Connectivity
Ambulatory Cardiac Monitor	Intellectual Property, LLC	–/✓	–	✓ (avg)	–	–	–	–	–/–	–	✓	–
Ambulatory Impedance Cardiograph MW1000A	Mindware Technologies LTD	✓/✓	–	✓	✓	–	✓	–	–/–	✓	–	✓
Berkeley Tricoder	University of Berkeley California	✓/✓	–	–	✓	✓	✓	–	✓/✓	✓	?	✓
VU-AMS Ambulatory Monitoring System	Vrije Universiteit, Netherlands	✓/✓	✓	✓	✓	✓	✓	-	–/–	–	✓	–
Fitbit Surge	Fitbit Inc.	–/✓*	–	–	–	✓	–	–	–/–	–	✓	✓
Jawbone UP4	Jawbone	–/✓+	–	–	✓	✓	✓	–	–/–	–	✓	✓
Bioharness 3	Zephyr Technology	–/✓	✓	–	✓	✓	–	–	–/–	–	✓	✓
Rhythm+	Scosche	–/✓*	–	–	–	✓	–	–	–/–	–	–	✓
Vanderbilt Health Monitor Platform	Vanderbilt University	✓/✓	✓	✓	✓	✓	✓	✓	✓/✓	✓	✓	✓

Heart rate determined by photoplethysmography (*) or impedance (+).

The majority of the devices listed in Table 2 are heart rate and cardiac monitors, both for the consumer and the professional market. Professional devices are typically applied to the patient in a clinical setting and record electrocardiograms and other physiological parameters, such as thoracic impedance or activity. To diagnose heart rhythm abnormalities, these parameters are usually stored to an internal memory and recorded over long periods. After a pre-defined recording time, which can be several hours to multiple days, the device has to be removed and the data manually extracted for offline diagnostics and data analysis. These devices do not allow for remote diagnostics of the patient's health condition and lack certain features. Therefore, immediate feedback by the primary care provider is not possible nor can the devices be configured for a larger clinical spectrum of patients, for example patients with orthostatic hypotension where posture and blood pressure measurements are critical.

The Berkeley Tricorder [13] and the Vanderbilt health monitor platform can be paired with a cell phone or tablet computer via Bluetooth and offers the acquisition of a multitude of physiological parameters at the same time. However, low sampling rates, limited resolution, low dynamic range, inflexible analog front-ends, inability to record thoracic impedance and blood pressure limit the Berkeley Tricorder's use to a few clinical applications. For example, low ECG sampling rates directly influence the error associated with the HRV analysis [15]. The most commonly used standard for HRV analysis (Taskforce of Electrophysiology [16]) recommend a sampling frequency between 250-500Hz, while most groups have moved to 0.5-1kHz [17]–[20].

The primary focus of this dissertation is to address a critical technological void in wearable healthcare monitors by developing a multi-sensor health monitor platform for data acquisition, analysis, and quasi real time transmission of several vital parameters to the patient and their care providers.

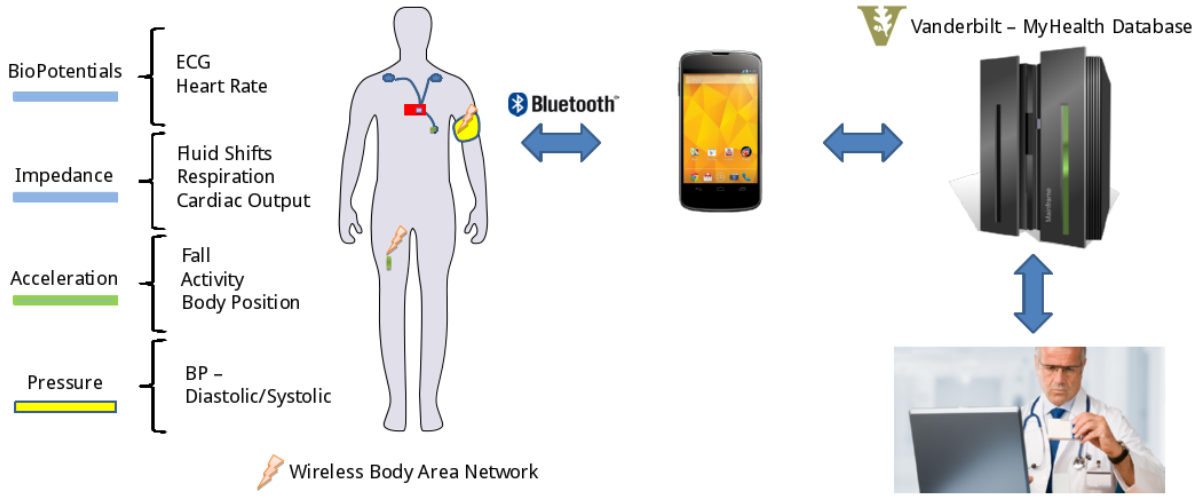

Figure 2: Concept of a wearable smart mobile health system configurable for specific patient population or particular clinical application

The health monitor, as shown in Figure 2, is designed to monitor changes in multiple physiological variables for diagnostics and early intervention in order to maintain an optimal health status, potentially preventing hospital readmissions. In addition, these systems can be integrated into a telemedical infrastructure to alert medical personnel in case of life-threatening events or worsening conditions. The

storage of medical data in a secure and central location provides easy access and opens new possibilities for enhanced data analysis and mining in order to identify previously unknown markers for diagnostics and optimal maintenance of chronic conditions. Further, remote access to a patient's medical data facilitates guidance during recovery and rehabilitation from an acute event or surgical procedure.

The health monitor platform is based on advanced sensor concepts and highly integrated embedded systems, which offer, in combination with distributed network technologies, the opportunity to customize the platform to a patient’s needs and to monitor a patient's health status continuously moving the point of care closer to the patient. Furthermore, this technology allows for large data sets to be recorded, which has the potential for the identification of early markers of a disease, timely intervention and consequently a reduction of costly hospital readmissions. In addition, smart health care and immediate feedback engages patients to take responsibility and play a more active role in their own health management and supports an independent active life style.

The specific aims of this dissertation were to develop a modular hardware platform and data infrastructure that is capable of recording multiple physiological parameters (1), evaluate the performance of the developed hardware by comparing it to clinically accepted and/or traditional methods (2), and apply the monitor platform to different clinical applications (3).

Chapter II presents an overview of the general hardware platform architecture and modules developed for this research project. The following Chapters III-V present the application of the health monitor platform to different well know clinical needs. Finally, the Conclusion and Future Work is presented in Chapter VI.

References

[1] Steven H. Woolf and Laudan Aron, ”U.S. Health in International Perspective: Shorter Lives, Poorer Health”, National Institutes of Health, 2013.

[2] M. Hartman, A. B. Martin, D. Lassman, A. Catlin, and the N. H. E. A. Team, ”National Health Spending In 2013: Growth Slows, Remains In Step With The Overall Economy”, *Health Affairs*, vol. 34, no. 1, pp. 150–160, Jan. 2015.

[3] G. Harsanyi, ”Sensors in Biomedical Applications: Fundamentals, Technology and Applications”. *CRC Press*, 2000.

[4] E. Kaniusas, ”Biomedical Signals and Sensors I: Linking Physiological Phenomena and Biosignals”. *Springer Science & Business Media*, 2012.

[5] G. Cybulski, ”Ambulatory Impedance Cardiography”, in *Ambulatory Impedance Cardiography*, Springer Berlin Heidelberg, 2011, pp. 39–56.

[6] ”Zephyr Bioharness 3”. [Online]. Available: www.zephyranywhere.com. [Accessed: 20-Jun-2015].

[7] ”Scosche Rythm+”. [Online]. Available: www.scosche.com. [Accessed: 20-Jun-2015].

[8] ”Jawbone UP4 Fitness Tracker”. [Online]. Available: www.jawbone.com. [Accessed: 20-Jun-2015].

[9] Fitbit Inc., ”Fitbit Surge - Product Manual”, Version 1.0, 2015.

[10] J. Parak and I. Korhonen, ”Evaluation of wearable consumer heart rate monitors based on photopletysmography”, in *2014 36th Annual International Conference of the IEEE Engineering in Medicine and Biology Society (EMBC)*, 2014, pp. 3670–3673.

[11] J. H. Kim, R. Roberge, J. Powell, A. Shafer, and W. Jon Williams, ”Measurement Accuracy of Heart Rate and Respiratory Rate during Graded Exercise and Sustained Exercise in the Heat Using the Zephyr BioHarnessTM”, *International Journal of Sports Medicine*, vol. 34, no. 06, pp. 497–501, Nov. 2012.

[12] R. J. Gusmer, T. A. Bosch, A. N. Watkins, J. D. Ostrem, and D. R. Dengel, ”Comparison of FitBit® Ultra to ActiGraph™ GT1M for Assessment of Physical Activity in Young Adults During Treadmill Walking”, *The Open Sports Medicine Journal*, vol. 8, no. 1, pp. 11–15, Apr. 2014.

[13] R. Naima and J. Canny, ”The Berkeley Tricorder: Ambulatory Health Monitoring”, in *Sixth International Workshop on Wearable and Implantable Body Sensor Networks, 2009. BSN 2009*, 2009, pp. 53–58.

[14] R. Harder, J. S. Whitfield, F. J. Baudenbacher, and A. Diedrich, ”Autonomic smart health system”, in *Clinical Autonomic Research*, Kohala Coast, Hawaii, 2013, vol. 23, p. 277.

[15] A. Voss, N. Wessel, A. Sander, H. Malberg, and R. Dietz, ”Influence of low sampling rate on heart rate variability analysis based on non-linear dynamics”, in *Computers in Cardiology 1995*, 1995, pp. 689–692.

[16] Task Force of the European Society of Cardiology the North American Society of Pacing Electrophysiology, ”Heart Rate Variability Standards of Measurement, Physiological Interpretation, and Clinical Use”, *Circulation*, vol. 93, no. 5, pp. 1043–1065, Mar. 1996.

[17] R. M. Baevsky, V. M. Baranov, I. I. Funtova, A. Diedrich, A. V. Pashenko, A. G. Chernikova, J. Drescher, J. Jordan, and J. Tank, ”Autonomic cardiovascular and respiratory control during prolonged spaceflights aboard the International Space Station”, *Journal of Applied Physiology*, vol. 103, no. 1, pp. 156–161, Jul. 2007.

[18] C. Daluwatte, J. H. Miles, S. E. Christ, D. Q. Beversdorf, T. N. Takahashi, and G. Yao, ”Atypical pupillary light reflex and heart rate variability in children with autism spectrum disorder”, *Journal of Autism and Developmental Disorders*, vol. 43, no. 8, pp. 1910–1925, Aug. 2013.

[19] M. Schiavenato, C. Oliu, E. Bello, J. Bohorquez, and N. Claure, ”Development of a System for the Assessment of Heart Rate Variability in the NICU”, in *Biomedical Engineering Conference (SBEC), 2013 29th Southern*, 2013, pp. 25–26.

[20] J. Tank, R. M. Baevsky, I. I. Funtova, A. Diedrich, I. N. Slepchenkova, and J. Jordan, ”Orthostatic heart rate responses after prolonged space flights”, *Clinical Autonomic Research*, vol. 21, no. 2, pp. 121–124, Dec. 2010.

CHAPTER II

MODULAR PLATFORM ARCHITECTURE

One of the main goals of this research project was to develop a platform technology, which can be configured and/or adapted for different patient needs. For this purpose, we designed a set of hardware modules, when integrated allow for the acquisition, processing and/or real-time transmission of various physiological signals. An overview of the platform developed for the project can be seen in Figure 3. For the development of these platform modules, emphasis was placed on the overall cost not exceeding $250 per device. The development of this platform technology led to an international patent application [1], which is included as Appendix D.1 in this dissertation. Subsequently, the intellectual property was licensed and provided the bases for an FDA approved commercial device for cardiac monitoring.

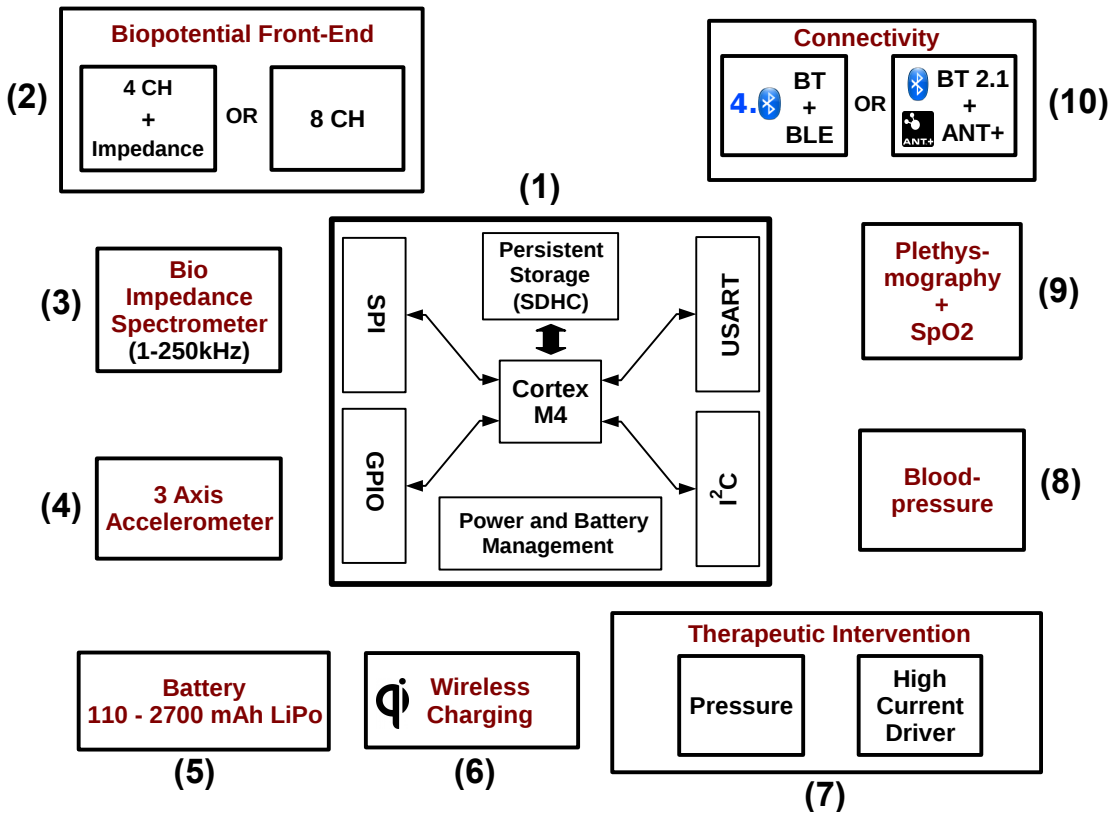

Figure 3: Overview of configurable hardware platform showing all available modules.

The terminology “module” in the sense used in this work, does not imply standalone, and if simply wired together result in ready to use and functional hardware. In fact, modules reflect a concept where pre-designed electrical templates can be placed together onto a single printed circuit board (PCB), and if interconnected via PCB traces enable the measurement of the desired physiological signals. Although these modules could be used to form standalone devices intended to acquire one physiological parameter, one would need to allocate more PCB real-estate and this was therefore not considered in this work.

The health monitor platform, as depicted in Figure 3, is organized into individual modules named as follows: platform core (1), biopotential front-end (2), bioimpedance spectrometer (3), 3 axis accelerometer (4), battery (5), wireless charging(6), therapeutic intervention (7), blood pressure (8), plethmography + SpO2 (9) and connectivity (10). The remainder of this chapter provides an in depth review of these platform modules.

Platform Core

The core is the heart of the platform (Figure 3) and the only component required to be included in each monitor configuration. It provides control, power, battery management and persistent storage to the modules. At the center of the core runs an ARM Cortex-M4F microprocessor (STM32F405, STMicroelectronics, Switzerland), a 32bit RISC processor targeted towards low power embedded systems that have a higher demand for control and signal processing. Some of the Cortex-M4F's key features are a limited DSP instruction set, floating point unit, 3 stage pipe-line, and hardware multiplier/divider [2].

The microprocessor unit (MCU) runs at 168MHz and executes the embedded system application (firmware) that logically combines module outputs to provide the monitor with its intended behavior. To preserve power, the MCU goes into sleep mode when idle and wakes up in periodic intervals to check for new data or events.

The core module provides stable supply voltage for all other modules, either at 3V or 5V. The 3V rail is generated using a linear regulator (MCP1802-3, Microchip Technology, USA) and provides a stabilized output for up to 150mA. Since the input voltage range is between 3.3V and 4.2V, the 5V rail is generated using a step up converter (LTC3525-5, Linear Technology, USA). In theory the DC/DC converter can supply up to 400mA; however, our circuit design only ensures stable output with a ripple voltage of ≤40mV for currents below 50mA. The MCU has full control over the supply voltage rails, such that they can be shutdown by the firmware if needed.

The core module, by default, does not offer a dedicated analog ground or rail, as is commonly found in mixed circuit designs, in an attempt to prevent digital ground currents to contaminate the analog circuitry. As research has shown in large, complex, and high-speed systems, a split-ground plane can cause substantial electromagnetic interferences if traces are routed improperly [3]–[6][2]–[5]. Since it is impossible to account for all variations of module placements, the system ground provided by the core module must be considered noisy. Thus, possible noise reduction strategies should be employed in the module design itself.

A battery charge management controller (MCP73833, Microchip Technology, USA) is integrated into the core module. The MCP73833 controls the charge cycle of the lithium polymer battery and reports information about charging status to the MCU. The required 5V supply voltage for charging can either be provided by the wireless charging module or an external AC/DC adapter. An integrated I2C fuel gauge (MAX17048G, Maxim Integrated, USA) tracks battery voltage and charge percentage, which can be retrieved by the MCU on demand.

The core module exposes digital interfaces that can be used to connect the modules. These interfaces include versatile high speed communications, like the serial programming interface (SPI) and universal asynchronous receiver/transmitters (UART), with clock frequencies of up to 24MHz and 8MHz, respectively. For sensor modules with low bandwidth requirements, two independent I2C buses as well as several general purpose input outputs (GPIO) are available.

Additionally, the core module is equipped with an internal Secure Digital (SD) card holder, that can be used as persistent storage for large amounts of data. The SD-card is connected to the MCU via a secure digital input output interface (SDIO) and can achieve data rates of up to 12MBytes/s.

A precise 32.768kHz crystal provides a slow clock to the MCU that is needed for time keeping with its embedded real time clock. The MCU is able to output a derived 32.678kHz clock signal that can be used by other peripheral modules, if required.

Biopotential Front-End

To measure potentials generated by human tissue, such as ECG, EMG or skin potential, two biopotential front-ends were designed. Both front-ends are based on the ADS129x series by Texas Instruments. The ADS129x series is a group of 24bit analog front-ends (AFE) specifically designed for ECG measurements [7]. However, many integrated features, like the internal reference driver or programmable gain amplifiers (PGA), are beneficial to other biopotential measurements as well.

The ADS1298/6/4, depending on which particular model is chosen, offers either 4, 6 or 8 differential input channels. Each channel is equipped with a dedicated programmable gain amplifier, with gain settings of 1x, 2x, 3x, 4x, 6x, 8x and 12x, as well as a 24bit delta-sigma analog-to-digital converter (ADC), with output data rates between 250SPS and 32kSPS. One of the greatest strengths of this AFE is its versatility, because many options are configurable by the application software. For example, the PGA input can be re-routed to measure internal temperature, analog or digital supply voltage, reference driver output or internal generated test signals. Further, signals from any of the lower 4 inputs can be combined arithmetically, e.g. building an average of multiple signals, and fed into the negative side of the PGA in channel 5, 6 or 7. This can be useful in applications where there is a need to derive a signal rather in analog then in digital. A functional overview of the ADS1298 showing some of its features, including multiplexer, PGA and reference driver, can be found in Figure 4.

To improve signal quality and provide reference for the differential inputs, the AFE has an integrated reference driver. The reference driver can be set to derive an output signal generated from any combination of input signals. Additional features include lead off detection, amplifiers to generate Wilson's central terminal [8] and dedicated outputs to facilitate hardware pacemaker detection (Figure 4).

The ADS129xR variant includes a fully integrated respiration impedance measurement feature, which allows for the measurement of respiratory activity by injecting a constant out of band AC current into the body and measuring the voltage drop generated due to volume changes of conductive tissue.

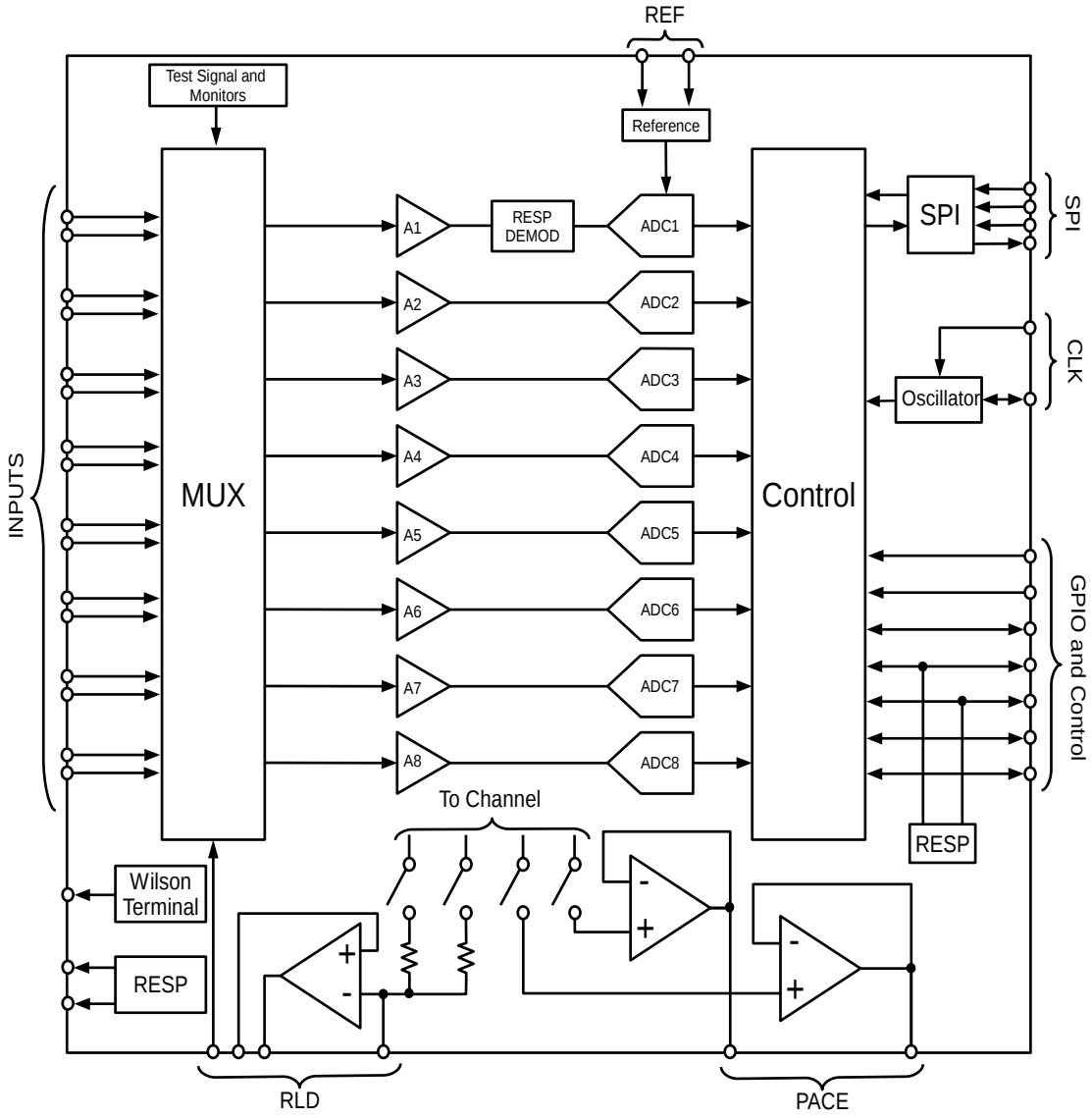

Figure 4: Schematic Block Diagram of ADS1298. Adapted from [7]

Bioimpedance Spectrometer

Bioelectrical impedance analysis (BIA) is a noninvasive and commonly used method for the assessment of body composition, including body water. This is achieved by the measurement of electrical responses to the introduction of low-level, alternating current into a living organism, and the application of biophysical models to estimate body composition [9].

Biological tissue can be seen as a complex conductor of resistive and reactive components. Electrical properties of biological tissue depend on the presence of body fluids and cell structures. BIA measures the voltage and phase angle of a signal generated by injecting a small sinusoidal electrical current at a single or multiple frequencies into the body and computes the complex impedance values.

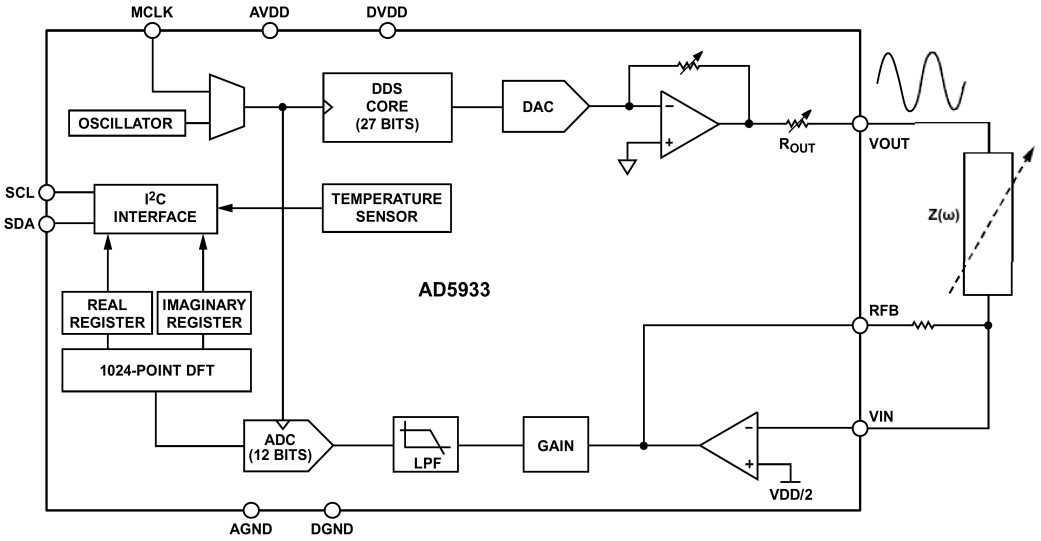

Figure 5: Block diagram of integrated impedance converter network analyzer AD5933 and overview of the build-in functions, like, frequency synthesizer, ADC, programmable gain amplifier, DFT and I2C interface. Adapted from [10]

To facilitate body composition measurements we designed an analog front-end module that is capable of performing bioelectrical impedance measurements. The front-end is based on the integrated impedance converter network analyzer AD5933, from Analog devices [10]. The AD5933 is a fully integrated impedance converter. As illustrated in Figure 5, the impedance converter includes a built in

sine wave frequency synthesizer, a 12bit ADC that can sample up to 1MSPS, and programmable gain input and output amplifiers. Further, to perform complex impedance measurements an integrated DSP applies a Discrete Fourier Transformation (DFT) to the digitized input signal and stores the real and imaginary results in its internal memory.

The impedance network analyzer allows for the direct measurement of impedance using a two-terminal measurement configuration, where the injecting and sensing electrodes are the same. Although bioelectrical impedance measurements have been performed in a bipolar (2 electrodes) configuration [11], the variable electrode-skin interface impedance adds an unpredictable bias to the measurement and; therefore, increases the observed error [12]. For this reason, current bioelectrical impedance analyzers perform impedance measurements using a tetrapolar measurement configuration. Furthermore, the network analyzer's voltage source impedance is approximately 200Ω, which adds a significant measurement error for whole body impedance, typically in the range from 100Ω to 1kΩ.

To overcome these issues, a precision wide-band constant current source using a differential receiver amplifier (AD8130, Analog Devices, USA) was designed. For bioelectrical impedance measurements, the internal resistance of a current source should be sufficiently high in order to minimize the error introduced by capacitance (cables, electrodes etc.) [13]. The wide-band current source, as seen in Figure 6 offers high internal resistance and, if combined with the AD5933, allows for precise tetra-polar impedance measurements. A more in depth analysis of the performance of this precision wide-band current source can be found in Chapter III.

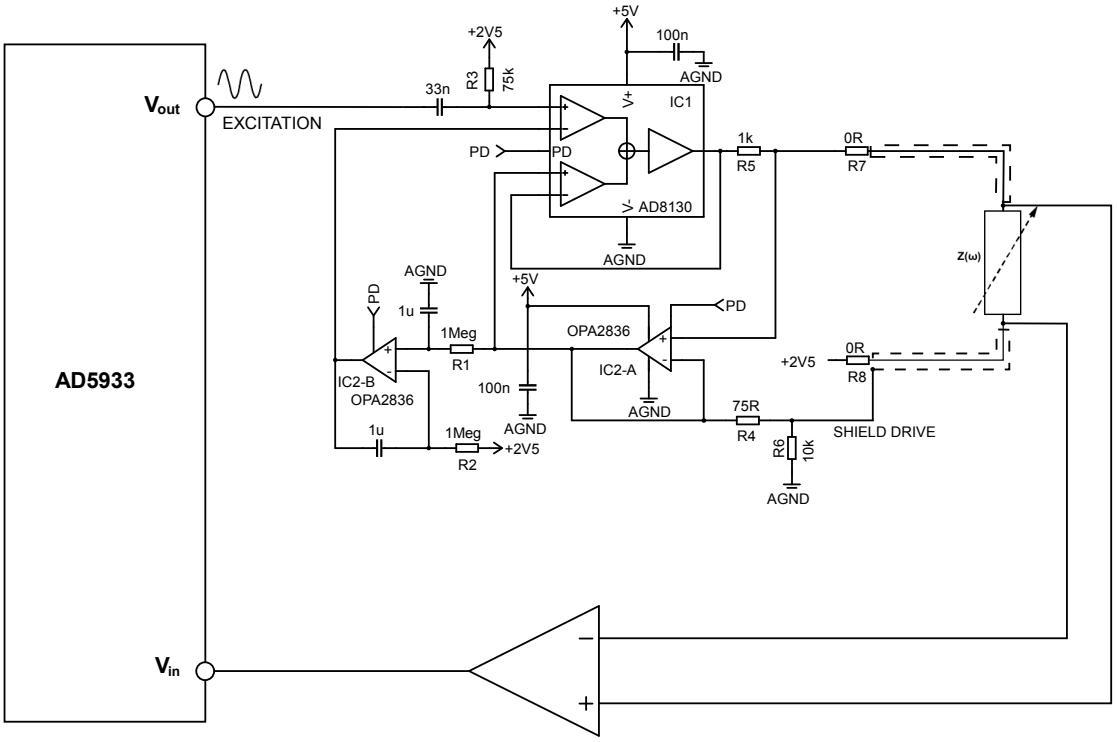

Figure 6: Simplified schematic of precision wide-band constant current source to enable tetra-polar impedance measurements. The differential amplifier AD8130 can be shutdown using the PD signal, to preserve power while not in use. Resistors R7 and R8 can be replaced with suitable capacitors to generate a fully bipolar output current.

3 Axis Accelerometer

Actigraphy is a method to study total activity, which is increasingly used in sleep research and clinical care to determine abnormalities in sleep patterns or circadian rhythms [14]–[17]. In addition, the detection of posture, movements, and falls can be applied for ambulatory health and medical monitoring [18], [19]. To facilitate the measurement of activity we designed a small motion module based on the 3-axis accelerometer (BMA180, Bosch Sensortec, Germany). The BMA180 provides a 14bit ADC with adjustable sampling rates of up to 2kSPS and full scale ranges between ±1g and ±16g. Additionally, a motion processor (Figure 7) allows for the automatic detection of low- and high-g events, slope changes, or orientation. Integration of the motion module into the final monitor is accomplished by using a I2C bus.

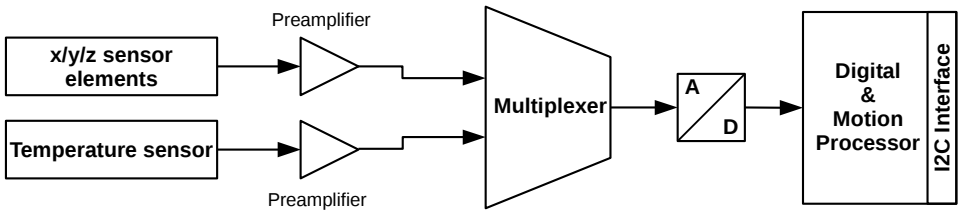

Figure 7: Block diagram of accelerometer BMA180, Adapted from [29]

Battery and Wireless Charging

The are significant disadvantages for any mobile monitoring solution to be directly connected to the mains during operation. Therefore, the health monitor platform is powered by a rechargeable lithium polymer battery pack. The battery pack contains safety measures, such as overvoltage, undervoltage and short circuit protection, to ensure the save operation of the battery at all times.

To enable charging of the battery, the core module requires a 5V and 1A supply, which can be provided by an external AC/DC adapter. However, most medical applications require full patient isolation, which can be achieved using wireless charging technology.

Wireless charging is a technology where energy is transferred from one object to another using electromagnetic fields. Energy transfer between devices is established through a transformer composed of loosely coupled coils embedded in the transmitter and receiver. A detailed overview of the technology can be found in Figure 8.

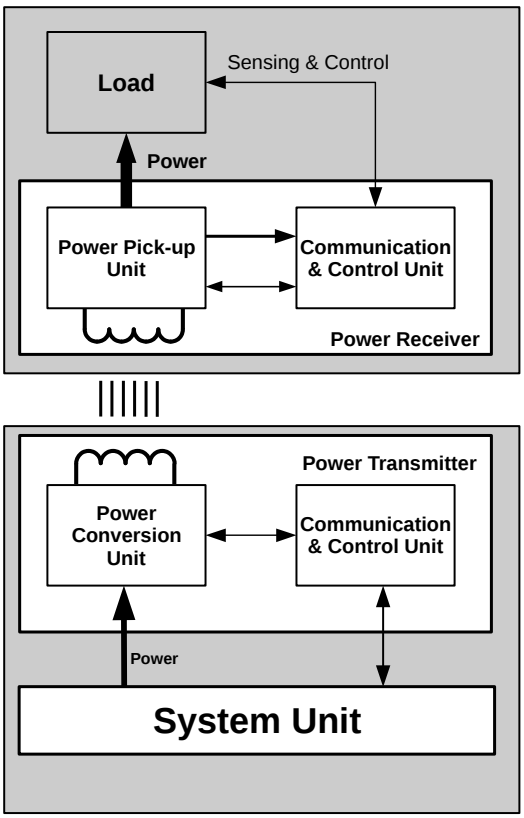

Figure 8: Overview of wireless power transfer from base station (bottom) to mobile device (top). Adapted from [20]

To address this need, a Qi compliant [20] wireless power receiver module was developed. Main functionality is provided by an integrated wireless power receiver circuit BQ51013B from Texas Instruments [21]. The BQ51013B is fully compliant with the Qi-standard and enables the use of commercially available charging stations. Altogether, the BQ51013B minimizes the required number of external components and offers features, such as output voltage rectification, foreign object detection and temperature control.

Therapeutic Intervention

Based on the recording of physiological variables and specific signal analysis, there may be a need to trigger therapeutic interventions and/or alarms. One of the therapeutic interventions would be the inflation of an abdominal binder, which applies pressure to the splanchnic region, in order to maintain blood pressure during upright position in patients with orthostatic hypotension [22]. The concept and implementation of such a device resulted in a patent application [23], which can be found in Appendix D.2.

Figure 9 shows the electronic components required to apply and maintain pressure to the splanchnic region of a patient. The module is composed of a pressure transducer (Honeywell, ASDX005PG2A5) as well as high current drivers. The high current drivers control diaphragm pump (Parker, T2-04) and two pneumatic solenoid values (Parker, X-Valve 8mm) in order to increase or decrease pressure in the abdominal binder. A bidirectional voltage translator (NXP Technology, GTL2002) ensures appropriate logic levels between the platform core and pressure transducer.

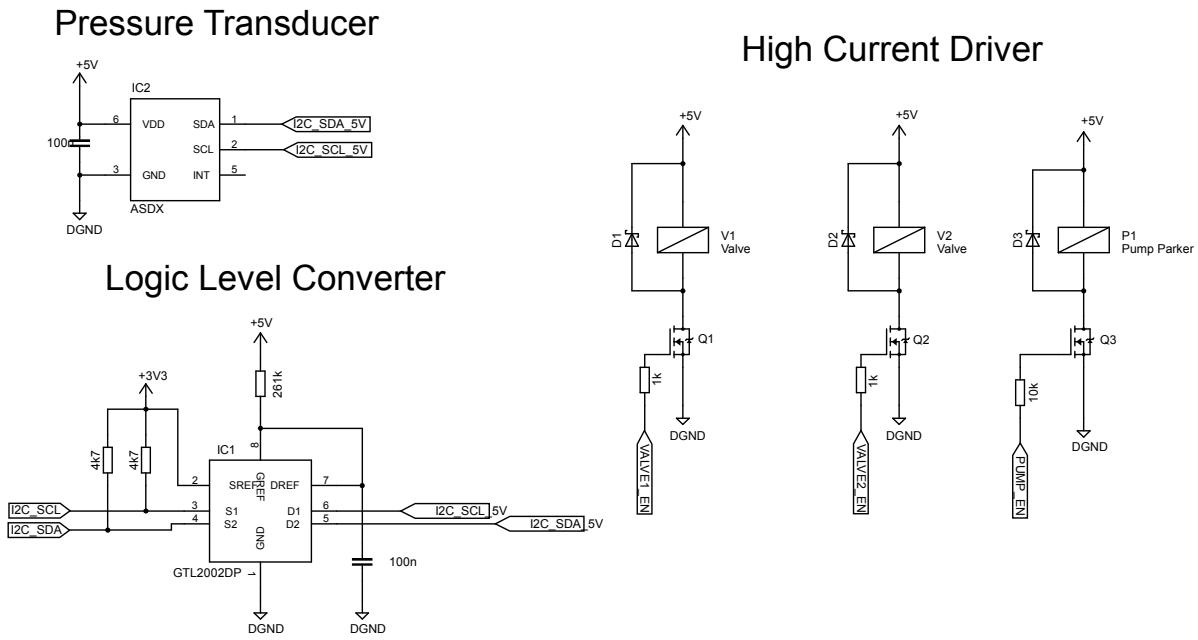

Figure 9: Schematic of therapeutic intervention module. Showing pressure transducer, high current drivers and logic level translator to inflate and maintain pressure of an abdominal binder.

Blood Pressure and Plethysmography/SpO2

Blood pressure, photoplethysmography and blood oxygen saturation are important parameters for patient monitoring. The technical design and development of these precise sensors is highly complex and beyond the scope of this work. In order to provide measurement capabilities of these physiological parameters in our health monitor platform, commercially available OEM modules from Corscience Germany (NIBP-2010 and ChipOx) were used. These OEM modules are equipped with a UART interface and; thus, can easily be integrated into the final monitor.

Connectivity

For smart and connected mobile health systems to be able to communicate with a remote medical data system or individual, the device requires the capability to transfer information freely and ubiquitous to the desired endpoint. With a growing number of mobile communication technologies, centralized server infrastructure and smartphones or tablet computers integrated into almost everyone's life, new possibilities to connect the patient wearing a mobile health monitor with a remote health care provider emerged.

Table 3: Wireless Communication Standards utilized by state of the art smartphones [24], [25]

Technology	Range	Date Rate	Max Power at TX	Frequency
Bluetooth (classic BT)	10-100 m	1-3 Mbit/s	2.5-100mW	2.4 Ghz
Bluetooth Low Energy (BLE)	50 m	1 Mbit/s	0.15-50mW	2.4 Ghz
ANT+	30 m	1 Mbit/s	0.18-56mW	2.4 Ghz
WiFi (Low energy device)	150-200 m	6-11 Mbit/s	150-210mW	2.4 Ghz or 5 Ghz

In addition to next generation wireless data technologies that link the smartphone to the internet, a variety of wireless short-range communication solutions are built into mobile devices [26]. A selection of most commonly used wireless communication standards in smartphones is provided in Table 3.

Virtually all mobile devices already include classic Bluetooth or WiFi technology, while BLE and ANT+ are emerging, ultra low-power and wireless technologies integrated into more modern or specialized purpose-built devices. To date, ANT+ has primarily been targeting the sports and fitness sector, particularly fitness and cycling performance monitoring [27].

To enable wireless communications with the outside world, two modules using miniature Bluetooth radios were designed. Both modules are based on wireless radios developed by Panasonic Europe and use either PAN1326 or PAN1327. PAN1326 is dual-mode Bluetooth radio that supports classic (BT) as well as Bluetooth low energy (BLE). The PAN1327 includes BT, and has added support for ANT+. ANT+ is a wireless personal network technology (WPAN) focusing mostly on the wellness and fitness sector, such as cadence sensors, cycling power meters, stride count sensors, etc.

While BLE and ANT+ compete for connecting short range and ultra-low power sensors that utilize very little bandwidth, BLE dominates the mobile phone market [28]. However, the author acknowledges that ANT+ is an emerging technology with steadily increasing mobile device support and is useful within very specific applications. Therefore, this technology was considered during module design and supported by utilizing the PAN1327 radio.

The two different radios are pin-compatible and only require a model specific software application service pack to be uploaded upon reset. Thus, during module development only the PAN1326 radio was considered.

For optimal power consumption, the radio requires multiple supply voltages. The digital supply is provided by a 1.8V step down DC/DC converter (ADP2108-1.8, Analog Devices, USA) and embedded into the module. In contrast, the RF circuitry of the radio requires a higher, but less stable supply voltage in order to maximize transmit power. The supply for the RF circuit can either come directly from the battery or the core module's digital system supply (3V).

The connectivity module is interfaced with the core module using UART. Logic level translation between both modules is achieved by adding the level translator TXB0106 (Texas Instruments, USA) into the signal path. A schematic of the connectivity module can be seen in Figure 10.

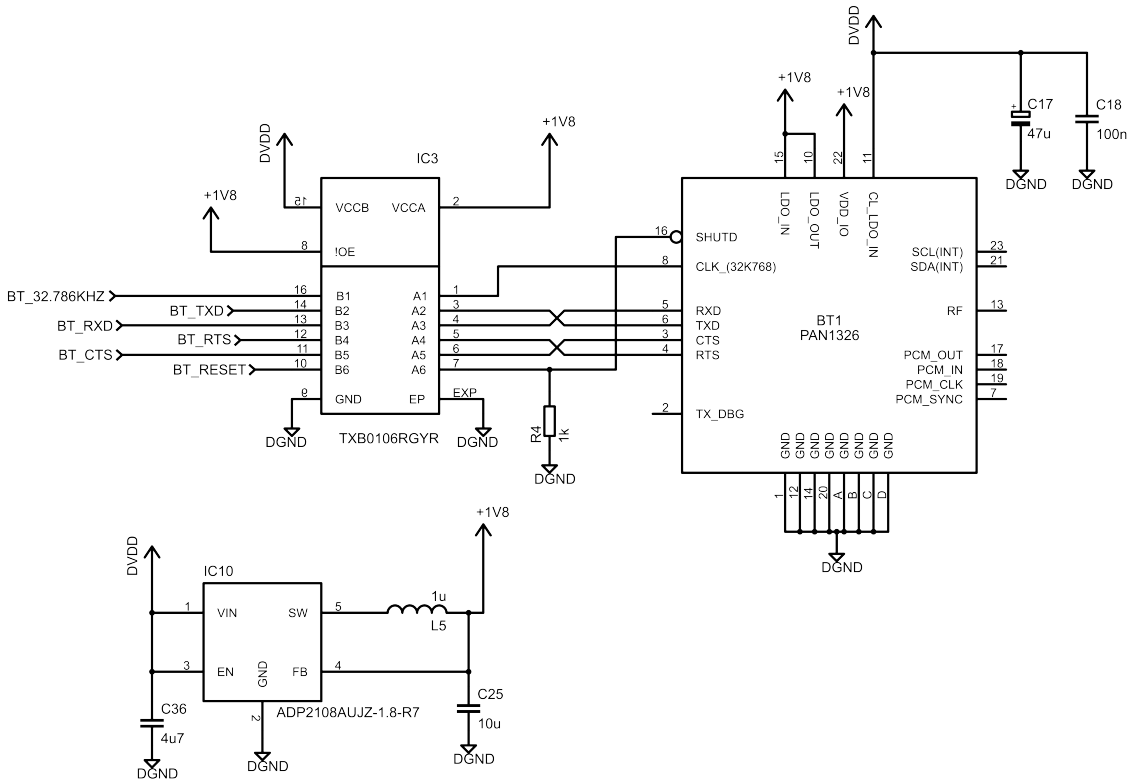

Figure 10: Schematic of connectivity module, showing Bluetooth radio PAN1326, logic level translator and step down DC/DC voltage converter.

References

[1] R. Harder, S. Eagle, F. Baudenbacher, J. Whitfield, A. Diedrich, J. B. Pietsch, and E.-J. Manders, ”Smart mobile health monitoring system and related methods”, *WO2014116968 A1*, 31-Jul-2014.

[2] ”STM32F405 Datasheet (Rev. 5)”. *ST Microelectronics*, 2015.

[3] M. I. Montrose, ”Printed circuit board design techniques for EMC compliance”, 2nd ed. *IEEE press*, 2000.

[4] H.-J. Liaw and H. Merkelo, ”Signal integrity issues at split ground and power planes”, in *Electronic Components and Technology Conference, 1996. Proceedings., 46th*, 1996, pp. 752–755.

[5] J. A. Roden, B. Archambeault, and R. D. Lyle, ”Effect of stitching capacitor distance for critical traces crossing split reference planes”, in *2003 IEEE International Symposium on Electromagnetic Compatibility*, 2003, vol. 2, pp. 703–707 vol.2.

[6] T.-L. Wu, S.-T. Chen, J.-N. Hwang, and Y.-H. Lin, ”Numerical and experimental investigation of radiation caused by the switching noise on the partitioned DC reference planes of high speed digital PCB”, *IEEE Transactions on Electromagnetic Compatibility*, vol. 46, no. 1, pp. 33–45, Feb. 2004.

[7] ”Analog Front End (AFE) - ECG / EEG Analog Front End - ADS1298R Datasheet (Rev. J)”. *Texas Instruments*, 2014.

[8] F. N. Wilson, F. D. Johnston, A. G. Macleod, and P. S. Barker, ”Electrocardiograms that represent the potential variations of a single electrode”, *American Heart Journal*, vol. 9, no. 4, pp. 447–458, Apr. 1934.

[9] H. C. Lukaski, ”Evolution of bioimpedance: a circuitous journey from estimation of physiological function to assessment of body composition and a return to clinical research”, *European Journal of Clinical Nutrition*, vol. 67, no. S1, pp. S2–S9, Jan. 2013.

[10] ”1 MSPS, 12 Bit Impedance Converter Network Analyzer - AD5933 Datasheet (Rev. E)”. *Analog Devices*, 2013.

[11] A. Boulier, J. Fricker, A. L. Thomasset, and M. Apfelbaum, ”Fat-free mass estimation by the two-electrode impedance method.”, *The American Journal of Clinical Nutrition*, vol. 52, no. 4, pp. 581–585, Oct. 1990.

[12] J. Rosell, J. Colominas, P. Riu, R. Pallas-Areny, and J. G. Webster, ”Skin impedance from 1 Hz to 1 MHz”, *IEEE Transactions on Biomedical Engineering*, vol. 35, no. 8, pp. 649–651, Aug. 1988.

[13] J. G. Webster, ”Medical Instrumentation Application and Design”, 4th ed. *Wiley*, 2010.

[14] A. C. Brown, M. H. Smolensky, G. E. D'Alonzo, and D. P. Redman, "Actigraphy: A Means of Assessing Circadian Patterns in Human Activity", *Chronobiology International*, vol. 7, no. 2, pp. 125–133, Jan. 1990.

[15] S. Ancoli-Israel, R. Cole, C. Alessi, M. Chambers, W. Moorcroft, and C. Pollak, "The role of actigraphy in the study of sleep and circadian rhythms. American Academy of Sleep Medicine Review Paper", *Sleep*, vol. 26, no. 3, pp. 342–392, 2003.

[16] A. Sadeh and C. Acebo, "The role of actigraphy in sleep medicine", *Sleep Medicine Reviews*, vol. 6, no. 2, pp. 113–124, May 2002.

[17] M. Chesson Jr, M. Coleman, M. Lee-Chiong, and D. Pancer, "Practice parameters for the use of actigraphy in the assessment of sleep and sleep disorders: an update for 2007", *Sleep*, vol. 30, no. 4, p. 519, 2007.

[18] N. Amini, M. Sarrafzadeh, A. Vahdatpour, and W. Xu, "Accelerometer-based on-body sensor localization for health and medical monitoring applications", *Pervasive and Mobile Computing*, vol. 7, no. 6, pp. 746–760, Dec. 2011.

[19] Q. Li, J. A. Stankovic, M. A. Hanson, A. T. Barth, J. Lach, and G. Zhou, "Accurate, Fast Fall Detection Using Gyroscopes and Accelerometer-Derived Posture Information", in *Sixth International Workshop on Wearable and Implantable Body Sensor Networks, 2009. BSN 2009*, 2009, pp. 138–143.

[20] Wireless Power Consortium, "Qi low power specification v1.1.2 : Wireless Power Transfer, System Description". Jun-2013.

[21] "Wireless Power Receiver - BQ51013B Datasheet (Rev. 05/2013)". *Texas Instruments*, 2013.

[22] L. E. Okamoto, A. Diedrich, F. J. Baudenbacher, R. Harder, J. S. Whitfield, A. Gamboa, C. Shibao, B. K. Black, S. R. Raj, and I. Biaggioni, "Comparative efficacy of an automated binder against midodrine in the treatment of orthostatic hypotension in autonomic failure", presented at the *24th International Symposium on the Autonomic Nervous System*, Kohala Coast, Hawaii, 2013.

[23] R. Harder, I. Biaggioni, F. Baudenbacher, A. Diedrich, and L. Okamoto, "Compression device, system, and method for decreasing abdominal venous pooling", *WO2014071292 A1*, 08-May-2014.

[24] "nRF51422 - ANT and ANT/Bluetooth low energy multiprotocol SoC". [Online]. Available: http://www.nordicsemi.com. [Accessed: 10-May-2013].

[25] Phill Smith, "Comparisons between Low Power Wireless Technologies". *CSR plc*, 2011.

[26] D. A. Gratton, "The Handbook of Personal Area Networking Technologies and Protocols". *Cambridge University Press*, 2013.

[27] M. J. McGrath and C. N. Scanaill, ”Sensor Technologies: Healthcare, Wellness and Environmental Applications”. *Apress*, 2013.

[28] D. A. Gratton, ”The Handbook of Personal Area Networking Technologies and Protocols”. *Cambridge University Press*, 2013.

[29] ”Triaxial, ultra high performance digital accelerometer - BMA180 Datasheet (Rev. 2.5)”. *Bosch Sensortec*, 2010.

CHAPTER III

A SMART MULTI-FREQUENCY BIOELECTRICAL IMPEDANCE SPECTROMETER FOR BIA AND BIVA APPLICATIONS

Introduction

Physiological Background

The electrical properties of tissues have been characterized in the late 19th century [1]. These properties have been studied for a wide range of frequencies on a variety of tissue types [2], [3]. Thomasset [2] was the first to conduct studies using electrical impedance as a means to determine total body water (TBW) composition using two subcutaneous needles [4]. Hoffer et al. [5] and Nyboer [5] later introduced the surface electrode bioelectrical impedance analysis (BIA) technique. The use of surface electrodes, as depicted in Figure 11 poses a disadvantage, because a higher current and higher voltage must be used to decrease the error in the measurement due to variation in the electrode-skin interface impedance [6].

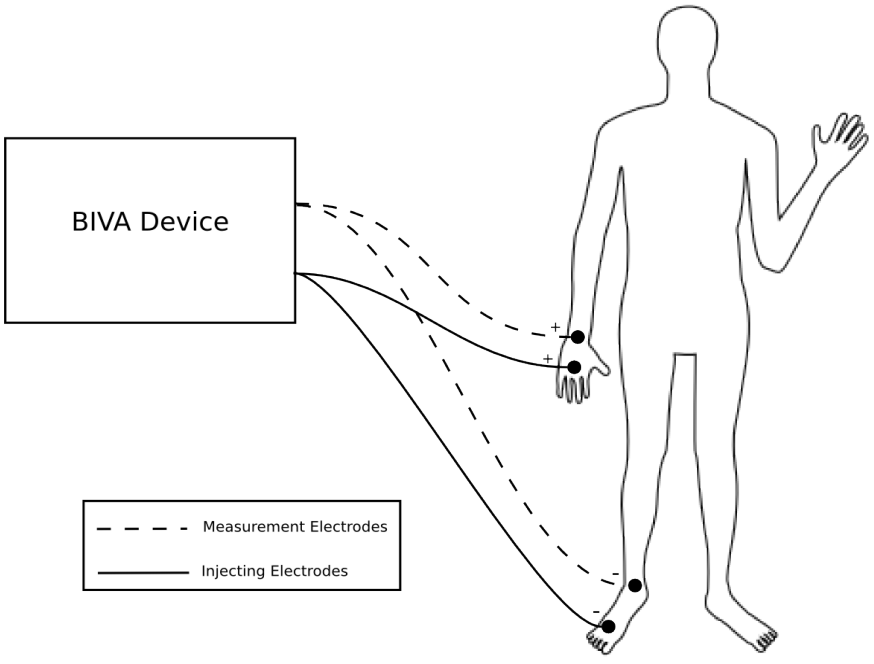

Figure 11: Common surface electrode placement for single segment BIA and BIVA measurements.

The method for determining body impedance is based upon the injection of a small alternating current into the human body. In human tissue the application of an alternating current results in an impedance profile that correlates with frequency [7]. Living tissue consist of intra- and extracellular space which acts as an ionic conductor and cellular membranes that have the property of an electrical insulator [4]. At low frequencies $(\leq 1\,kHz)$ the current is mainly carried by the extra-cellular fluid, while at higher frequencies $(\geq 500\,kHz)$ the current passes through the intra- and extracellular compartment [8], see Figure 12 for illustration.

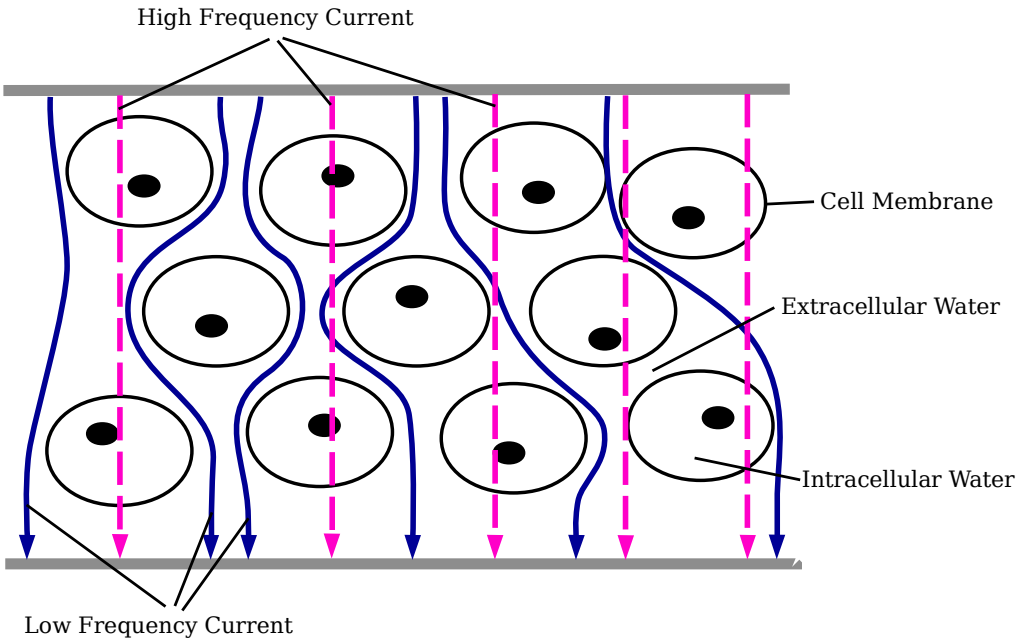

Figure 12: The current path through tissue at lower and higher frequencies.

This in vivo tissue behavior can be modeled by an equivalent circuit, depicted in Figure 13-left. The extracellular fluid is represented by resistor in parallel to a second arm, consisting of a capacitance and resistance of the intracellular fluid and the cell membrane connected in series [4], [9].

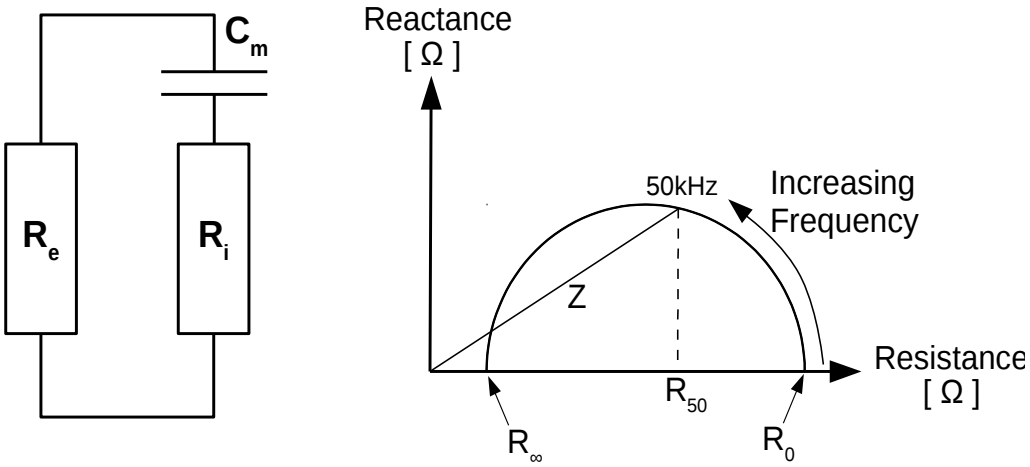

*Figure 13: Equivalent circuit of tissue (**left**), variation of impedance with frequency (**right**).*

Resistive and capacitive tissue components can be characterized at different frequencies, which results in a different phase of the current with respect to the voltage drop across the tissue, commonly referred to as phase angle. The vector of the impedance with components termed resistance and reactance is depicted in Figure 13-right. Cole et al. discovered that impedance values recorded in biological tissue resemble a perfectly circular locus with a center point slightly depressed the resistance axis [10].

Practical and physical constraints prevent the use of direct current and infinitive frequency. Therefore, resistance values in the limit of f=0 and f=∞ (Figure 13) can be predicted from a finite number of measurements at different frequencies using the Cole model and least mean square fits [11], The volume of total body water as well as fat free mass can be estimated utilizing a compartment model that considers R_0, R_∞, the patient's height and weight [4].

Another approach that does not require any assumption about body geometry, electrical tissue models or regression analysis is known as bioelectrical impedance vector analysis (BIVA).

In the BIVA representation, body composition is described as a vector with resistance (R) as the abscissa, and reactance (Xc) as the ordinate, normalized by the subjects height (H). The location of the vector is directly influenced by the body composition of an individual, as first described by Piccoli et al. [12], [13] The individual BIVA vectors are frequently displayed with the bivariate ellipsoidal 95th, 75th and 50th percentile confidence intervals (tolerance ellipse) of a normal healthy reference population in a two dimensional coordinate system with abscissa R/H (Ω/m) and ordinate Xc/H (Ω/m), see Figure 14.

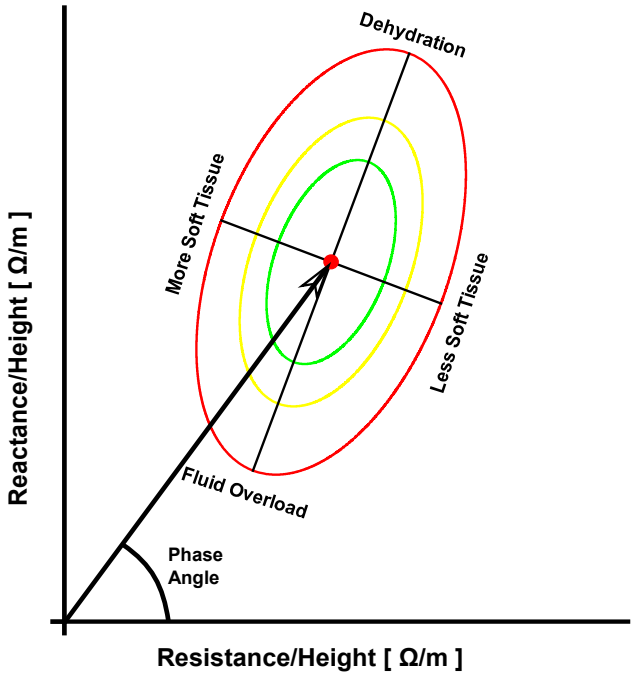

Figure 14: Bioelectrical Impedance Vector Analysis (BIVA) [4], [29].

Clinical Relevance

Undernutrition is a prevalent syndrome, generally in elderly and children, especially in developing countries [14]. Although undernutrition can be assessed using anthropometric measures, such as changes in weight or body mass index, waist circumferences, waist-to-hip ratio, mid-arm circumference, or skinfold thickness. These measurements are often difficult to interpret in clinical practice due to a lack of reference data for specific populations or ethnic groups. Anthropometric measurements are simple and inexpensive procedures, but a large variety of reliability among studies was found [15].

Anthropometric measurements are commonly used as proxy measures for body composition assessment in clinical practice. In recent decades, computer tomography, magnetic resonance imaging, and dual-energy X-ray absorptiometry (DXA) have been developed as new clinical standards to assess body composition [16]. While DXA has increasingly been used as a reference standard to estimate body composition [16], [17], these methods require costly clinical environments, well trained medical personal and are not applicable for frequent ambulatory monitoring of children or elderly in their natural living environment.

Bioelectrical impedance analysis (BIA) is a non-invasive, safe, inexpensive and portable technique for rapid assessment of body composition and body water that requires minimal patient collaboration. A detailed review of the technology has been published recently by Lukaski et al. [18].

BIA measures the voltage and phase angle of a signal generated by injecting a small sinusoidal electrical current at a single or multiple frequencies into the body, typically from hand-to-foot and computes the complex impedance values, with the real part of the impedance representing resistance (R) and imaginary part the reactance (Xc). It is well known that the volume of a homogeneous conductor with uniform cross-section can be computed based on its length, specific conductance and resistivity. Although the human body is not an object with uniform cross-sectional area or constant conductivity, semi-empirical relationships between impedance, height and body mass have been established [19]. These predictive equations are often obtained from linear regression analysis

using cross-validated DXA and body composition data obtained from specific populations in which they are valid [20]. Using this approach Kyle et al. derived a set of equations to estimate the fat-free mass (FFM) from BIA measurements with a correlation of r=0.986 compared to DXA in 343 healthy subjects aged 20-94 [21].

Multi-frequency analysis is used to determine extracellular (ECW) and intracellular water (ICW) based on a simple model of a purely capacitive membrane separating intra- and extracellular space and a purely resistive intra- and extracellular space. Therefore, ECW can be estimated from the impedance at low frequency and total body water (TBW) from the real component of the impedance at high frequency, where the capacitive effect of the cell membrane can be neglected [22]. ICW can be calculated from the difference between TBW and ECW.

In contrast to BIA, bioelectrical impedance vector analysis (BIVA) does not require any assumption about body geometry, electrical tissue models or regression analysis [23]. In the BIVA representation, body composition is described as a vector with resistance (R) as the abscissa, and reactance (Xc) as the ordinate, normalized by the subjects height (H) (see Figure 14). The individual BIVA vectors are quite often displayed with the bivariate ellipsoidal 95th, 75th and 50th percentile confidence intervals (tolerance ellipse) of a normal healthy reference population in a two dimensional coordinate system with abscissa R/H (Ω/m) and ordinate Xc/H (Ω/m). Bosy-Westphal et al. published reference BIVA standards of vector distributions according to sex, BMI and age in large populations of white children, adolescents and adults [24].

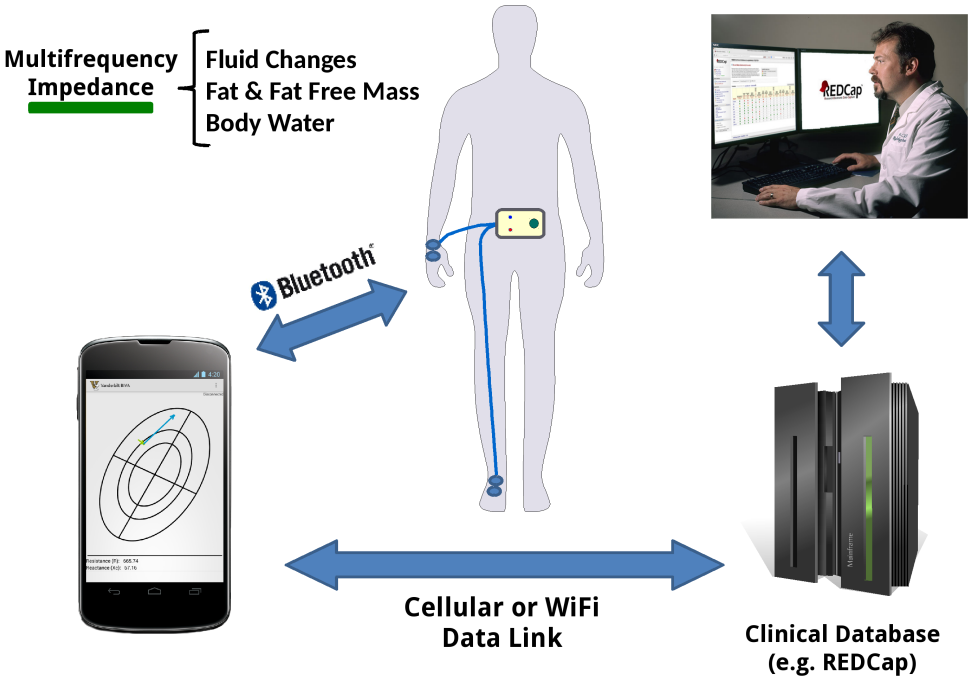

Figure 15: Concept of smart multi-frequency impedance spectrometer tethered to a smart phone and data transfer to a data server to facilitate immediate feedback from health care provider or aggregation of impedance measurements across multiple studies in a clinical database.

With the introduction of smart phones, new mobile applications are developed to aid in health management and offer guidance for a better healthy living. Professional caretakers are using smart phones frequently in making decisions to improve the outcomes of clinical care [25]. The integration with smart mobile devices offer ubiquitous network access that provides a path for data synchronization with a centralized database and facilitates immediate feedback from health care providers for longitudinal monitoring, guidance and intervention in clinical or home environments (Figure 15).

To achieve a wider use of BIA/BIVA applications, we developed a portable, low cost, battery operated and rugged multi-frequency impedance spectrometer. The spectrometer is tethered wirelessly to a smart phone or tablet computer and runs BIA and BIVA graphical applications to promote the use of BIA technology by patients and health care providers with limited training (Figure 16).

*Figure 16: Wireless multi-frequency impedance spectrometer (**left**) used for bioelectrical impedance vector analysis (BIVA) in a rugged dust and water protected (IP 54) enclosure and snap on lead wires for easy and robust electrode attachment. Mobile application running on Nexus 7 tablet computer (**right**) that displays multiple BIVA measurements and allows for tracking of patient progress, patient management and data export.*

Hardware

The platform consists of an ARM cortex-M4 microprocessor (STM32F415, STMicroelectronics). The cortex-M4 was selected as it offers a good balance between power consumption and computational power. Further, the integration of a floating point unit and limited DSP instruction set creates a powerful controller for bioelectrical impedance measurements and signal processing (Figure 17).

The hardware is placed in a dust- and water-protected (IP54) enclosure (OKW Enclosures Inc., USA) to ensure proper device functionality in harsh environments (Figure 16). The integration of wireless charging provides patient safety while maintaining low circuit complexity and improved ruggedness of the

spectrometer due to the galvanic discontent between the charging device and mains. The only wires leading into the enclosure are the patient lead wires, which can be sealed hermetically.

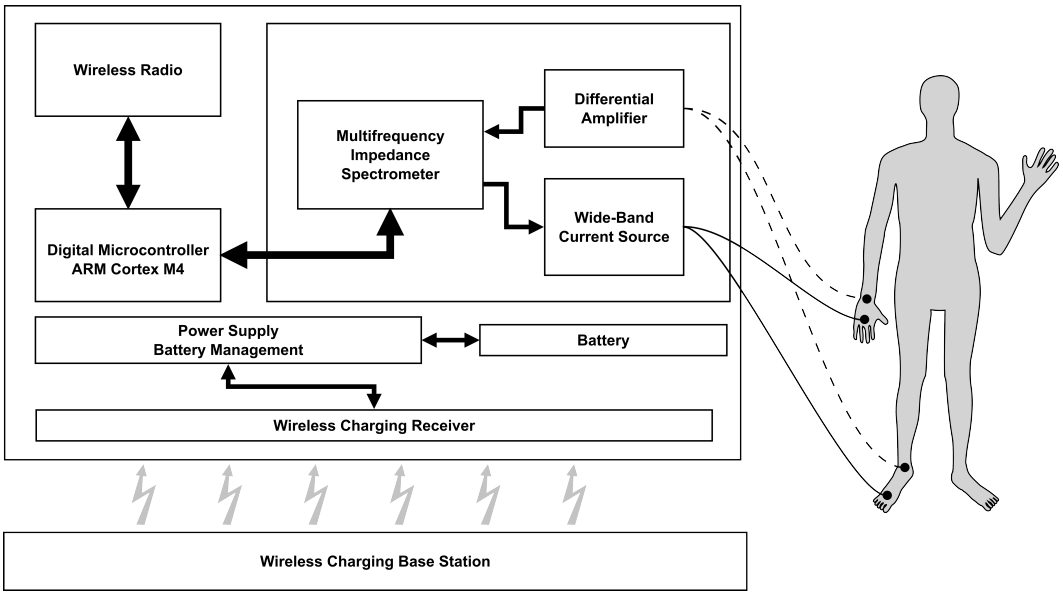

Figure 17: Simplified block diagram of wireless multi-frequency impedance spectrometer and standard BIA electrode placement on hand/wrist and foot/ankle.

Communication to the mobile device is established via a Bluethooth v2.1 connection and allows for the setting of measurement parameters, like excitation amplitude, start and stop frequency and frequency increment. Upon completion of the measurement sequence the recorded impedance for each frequency is transferred to the mobile device. At all times it is ensured that the measurement parameters are within functional and safe limits by the spectrometer firmware.

Analog front-end

The analog front-end is built around a high precision digital impedance network analyzer AD5933 from Analog Devices. The AD5933 is a fully integrated impedance analyzer with a built in frequency generator that allows for the determination of an impedance over a wide range of selectable frequencies. A 12-bit analog to digital converter (ADC) samples the input signal at a rate of 1MSPS and an integrated DSP applies a discrete Fourier transformation (DFT) to the digitized input signal and returns real and imaginary components. These features combined with the ease of programming via I2C bus makes the AD5933 an excellent component for a smart bioelectrical impedance analyzer.

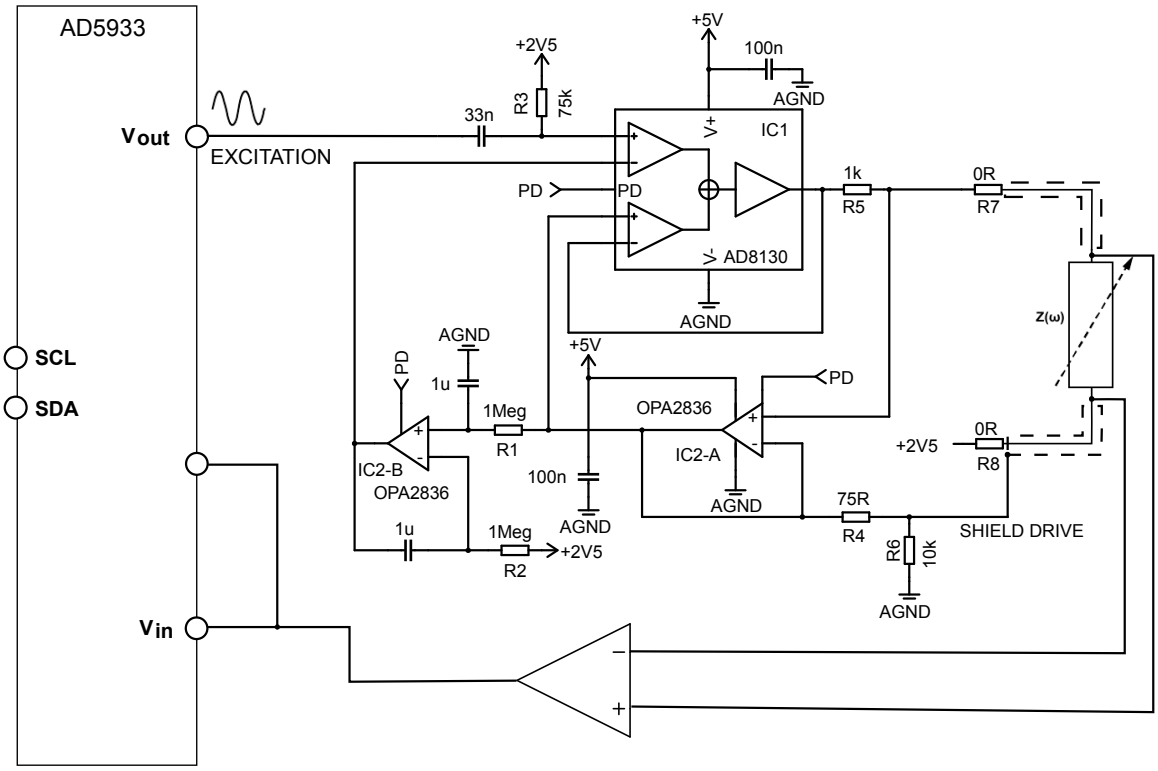

Figure 18: Analog front-end of the bioelectrical impedance spectrometer including precision wide-band constant current source using the differential receiver amplifier AD8130 that allows for tetrapolar impedance measurements, high output impedance and high CMRR. The front-end can be disabled when not in use through a power down signal (PD) to reduce the overall power consumption of the spectrometer.

A precision wide-band constant current source was designed to overcome output impedance limitations and to allow for precise tetrapolar impedance measurements. The complete circuit diagram is shown in Figure 18. Most instrumentation amplifier based constant current sources provide relatively high output impedance and high common mode rejection ratio (CMRR) at lower frequencies. However, bandwidth, slew rate and CMRR limitations make instrumentation amplifier an inadequate choice for precision high frequency constant current sources. The differential receiver amplifier AD8130 from Analog Devices offers high CMRR (80dB @ 2MHz) at high frequencies and has been successfully used for bioelectrical impedance measurement [26], [27].

This amplifier has a comparatively high input bias current of maximal ±3.5μA. The large bias current poses a problem, since it affects the output current for small excitation signals and prevents accurate impedance measurements. However, this issue can be overcome by adding a unity gain amplifier (Figure 18, IC2-A, OPA2836) into the feedback path. Furthermore, to allow for single supply operation of the current source as well as for purely capacitive or ac coupled loads, a DC stabilization loop (Figure 18, IC2-B, OPA2836) was introduced. The cut-off frequency of the DC stabilization loop was chosen small enough (below 0.5Hz) to have a negligible effect on bioelectrical impedance measurements.

To achieve a fully bipolar current source, the output can be AC coupled by replacing resistors R7 and R8 with suitable coupling capacitors. The maximum possible output current with this design is limited by the maximum output voltage swing of IC1 and current sense resistor R5 to 1.7mA_{RMS}.

Software

The mobile application was developed using Android operating system (Google & Open Handset Alliance, Ice Cream Sandwich, API level 14) and provides management of the patient record, archiving of data, impedance spectrometer device controls and visualization of BIA/BIVA measurements.

Patient record and anthropomorphic data for each visit are saved in conjunction with each BIVA measurement in a relational database. Hence, the health care provider and patient can track the patient's performance over an extended period for early diagnosis or adjustments to treatment plans (Figure 19).

The individual BIVA measurements are displayed with the bivariate ellipsoidal 95th, 75th and 50th percentile confidence intervals (confidence ellipses) of a normal healthy reference population, which is based on the work of Picolli et. al. [28], [29], (Figure 19, Figure 16).

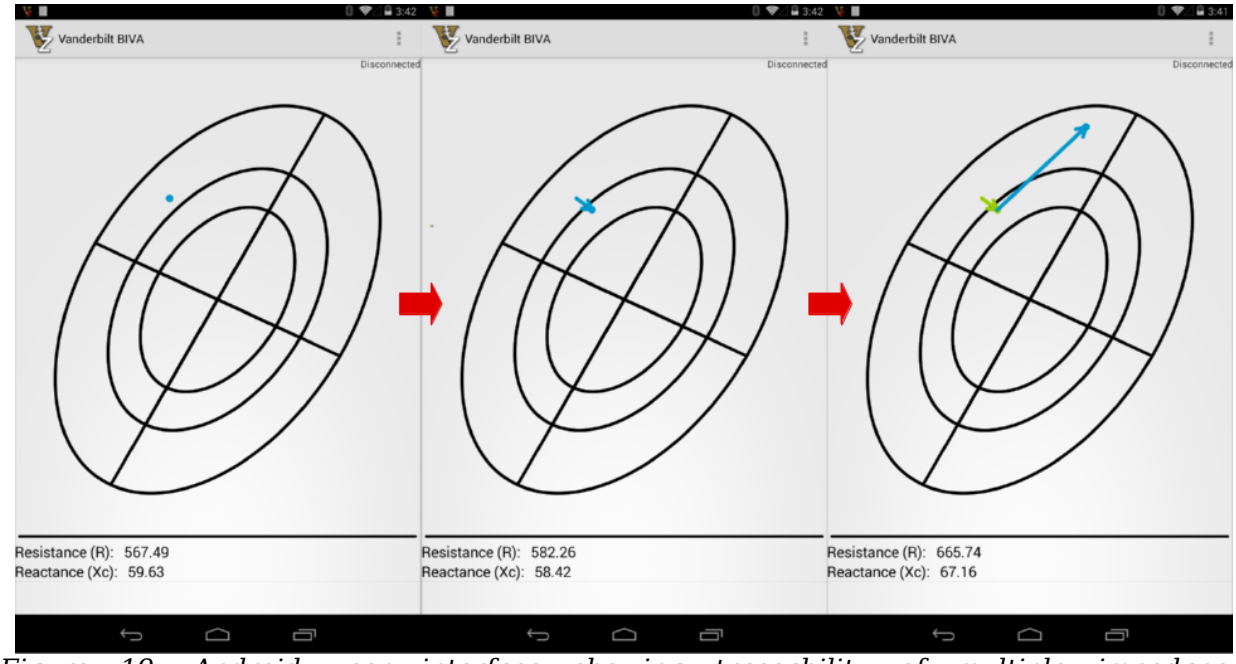

Figure 19: Android user interface showing traceability of multiple impedance measurements over prolonged time.

An export of impedance measurements and anthropometric data into a Research Electronic Data Capture (REDcap)[30] database allows for the aggregation of measurements across multiple devices and studies. This capability, facilitates the monitoring of larger patient groups at multiple locations or the creation of new reference population data sets.

An integrated software update mechanism ensures that devices run the most recent mobile application, such that the hardware does not need to be recalled and the operator benefits from new features, such as an updated reference population database or different protocols and algorithms to determine body composition. A more in depth description of the user interface can be found in Appendix B.

Hardware Validation

Hardware Performance Evaluation

To evaluate the performance of the bioelectrical impedance spectrometer, we used a tissue equivalent model with 2 resistors representing the extra- and intracellular space and 1 capacitor representing the cell membrane [31]. The resistor and capacitor values were determined by fitting whole body impedance values at different frequencies to the equivalent circuit model. The impedance data for the model corresponds to a healthy 20-35 year old male adult. The model values obtained are a resistance R1=549Ω (extracellular) in parallel with a series combination of capacitance C=2.2nF and a resistance R2=1098Ω (intracellular). All resistors had tolerances of 0.1% and 1% for the capacitor. Prior the performance evaluation, the spectrometer output was calibrated in the frequency range of 1kHz to 300kHz, with 1kHz increments using a 500Ω 0.01% calibration resistor.

Measurements from the multi-frequency impedance spectrometer were validated using the tissue equivalent model at 22 different frequencies, between 1kHz and 300kHz. The upper frequency limit was chosen higher than the recommended maximum of AD5933 (100kHz) to fully evaluate the limitations of this impedance spectrometer. A measurement consists of data obtained at 22

frequencies and after each measurement the lead wires were repositioned to account for capacitive coupling between leads. Based on 20 measurements we computed mean, percentage error and standard deviation.

Furthermore, during each measurement we fitted impedance values at 5 different frequencies (3kHz, 10kHz, 50kHz 75kHz and 100kHz) to a circular impedance locus using a least mean square estimator and determined the Cole parameters R_0, R_∞, α and τ [10], [11]. Using these Cole parameters, impedance values and errors were determined for each measurement over an extended frequency range from 1kHz to 3MHz.

Body Composition

We conducted a study where 9 healthy volunteers with median age 53 (lower-upper quartile: 36.8-70.3) years underwent DXA. DXA, impedance measurements, weight and height were taken the same day. Body height was measured within 0.5cm using a calibrated wall-mounted stadiometer (Perspective Enterprises, Portage, MI). Body weight was measured within 0.1kg using a calibrated beam platform scale (Detecto-Medic, Detecto Scales, Inc, Northbrook, IL) with participants wearing light clothing and no shoes. The scans were completed with a whole body DXA (Lunar Prodigy; GE Medical Systems, Madison, WI, USA) in supine position and body composition (fat and fat-free mass) was calculated using manufacturer provided software. Directly after the DXA scan without any change in position whole body impedance was measured.

Based on the impedance values at 50kHz the subject's fat free mass (FFM) (Equation 1) and fat mass (FM) (Equation 2) was estimated using an empirical prediction algorithm proposed by Kyle et al. [21]. The measurements were performed using Ag/AgCl gel electrodes (3M, Red Dot Monitoring Electrode) and standard tetrapolar electrode placement on the back of the patient's hand and foot [32]. The sensing electrodes were placed at the levels of the prominent bones on the dorsal face of the wrist and ankle. The current injecting electrodes were placed 5 cm distal from the sensing electrodes. The preparation and cleaning of the skin

with alcohol, the use of pre-gelled electrodes, and standard placement at well defined anatomical points minimizes the error introduced by variances in electrode position and electrode-skin interface impedance [32]–[34].

$$FFM_{kg} = -4.104 + 0.518 \cdot \frac{Height(cm)^2}{Resistance} + 0.231 \cdot Weight(kg) + 0.130 \cdot Reactance + 4.229 \cdot Sex(men = 1, women = 0) \quad (1)$$

$$FM_{\%} = \left(1 - \frac{FFM(kg)}{Weight(kg)}\right) * 100\% \quad (2)$$

To characterize the relationship between impedance based and DXA fat mass estimates, we used a simple linear regression model, means and differences.

Body Water Changes

Body water is important for cell and circulatory body functions, its maintenance and control is critical in renal failure patients, heart failure patients and patients with hypertension. Salt and volume regulation are closely related and are affected by salt intake and water consumption [35]. Impedance techniques could be used to monitor body water retention during diuresis or low salt diets.

To determine changes in the ECW and ICW during different amounts of daily sodium intake, we obtained data from one healthy female (39 years, 163cm height, 71kg weight) on a low (LS, 10 mE Na+ per day), normal (60 mE Na+ per day), and high sodium diet (300 mE Na+ per day). After 6 days on each diet, impedance measurements were taken at the same anatomical position of left wrist and left ankle in supine position in the morning after an overnight fast.

ECW (Equation 3) and TBW (Equation 4) at 5kHz and 100kHz were calculated based on the semi-empirical formulas obtained by Deurenberg et al. [36]. The calculations are based on linear regression analysis of bioimpedance data compared with DXA, as clinical accepted standard.

$$ECW_{kg} = 2.53 + 0.18903 \cdot \frac{Height(cm)^2}{Z_{5kHz}} + 0.06753 \cdot Weight(kg) - 0.02 \cdot Age \quad (3)$$

$$TBW_{kg} = 6.69 + 0.34573\frac{Height(cm)^2}{Z_{100\,kHz}} + 0.17065 \cdot Weight(kg) - 0.11 \cdot Age + 2.66 \cdot Sex(men = 1, women = 0) \quad (4)$$

These formulas are based on the fact that the injected current at lower frequencies is unable to couple effectively across the capacitive cell membrane (Figure 12). Therefore, the body impedance measured at low frequency is mostly affected by the extracellular water. For higher frequencies, the cell membrane couples more efficiently and intracellular currents lead to a larger contribution of the intracellular resistance (Figure 4). Hence, the body impedance at high frequencies is dominated by a parallel configuration of intra- and extracellular resistance [2], [37]. As a result, impedance measurements at different frequencies can be used as a proxy for total body, intra- and extracellular water.

All applicable institutional and governmental regulations concerning the ethical use of human volunteers were followed during these studies, in accordance with the ethical principles of the Helsinki-II Declaration. All participants signed an informed consent document approved by the Vanderbilt University Institutional Review Board.

Results

Hardware Performance Evaluation

The mean resistance and reactance values at different frequencies obtained from our tissue equivalent model are plotted in Figure 20. Resistance measurements show a nearly constant error of less than ±1% across the frequency range from 3kHz to 300kHz. Further, the resistance exhibits a standard deviation of 0.01% for frequencies between 3kHz and 175kHz and approaches 0.017% at high frequencies. The reactance measurements exhibit a slightly larger error of ±5% in the frequency range between 4kHz and 150kHz which significantly increases at low and high frequencies and has a maximum of -15% at 300kHz. The standard deviation of the reactance closely follows those of the resistance measurements up to a frequency of 100kHz, but increases nearly 10 fold toward both ends of the spectrum. The impedance spectrometer did not produce reliable impedance measurements for frequencies of 1kHz and 2kHz.

The resistance values derived from the Cole estimation exhibit an error and standard deviation of ±0.2% and 0.05%, respectively, over the extended frequency range from 1kHz to 3MHz. For the reactance estimation, the error (standard deviation) exhibits a minimum of 0.6% (0.08%) at 50kHz, but increases to a maximum of 4.4% (0.5%) at 1kHz and 3MHz.

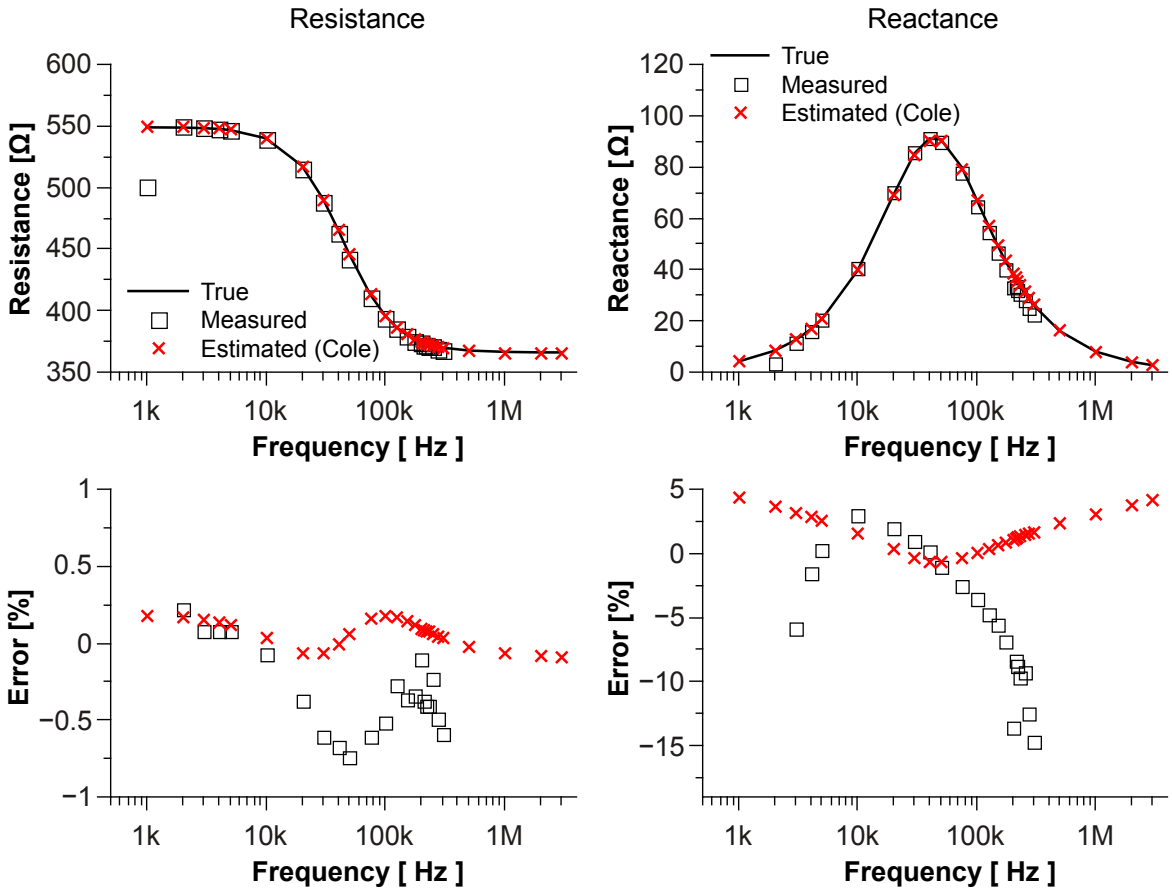

Figure 20: BIA measurements with a tissue equivalent circuit model measured at multiple frequencies (square) compared to impedance estimations based on the Cole model (cross) using five BIA measurements between 3kHz and 100kHz. Absolute resistance and reactance over frequency (top). Absolute error of measurement with respect to true resistance (bottom-left) and true reactance (bottom-right). Values for 1kHz and 2kHz partially omitted due to significant measurement error.

Body Composition

We compared body FM estimation using BIA and DXA. The results of the linear regression indicate that there is a strong positive correlation (r^2=0.985) between the measures (Figure 21). The null hypothesis of the slope equal zero was rejected with a p-value of less than 0.0001. The largest deviation of the FM from the reference standard was 4.8%, which corresponds to an absolute error of 6.5% with respect to the subjects total body weight. Further, for the majority of the measurements (8 out of 9) the BIA estimation showed a tendency to underestimate FM compared to DXA measurement in this subject group, with a mean (median) bias of 2.62% (2.79%).

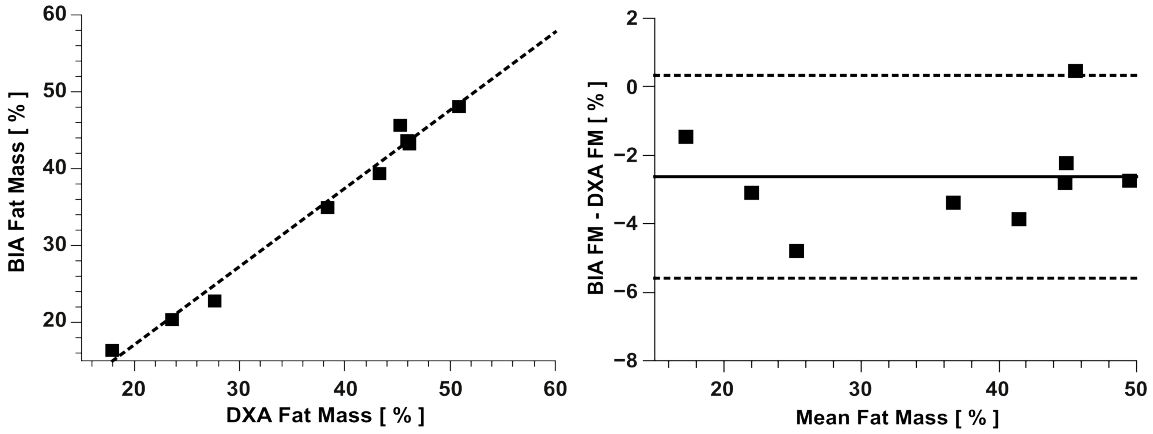

Figure 21: Comparison of body fat mass estimation in 9 subjects via bioelectrical impedance spectrometer (BIA) and dual-energy X-ray absorptiometry (DXA) (left) and Bland-Altman plot (right) with mean difference (solid line) and 95% limit of agreement (dashed lines).

Body Water Changes

Figure 22 shows changes of impedance and reactance (Figure 22-left) and estimation of TBW and ECW using multi-frequency impedance (Figure 22-right) during low, normal, and high sodium diet in a healthy subject. The results demonstrate that increasing sodium load causes impedance and reactance changes towards the direction of more hydration in the BIVA graphical representation. Further, the estimates of ECW and TBW increased with increasing sodium load, as expected.

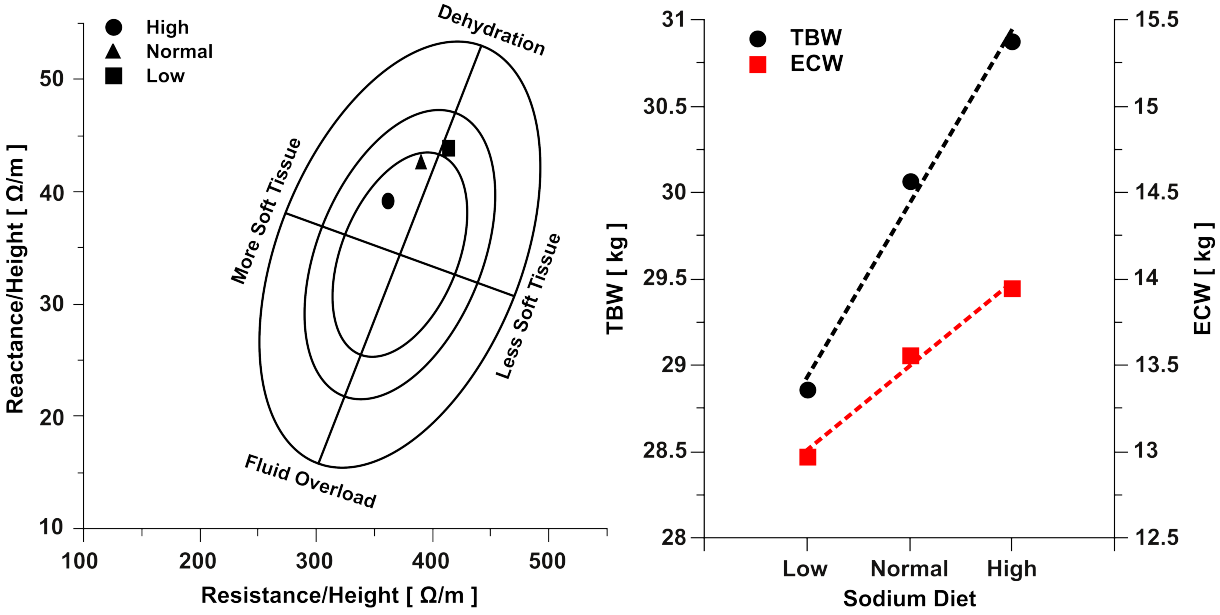

*Figure 22: BIVA with RXc graph of a female subject fed diets with low, normal and high sodium content (**left**). The population specific bivariate tolerance intervals are displayed as tolerance ellipses (95%, 75% and 50%). The reference population used for the tolerance ellipses was based on healthy Caucasian females (n=372, age 16-84yr) [47]. Estimation of TBW and ECW of the same subject (**right**) determined by using multiple frequencies, 100kHz for TBW and 5kHz for ECW. Estimation based on BIA equations reported by Deurenberg et al. [36].*

Discussion

Utilizing an integrated programmable impedance network analyzer allows for a simple and low cost circuit design to measure the impedance over a range of frequencies particularly suited for BIA assessments. The multi-frequency impedance spectrometer shows a significantly higher error at low frequencies. The observed error of the AD5933 is as expected , since the integrated circuit is driven with a 16MHz system clock, which results in a 1MSPS sampling rate. Therefore, the period of an input signal at low frequencies is not fully captured by the 1024 point DFT and spectral leakage becomes a significant source of errors. If necessary the lower frequency limit can be reduced by scaling the system clock frequency. However, adjusting the clock frequency will directly impact the sampling frequency of the ADC and; therefore, significantly limits its measurable frequency range and use for BIA applications.

The AD5933's internal low pass filtering (fc~100kHz), before analog to digital conversion, restricts the upper frequency limit of this impedance spectrometer [38]. Therefore, it is expected that the measurement error will increase above 100kHz due to the reduced sensitivity. Our measurements have shown that accuracy for resistance measurements stay below ±1% for a frequency range of 3kHz-300kHz and ±5% (3kHz to 150kHz) for reactance measurements. Hence, the suitable frequency range for this impedance spectrometer, with respect to BIA/BIVA application, is 3kHz to 150kHz. Studied that performed BIA measurements outside this frequency range have raised some controversy about the effectiveness of impedance measurements to determine body composition due to limited reproducibility [19], [39] and effects of electrode mismatches at high and low frequencies [40].

These limitations can be overcome by utilizing a least mean square approximation of multiple impedance measurements at different frequencies to a tissue equivalent circuit model. Using this estimation, the error for the resistance and reactance determinations could be reduced to less than 0.2% and 5%

respectively at high and low frequencies over an extended frequency range from 1kHz to 3MHz. The algorithm is sufficiently simple to be implemented directly on the microcontroller for real-time estimation of R_0 and R_∞.

There is an extensive body of literature showing that anthropometric measures do not provide accurate information about body fat in all populations, especially in children, elderly and athletes [41]–[43], leading to a wrong diagnosis and potentially harmful intervention. Although, we did not validate the device in children and athletes, we have shown that our impedance spectrometer estimates FM in normal healthy adults, median age 53 years, with a regression coefficient of r2=0.985 and 6.5% maximum error compared to DXA measurements.

We also showed that our device can be used to track body water changes during different dietary interventions. The BIVA graphical presentation allows for a simple tracking of body water content and/or body composition in a clinical or home setting. Utilizing a tissue equivalent model and least mean square approximation, we demonstrated an extension of our measurement range. We hypothesis that the extension of the measurement range will lead to a more accurate determination of TBW and ECW, which is subject to further clinical studies.

It has been shown than BIA can be a valuable tool for determining a subject's body composition within specific patient groups [14], [44], [45]. Some studies demonstrated that BIA has limitations for assessing body composition [46] due to utilizing compartmental models and regression analysis derived for specific patient populations, which cannot be generalized [45]. In contrast, our device can be customized for various patient groups and populations leading to a more accurate estimation of body composition.

The main advantage of our current solution, compared to other BIA/BIVA devices commercially available, is cost effectiveness, ruggedness and integration into a centralized data management infrastructure. The tight integration of software with hardware allows for "on-the-fly" customization. Therefore, we can implement new and group-specific algorithms for determining body composition or

tracking of nutritional status and body water for each individual patient not only in the clinical setting, but also at home. The implementation of server data link can provide an immediate feedback to the patients and/or health care provider.

Conclusion

The presented smart multi-frequency bioelectrical impedance spectrometer for BIA and BIVA applications is able to track nutritional and hydration status in healthy subjects and patients. The simplicity of BIA/BIVA measurements and the simple visual representation of impedance data enables patients to compare and determine body composition during the time course of a specific treatment plan. Hence, patients may be actively engaged in their health and take responsibility leading to a higher adherence to the treatment plan, early diagnosis and be proactive for their health.

References

[1] L. Hermann, ”Ueber eine Wirkung galvanischer Stroeme auf Muskeln und Nerven”, *Archiv für die gesamte Physiologie des Menschen und der Tiere*, vol. 5, no. 1, pp. 223–275, Dec. 1872.

[2] A. Thomasset, ”Bio-electric properties of tissues. Estimation by measurement of impedance of extracellular ionic strength and intracellular ionic strength in the clinic”, *Lyon médical*, vol. 209, pp. 1325–1350, Jun. 1963.

[3] M. Y. Jaffrin and H. Morel, ”Body fluid volumes measurements by impedance: A review of bioimpedance spectroscopy (BIS) and bioimpedance analysis (BIA) methods”, *Medical Engineering & Physics*, vol. 30, no. 10, pp. 1257–1269, Dec. 2008.

[4] U. G. Kyle, I. Bosaeus, A. D. De Lorenzo, P. Deurenberg, M. Elia, J. M. Gómez, B. L. Heitmann, L. Kent-Smith, J.-C. Melchior, M. Pirlich, H. Scharfetter, A. M. W. J. Schols, and C. Pichard, ”Bioelectrical impedance analysis—part I: review of principles and methods”, *Clinical Nutrition*, vol. 23, no. 5, pp. 1226–1243, Oct. 2004.

[5] J. Nyboer, M. M. Kreider, and L. Hannapel, ”Electrical Impedance Plethysmography A Physical and Physiologic Approach to Peripheral Vascular Study”, *Circulation*, vol. 2, no. 6, pp. 811–821, Dec. 1950.

[6] A. Boulier, J. Fricker, A. L. Thomasset, and M. Apfelbaum, ”Fat-free mass estimation by the two-electrode impedance method.”, *The American Journal of Clinical Nutrition*, vol. 52, no. 4, pp. 581–585, Oct. 1990.

[7] R. F. Kushner, ”Bioelectrical impedance analysis: a review of principles and applications.”, *Journal of the American College of Nutrition*, vol. 11, no. 2, pp. 199–209, 1992.

[8] M. Y. Jaffrin and H. Morel, ”Body fluid volumes measurements by impedance: A review of bioimpedance spectroscopy (BIS) and bioimpedance analysis (BIA) methods”, *Medical Engineering & Physics*, vol. 30, no. 10, pp. 1257–1269, Dec. 2008.

[9] H. C. Lukaski, ”Evolution of bioimpedance: a circuitous journey from estimation of physiological function to assessment of body composition and a return to clinical research”, *European Journal of Clinical Nutrition*, vol. 67, no. S1, pp. S2–S9, Jan. 2013.

[10] K. S. Cole, ”Electric Impedance of Suspensions of Spheres”, *The Journal of General Physiology*, vol. 12, no. 1, pp. 29–36, Sep. 1928.

[11] B. H. Cornish, B. J. Thomas, and L. C. Ward, ”Improved prediction of extracellular and total body water using impedance loci generated by multiple frequency bioelectrical impedance analysis”, *Physics in Medicine and Biology*, vol. 38, no. 3, p. 337, Mar. 1993.

[12] A. Picolli, P. Piazza, D. Noventa, L. Pillon, and M. Zaccaria, ”A new method for monitoring hydration at high altitude by bioimpedance analysis”, *Medicine & Science in Sports & Exercise December 1996*, vol. 28, no. 12, pp. 1517–1522, 1996.

[13] A. Piccoli, L. Pillon, and F. Dumler, ”Impedance vector distribution by sex, race, body mass index, and age in the United States: standard reference intervals as bivariate Z scores”, *Nutrition*, vol. 18, no. 2, pp. 153–167, Feb. 2002.

[14] M. A. Camina Martín, B. de Mateo Silleras, and M. P. Redondo del Río, ”Body composition analysis in older adults with dementia. Anthropometry and bioelectrical impedance analysis: a critical review”, *European Journal of Clinical Nutrition*, vol. 68, no. 11, pp. 1228–1233, Nov. 2014.

[15] S. J. Ulijaszek and D. A. Kerr, ”Anthropometric measurement error and the assessment of nutritional status”, *British Journal of Nutrition*, vol. 82, no. 03, pp. 165–177, Sep. 1999.

[16] A. Andreoli, G. Scalzo, S. Masala, U. Tarantino, and G. Guglielmi, ”Body composition assessment by dual-energy X-ray absorptiometry (DXA)”, *La radiologia medica*, vol. 114, no. 2, pp. 286–300, Mar. 2009.

[17] A. Pietrobelli, Z. Wang, C. Formica, and S. B. Heymsfield, ”Dual-energy X-ray absorptiometry: fat estimation errors due to variation in soft tissue hydration”, *American Journal of Physiology - Endocrinology and Metabolism*, vol. 274, no. 5, pp. E808–E816, May 1998.

[18] H. C. Lukaski, ”Evolution of bioimpedance: a circuitous journey from estimation of physiological function to assessment of body composition and a return to clinical research”, *European Journal of Clinical Nutrition*, vol. 67, no. S1, pp. S2–S9, Jan. 2013.

[19] U. G. Kyle, I. Bosaeus, A. D. De Lorenzo, P. Deurenberg, M. Elia, J. M. Gómez, B. L. Heitmann, L. Kent-Smith, J.-C. Melchior, M. Pirlich, H. Scharfetter, A. M. W. J. Schols, and C. Pichard, ”Bioelectrical impedance analysis—part I: review of principles and methods”, *Clinical Nutrition*, vol. 23, no. 5, pp. 1226–1243, Oct. 2004.

[20] R. A. Brownbill and J. Z. Ilich, ”Measuring body composition in overweight individuals by dual energy x-ray absorptiometry”, *BMC Medical Imaging*, vol. 5, no. 1, p. 1, Mar. 2005.

[21] U. G. Kyle, L. Genton, L. Karsegard, D. O. Slosman, and C. Pichard, ”Single prediction equation for bioelectrical impedance analysis in adults aged 20–94 years”, *Nutrition*, vol. 17, no. 3, pp. 248–253, Mar. 2001.

[22] K. S. Cole, ”Membranes, ions, and impulses: a chapter of classical biophysics”, vol. 1. *Univ of California Press*, 1968.

[23] A. Piccoli, B. Rossi, L. Pillon, and G. Bucciante, ”A new method for monitoring body fluid variation by bioimpedance analysis: The RXc graph”, *Kidney Int*, vol. 46, no. 2, pp. 534–539, Aug. 1994.

[24] A. Bosy-Westphal, S. Danielzik, R.-P. Dörhöfer, A. Piccoli, and M. J. Müller, ”Patterns of bioelectrical impedance vector distribution by body mass index and age: implications for body-composition analysis”, *The American Journal of Clinical Nutrition*, vol. 82, no. 1, pp. 60–68, Jul. 2005.

[25] P. Divall, J. Camosso-Stefinovic, and R. Baker, ”The use of personal digital assistants in clinical decision making by health care professionals: A systematic review”, *Health Informatics Journal*, vol. 19, no. 1, pp. 16–28, Mar. 2013.

[26] A. H. Ar-Rawi, M. Moghavvemi, and W. M. A. Wan-Ibrahim, ”Wide Band Frequency Fixed Current Source for BIT and BIA”, in *World Congress on Medical Physics and Biomedical Engineering, September 7 - 12, 2009, Munich, Germany*, O. Dössel and W. C. Schlegel, Eds. Springer Berlin Heidelberg, 2009, pp. 522–524.

[27] U. Pliquett and A. Barthel, ”Interfacing the AD5933 for bio-impedance measurements with front ends providing galvanostatic or potentiostatic excitation”, *Journal of Physics: Conference Series*, vol. 407, no. 1, p. 012019, Dec. 2012.

[28] A. Piccoli, L. Pillon, and F. Dumler, ”Impedance vector distribution by sex, race, body mass index, and age in the United States: standard reference intervals as bivariate Z scores”, *Nutrition*, vol. 18, no. 2, pp. 153–167, Feb. 2002.

[29] A. Piccoli, P. Piazza, D. Noventa, L. Pillon, and M. Zaccaria, ”A new method for monitoring hydration at high altitude by bioimpedance analysis”, *Medicine and Science in Sports and Exercise*, vol. 28, no. 12, pp. 1517–1522, Dec. 1996.

[30] P. A. Harris, R. Taylor, R. Thielke, J. Payne, N. Gonzalez, and J. G. Conde, ”Research electronic data capture (REDCap)—A metadata-driven methodology and workflow process for providing translational research informatics support”, *Journal of Biomedical Informatics*, vol. 42, no. 2, pp. 377–381, Apr. 2009.

[31] K. S. Cole, ”Membranes, Ions, and Impulses: A Chapter of Classical Biophysics”. *University of California Press*, 1968.

[32] A. Gartner, B. Maire, F. Delpeuch, P. Sarda, R. P. Dupuy, and D. Rieu, ”Importance of electrode position in bioelectrical impedance analysis.”, *The American Journal of Clinical Nutrition*, vol. 56, no. 6, pp. 1067–1068, Dec. 1992.

[33] B. J. B. S. Thomas, B. H. M. S. Cornish, and L. C. Ward, ”Bioelectrical Impedance Analysis For Measurement of Body Fluid Volumes: A Review”, *Journal of Clinical Engineering*, vol. 17, no. 6, Nov. 1992.

[34] A. Searle and L. Kirkup, ”A direct comparison of wet, dry and insulating bioelectric recording electrodes”, *Physiological Measurement*, vol. 21, no. 2, p. 271, May 2000.

[35] A. C. Guyton and J. E. Hall, ”Guyton and Hall Textbook of Medical Physiology”. *Elsevier Health Sciences*, 2010.

[36] P. Deurenberg, A. Tagliabue, and F. J. M. Schouten, ”Multi-frequency impedance for the prediction of extracellular water and total body water”, *British Journal of Nutrition*, vol. 73, no. 03, pp. 349–358, 1995.

[37] E. C. Hoffer, C. K. Meador, and D. C. Simpson, ”Correlation of whole-body impedance with total body water volume.”, *Journal of Applied Physiology*, vol. 27, no. 4, pp. 531–534, Oct. 1969.

[38] Analog Devices, ”AD5933 Evaluation Board User Guide”. Feb-2012.

[39] D. B. Stroud, B. H. Cornish, B. J. Thomas, and L. C. Ward, ”The use of Cole-Cole plots to compare two multi-frequencybioimpedance instruments”, *Clinical Nutrition*, vol. 14, no. 5, pp. 307–311, Oct. 1995.

[40] R. Buendía, P. Bogónez-Franco, L. Nescolarde, and F. Seoane, ”Influence of electrode mismatch on Cole parameter estimation from Total Right Side Electrical Bioimpedance Spectroscopy measurements”, *Medical Engineering & Physics*, vol. 34, no. 7, pp. 1024–1028, Sep. 2012.

[41] A. M. Prentice and S. A. Jebb, ”Beyond body mass index”, *Obesity Reviews*, vol. 2, no. 3, pp. 141–147, Aug. 2001.

[42] J. Van den Broeck and J.-M. Wit, ”Anthropometry and body composition in children”, *Hormone Research in Paediatrics*, vol. 48, no. Suppl. 1, pp. 33–42, 1997.

[43] D. Gallagher, M. Visser, D. Sepúlveda, R. N. Pierson, T. Harris, and S. B. Heymsfield, ”How Useful Is Body Mass Index for Comparison of Body Fatness across Age, Sex, and Ethnic Groups?”, *American Journal of Epidemiology*, vol. 143, no. 3, pp. 228–239, Feb. 1996.

[44] R. Buffa, B. Saragat, S. Cabras, A. C. Rinaldi, and E. Marini, ”Accuracy of Specific BIVA for the Assessment of Body Composition in the United States Population”, *PLoS ONE*, vol. 8, no. 3, p. e58533, Mar. 2013.

[45] M. S. Mialich, J. M. F. Sicchieri, and A. A. J. Junior, ”Analysis of Body Composition: A Critical Review of the Use of Bioelectrical Impedance Analysis”, *International Journal of Clinical Nutrition*, vol. 2, no. 1, pp. 1–10, 2014.

[46] P. Ritz, A. Sallé, M. Audran, and V. Rohmer, ”Comparison of different methods to assess body composition of weight loss in obese and diabetic patients”, *Diabetes Research and Clinical Practice*, vol. 77, no. 3, pp. 405–411, Sep. 2007.

[47] A. Piccoli, S. Nigrelli, A. Caberlotto, S. Bottazzo, B. Rossi, L. Pillon, and Q. Maggiore, ”Bivariate normal values of the bioelectrical impedance vector in adult and elderly populations.”, *The American Journal of Clinical Nutrition*, vol. 61, no. 2, pp. 269–270, Feb. 1995.

CHAPTER IV

A COST EFFECTIVE WIRELESS 12-LEAD ECG SYSTEM TO IMPROVE TIME TO DIAGNOSING OF ACUTE CARDIAC DISORDERS IN THE INTENSIVE CARE UNIT

Introduction

Physiological Background

The heart's electrical activity results in the generation of surface potentials across the thorax, which are recorded as Electrocardiogram (ECG or EKG). A simple model for the heart's electrical activity is a current dipole changing direction and amplitude during each heart cycle. The electrical potentials recorded between two points on the surface of the thorax are a result from the projections of said current dipole onto this axis [1]. A typical ECG trace with two electrodes placed at each shoulder is shown in Figure 23.

The ECG is commonly used to diagnose arrhythmias, abnormalities in the heart's conduction system, or ischemia, a lack of heart muscle perfusion [2].

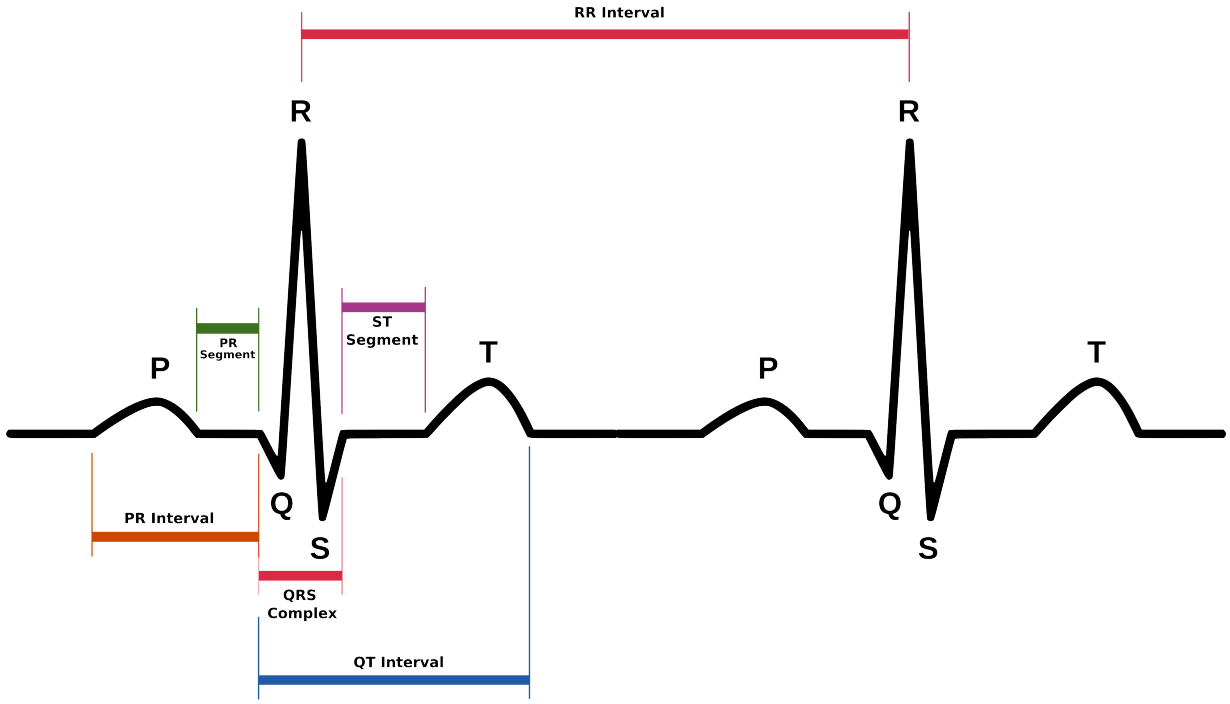

Figure 23: Representation of an ideal ECG showing important markers (P,Q,R,S,T) and intervals within an ECG waveform.

The ECG trace is classified in different segments, which result from de- and repolarization of different compartments of the heart. The P-wave represents atrial depolarization and always precedes a QRS complex (Figure 23) in healthy individuals. The QRS complex is a representation of the depolarization of the ventricles and is often used as a reference point in an ECG due to its large well defined amplitude, in comparison to the T-wave, which results from the repolarization of the ventricles [3]. The interval between two R-peaks (Figure 23) represents the time between heart beats and is used to determine heart rate (Equation 5).

$$HR_{bpm} = \frac{60}{RR_{\text{int}}} \quad ; \quad RR_{\text{int}} \text{ in seconds} \tag{5}$$

The classification of the ECG in different segments carries high diagnostic relevance. The ST-segment (Figure 23) represents ventricular repolarisation and is used to diagnose myocardial infarction, ischemia or electrolyte abnormalities etc. [4]. The PR-segment begins at the end of the P-wave and lasts until the start of the Q-wave and represents the conduction time of the atrioventricular (AV) node. This parameter allows for the detection of a disturbed pathway between the AV node and the “Bundle of His”. A prolonged PR-segment is an indicator for a 1st degree heart block or a bundle branch block [4].

In order to capture the complex electrical activity of the heart in greater detail, multiple projections of the heart vector are needed. A standard 12-lead ECG uses 10 leads and computes 12 projections of the heart vector to determine the orientation of the heart vector over time. A 12-lead ECG is used to determine for example the location of a myocardial infarction.

Figure 24 depicts the placement of 10 electrodes at well defined positions on the chest and limbs of an individual, as commonly used for standard 12-lead ECG.

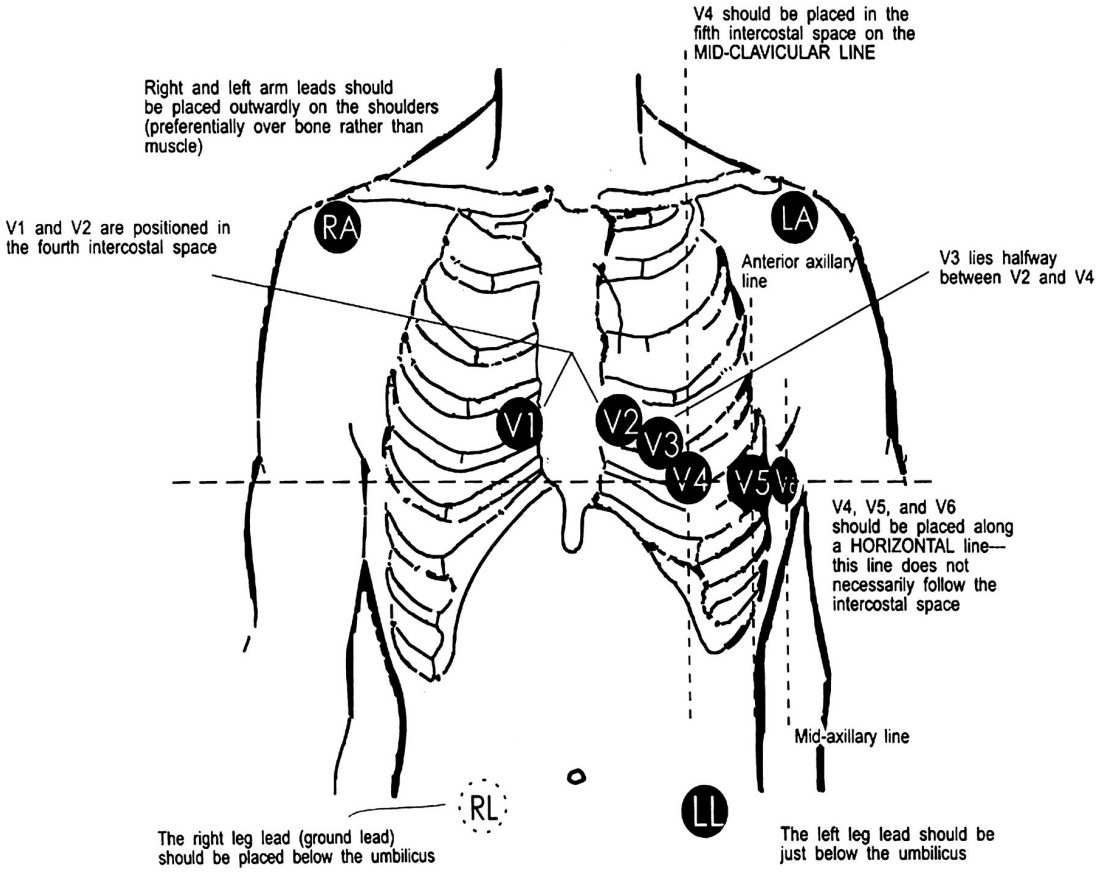

Figure 24: Standard 12-lead ECG electrode placement [27]

Clinical Relevance

Cardiovascular disease is the number one cause of morbidity and mortality in the U.S., affecting 1.5 million people per year and resulting in greater than $300 billion per year in health care costs and lost productivity [5]. The most serious and time-sensitive acute coronary event is a ST-elevation myocardial infarction (STEMI) (Figure 25-left). The primary diagnostic tool for diagnosing STEMI is the 12-lead electrocardiogram (ECG). Once the ECG diagnosis of STEMI has been confirmed, the gold standard for therapy is restoration of coronary blood flow via percutaneous coronary intervention (PCI), also called angioplasty (Figure 25-right). PCI must commence rapidly, as each 30 minutes of delay significantly increases mortality [6]. Pre-hospital ECG transmission to cardiologists at off-site or tertiary care centers allows for timely triage of patients to PCI centers and the activation of catheterization laboratories in advance. As a result, national guidelines have been set forth to decrease time to PCI, resulting in notable improvements of door-to-balloon times, reduced cardiac muscle damage, and decreased length of hospital stay [7] for outpatient-onset STEMI [8], [9].

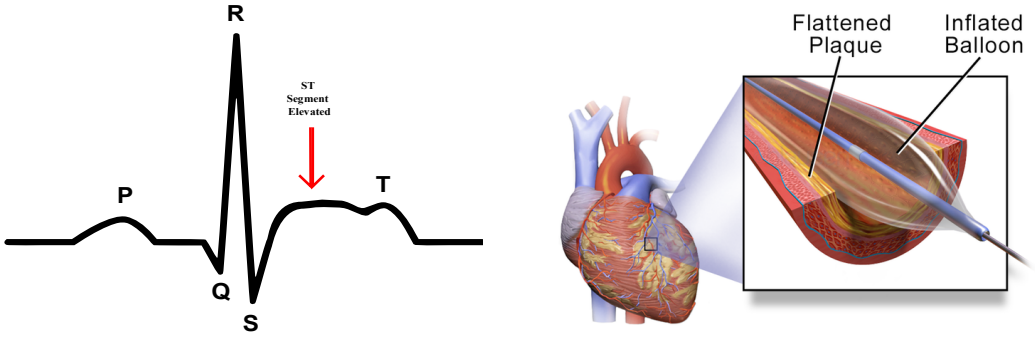

*Figure 25: Abnormal ECG with ST segment elevation (**left**); Angioplasty - Balloon inflating in artery (**right**) [28]*

However, quality improvement efforts and databases, such as the National Cardiovascular Data Registry, have largely excluded patients who are already hospitalized for non-coronary conditions (inpatient-onset STEMI) [10]. It has recently been discovered that inpatient-onset STEMI have a higher mortality than those who present as an outpatient [11]–[13]. In one study, the difference between inpatient and outpatient-onset STEMI was a striking 39.6% versus 4%, respectively

[12]. While such differences may be multifactorial, studies highlight notable differences in time from onset of MI to acquiring inpatient ECGs [12]. Further, there is a significantly prolonged ECG-to-angiograpy time compared to outpatient-onset STEMI cases [12].

Barriers to obtaining and transmitting ECG data in the outpatient setting include paper based printouts and expensive proprietary receiving stations that prohibit universal acceptance of ECG data [14], [15]. Attempts to overcome these barriers include transmission of ECG data via facsimile or cellphone images of paper-based 12-lead ECG printouts [16]. This practice leads to poor data transmission quality, violation of HIPAA standards, and lost patient data. However, there is a paucity of literature addressing these barriers within a hospital setting.

Similar obstacles exist in tertiary care centers, even ones with the most sophisticated and cloud-based systems. Once an inpatient ECG is obtained, options for transmitting data to a cardiologist include hand-delivery of a paper copy, facsimile, or text messaging a picture of the printed 12-lead ECG. Another option is a cloud-based hospital ECG reading system. However, these systems require modulation of hospital information technology infrastructure that is costly, especially for rural or underserved hospitals. Further, even cloud-based ECG reading systems require the cardiologist be alerted first via phone or pager to read the ECG. The cardiologist must then access a desktop computer, which detracts from patient care and interrupts workflow. Leading commercially available ECG systems do not offer instantaneous bidirectional communication between the referring physician and the cardiologist interpreting the ECG. The multitude of steps and inefficiencies around obtaining and interpreting ECGs may be a contributing factor in the delayed care of inpatients with acute cardiac disorders.

In this work, we describe a novel solution utilizing smart phone and tablet computer technologies for obtaining and transmitting ECG data from a wireless, miniaturized ECG device and data transmission to an internet hosted medical device data system (MDDS) in a tertiary medical center.. The MDDS provides HIPAA-compliant data storage and distribution of clinical data, as well as facilitates secure communication between health care providers. An overview of our system, including an exemplary workflow can be seen in Figure 26.

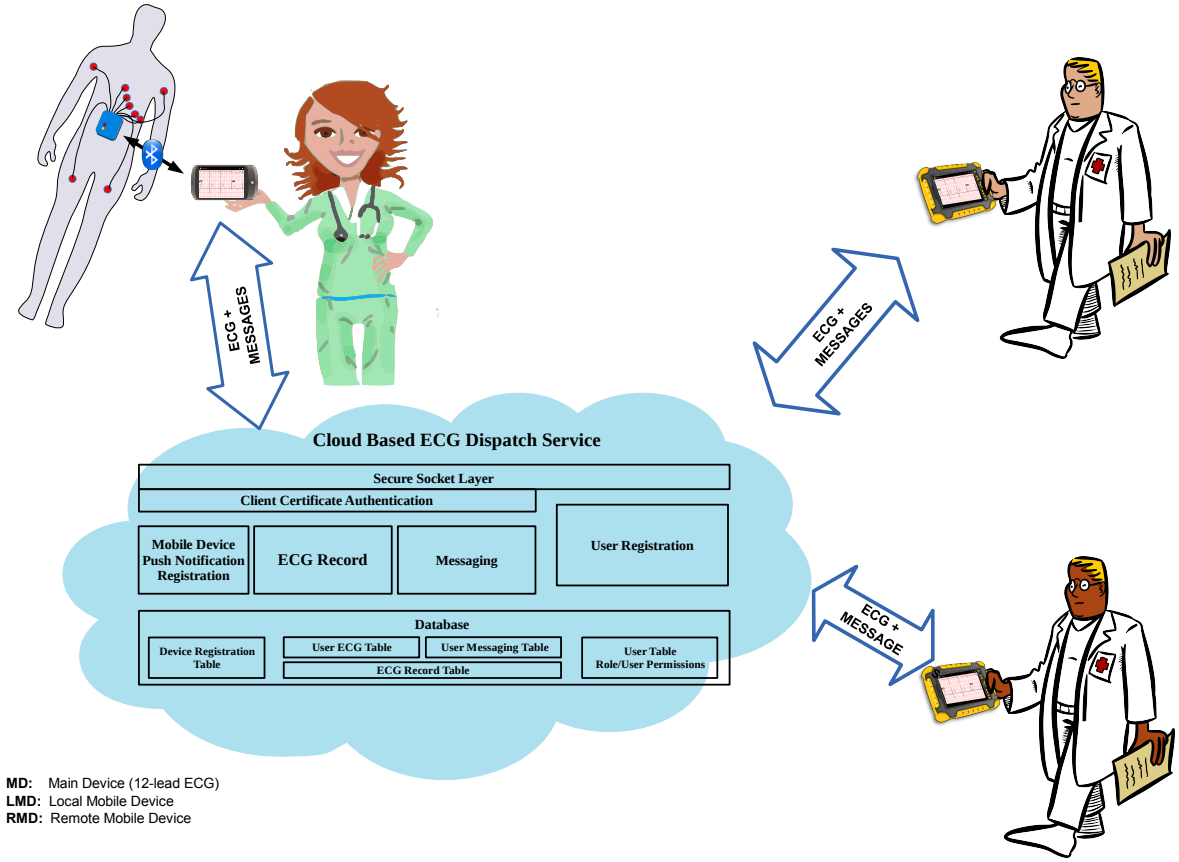

Figure 26: Concept and example application of a cloud based 12-lead ECG system. Showing an ECG technician recording a 12-lead ECG from a patient and sending the record via the ECG Dispatch Service (MDDS) to multiple physicians. Each physician is notified about the event and able to retrieve the ECG record for adjudication. The physician is able to communicate with the technician via secure messaging service, to allow for immediate response.

Wireless 12-lead ECG Monitor

Hardware

We designed a miniaturized wireless ECG monitor, that can be used for the acquisition of static 12-lead ECGs (Figure 27). During hardware development, emphasis was placed on the overall device costs (<$250), portability, small form factor, and wireless capabilities, while maintaining patient safety and competitive signal qualities.

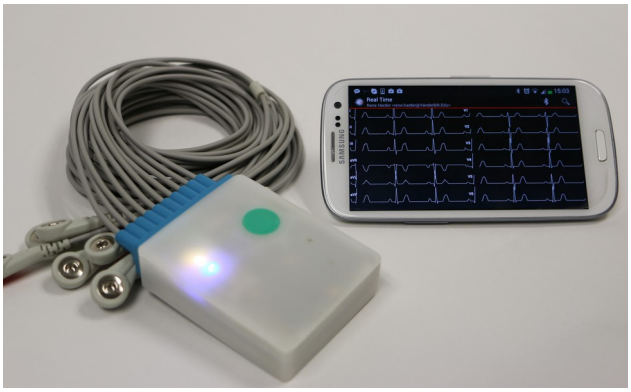

Figure 27: Wireless 12-lead ECG monitor

The wireless ECG monitor is comprised of a 32bit ARM cortex-M4F microprocessor (STM32F405, STMicroelectronics, Switzerland), a dual-mode Bluetooth radio (PAN1326, Panasonic Europe, Germany) and 8 channel analog front-end (AFE, ADS1298, Texas Instrument, USA) (Figure 28).

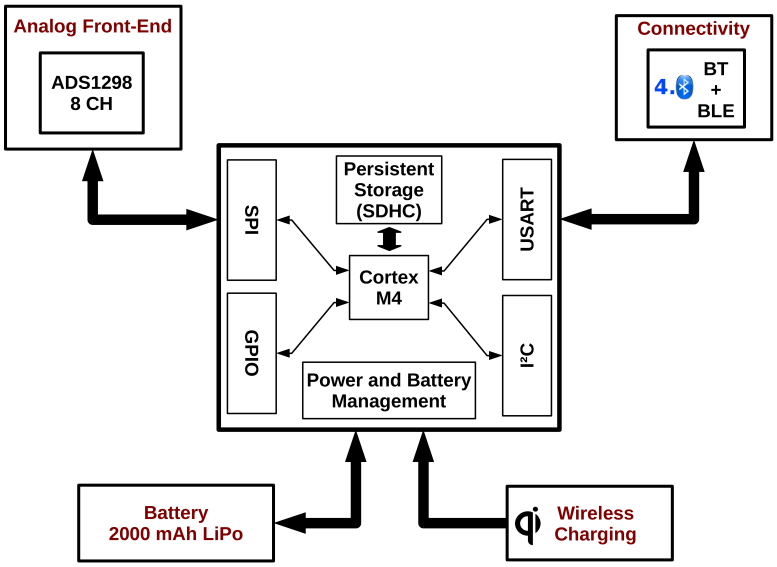

Figure 28: Simplified Block Diagram of wireless 12-lead ECG monitor

To achieve portability of the ECG monitor, allowing it to be carried in a physicians coat pocket and ready to use when needed, we chose a battery operated design. A 2000mAh rechargeable lithium polymer (LiPo) battery is incorporated to power the 12-lead ECG monitor. The battery provides the health care provider, with at least 24h of continuous use, considering the monitor's maximum current consumption of 75mA. The current consumption was determined during wireless streaming of high resolution 12-lead ECG data.

Further, to ensure patient safety, while maintaining a small form factor, we added support for wireless charging. Wireless charging removes the need for an additional means of isolating the ECG monitor from the mains and ensures that ground leakage currents, potentially flowing through the patient, stay below the required safety limits [17].

The ADS1298 is an AFE, specifically designed by Texas Instruments for biopotential measurements. The AFE offers 8 simultaneous sampling 24bit delta-sigma analog-to-digital converters (ADC), reference electrode driver, programmable gain amplifiers (PGA), internal bandgap voltage reference, and serial programming interface (SPI) for configuration and data transfer to the microcontroller unit (MCU). The digitized signal data rate (fd) can be set between 250 samples per second (SPS) and 8kSPS at full, and up to 32kSPS at reduced resolution (17bit) with a bandwidth (-3dB cutoff) of 0.265*fd. National standards applicable to diagnostic ECG machines require a minimum sampling rate of 500SPS [18]. Further, to meet said frequency response and input offset voltage requirements, the AFE was configured to sample at 1kSPS and the pre-amplifier gain was set to 6x for all ECG measurements.

To improve common mode noise susceptibility of the ECG, a portion of the common mode signal, observed at the pre-amplifier output, is inverted and injected back into the patient via the right leg electrode. As per common ECG practices, the precordial leads (V1 to V6) are referenced to the Wilson's central terminal (WCT) [19], [20]. Hence, the right leg drive (RLD) is configured to superimpose an average of right-arm (RA), left-arm (LA) and left-leg (LL) electrodes onto the

patient. To maintain patient safety, current limiting resistances were added to the output of the RLD that limit the maximum current injected into the patient under normal operating conditions to less than 50µA.

Input Transient Voltage Protection

During normal operation, a 12-lead ECG monitor will rarely see input voltages larger than a few 100 millivolts. However, in clinical settings, ECG machines may be exposed to defibrillator discharges in an attempt to restore a normal cardiac rhythm.

A defibrillator generates pulses with several 10th of milliseconds duration and voltages of up tp 5kV [21], [22]. These high energy transients are injected through the lead wires into the ECG monitor. Special care must be taken in order to prevent damage to the input AFE during such an event. Input protection is achieved by adding voltage clamping or isolating devices, such as gas-discharge tubes, Zener diodes or opto-isolators, into the signal path that restrict the voltage observed at the analog input to save limits. Furthermore, the ECG device must ensure that the majority of the energy delivered by the defibrillator is injected into the body and not dissipated within the ECG monitor. Consequently, a current limiting device must be added to the protection circuit, such that at a maximum 10% of the energy is shunted within the ECG machine [23].

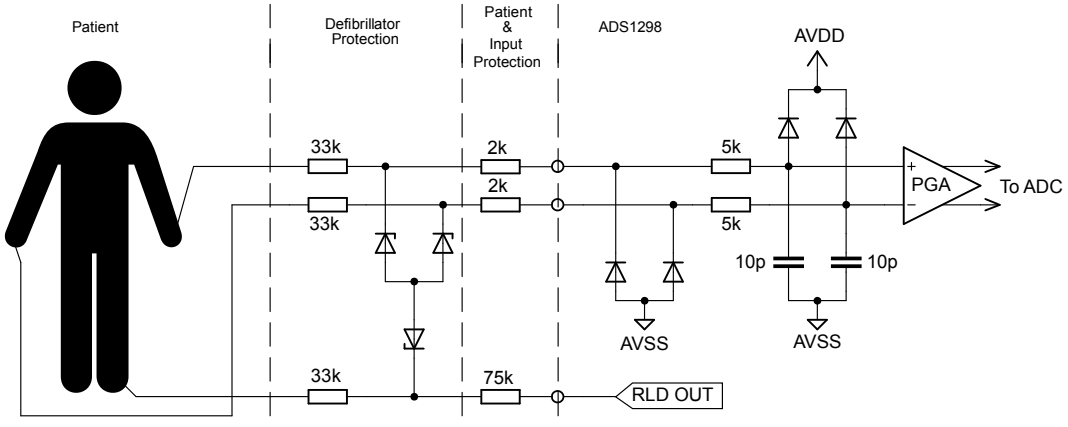

Figure 29: Simplified schematic of analog input protection circuit for 12-lead wireless ECG monitor.

The analog input protection circuit of our miniature wireless 12-lead ECG monitor is illustrated in Figure 29. To shunt the defibrillator energy within the device, we have chosen transient voltage suppressors (TVS) (PTVS14VS1UR, NXP Semiconductor, Netherlands). These TVS offer small leakage (≤100nA) and high pulse power rating (400W, 10/1000 µs pulse) in a much smaller form factor than the more commonly found gas-discharge tubes. To restrict the amount of current injected into the leads, we added 33kΩ high power thick film SMD resistors (CRCW251233K, Vishay Intertechnology, USA) in series with the voltage clamping diodes. The protection circuit limits the energy dissipated within the ECG monitor to a maximum of 1.1J or 0.2% of a 400J defibrillator discharge.

Common Mode Rejection

Due to physical limitations, the output of any equipment that measures differential voltages is generally affected by a signal common to each input. This common mode signal offsets the voltage observed at the input of the differential amplifier by shifting the operational point of the inputs toward the rails and reduces the maximum differential signal that can be amplified without any distortion. Further, because of impedance imbalances in the electrode-skin interface, input circuitry, and amplifier, the common mode signal can be translated into a differential signal, with its amplitude depending on the different gains seen from each input to the output. The ability of a system to reject the unwanted common mode signal is referred to a common mode rejection (CMR) or expressed as common mode rejection ration (CMRR), if referenced to the differential input signal.

ECGs are often taken in uncontrolled environments and are immersed in electromagnetic interferences typically generated by power lines, resulting in noise with their fundamental frequencies and harmonics. On that account, federal and international standards require that diagnostic ECGs maintain a CMRR of ≥89dB and an input offset range of ±350mV under normal operation [18], [23].

To evaluate the CMR of our AFE we applied a $10V_{rms}$ sine wave (60Hz) with source capacitance of 200pF to all electrode terminals shorted together. In order to reflect the variable resistance of the electrode-skin interface, an imbalance of

51kΩ || 47nF was added in series to one electrode terminal [24]. Figure 30 shows the captured waveform with the electrode imbalance placed into the RA electrode. As expected the largest observed common mode noise is seen in lead-I (LA-RA) and lead-II (LL-RA). The observed worst-case CMRR of our wireless 12-lead ECG monitor was determined to be ≥98dB.

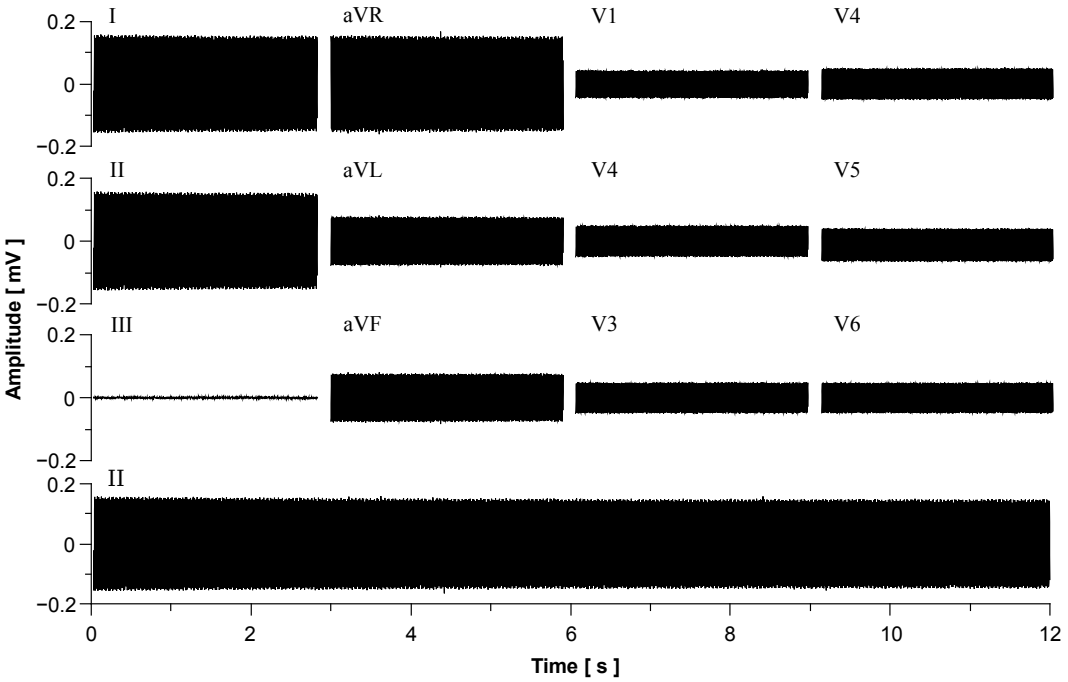

Figure 30: Recording of common mode signal with electrode imbalance in RA electrode. Sinusoidal common mode signal applied to all leads with amplitude and frequency of 10V_{rms} and 60Hz, respectively.

Input Referred Noise

The amount of noise observed in any ECG trace can be detrimental in forming an accurate diagnosis. Hence, for diagnostic ECGs, the International Electrotechnical Commission (IEC) specifies that the maximum noise during a 10 second recording must be less than $30\mu V_{pp}$, as defined in the essential performance requirements of IEC60601-2-25 [23]. The input noise of the ADS1298 at 500SPS and 1kSPS with a gain setting of 6x is specified to be less than $3.5\mu V_{pp}$, and $5.0\mu V_{pp}$ respectively. However, the thermal noise observed in the ECG recording is mostly caused by resistances (e.g. electrode-skin interface impedance) and amplifiers [25], [26]. Consequently, to quantify the observed noise one must consider the entire input circuitry, composed of AFE, anti alias filters, defibrillator protection circuit, and electrode skin contact.

To evaluate the peak input noise of the analog input circuitry all electrodes were shorted together. The electrode skin interface is simulated according to IEC specification [23] using a resistor and capacitor parallel combination (51kΩ || 47nF). The ECG was recorded for 10 seconds with a data rate of 1kSPS and saved to internal storage without any signal processing. Figure 31 shows the noise acquired using this setup. The maximum noise observed over the whole recording bandwidth (0-265Hz) is $8.5\mu V_{pp}$ (standard deviation: 4.2μV), which is much less than the allowed limit of $30\mu V_{pp}$.

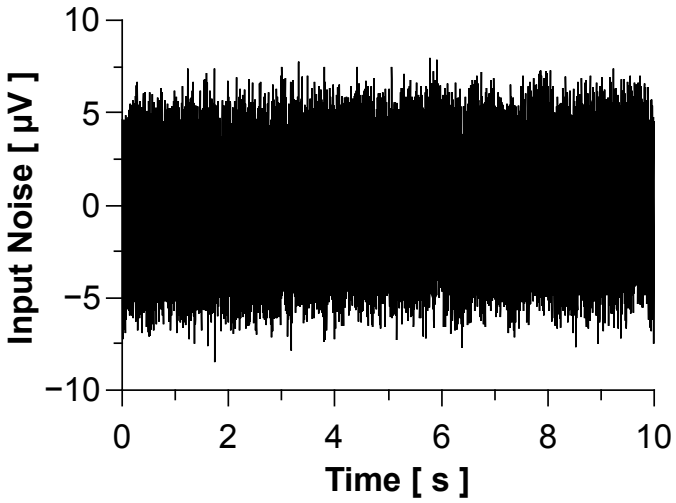

Figure 31: Input referred noise on ECG lead-II over 10s, recorded at 1kSPS and gain of 6x.

Software Architecture

To utilize the wireless 12-lead ECG monitor we developed a software application that can be deployed on mobile devices running the Android operating system (Google & Headset Alliance, Android version 4.0 and up). The Android application (app) provides the health care provider with a means to manage the connection status as well as controlling the ECG monitor in order to capture and transmit high resolution (47nV/LSB, 1kSPS) ECG records. The application integrates into a central server based MDDS that provides user account management, notifications, messaging and routing of ECG information.

The MDDS's account management is integrated into a central institutional authentication system, using the lightweight directory access protocol (LDAP), and allows users registered within our institution the immediate use of the ECG monitor and gives access to private health information (PHI) content in the system. The MDDS is designed in a modular fashion that allows for the integration of other single-sign on solutions via a plugin framework. Within the entire system all data including patient identifiers, messages and ECG records are signed by the sender/creator and protected using 2048bit asymmetric cryptography in transport and at rest.

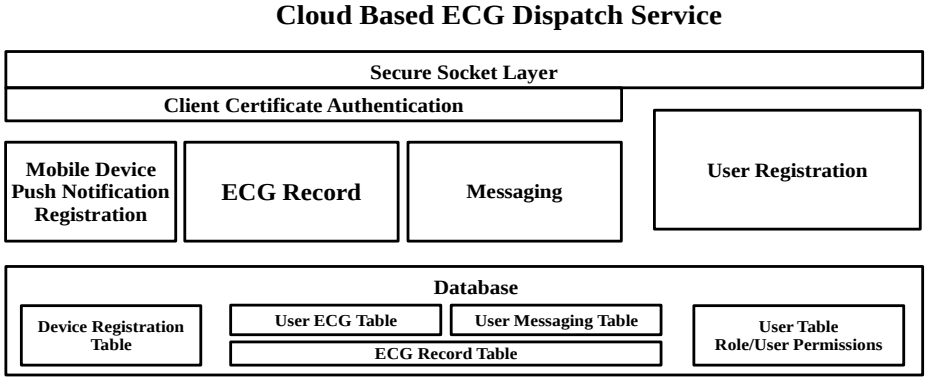

Figure 32: Functional components of Vanderbilt ECG Dispatch Service

A block diagram describing the functional components of the MDDS can be seen in Figure 32. For a more in depth description of the Vanderbilt ECG Dispatch System or MDDS and its application programming interface (API) please refer to Appendix C.

The workspace of the application is partitioned on a per user basis, such that multiple users only have access to their personal content, like ECG and messages. All content is encrypted on the mobile device and only accessible by an authenticated user.

Prior to the first use of the application the user must setup a local account by entering his institutional username and password which are validated with the MDDS. For successive use, the user can access content by simply entering a predefined 4-6 digit pin code. To enhance security, a symmetric encryption key is generated by applying a key stretching algorithm to the pin code, such as the Password-Based Key Derivation Function 2 (PKDBF2). Once the encryption key is derived, it unlocks and decrypts the user specific content and allows the operator to view previously captured and transmitted ECGs. Public-key cryptography is used to provide secure communication between clinicians and/or technicians. Further, once an account has been setup within the application, the mobile device has been registered for push notification, for example the MDDS is able to notify the user of the mobile device about new or updated events.

In order to reduce in-hospital response times, we improved upon the current procedures in tertiary hospitals, as depicted in Figure 33. The revised workflow is presented in the following section.

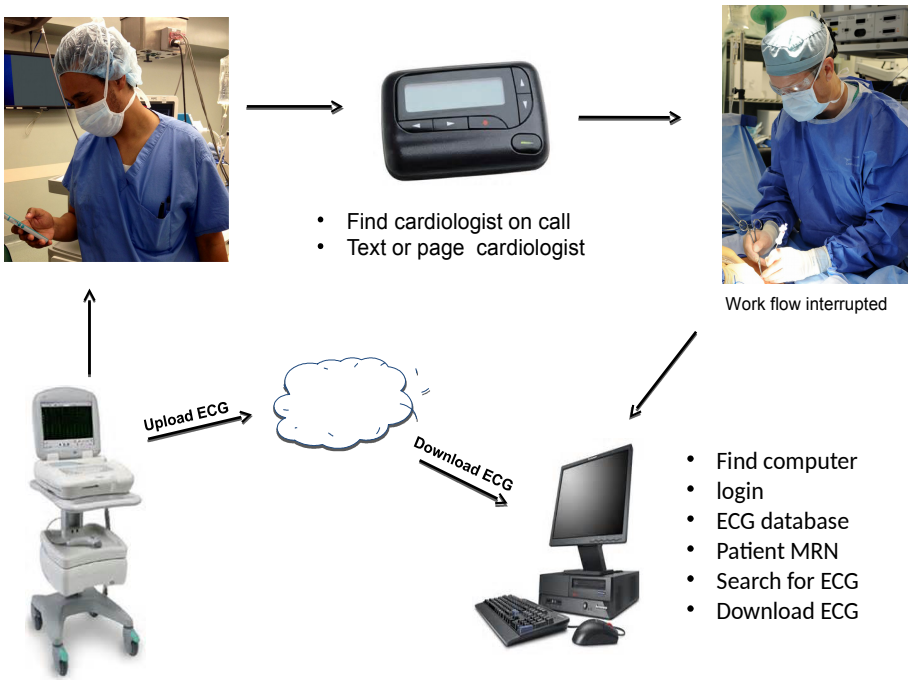

Figure 33: Example 12-lead ECG workflow in tertiary care center. Visualizing the steps required from acquisition to diagnosis of ECG.

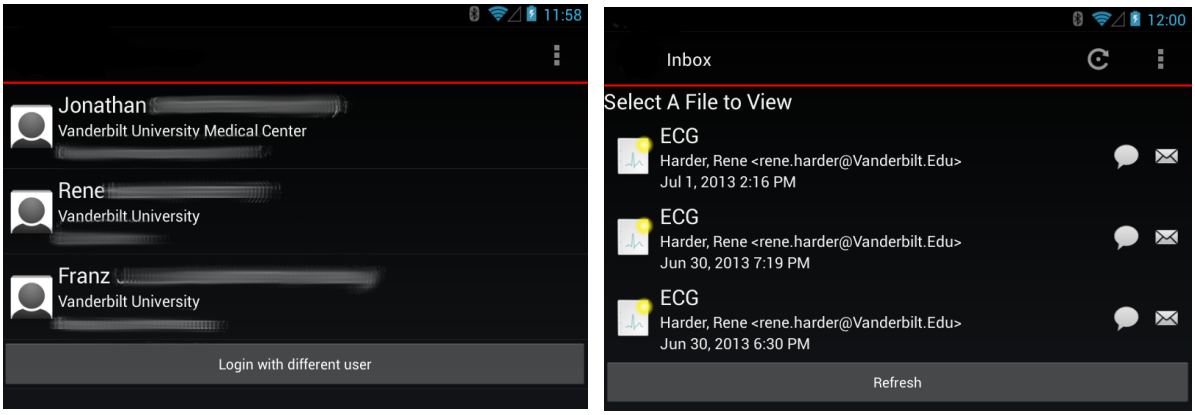

*Figure 34: User selector/login screen (**left**) and inbox, listing all received ECGs (**right**)*

Proposed Workflow for Wireless ECG

The proposed workflow allows technicians to transmit the ECG data through a cloud-based service directly to a cardiologist eliminating any intermittent steps. First, the technician logs into the application (Figure 34-left), then the mobile device automatically establishes a Bluetooth connection to an available preset wireless 12-lead ECG monitor. When connected, the ECG starts streaming a preview of the 12-lead ECG, such that the technician is able to verify proper lead placement, electrode-skin contact and quality of signal (Figure 35). If satisfied with the ECG signal, the technician is able to initiate capture of a static 12-lead ECG recording, that will be displayed onscreen about 15 seconds later. The technician is then able to either discard, or transmit the ECG record to a remote physician for review. Once transmitted, the receiving physician is notified and able to open the ECG either via their inbox (Figure 34-right) or directly through the notification message. An example of a received ECG record can be seen in Figure 36. Furthermore, the cardiologist is able to communicate securely with the practitioner caring for the patient (Figure 37).

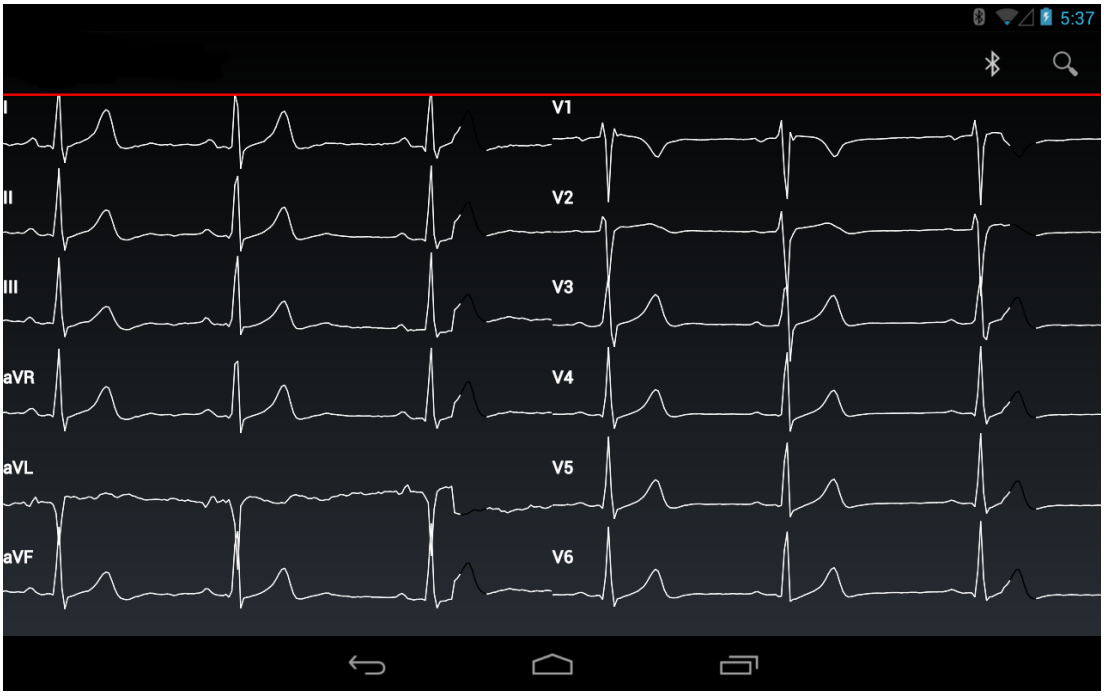

Figure 35: Real-time streaming of low resolution (125 SPS) 12-lead ECG waveform before, during, and after capture of high resolution ECG

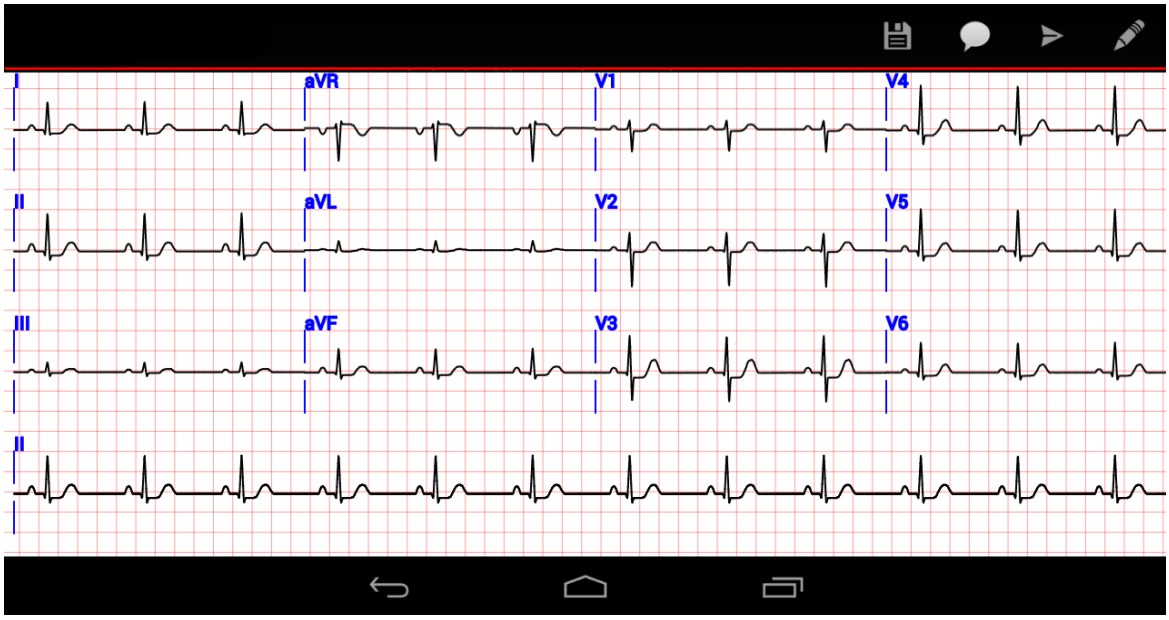

Figure 36: High resolution static 12-lead ECG record, as seen by the receiving physician. The user is able to zoom and drag the ECG across a static grid (10mm/mV) using finger gestures to enhance smaller features and enable the extraction of accurate time information.

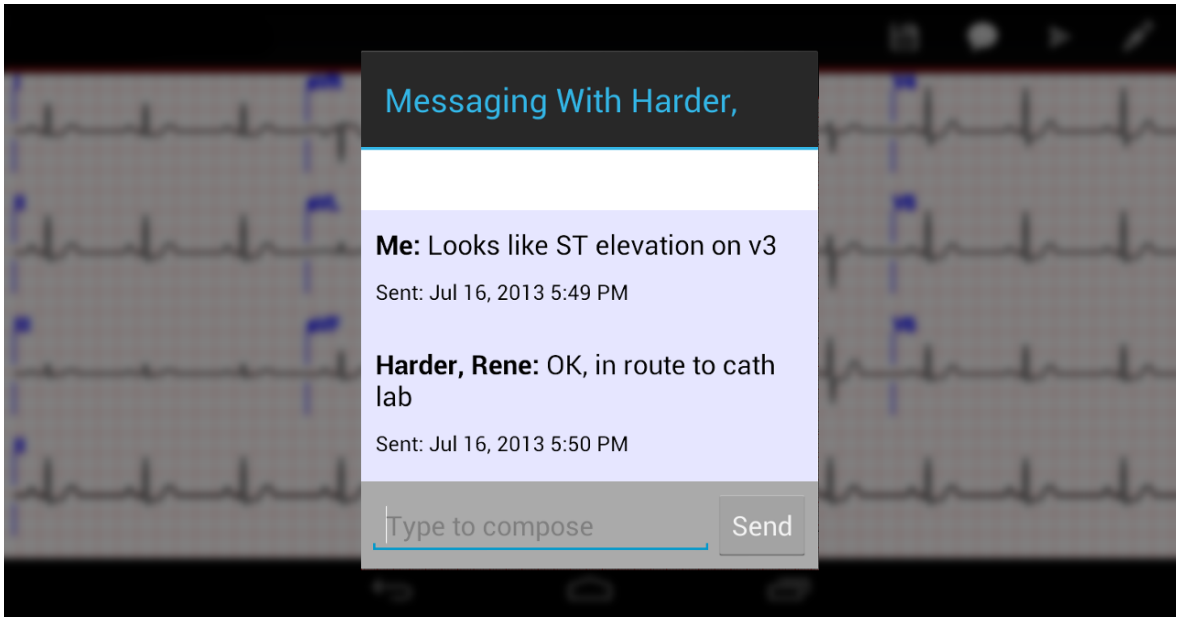

Figure 37: In app secure messaging between cardiologist and practitioner treating the patient.

Experiments and Results

We performed a pilot study on inpatients with acute cardiac disorders and compared the results to standard practice within a tertiary, high-volume cardiac hospital.

Study Design

The clinical study was approved by Vanderbilt University's Institutional Review Board. We enrolled adult patients at Vanderbilt University Medical Center's Cardiovascular Intensive Care Unit (CVICU) who required a routine or urgent 12-lead ECG. Either the CVICU staff physician and/or that patient's cardiovascular surgeon determined the clinical need for an urgent 12-lead ECG. Once the decision was made, both the standard ECG and the wireless ECG were performed. Per standard practice, the 12-lead ECG machines arrived and were performed via an ECG technologist. Once the 12-lead ECG was ordered by the CVICU team, the staff physician, who would carry the wireless 12-lead ECG monitor in his coat pocket, would place the wireless 12-lead ECG on the patient and obtain the digital ECG.

The primary outcomes measured were the times and number of steps from the ECG order being placed to it being digitally available for clinical interpretation. We recorded time from physician order to completion of the standard 12-lead ECG via technologist, as well as the wireless 12-lead ECG monitor. Standard ECGs were sent to Vanderbilt's cloud-based server for cardiologist interpretation, performed on a desktop computer. The wireless 12-lead ECGs were transmitted via the Internet to the cardiologist's electronic tablet. Successful transmission rates and time to successful acceptance on cardiologists' electronic tablets were also recorded. Lastly, the steps involved from the order being placed to the ECG being available to the cardiologist were also obtained for each ECG.

Results

We enrolled 5 patients in the CVICU, all requiring a routine or urgent 12-lead ECG to exclude acute myocardial infarction. Wireless 12-lead ECGs were obtained and transmitted with a 100% success rate. Time from ECG ordering to wireless ECG acquisition was negligible as the system was immediately available to the staff physician ordering the test. The receiving cardiologist received alerts on their smart phone for all 5 ECGs within 1s of ECG transmission, with one step required for visualizing the ECG.

Table 4: Time to acquisition of standard and wireless 12-lead ECG.

Patient	**Diagnosis**	**Time to obtain 12-lead ECG**		
		Expected	**Standard ECG**	**Wireless ECG**
1	Left bundle branch block, 1st degree AV block	45min*	40min	<5min
2	Anterolateral ischemia, NSTEMI	10min**	31min	<5min
3	Left ventricular hypertrophy, prolonged QT interval	45min*	47min	<5min
4	Anterior infarct, old	45min*	11min	<5min
5	Right bundle branch block, inferior infarct, old	45min*	72min	<5min

Expected: the time expected as per standard hospital guidelines. Routine, ** Urgent*

Standard 12-lead ECGs obtained via ECG technicians took an average of 40.2 minutes. Receiving cardiologists were alerted by pager system and required an additional 8 steps to visualize the ECG for interpretation (Figure 33).

Discussion & Conclusion

We have demonstrated the accuracy, feasibility and advantages of our wireless 12-lead ECG monitor in a tertiary hospital setting. While such studies have been performed in the pre-hospital setting for several years, there remains a void of literature describing ECG metrics within hospital systems [14], [15]. However, recent attention to increased cardiac mortality in hospitalized patients due to prolonged time to diagnosis of acute cardiac disorders highlights the significance of inpatient workflow [11]. The striking discoveries surrounding inpatient mortality is a motivating factor to establish new metrics for in-hospital workflow of patients with acute cardiac disorders.

Although the increased mortality associated with inpatient STEMI is multifactorial, the time delay in obtaining the diagnostic 12-lead ECG subsequently extends the overall time to treatment. The findings of our small pilot study, corroborate those at other institutions, particularly with regard to the delayed times in acquiring standard 12-lead ECGs [11], [12].

Several factors may contribute to this delay. For example, inpatient ECG acquisition is limited by the number of devices and availability of technicians, who are often responding to multiple urgent situations at the same time. Our wireless ECG provides a cost-effective option for placement of devices in several areas of the hospital, particularly in critical care and perioperative settings. Also, compared to standard 12-lead ECGs, the small form factor of the wireless 12-lead ECG monitor makes it easy to obtain in patient rooms, often occupied by other equipment and personnel.

Another potential factor for delayed inpatient cardiac diagnoses is transmission of ECG data to the cardiologist once the 12-lead ECG is obtained, an often cumbersome process in a large tertiary care center (Figure 33). Currently, paper copies of printed ECGs are hand-delivered to the cardiologist.

There remains a critical unmet need for a cost-effective ECG platform that obtains and transmits data in a HIPAA-compliant manner across cellular and wireless networks within a tertiary hospital setting. Even with state-of-the-art ECG

technology, our study demonstrated an 8-step process with workflow disruption during the process of transmitting and receiving ECG data. The multitude of steps and inefficiencies around obtaining and interpreting ECGs may be a contributing factor in the delayed care of inpatients with acute cardiac disorders.

We have shown a proof-of-concept model for wireless ECG monitoring in hospitalized patients with acute cardiac disorders without the need for costly hospital infrastructure modifications. This is particularly important for rural or underserved hospitals.

While pre-hospital use of the wireless 12-lead ECG system is self-evident, there are also several advantages for the use of this technology within large tertiary care centers. A locally available, wireless 12-lead ECG monitor is an economical viable solution that may reduce the time to diagnosis of acute cardiac disorders in the hospital setting.

For further verification a larger, prospective and multicenter trial to compare outcomes with the wireless versus standard 12-lead ECG in the inpatient arena is needed.

In summary, our wireless 12-lead ECG monitor is a cost effective, safe and easy to use solution that allows for fast communication between on site staff and off site cardiologist, resulting in immediate diagnosis and potentially improve patient outcome.

References

[1] J. Malmivuo and R. Plonsey, ”The Basis of ECG Diagnosis”, in *Bioelectromagnetism: Principles and Applications of Bioelectric and Biomagnetic Fields*, Oxford University Press, 1995, p. 512.

[2] L. S. Lilly, ”Braunwald’s Heart Disease: A Textbook of Cardiovascular Medicine”. *Elsevier Health Sciences*, 2012.

[3] J. Malmivuo and R. Plonsey, ”The Heart”, in *Bioelectromagnetism: Principles and Applications of Bioelectric and Biomagnetic Fields*, Oxford University Press, 1995, p. 512.

[4] E. A. Ashley and J. Niebauer, ”Conquering the ECG”. *Remedica*, 2004.

[5] A. S. Go, D. Mozaffarian, V. L. Roger, E. J. Benjamin, J. D. Berry, W. B. Borden, D. M. Bravata, S. Dai, E. S. Ford, C. S. Fox, S. Franco, H. J. Fullerton, C. Gillespie, S. M. Hailpern, J. A. Heit, V. J. Howard, M. D. Huffman, B. M. Kissela, S. J. Kittner, D. T. Lackland, J. H. Lichtman, L. D. Lisabeth, D. Magid, G. M. Marcus, A. Marelli, D. B. Matchar, D. K. McGuire, E. R. Mohler, C. S. Moy, M. E. Mussolino, G. Nichol, N. P. Paynter, P. J. Schreiner, P. D. Sorlie, J. Stein, T. N. Turan, S. S. Virani, N. D. Wong, D. Woo, and M. B. Turner, ”Heart Disease and Stroke Statistics—2013 Update A Report From the American Heart Association”, *Circulation*, vol. 127, no. 1, pp. e6–e245, Jan. 2013.

[6] B. K. Nallamothu and E. R. Bates, ”Percutaneous coronary intervention versus fibrinolytic therapy in acute myocardial infarction: is timing (almost) everything?”, *The American Journal of Cardiology*, vol. 92, no. 7, pp. 824–826, Oct. 2003.

[7] M. Sanchez-Ross, G. Oghlakian, J. Maher, B. Patel, V. Mazza, D. Hom, V. Dhruva, D. Langley, J. Palmaro, S. Ahmed, E. Kaluski, and M. Klapholz, ”The STAT-MI (ST-Segment Analysis Using Wireless Technology in Acute Myocardial Infarction) Trial Improves Outcomes”, *JACC: Cardiovascular Interventions*, vol. 4, no. 2, pp. 222–227, Feb. 2011.

[8] E. M. Antman, D. T. Anbe, P. W. Armstrong, E. R. Bates, L. A. Green, M. Hand, J. S. Hochman, H. M. Krumholz, F. G. Kushner, G. A. Lamas, C. J. Mullany, J. P. Ornato, D. L. Pearle, M. A. Sloan, J., Sidney C. Smith, J. S. Alpert, J. L. Anderson, D. P. Faxon, V. Fuster, R. J. Gibbons, G. Gregoratos, J. L. Halperin, L. F. Hiratzka, S. A. Hunt, and A. K. Jacobs, ”ACC/AHA Guidelines for the Management of Patients With ST-Elevation Myocardial Infarction—Executive SummaryA Report of the American College of Cardiology/American Heart Association Task Force on Practice Guidelines (Writing Committee to Revise the 1999 Guidelines for the Management of Patients With Acute Myocardial Infarction)”, *Journal of the American College of Cardiology*, vol. 44, no. 3, pp. 671–719, Aug. 2004.

[9] E. M. Antman, M. Hand, P. W. Armstrong, E. R. Bates, L. A. Green, L. K. Halasyamani, J. S. Hochman, H. M. Krumholz, G. A. Lamas, C. J. Mullany, D. L. Pearle, M. A. Sloan, and J., Sidney C. Smith, ”2007 Focused Update of the ACC/AHA 2004 Guidelines for the Management of Patients With ST-Elevation Myocardial Infarction”, *Journal of the American College of Cardiology*, vol. 51, no. 2, pp. 210–247, Jan. 2008.

[10] E. D. Peterson, M. T. Roe, J. S. Rumsfeld, R. E. Shaw, R. G. Brindis, G. C. Fonarow, and C. P. Cannon, ”A Call to ACTION (Acute Coronary Treatment and Intervention Outcomes Network) A National Effort to Promote Timely Clinical Feedback and Support Continuous Quality Improvement for Acute Myocardial Infarction”, *Circulation: Cardiovascular Quality and Outcomes*, vol. 2, no. 5, pp. 491–499, Sep. 2009.

[11] P. Kaul, J. J. Federspiel, X. Dai, S. C. Stearns, S. C. Smith Jr., M. Yeung, H. Beyhaghi, L. Zhou, and G. A. Stouffer, ”Association of inpatient vs outpatient onset of st-elevation myocardial infarction with treatment and clinical outcomes”, *JAMA*, vol. 312, no. 19, pp. 1999–2007, Nov. 2014.

[12] X. Dai, J. Bumgarner, A. Spangler, D. Meredith, S. C. Smith, and G. A. Stouffer, ”Acute ST-Elevation Myocardial Infarction in Patients Hospitalized for Noncardiac Conditions”, *Journal of the American Heart Association*, vol. 2, no. 2, p. e000004, Apr. 2013.

[13] C. Maynard, E. Lowy, R. J, J. Rumsfeld, A. E. Sales, H. Sun, B. Kopjar, B. Fleming, R. L. Jesse, R. Rusch, and S. D. Fihn, ”The prevalence and outcomes of in-hospital acute myocardial infarction in the department of veterans affairs health system”, *Archives of Internal Medicine*, vol. 166, no. 13, pp. 1410–1416, Jul. 2006.

[14] H. H. Ting, H. M. Krumholz, E. H. Bradley, D. C. Cone, J. P. Curtis, B. J. Drew, J. M. Field, W. J. French, W. B. Gibler, D. C. Goff, A. K. Jacobs, B. K. Nallamothu, R. E. O’Connor, and J. D. Schuur, ”Implementation and Integration of Prehospital ECGs Into Systems of Care for Acute Coronary Syndrome A Scientific Statement From the American Heart Association Interdisciplinary Council on Quality of Care and Outcomes Research, Emergency Cardiovascular Care Committee, Council on Cardiovascular Nursing, and Council on Clinical Cardiology”, *Circulation*, vol. 118, no. 10, pp. 1066–1079, Sep. 2008.

[15] B. A. Afolabi, G. M. Novaro, S. L. Pinski, K. R. Fromkin, and H. S. Bush, ”Use of the prehospital ECG improves door-to-balloon times in ST segment elevation myocardial infarction irrespective of time of day or day of week”, *Emergency Medicine Journal*, vol. 24, no. 8, pp. 588–591, Aug. 2007.

[16] J.-C. Hsieh, B.-X. Lin, F.-R. Wu, P.-C. Chang, Y.-W. Tsuei, and C.-C. Yang, ”Ambulance 12-Lead Electrocardiography Transmission via Cell Phone Technology to Cardiologists”, *Telemedicine and e-Health*, vol. 16, no. 8, pp. 910–915, Oct. 2010.

[17] ”IEC standard for Medical electrical equipment - Part 1: General requirements for basic safety and essential performance”. *IEC 60601-1:2005*.

[18] ”AAMI standard for Medical electrical equipment - Part 2-25: Particular requirements for the basic safety and essential performance of electrocardiographs”. *ANSI/AAMI/IEC 60601-2-25:2011*.

[19] F. N. Wilson, F. D. Johnston, A. G. Macleod, and P. S. Barker, ”Electrocardiograms that represent the potential variations of a single electrode”, *American Heart Journal*, vol. 9, no. 4, pp. 447–458, Apr. 1934.

[20] L. Bacharova, R. H. Selvester, H. Engblom, and G. S. Wagner, ”Where is the central terminal located?: In search of understanding the use of the Wilson central terminal for production of 9 of the standard 12 electrocardiogram leads”, *Journal of Electrocardiology*, vol. 38, no. 2, pp. 119–127, Apr. 2005.

[21] A. Y. K. Chan, ”Biomedical Device Technology: Principles and Design”. *Charles C Thomas Publisher*, 2008.

[22] D. D. Dobrev, T. Neycheva, and N. Mudrov, ”Simple two-electrode biosignal amplifier”, *Medical and Biological Engineering and Computing*, vol. 43, no. 6, pp. 725–730, Nov. 2005.

[23] ”IEC standard for Medical electrical equipment - Part 2-25: Particular requirements for the basic safety and essential performance of electrocardiographs”. *IEC 60601-2-25:2011*.

[24] E. Huigen, D. A. Peper, and C. A. Grimbergen, ”Investigation into the origin of the noise of surface electrodes”, *Medical and Biological Engineering and Computing*, vol. 40, no. 3, pp. 332–338, May 2002.

[25] C. Gondran, E. Siebert, S. Yacoub, and E. Novakov, ”Noise of surface bio-potential electrodes based on NASICON ceramic and Ag−AgCl”, *Medical and Biological Engineering and Computing*, vol. 34, no. 6, pp. 460–466, Nov. 1996.

[26] J. H. Nagel, ”Biopotential Amplifiers”, in *The Biomedical Engineering Handbook*, 2000.

[27] R. Freeman, W. Wieling, F. B. Axelrod, D. G. Benditt, E. Benarroch, I. Biaggioni, W. P. Cheshire, T. Chelimsky, P. Cortelli, C. H. Gibbons, D. S. Goldstein, R. Hainsworth, M. J. Hilz, G. Jacob, H. Kaufmann, J. Jordan, L. A. Lipsitz, B. D. Levine, P. A. Low, C. Mathias, S. R. Raj, D. Robertson, P. Sandroni, I. J. Schatz, R. Schondorf, J. M. Stewart, and J. G. van Dijk, ”Consensus statement on the definition of orthostatic hypotension, neurally mediated syncope and the postural tachycardia syndrome”, *Autonomic Neuroscience*, vol. 161, no. 1–2, pp. 46–48, Apr. 2011.

[28] Blausen Medical Communications, Inc., ”Angioplasty Balloon Inflated, (CC BY 3.0 License)”.

CHAPTER V

AMBULATORY AUTONOMIC HEALTH MONITOR

Introduction

Maintaining blood flow in order to ensure the supply of oxygen and nutrition to the organs is the main function of the cardiovascular system. Cardiovascular monitoring is commonly employed to evaluate electrical function and structural components. Such monitoring is multimodal and includes ultrasound, electrocardiogram (ECG), invasive catheter placement, and advanced imaging techniques, like magnetic resonance imaging (MRI) [1], [2]. All of these methods are readily available in the hospital setting. However, high hospital costs and reduced reimbursements for hospital readmissions for cardiovascular disorders have resulted in increased need for outpatient monitoring.

The challenge, monitoring electrical and functional components of the cardiovascular system, is the need for multiple sensors.

The use of ECG Holter systems is common practice to monitor electrical activity of the heart in a clinical and home environment. While these Holter devices can detect arrhythmias and ischemic episodes, there is no real-time signal processing or immediate availability to the practitioner for diagnosis. Mobile devices such as AliveCor (AliveCor Inc., San Francisco, USA) depend on the patient holding the device, often during symptomatic episodes. Events will be missed if the patient is asleep, asymptomatic, or during loss of consciousness.

Blood pressure, which is the pressure resulting from the force of circulating blood against the vessels, is another important parameter characterizing the cardiovascular system and is used to assess short and long term cardiovascular risk. Blood pressure can be measured in real-time by placing a catheter based pressure transducer directly into an artery, an invasive method that can only be done in a hospital setting. A more commonly used practice is the measurement of blood pressure by placing an inflatable cuff on the extremities of the patient. However, cuff measurements do not allow for continuous monitoring of blood pressure.

Further, blood pressure is the product of cardiac output and peripheral resistance (Figure 38), which is determined by the cross section of the vasculature. Blood pressure is regulated through the baroreflex of the autonomic nervous system. Baroreceptors are located in the aortic arch and the carotid sinuses and monitor changes in blood pressure. Baroreceptors are stretch receptors providing a fast negative feedback loop, and either increase or decrease the blood pressure by decreasing or increasing the heart rate, respectively via the autonomic nervous system. Sympathetic innervation of the vessels causes vasoconstriction, which increases peripheral resistance. Vasoconstriction increases venous return (preload) and afterload of the heart, helping the system to maintain blood pressure. Additionally, sympathetic activation and parasympathetic withdraw of the autonomic nervous system is modulating heart rate and contractility of the heart, thus affecting the cardiac output [3].

Contractility is determined by measuring volume or pressure changes during catheterization in highly specialized laboratories in the hospital. But contractility can be estimated indirectly by measurements of pre-ejection period (PEP) and left ventricular ejection time (LVET) noninvasively using impedance techniques [4].

Circulation volume and venous return is another important variable for the pump function of the heart. Circulating volume is affected by position dependent fluid shifts and hydration status. Low blood volume can cause hypotension (low blood pressure) or postural orthostatic tachycardia syndrome (POTS) [5]. Fluid status is critical in heart failure patients and has to be controlled carefully to prevent volume overload and decompensation of the heart [6].

Failure of the autonomic system can cause hypertension (high blood pressure) and increase cardiovascular risk of mortality. Autonomic dysfunction can also cause orthostatic hypotension (OH), also called postural hypotension. OH is caused by a sudden drop in blood pressure of at least 20mmHg in systolic blood pressure (SBP) or 10mmHg in diastolic blood pressure (DBP) when a person suddenly stands up from a sitting or lying position. A drop in blood pressure can cause lightheadedness, a “dizzy spell” or fainting, which greatly increases the risk of falls. Paradoxically, 50% of these patients develop supine hypertension, which is not rec-

ognized by many physicians and caregivers. The combination of orthostatic hypotension with supine hypertension poses a difficult diagnostic and therapeutic challenge [7].

There is need for an ambulatory device, which integrates measurements of heart pump function and blood pressure in combination with posture and activity for use outside of the clinical setting. Additionally this ambulatory device should give immediate feedback to the patient as well as the caregiver to permit rapid therapeutic interventions, such as blood pressure control and improvement of heart function.

We developed an ambulatory smart health monitor that integrates monitoring of pump function, blood pressure and autonomic control. Figure 38 shows the concept of this ambulatory health monitor, including the relationships between physiological measures (acceleration, cuff blood pressure, ECG and thoracic impedance), and established cardiovascular performance parameters (contractility, heart rate, stroke volume, cardiac output and beat-to-beat blood pressure). A summary of target parameters, sensors, and approach is shown in Table 5.

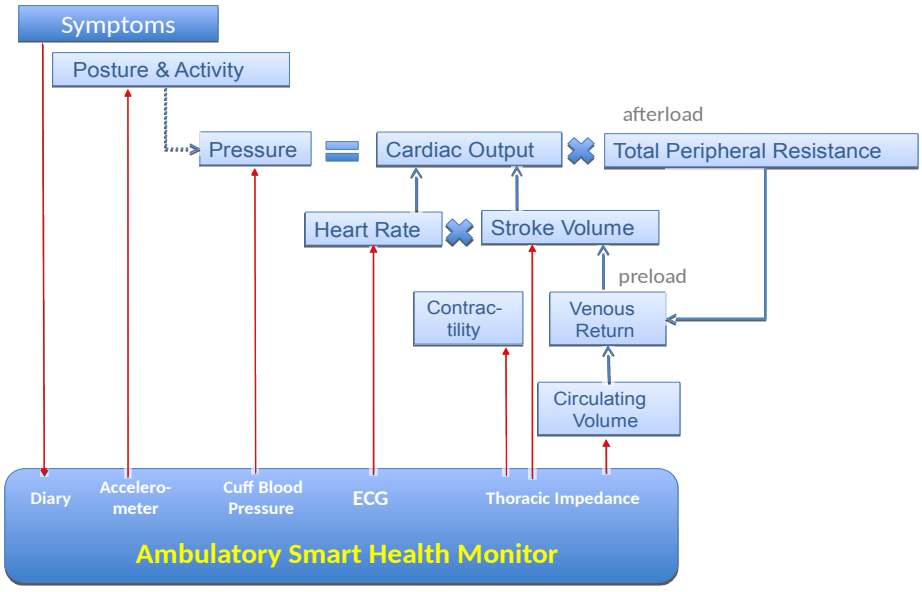

Figure 38: Concept of an ambulatory health monitor for patients with heart failure, hypertension or autonomic failure.

Table 5: Target Parameter and Sensors for Proposed Ambulatory Health Monitor

Parameter	Sensors	Implementation
Symptoms and Comments	Phone keyboard and Voice Input	Time stamped Diary and Log
Posture	Accelerometer	Posture Detection (Angle)
Movement		Activity Level Measurements (Power)
Fall		
Blood Pressure	Arm Cuff	Oscillometric Non Invasive Blood Pressure
Heart Rate	ECG	Lead II, QRS Detection and RRI measurements
Arrhythmias	ECG	5 Lead ECG, Rhythm Analysis
Ischemic Events	ECG	Detection of ST-Elevation
Cardio-Vagal Autonomic Control	ECG	Spectral Analysis of Heart Rate Variability and its components
Fluid Status	Impedance	Thoracic Fluid Content (Z0)
Stroke Volume (SV)	Impedance	Estimation of SV by Kubicek or Sramek
Contractility	Impedance	Pre ejection Period
		Left Ventricular Ejection Time
		(dZ/dt)max

The next sections provide a detailed description of the hardware and software implementation for measuring the different physiological variables described in the table above.

System Design

Over the past decade advances in sensor and mobile device technologies offer high quality signal computing and wireless networking capabilities. Taking advantage of these technologies, we designed a prototype battery operated wireless health care monitor based on an 8bit micro-controller (ATxmega256A3BU, Atmel, USA) [8], [9].

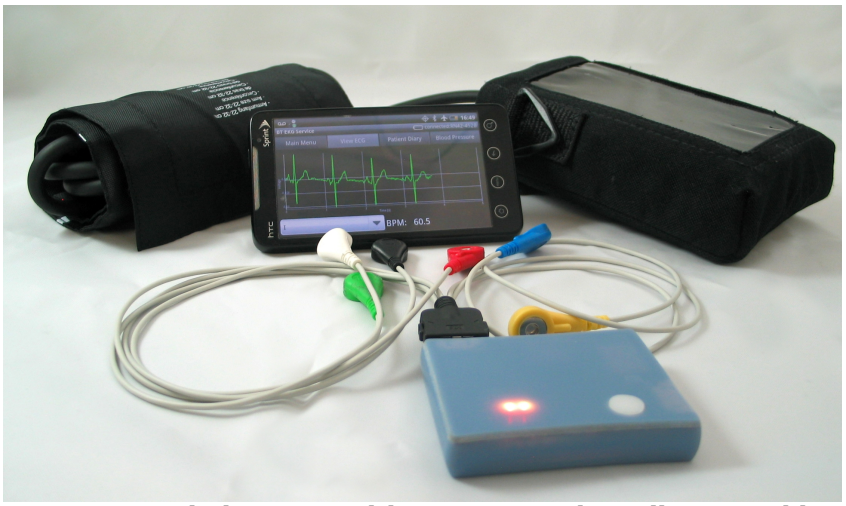

Figure 39: Ambulatory Health Monitor and oscillometric blood pressure module connected to a smartphone, that is showing a real-time ECG trace.

Due to the limited computational power of an 8bit micro-controller and increasing demand for wireless peripheral sensors, we developed the next generation of a mobile ambulatory health monitor (Figure 39) based on an ARM Cortex-M4F (STM32F405, STMicroelectronics, Switzerland). We have chosen the Cortex-M4F platform, because it offers a good balance between power consumption and computational power. A limited DSP instruction set enables real time signal processing for feature extraction, such as cardiac output estimation, and high level alerts.

Furthermore, the integration of a different wireless radio that supports classic and Bluetooth low energy provides more flexibility in interfacing peripheral sensor nodes as commonly found in body area networks (BAN). A block diagram of the health monitor can be seen in Figure 40.

The ambulatory health monitor was equipped with a 2000mA lithium polymer battery that allows for a maximum recording time of up to 30h during normal monitoring with an active Bluetooth connection.

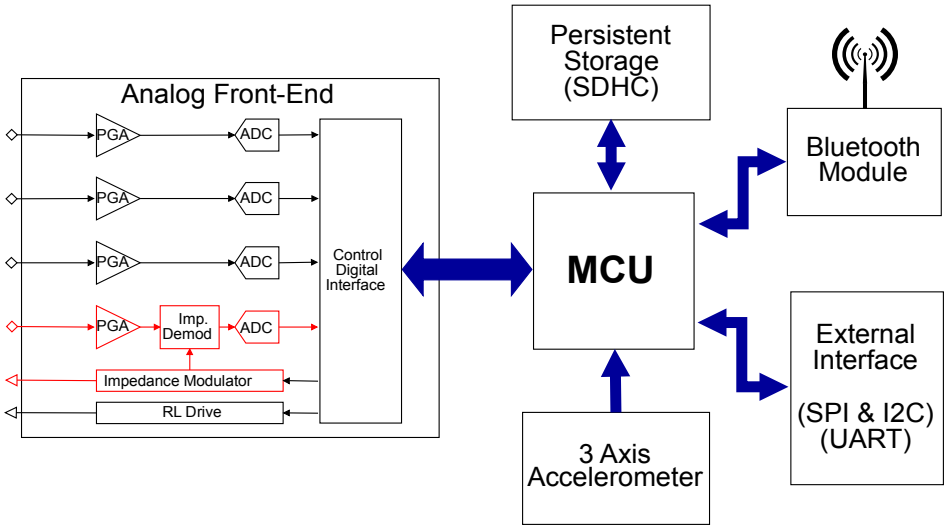

Figure 40: Simplified hardware block diagram of autonomic health monitor

Biopotential

To enable biopotential measurements, like electrocardiogram (ECG) or electromyography (EMG) a 4 channel analog front-end (AFE) ADS1294R (Texas Instruments, USA) was integrated. The ADS1294R provides programmable gain preamplifiers (1x to 12x), 4 dedicated 24bit delta-sigma analog-to-digital converters (ADC), reference electrode driver and serial programming interface (SPI) for configuration and high-speed data transfer to the microcontroller unit (MCU).

In our configuration, the delta sigma modulator continuously samples the input signal at 512 kSPS, referred to as modulation frequency (f_{MOD}). However, the output data rate (f_d) of the AFE can be set between 250SPS and 8kSPS at full resolution and up to 32kSPS at reduced resolution (17bit). The output data rate is achieved by feeding the output of the delta-sigma modulator through a decimation stage composed of a third-order sinc filter (Equation 6). The sinc filter provides a -3dB cut off at approximately $0.265*f_d$ (Figure 41).

$$|H(z)| = \left| \frac{1 - z^{-N}}{N \cdot (1 - z^{-1})} \right|^3 \qquad (6)$$

N : *Decimation Factor*

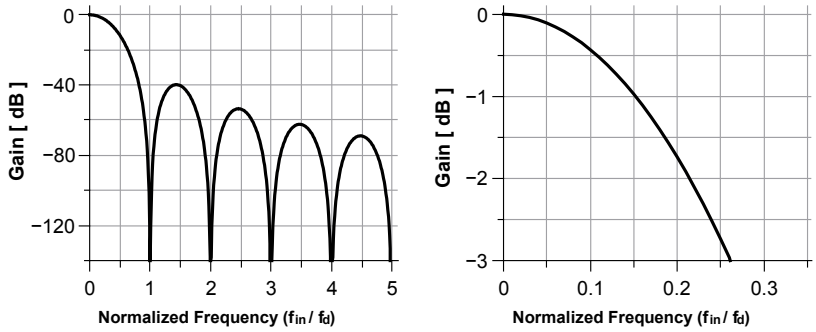

*Figure 41: Sinc filter frequency response (**left**) and roll-of (**right**)*

Due to the internal decimation filter and high modulation frequency of the delta-sigma modulator, there is little need for complex higher-order anti alias filter. Hence, we added a second order RC input lowpass filter with a cut-off frequency of 60kHz to sufficiently attenuate signals with frequencies higher than or equal to $f_{MOD,}$ while maintaining flexibility with respect to physiological parameters that require higher data rates.

The ability to configure the output data rate and filter setting on demand, allows for the measurement of a variety of biopotentials, which enures that optimal recording parameters are used for each specific application.

Electrocardiogram

The most important diagnostic and clinical relevant parameter for any cardiac monitor is the ECG, which represents the surface potential generated by the heart. To a trained health care provider, the ECG offers a substantial amount of information regarding the structure and electrical function of the heart.

For ECG measurements, the internal reference driver is configured to generate a signal that represents the average of right arm (RA), left arm (LA) and left leg (LL) electrodes, also know as Wilson's central terminal [10]. This reference

drive is applied to the body via the right leg (RL) electrode. If desired for a specific application, the AFE can be configured to derive a reference drive from any input electrode configuration or simply buffer mid-voltage.

To maintain patient safety, independent of reference drive configuration, current limiting resistances were added to the output of the driver and limit the maximum output current to less than 50µA. Furthermore, this reference drive configuration feeds back common mode signal observed after the pre-amplifier stage. In conjunction with the low output impedance of the amplifier, the right leg drive improves the common mode rejection ratio (CMRR) of the AFE, which was determined to be larger than 95dB at a pre-amplifier gain setting of 3x.

In order to evaluate the device performance, ECG data were collected from three healthy volunteers on a tilt table. The tilt table creates a controlled change in posture, from supine to upright and vice versa. After approximately 300s in supine the tilt table was activated and the individual was gradually positioned almost upright (60-70 degrees). During the performance of this test, the health monitor continuously recorded ECG leads I, II, and III from the subject at a sampling rate of 500SPS and stored the waveforms into its internal persistent memory.

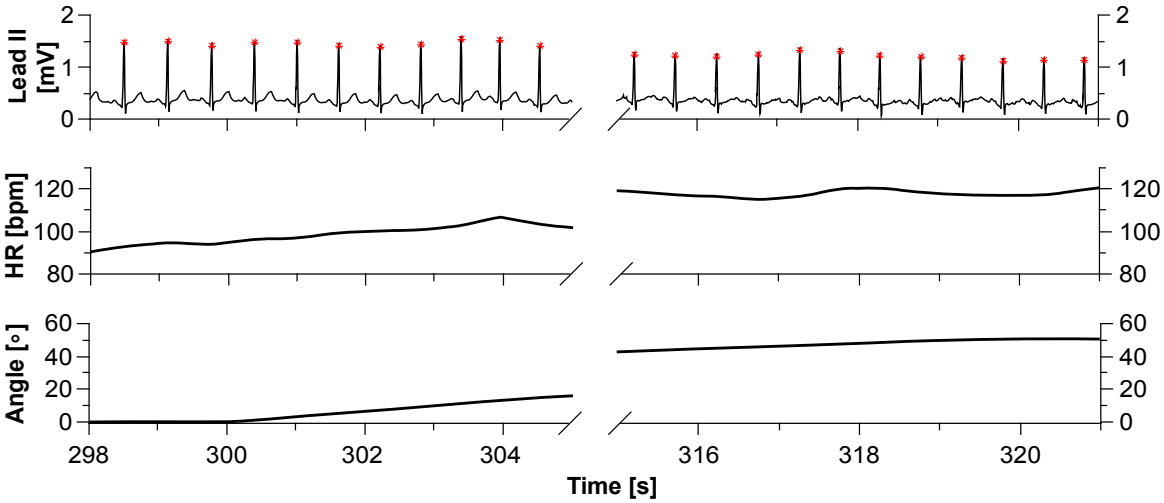

*Figure 42: Lead-II of ECG recording from healthy subject undergoing tilt table test (**top**). Estimated HR based on Pan & Tompkins QRS detection algorithm [11] (**middle**). Angle of tilt table during the experiment (**bottom**).*

To analyze the ECG and determine the heart rate (HR), we applied a self learning QRS detection algorithm to ECG lead-II, as proposed by Pan and Tompkins [11]. The advantage of this algorithm is to maintain high accuracy and noise tolerance, while only relying on integer operations for signal filtering and detection of R-peaks. This algorithm is ideally suited for real time QRS detection in embedded systems, since it provides high detection rates, but at the same time frees microcontroller resources that can be used for other more computational intense tasks. Lead-II and HR recorded for one subject during this experiment is shown in Figure 42. The HR increases as expected with the tilt angle, which was determined utilizing the internal accelerometer.

Electromyography

Electromyography or EMG is a method for recording the electrical potentials generated by skeletal muscle when activated. EMG is a tool used to identify neuromuscular diseases, muscle fatigue or as control signal for prosthetic devices.

The action potential generated by the muscle cells can either be recorded using intramuscular or surface electrodes. For intramuscular measurement, a needle electrode is inserted directly into the muscle, and the potential is recorded in reference to the surface of the skin. Surface measurement is performed by placing at minimum 2 electrodes above the muscle on the skin. Surface electrode measurements are restricted to superficial muscles. The use of surface electrodes is limited, because the action potentials of underlying muscles will be indistinguishable from the potentials of adjacent muscles or are unable to surpass the signals generated by muscles above.

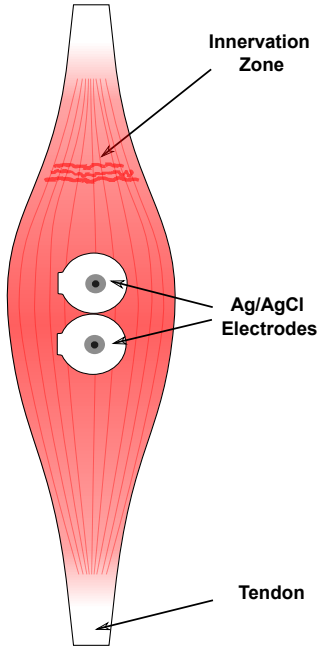

Figure 43: Preferred electrode placement for maximum output signal power.

To record EMG data from a healthy volunteer, we applied 2 Ag/AgCl gel electrodes, center point of disk electrodes spaced 5cm apart, to the biceps brachii, which is a large flexor muscle in the upper arm. The electrodes were placed in the center of the muscle belly, between the motor point (innervation zone) and the musculotendinous junction (Figure 43). This electrode placement has been found to result in a signal measurement with the largest energy [12]. The electrodes were connected to a differential input of the AFE with standard ECG lead wire and the front-end was configured to record at a sampling rate of 1kSPS to fully capture action potentials with frequency components ranging from 0Hz-350Hz [13], [14]. To minimize power line interferences, we placed an additional electrode on the inner surface of the

forearm in close proximity to the wrist. This electrode was fed by the reference driver of the AFE, which generated a signal composed of the inverted average of both inputs.

The subject was placed in sitting position with his forearm stretched out horizontally, on a flat solid surface, while holding a 4.54kg (10lbs) dumbbell in his hand. During the experiment the subject contracted his biceps muscle and was holding the contraction for approximately 3 seconds. This step was repeated for an additional 2 times. Post experiment, we extracted the EMG data from the internal persistent storage of the health monitor and estimated the power spectral density (PSD) for every second of the EMG signal with a window length of 5s. Figure 44 shows the EMG recording and PSD before and during muscle contraction.

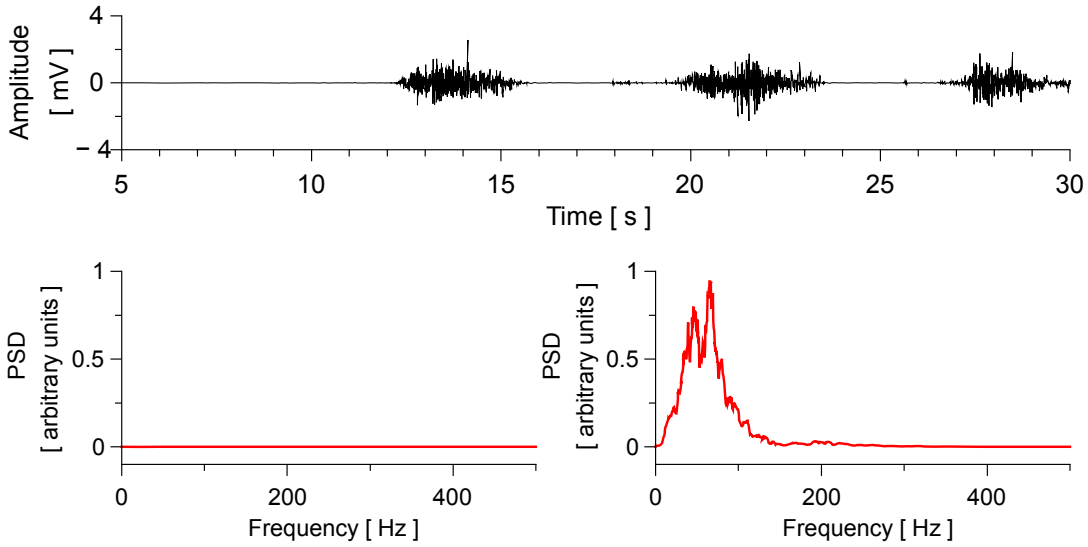

*Figure 44: EMG measurement of biceps brachii before, during, and after multiple voluntary contractions, recorded with health monitor at sampling rate of 1kSPS (**top**). Power spectral density before activation, calculated for time segment 5-10s. (**bottom-left**). Power spectral density during activation at time segment 11-16s. (**bottom-right**)*

Thoracic Impedance

Thoracic impedance, also known as impedance plethysmography, is a method of measuring the electric impedance across the thorax to estimate volume changes of tissue, via surface electrodes (Figure 49).

Considering a simplified model, the resistance of the thorax is determined by the cross section, length and resistivity. If the individual is stationary and not breathing, the resistance of the thorax is mainly affected by the volume and the resistivity of blood.

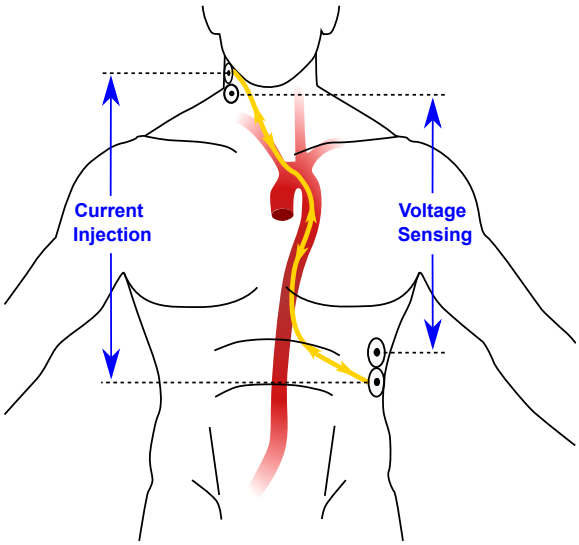

Figure 45: Placement of electrodes for measurement of thorax impedance. Showing location of tetrapolar electrode configuration. Outer electrodes inject current into the thorax, inner electrodes sense voltage changes.

At each cardiac cycle, the heart ejects a certain amount of blood through the right ventricle into the lungs. The pressure increase in the lungs forces oxygen rich blood back through the pulmonary vein into the left atrium. These fluid distribution changes within the thorax can be observed by fluctuations of the impedance across the chest. The amount of blood injected into the lungs at each cycle is equivalent to the stroke volume, characterizing the cardiac output and contractility [15].

Impedance plethysmography is used as a proxy measure to determine respiration activity, fluid level changes in the thorax or cardiac output.

Respiration Activity

The ADS1294R has an integrated modulation signal generator with 2 user selectable frequencies of 32kHz and 64kHz, the appropriate demodulation circuit can be enabled for input channel 1 of the AFE. This feature is designed for the measurement of respiration impedance via any two ECG electrodes. Most commonly used are LA and RA electrodes. However, if the modulation signal is routed out via an independent set of electrodes, it enables the tetra-polar measurements (Figure 45) of thoracic impedance.

To facilitate respiration measurements, the AFE injects a current with an approximate amplitude of 750µA and frequency of 64kHz into the thorax. The sampled impedance signal is band-pass filtered (0.05Hz to 2Hz) in order to extract respiration activity. An example of respiration activity is shown in Figure 46.

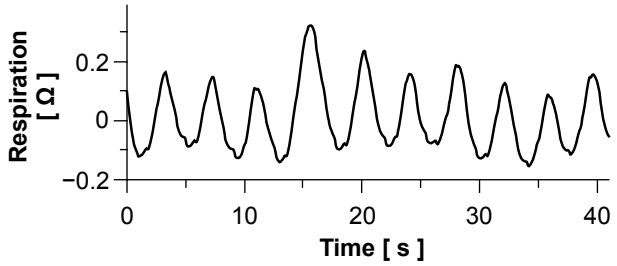

Figure 46: Respiration activity derived from thorax impedance signal by band-pass filtering (0.05-2Hz).

Fluid Accumulation

If a human body is in the upright position, the earth's gravity exerts a downward force on the fluid mass of the body, only compensated by the fluid pumped back via the venus return, which causes approximately 700ml of blood to aggregate in the lower extremities or abdominal region of the body [16]. Due to the depletion of fluid in the thorax, the resistivity of the volume conductor slowly increases until a steady state of fluid displacement is reached.

With simple filtering techniques, the influence of thoracic impedance caused by static fluid redistribution can be extracted. Figure 47 shows a healthy subject during a change in posture, from supine to upright and back. The recorded impedance was processed through a low pass filter with a 0.05Hz cut off frequency (-3dB).

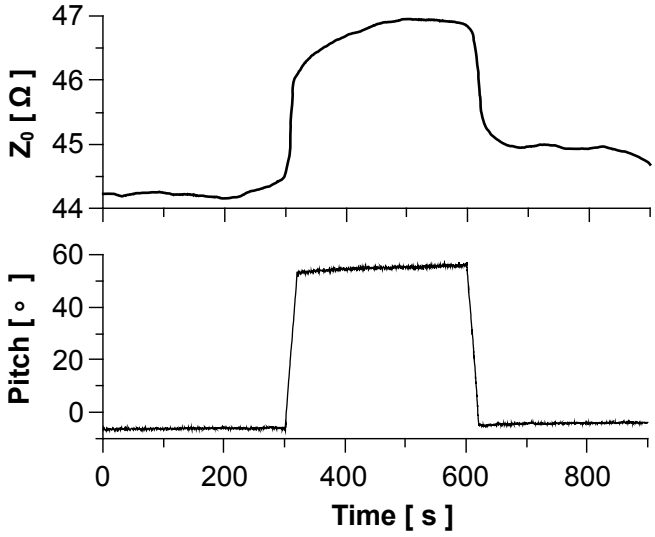

Figure 47: Thoracic impedance signal showing influence of fluid redistribution within the body.

Cardiac Performance

Because the modulation and demodulation circuit was designed by Texas Instruments specifically for respiration impedance measurement, which has lower bandwidth requirements (0.05Hz to 3Hz) compared to impedance cardiography (0.05Hz to 25Hz), the input circuitry needed to be characterized. We; therefore, designed an impedance simulator to evaluate the input characteristic of the demodulation circuitry. A circuit diagram of this impedance simulator can be found in Figure 48. The tolerances of the resistors used were less than 1% and less than 10% for the capacitance. The resistance between the output pins V+ and V- was set to 28Ω by adjusting the precision 10kΩ potentiometer. The output resistance was verified using a calibrated LCR meter (Agilant U1733C) at 10kHz measurement frequency. The nonlinearity of this simulator over an output resistance range of ±0.6Ω was determined to be less then 3.4%.

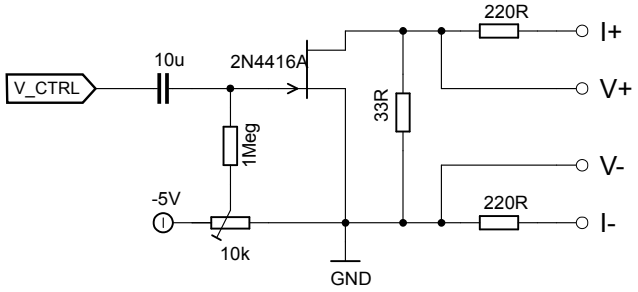

Figure 48: Circuit diagram of thoracic impedance simulator, based on JFET 2N4416A (Vishay Intertechnology Inc.)

Once the impedance simulator was properly adjusted, the current injecting leads of the health monitor were connected to pin I+ and I-, and the voltage measurement leads RA and LL to pins V+ and V-. A frequency synthesizer was connected to the control voltage BNC port (V_CTRL) of the simulator. The synthesizer was configured for single frequency sinewave output with a signal amplitude of 300mV. Impedance measurements with our health monitor were performed at 36 different fre-

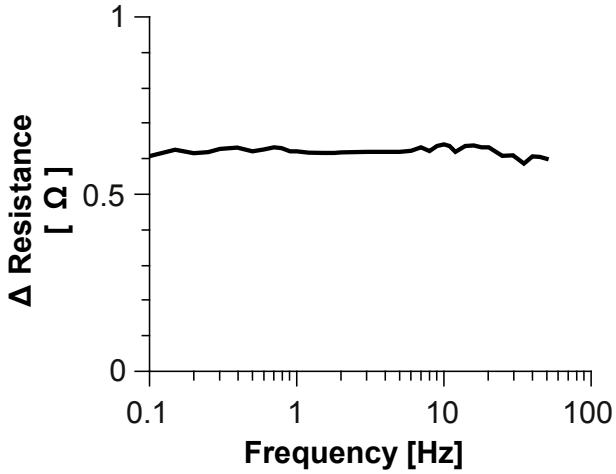

Figure 49: Frequency characterization of impedance input circuitry. Modulation of resistance with amplitude of 0.6Ω and frequency in the range of 0.1Hz to 50Hz.

quencies ranging from 0.1Hz to 50Hz. In order to capture multiple periods of the input signal, the impedance output at each frequency was recorded with the health monitor for 60 seconds for frequencies less than 0.15Hz and 30 seconds for higher excitation frequencies. For the measurement of thorax impedance, the health monitor injected a current of 750µA amplitude and 64kHz frequency into the variable resistor. The AFE was configured with a data rate of 500SPS and the sampled data was written to the internal persistent memory without further signal processing or conditioning. The resulting impedance spectrum is displayed in Figure 49.

The measured impedance spectrum, in the frequency range of 0.1Hz to 50Hz, is constant within 6.5% of the expected value. Thus, the respiration impedance circuitry of the AFE is suited for impedance cardiography.

In order to estimate stroke volume, we have chosen the exact same test setup as described in section “Electrocardiogram”. Silver/Silver-Chloride (Ag/AgCl) gel-electrodes were applied to the upper thorax of a test subject, as shown in Figure 45.

At the beginning of the experiment, the volunteer was placed on the tilt table in supine position. After approximately 300s the tilt table was activated and moved the subject in a slow and continuous motion into an almost upright position (60-70 degrees), with the health monitor configured to record impedance and ECG data during the tilt.

Upon completion of the experiment, the data on the health monitor was extracted and the stroke volume was calculated (Equation 7) [15], as first described by Kubicek et. al. [17], [18]. To enhance visibility with respect to impedance cardiography and stroke volume calculation, we extracted a small time segment of the recording prior to the tilt, which is illustrated in Figure 50. A more detailed and in depth description of the methods used to estimate stroke volume can be found in the book “Bioelectromagnetism” by Jaakko Malmivuo [33].

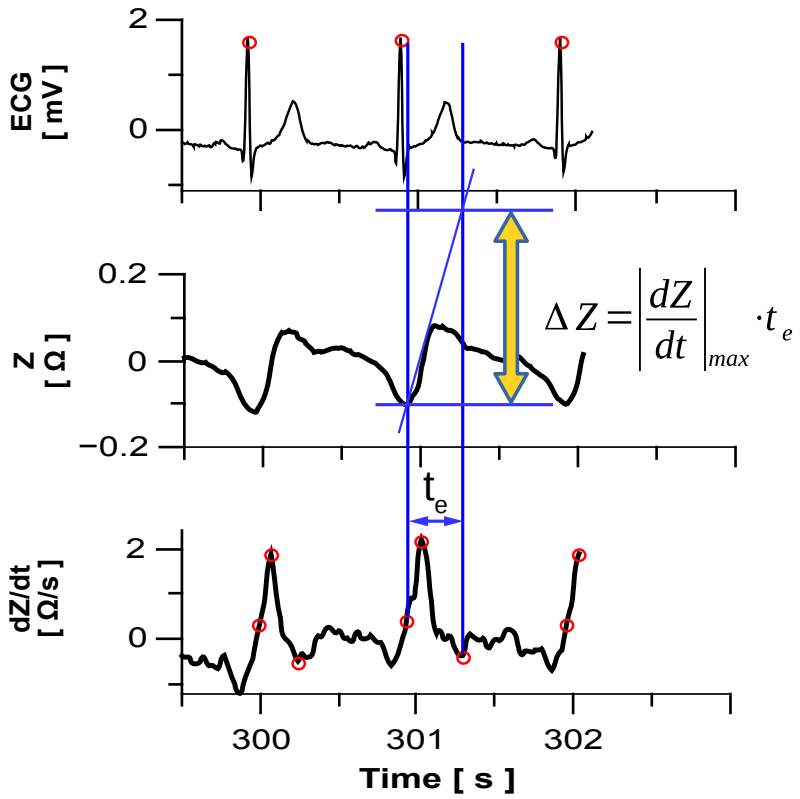

*Figure 50: Impedance cardiography: ECG with R-point marker (**top**). Impedance signal without baseline and respiration influences (**middle**). First derivative of impedance including important markers (begining, max and end point of ejection) used for cardiac stroke volume estimation (**bottom**).*

$$SV = \rho_b \frac{l^2}{Z^2} \left|\frac{dZ}{dt}\right|_{max} \cdot t_e \tag{7}$$

with:

SV = stroke volume [ml]

ρ_b = resistivity of the blood [Ω·cm]

l = mean distance between the inner electrodes [cm]

Z = mean impedance of the thorax [Ω]

$\left|\frac{dZ}{dt}\right|_{max}$ = absolute value of the maximum deviation of the first derivative signal during systole [Ω/s]

t_e = ejection time [s]

The impedance measurement for the tilt table experiment and analysis outcome are displayed in Figure 51. With increasing tilt, the stroke volume decreases due to a pooling of blood in the leg veins. In order to compensate for the decreased stroke volume, the carotid baroreceptor reflex increases the heart rate to maintain blood pressure, as shown in Figure 42.

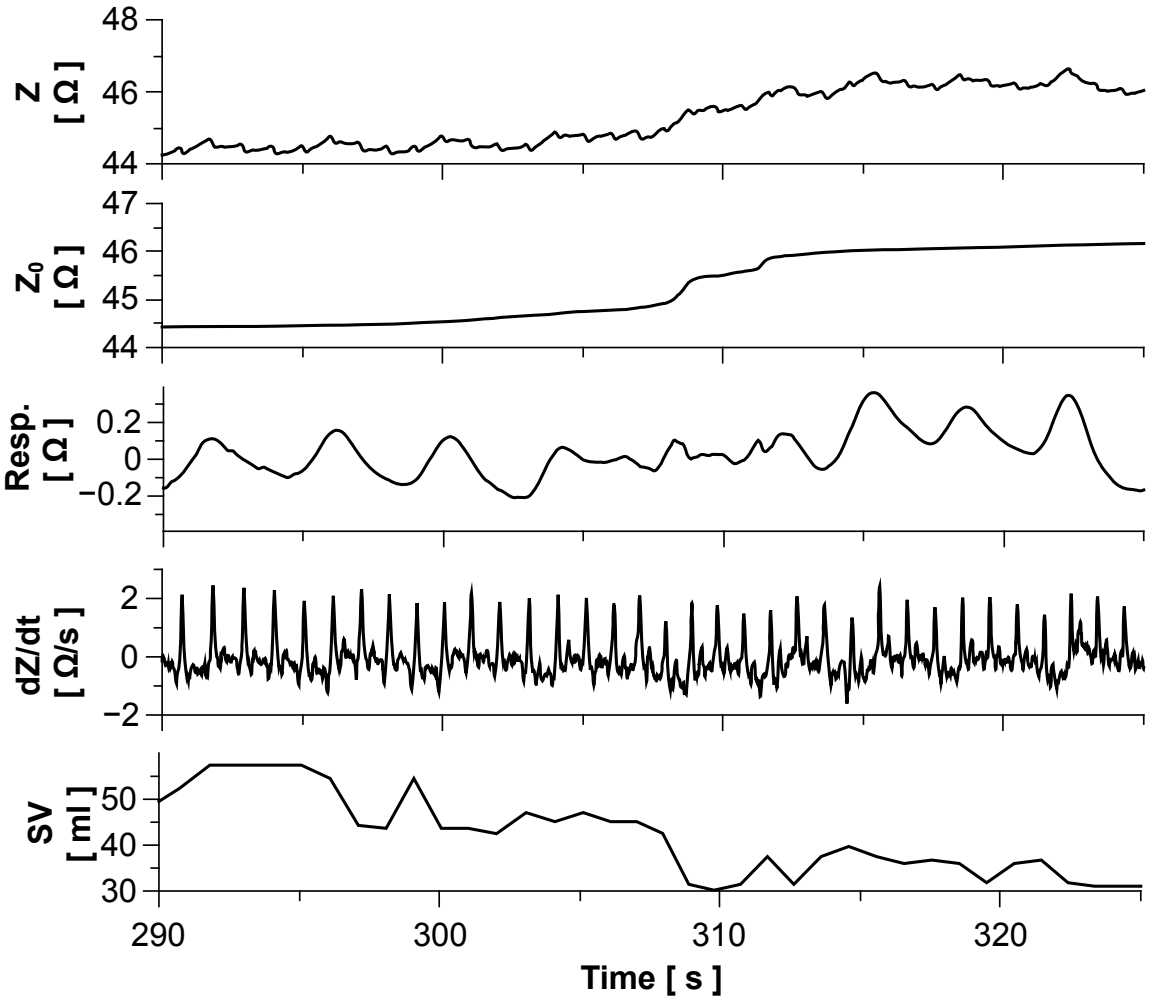

*Figure 51: Thoracic impedance measurement of one human volunteer undergoing a tilt table test. Showing different information that can be extracted using signal processing. Raw thoracic impedance signal (**top**). Z_0 - baseline impedance component with $f(Z_0) \leq 0.05Hz$, representing change resulting from quasi static fluid redistribution inside the body (**2_{nd} from top**). Respiration signal that indicates inhales and exhales of the subject (**middle**). dZ/dt – differentiated impedance signal that reflects the dynamic changes of impedance, influenced by circulation of blood (**2_{nd} from bottom**). SV – stroke volume estimation, determined by using prediction algorithm proposed by Kubicek et. al. (**bottom**)*

Accelerometer

To facilitate actigraphy and support posture detection, a 14bit 3D accelerometer (BMA180, Bosch Sensortec, Germany) was integrated into the ambulatory health monitor.

Due to the size constraints of the health monitor, the real-estate for additional components was limited. Hence, we have opted for a single 3-axis accelerometer, instead of a gyroscope or gyroscope / accelerometer combination. Further, compared to a gyroscope, an accelerometer has the advantage of being able to measure static as well as dynamic forces, given they are the result of linear acceleration.

Actigraphy and Posture Tracking

Actigraphy, a method to study patient movements, is increasingly used in sleep research and clinical care to determine abnormalities in sleep pattern or circadian rhythm [19]–[22]. Furthermore, during continuous monitoring of an individual, especially during daily activities, the knowledge about posture (standing, lying, sitting or rapid change of position) can be an important parameter to determine the context of clinical symptoms [23]. Symptoms could, for example be increased heart rate, dizziness, fatigue or syncope and context might be exercise, changes in posture or sleep.

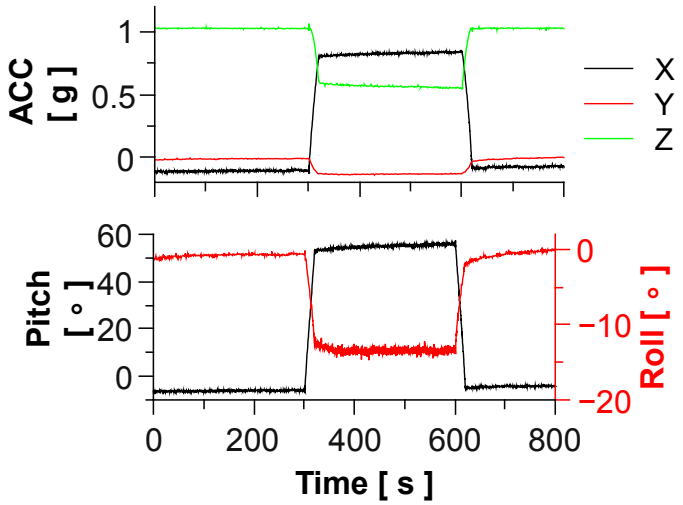

*Figure 52: Accelerometer output during change of posture from supine to upright and back (**top**). Pitch and Roll angle derived from acceleration data (**bottom**)*

Figure 52 shows the output recorded by the accelerometer during a steady incline of one volunteer from supine to nearly upright (about 70 degrees). During this procedure, the health

monitor was fixed to the patient's chest. We calculated the pitch and roll using simple trigonometric functions. Where pitch and roll reflect the rotation of the body around the transverse (Y) and longitudinal (X) axis, respectively.

It must be noted that the use of an accelerometer poses certain disadvantages. Due to the inherit nature of an accelerometer, it is impossible to estimate a slow rotation of the object of interest around the gravitational vector, if a single axis of the sensor is in perfect alignment with the direction of the gravitational force. This phenomenon is caused by the lack of a static force perpendicular to the gravitational force, which would allow for the measurement of linear acceleration on rotation around said axis.

External Peripheral Sensors

Certain applications may require the acquisition of physiological parameters that cannot be recorded with the health monitor itself. Therefore, we designed an external interface that can used to integrate external physiological sensors. In an earlier version of the heath monitor, the interface was exposed through a 24pin external connector. This connector allowed the peripheral device to interact with the MCU via either a universal asynchronous receiver/transmitter (UART) interface, inter inter circuit (I2C) bus or SPI. (See Appendix A.1 for connector pin out).

However, due to the availability of one physical interface, only a single peripheral sensor could be directly attached to the monitor at any given time. If multiple sensors are used, they have to be daisy chained together, which introduced a number of issues. At first, we noticed that the vast amount of cable required to interconnect these sensors needed to be routed across the body and potentially restricted the movement of the patient. Further, the exposed interfaces UART, I2C and SPI were designed for use within one system, with relatively short and well-controlled trace length. Consequently, these interfaces offer limited noise immunity, error correction or detection. Introducing long cables, comparatively longer than one would normally find within an embedded system, caused sporadic communication errors or even total communication breakdown between MCU and peripheral device. Although, we used shielded cables between devices to reduce crosstalk and improve noise immunity, communication errors occurred over long

times (24h periods). To address this issue, we had to modify the health monitor firmware to validate or correct received data and restore communication if necessary, which substantially complicated peripheral device driver development.

Thus, in the current version of the health monitor (Rev. 3.2.2, Appendix A.1), the physical interface has been removed and connections to peripheral devices are facilitated using Bluetooth classic or low energy. Additionally, the use of Bluetooth potentially enables the integration of new, emerging and commercially available wireless sensor and wearables, like noninvasive blood pressure cuffs, scales or pulse oximeter.

Blood Pressure

In order to determine a subject's blood pressure, we connected a noninvasive oscillometric blood pressure OEM module (NIBP-2010, Corscience, Erlangen, Germany) to the health monitor. Figure 53 shows a 24 hour recording of systolic and diastolic blood pressure of one healthy subject during a normal daily routine. Blood pressure measurements were taken in periodic intervals of 20min. A 24h blood pressure profile, as shown in Figure 53, helps in identifying if a patient's blood pressure drops during sleep. In the general population, a blood pressure drop of at least 10% during the night is observed and autonomic failure patients, that do not drop (non-dipper), face a higher risk of cardiovascular diseases [24]. In addition, the built in accelerometer assists in identifying sleep patterns, such as sleep onset, especially in patients that are classified as non-dippers.

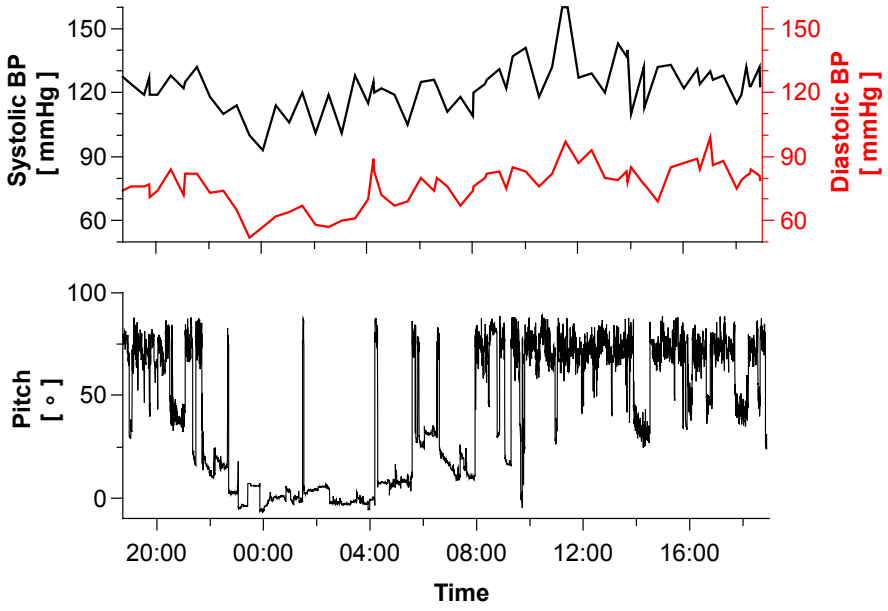

*Figure 53: 24h oscillometric blood pressure recording of one healthy subject (**top**). Rotation (pitch) of subject around the transverse axis with respect to the earth gravitational force using data provided by the health monitor's internal accelerometer (**bottom**). The pitch can also be used as one parameter to help in the investigation of sleep pattern abnormalities.*

Photoplethysmography and SpO2

Photoplethysmography (PPG) measures volume changes of blood during one cardiac cycle, typically performed on the finger tip using reflection or transmission of light [25]. Research has shown that the amplitude of the pulse waveform, or more specifically the pulse pressure, is proportional to the difference of systolic and diastolic arterial pressure [26]–[28]. In addition, it has been used as an estimate of cardiac output by determining the time difference between blood ejected from the heart (ECG) and pressure wave reaching the periphery (PPG) [29], [30].

If light is passed through blood perfused tissue, a fraction of the light is absorbed. Given that oxygen rich hemoglobin (HbO_2) and reduced hemoglobin (Hb) absorb different amounts of light depending on the wavelength, one can estimate the blood oxygen saturation (SpO_2)[31]. This effect is taken advantage of in most PPG monitors by employing LEDs with two different wavelengths, typically in the red (660nm) and infrared (900nm) spectrum [32].

To measure PPG and SpO_2, the health monitor utilizes an OEM pulse oximetry module from Corscience, Germany (ChipOx). The pulse oximeter captures the pulse waveform with 100Hz at 128bit resolution and calculates blood oxygen saturation once a second.

Figure 54 shows a recording of pulse waveform and oxygen saturation captured from one healthy volunteer. In order to stimulate apnea with a change in SpO2, the subject would cease breathing until an output change was observed or he could no longer voluntarily hold his breath. As expected the oxygen saturation reduces during periods of apnea (Figure 54).

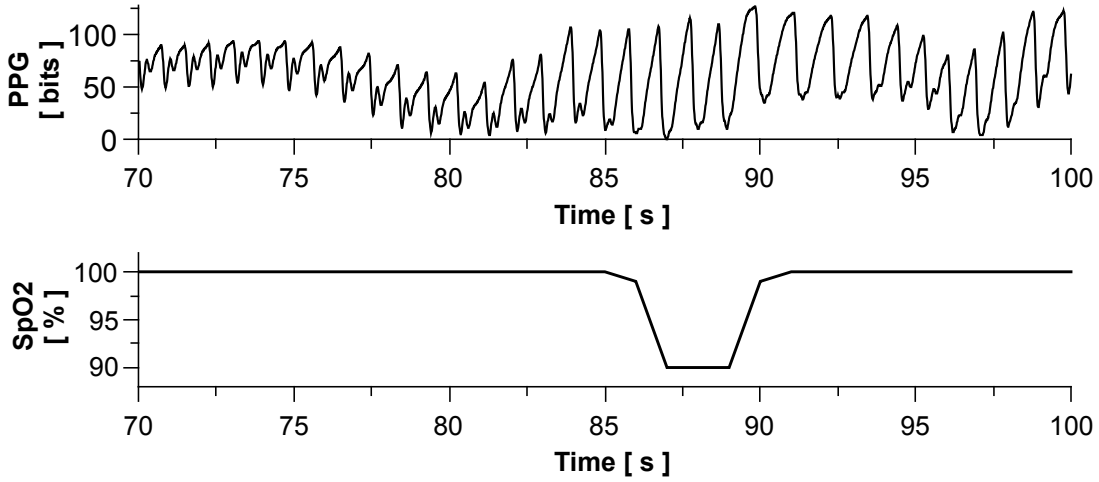

*Figure 54: Trace of photoplethysmograph waveform (**top**) and blood oxygen saturation (**bottom**). Recorded from one subject during simulation of apnea by voluntary cessation of breathing. Simulation of apnea was terminated at 82 seconds.*

Mobile Phone/Tablet Application

To visualize data and to provide the patient and/or health care provider with a user interface, we developed a mobile application for the Android operating system (Google & Open Handset Alliance, 2.3 and higher). The mobile application communicates with the health monitor wirelessly through a Bluetooth connection. Connection parameters, such as device pairing or auto connect, can be set within the application's setting menu.

Within the application the user is able to select and stream a physiological parameter directly to the smart phone, which enables the user to monitor the signal and ensure proper electrode-skin contact in order to maintain a high quality recording (Figure 55). A configurable patient diary (Figure 56) enables the user to enter symptoms and events that can aid in forming a diagnosis by the health care provider. These event markers are timestamped and stored with the real time physiological data in the health monitor's persistent storage.

In addition, the mobile application automatically detects peripheral sensor modules attached to the health monitor, for instance the blood pressure or pulse oximetry module, and presents control, real-time streaming or other device specific options. For example, Figure 57 shows the BP control view, that allows the user to start an individual BP recording and visualized BP values collected since start of the recording.

Depending on the connection setting, the mobile application can stay in contact with the health monitor for the entire duration of the recording. This feature allows for the integration of decision trees within the mobile application that logically combine health monitor outputs and consequently trigger a response to a detected and potentially important event.

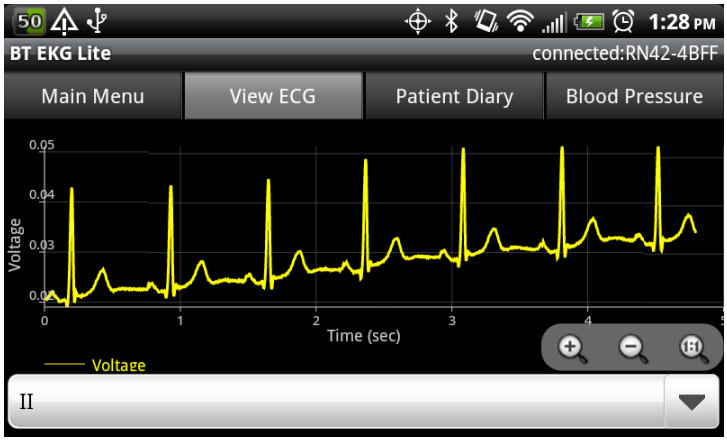

Figure 55: Mobile Application: Real-time streaming of ECG lead-II from the health monitor to the application in order monitor signal quality and proper electrode-skin contact.

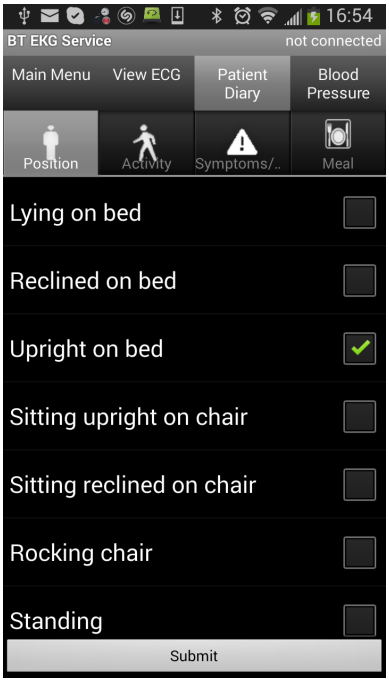

Figure 56: Patient diary in mobile application allows user to select symptoms or specify events.

Figure 57: Mobile application: Blood pressure view offers control and visualization of blood pressure measurements over time.

Conclusion

We presented an ambulatory wireless health care monitor that is capable of recording high quality ECGs, activity, thoracic impedance, blood pressure, oxygen saturation and peripheral pulse waveform in patients for at least 24 hours. Software and firmware modifications allow us to customize and adapt the device to monitor different patient populations ranging from heart failure, syncopy to orthostatic hypotension and other autonomic failures, like baroreflex failure or postural tachycardia syndrome.

The health care monitor system is an evidence-based, person-centric diagnostic platform, which provides a new focus on the patient rather than the disease. Data generated with the platform can be explored to identify early markers for disease to prevent hospital re-admissions or management of disease. Ultimately the platform is expected to increase the quality of life and foster a greater independence of patients.

References

[1] R. Fagard and J. Conway, ”Measurement of cardiac output: Fick principle using catheterization”, *European Heart Journal*, vol. 11, no. suppl I, pp. 1–5, Jan. 1990.

[2] J. D. Collins, ”Global and Regional Functional Assessment of Ischemic Heart Disease with Cardiac MR Imaging”, *Radiologic Clinics of North America*, vol. 53, no. 2, pp. 369–395, Mar. 2015.

[3] D. Robertson, A. Diedrich, and M. W. Chapleau, ”Editorial on Arterial Baroreflex Issue”, *Autonomic Neuroscience*, vol. 172, no. 1–2, pp. 1–3, Dec. 2012.

[4] S. Rl, ”Noninvasive estimation of the end systolic pressure-volume relationship using impedance cardiography.”, *Journal of the Mississippi State Medical Association*, vol. 41, no. 5, pp. 575–578, May 2000.

[5] J. M. Stewart, ”Common Syndromes of Orthostatic Intolerance”, *Pediatrics*, vol. 131, no. 5, pp. 968–980, May 2013.

[6] T. Tuy and W. F. Peacock IV, ”Fluid Overload Assessment and Management in Heart Failure Patients”, *Seminars in Nephrology*, vol. 32, no. 1, pp. 112–120, Jan. 2012.

[7] C. Shibao, A. Gamboa, A. Diedrich, and I. Biaggioni, ”Management of hypertension in the setting of autonomic dysfunction”, *Current Treatment Options in Cardiovascular Medicine*, vol. 8, no. 2, pp. 105–109, Mar. 2006.

[8] R. Harder, J. S. Whitfield, F. J. Baudenbacher, and A. Diedrich, ”Ambulatory Autonomic Health Monitor System for Patients with Autonomic Dysfunction”, presented at the *35th Annual Interational Conference of the IEEE Engineering in Medicine and Biology Society*, Osaka, Japan, 2013.

[9] R. Harder, J. S. Whitfield, F. J. Baudenbacher, and A. Diedrich, ”Autonomic smart health system”, in *Clinical Autonomic Research*, Kohala Coast, Hawaii, 2013, vol. 23, p. 277.

[10] F. N. Wilson, F. D. Johnston, A. G. Macleod, and P. S. Barker, ”Electrocardiograms that represent the potential variations of a single electrode”, *American Heart Journal*, vol. 9, no. 4, pp. 447–458, Apr. 1934.

[11] J. Pan and W. J. Tompkins, ”A Real-Time QRS Detection Algorithm”, *IEEE Transactions on Biomedical Engineering*, vol. BME-32, no. 3, pp. 230–236, Mar. 1985.

[12] C. J. De Luca, ”The use of surface electromyography in biomechanics”, *Journal of applied biomechanics*, vol. 13, pp. 135–163, 1997.

[13] R. Merletti and P. Di Torino, ”Standards for reporting EMG data”, *Journal of Electromyography and Kinesiology*, vol. 9, no. 1, pp. 3–4, 1999.

[14] A. Van Boxtel, ”Optimal signal bandwidth for the recording of surface EMG activity of facial, jaw, oral, and neck muscles”, *Psychophysiology*, vol. 38, no. 01, pp. 22–34, Jan. 2001.

[15] J. Malmivuo and R. Plonsey, ”Bioelectromagnetism: principles and applications of bioelectric and biomagnetic fields”. *Oxford University Press*, 1995.

[16] A. Diedrich and I. Biaggioni, ”Segmental orthostatic fluid shifts”, *Clinical Autonomic Research*, vol. 14, no. 3, pp. 146–147, Jun. 2004.

[17] W. G. Kubicek, J. Karnegis, R. P. Patterson, D. A. Witsoe, and R. Mattson, ”Development and evaluation of an impedance cardiac output system.”, *Aerospace medicine*, vol. 37, no. 12, pp. 1208–1212, Dec. 1966.

[18] W. G. Kubicek, R. P. Patterson, and D. A. Witsoe, ”Impedance Cardiography as a Noninvasive Method of Monitoring Cardiac Function and Other Parameters of the Cardiovascular System*”, *Annals of the New York Academy of Sciences*, vol. 170, no. 2, pp. 724–732, Jul. 1970.

[19] A. C. Brown, M. H. Smolensky, G. E. D’Alonzo, and D. P. Redman, ”Actigraphy: A Means of Assessing Circadian Patterns in Human Activity”, *Chronobiology International*, vol. 7, no. 2, pp. 125–133, Jan. 1990.

[20] S. Ancoli-Israel, R. Cole, C. Alessi, M. Chambers, W. Moorcroft, and C. Pollak, ”The role of actigraphy in the study of sleep and circadian rhythms. American Academy of Sleep Medicine Review Paper”, *Sleep*, vol. 26, no. 3, pp. 342–392, 2003.

[21] A. Sadeh and C. Acebo, ”The role of actigraphy in sleep medicine”, *Sleep Medicine Reviews*, vol. 6, no. 2, pp. 113–124, May 2002.

[22] M. Chesson Jr, M. Coleman, M. Lee-Chiong, and D. Pancer, ”Practice parameters for the use of actigraphy in the assessment of sleep and sleep disorders: an update for 2007”, *Sleep*, vol. 30, no. 4, p. 519, 2007.

[23] M. Ovadia, K. Gear, D. Thoele, and F. I. Marcus, ”Accelerometer Systolic Time Intervals as Fast-Response Sensors of Upright Posture in the Young”, *Circulation*, vol. 92, no. 7, pp. 1849–1859, Oct. 1995.

[24] L. E. Okamoto, A. Gamboa, C. Shibao, B. K. Black, A. Diedrich, S. R. Raj, D. Robertson, and I. Biaggioni, ”Nocturnal Blood Pressure Dipping in the Hypertension of Autonomic Failure”, *Hypertension*, vol. 53, no. 2, pp. 363–369, Feb. 2009.

[25] K. H. Shelley, ”Photoplethysmography: beyond the calculation of arterial oxygen saturation and heart rate”, *Anesthesia & Analgesia*, vol. 105, no. 6, pp. S31–S36, 2007.

[26] A. P. Avolio, M. Butlin, and A. Walsh, ”Arterial blood pressure measurement and pulse wave analysis—their role in enhancing cardiovascular assessment”, *Physiological Measurement*, vol. 31, no. 1, p. R1, Jan. 2010.

[27] X. F. Teng and Y. T. Zhang, ”Continuous and noninvasive estimation of arterial blood pressure using a photoplethysmographic approach”, in *Proceedings of the 25th Annual International Conference of the IEEE Engineering in Medicine and Biology Society, 2003*, 2003, vol. 4, pp. 3153–3156 Vol.4.

[28] Y. Yoon, J. H. Cho, and G. Yoon, ”Non-constrained Blood Pressure Monitoring Using ECG and PPG for Personal Healthcare”, *Journal of Medical Systems*, vol. 33, no. 4, pp. 261–266, Jul. 2008.

[29] M. M. Hirschl, H. Kittler, C. Woisetschläger, P. Siostrzonek, T. Staudinger, J. Kofler, E. Oschatz, A. Bur, M. Gwechenberger, and A. N. Laggner, ”Simultaneous comparison of thoracic bioimpedance and arterial pulse waveform-derived cardiac output with thermodilution measurement”, *Critical care medicine*, vol. 28, no. 6, pp. 1798–1802, 2000.

[30] O. Goedje, K. Hoeke, M. Lichtwarck-Aschoff, A. Faltchauser, P. Lamm, and B. Reichart, ”Continuous cardiac output by femoral arterial thermodilution calibrated pulse contour analysis: comparison with pulmonary arterial thermodilution”, *Critical care medicine*, vol. 27, no. 11, pp. 2407–2412, 1999.

[31] K. K. Tremper, ”Pulse oximetry.”, *CHEST Journal*, vol. 95, no. 4, pp. 713–715, 1989.

[32] P. D. Mannheimer, J. R. Cascini, M. E. Fein, and S. L. Nierlich, ”Wavelength selection for low-saturation pulse oximetry”, *IEEE Transactions on Biomedical Engineering*, vol. 44, no. 3, pp. 148–158, Mar. 1997.

CHAPTER VI

CONCLUSION

The primary contribution of this dissertation is the development of a wireless and modular health care platform to monitor multiple physiological variables that can be configured for different clinical and patient needs. The platform is composed of individual hardware modules, which integrate specific measurement capabilities, such as ECG, EMG, cardiac stroke volume, intra- and extracelluar water, body composition, activity and posture, blood pressure, pulse wave and SpO2.

As described in the previous chapters, these hardware modules enable the development of physiological monitoring solutions that provide novel measurement modalities, such as continuous blood pressure or noninvasive beat-to-beat cardiac stroke volume and pulse wave, in a small and mobile form factor. Further, we have shown that the analog front-ends produce digital outputs according to what is defined in the reference literature. The experimental results, presented in Chapter III-V, indicate that the physiological signals recorded with our health monitor platform are comparable in signal quality to equipment used in clinical environments, while maintaining an overall cost of less than $250 per device.

Another contribution of this dissertation is the design and implementation of real-time high bandwidth streaming of physiological data to mobile devices, such as smartphone or tablet computer and a cloud based data infrastructure for alerts, signal processing, remote data access and messaging. The integration of our platform into these mobile device technologies provides the patient with control and visualization of his/her own health data. Thus, patients can become actively engaged in their health and take responsibility leading to a potentially higher adherence to the treatment plan or early diagnosis of critical conditions potentially preventing hospital re-admissions.

As a result, real-time monitoring and advanced signal processing allows for feature extraction and the detection of clinically important markers for patient specific event handling.

Furthermore, mobile device technologies enable real-time transfer, storage of medical data in a central location, and facilitate communication between healthcare providers and/or patients. The aggregation of large amounts of real time medical data integrated into the medical record system enables exploratory research to extract hidden and previously unknown markers, which are impossible to identify with conventional technologies. Consequently, leading to new metrics for identification of early markers or improved treatment of a disease.

The integration into a remote infrastructure favors management of the health monitor platform and allow for firmware updates or adjustments of feature extraction algorithms employed on the monitoring device. We have presented in Chapter III that remote updates can be initiated by the health care provider to take into account changes in the patient's health status or to accommodate for patient specific variation in physiology without a clinic or hospital visit.

In summary, this dissertation presented a highly modular smart health platform integrated with mobile device technologies and cloud based data infrastructure. We demonstrated the utilization of the technology to access intra- and extracellular water, fat mass, cardiac electrophysiology, heart rate, cardiac stroke volume, blood pressure, pulse wave velocity and oxygen saturation in an ambulatory setting. The obtained physiological signals can be used to monitor the nutritional status, the electrical and mechanical activity of the heart, respiration, the vascular compliance, activity, posture and blood oxygen saturation in a wide spectrum of patients in an ambulatory setting for diagnostics and to improve treatment strategies to prevent hospital readmissions in the future.

Future Directions

The modular health platform evaluated in this work offers a multitude of physiological variables the can be measured. However, some research implies that the accuracy of monitoring patient's activity over a prolonged period can substantially be improved by combining the output of an accelerometer with a gyroscope and/or magnetometer. Improvements in manufacturing technologies resulted in advanced single chip solutions for motion and orientation tracking. These 9-axis sensors, such as BNO055 (Bosh Sensortec, Germany), can easily be integrated into future hardware version.

While the studies performed in this work were small pilot studies, we obtained physiological signals better or comparable to instrumentation used in the clinic. The different sensing modalities can be adapted to different clinical needs and in combination with mobile technologies will eventually enable the integration of real time data into the medical record system and therefore reduce hospital stays or prevent readmissions. However, to fully understand the scope and limitations of smart wearable health monitoring systems in general population or specific patient groups larger clinical trails are necessary. Additionally, this research only focused on the delivery of health care within the United States, in other parts of world the outcomes may be less prominent and need to be researched.

Besides, ethical, legal and privacy concerns an emerging field of research focuses on the extraction of relationships and patterns in large quantities of medical data. This field is often referred to as medical datamining (Big Data) and in combination with smart health care technologies that collect huge amounts of health information in larger population or patient groups will enable the identification of patterns and health risks to implement preventive measurements to reduce health care cost and enhancing the quality of life in a larger population segments.

APPENDIX

A. Schematics and Printed Circuit Board Layouts

A.1 Ambulatory Health Monitor

Ambulatory Health Monitor Rev. 3.2.2

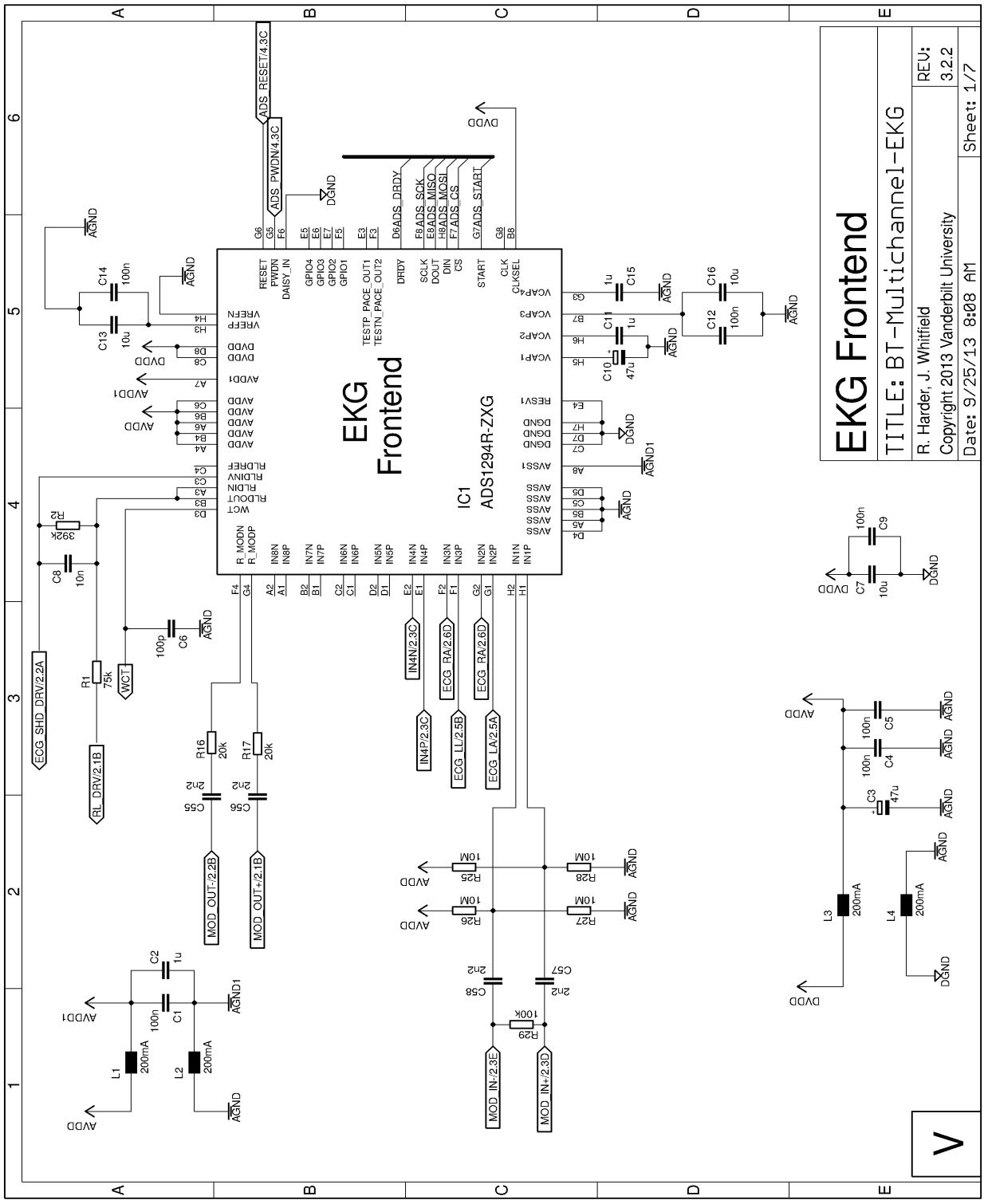

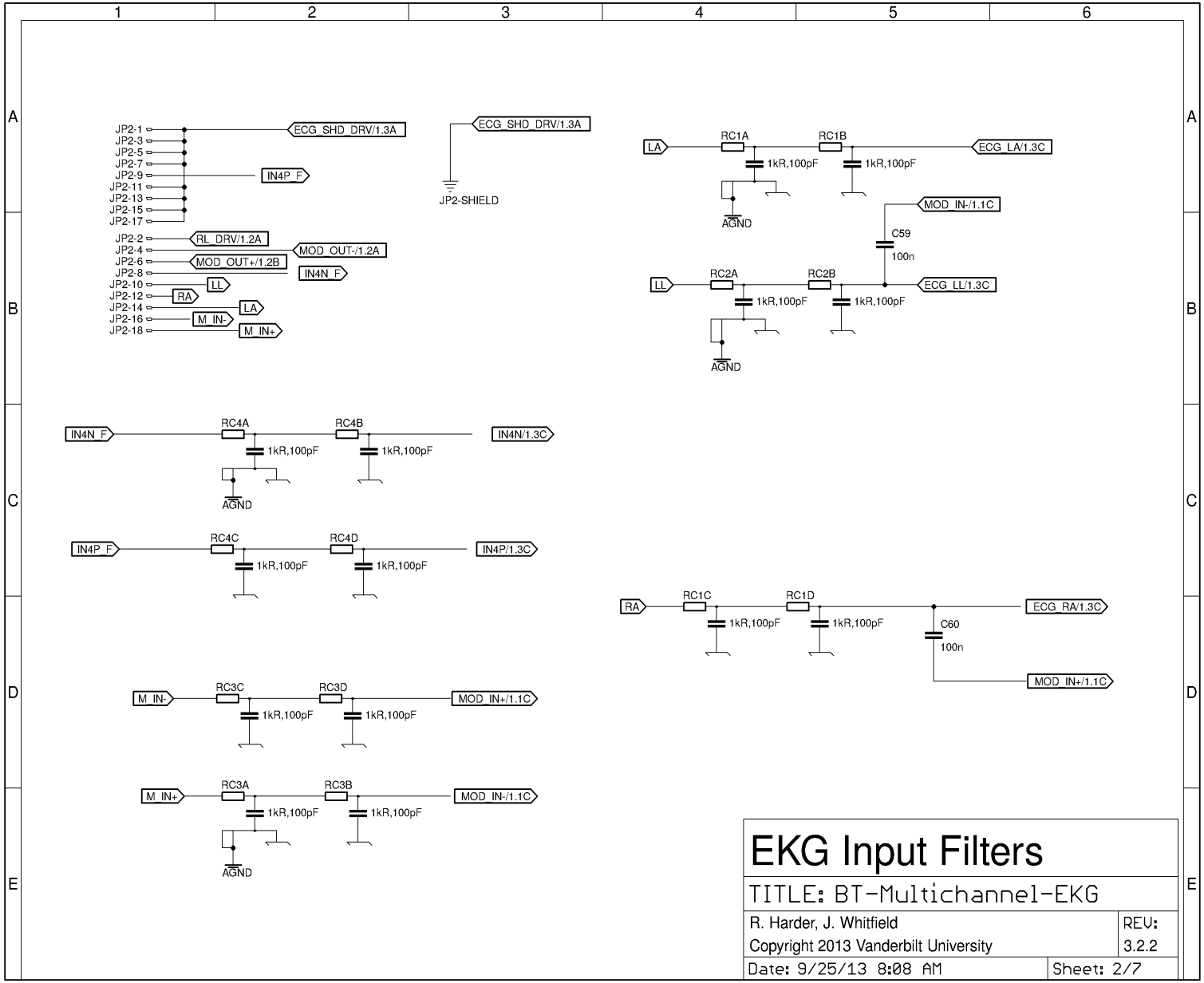
1
2
3
4
5
6
A
B
C
D
E
JP2-1
JP2-3
JP2-5
JP2-7
JP2-9
JP2-11
JP2-13
JP2-15
JP2-17
ECG_SHD_DRV/1.3A
IN4P_F
JP2-2
JP2-4
JP2-6
JP2-8
JP2-10
JP2-12
JP2-14
JP2-16
JP2-18
RL_DRV/1.2A
MOD_OUT-/1.2A
MOD_OUT+/1.2B
IN4N_F
LL
RA
LA
M_IN-
M_IN+
ECG_SHD_DRV/1.3A
JP2-SHIELD
LA
RC1A
RC1B
1kR,100pF
1kR,100pF
ECG_LA/1.3C
AGND
MOD_IN-/1.1C
C59
100n
LL
RC2A
RC2B
1kR,100pF
1kR,100pF
ECG_LL/1.3C
AGND
IN4N_F
RC4A
RC4B
1kR,100pF
1kR,100pF
IN4N/1.3C
AGND
IN4P_F
RC4C
RC4D
1kR,100pF
1kR,100pF
IN4P/1.3C
RA
RC1C
RC1D
1kR,100pF
1kR,100pF
C60
100n
ECG_RA/1.3C
MOD_IN+/1.1C
M_IN-
RC3C
RC3D
1kR,100pF
1kR,100pF
MOD_IN+/1.1C
M_IN+
RC3A
RC3B
1kR,100pF
1kR,100pF
MOD_IN-/1.1C
AGND
EKG Input Filters
TITLE: BT-Multichannel-EKG
R. Harder, J. Whitfield
Copyright 2013 Vanderbilt University
REV:
3.2.2
Date: 9/25/13 8:08 AM
Sheet: 2/7

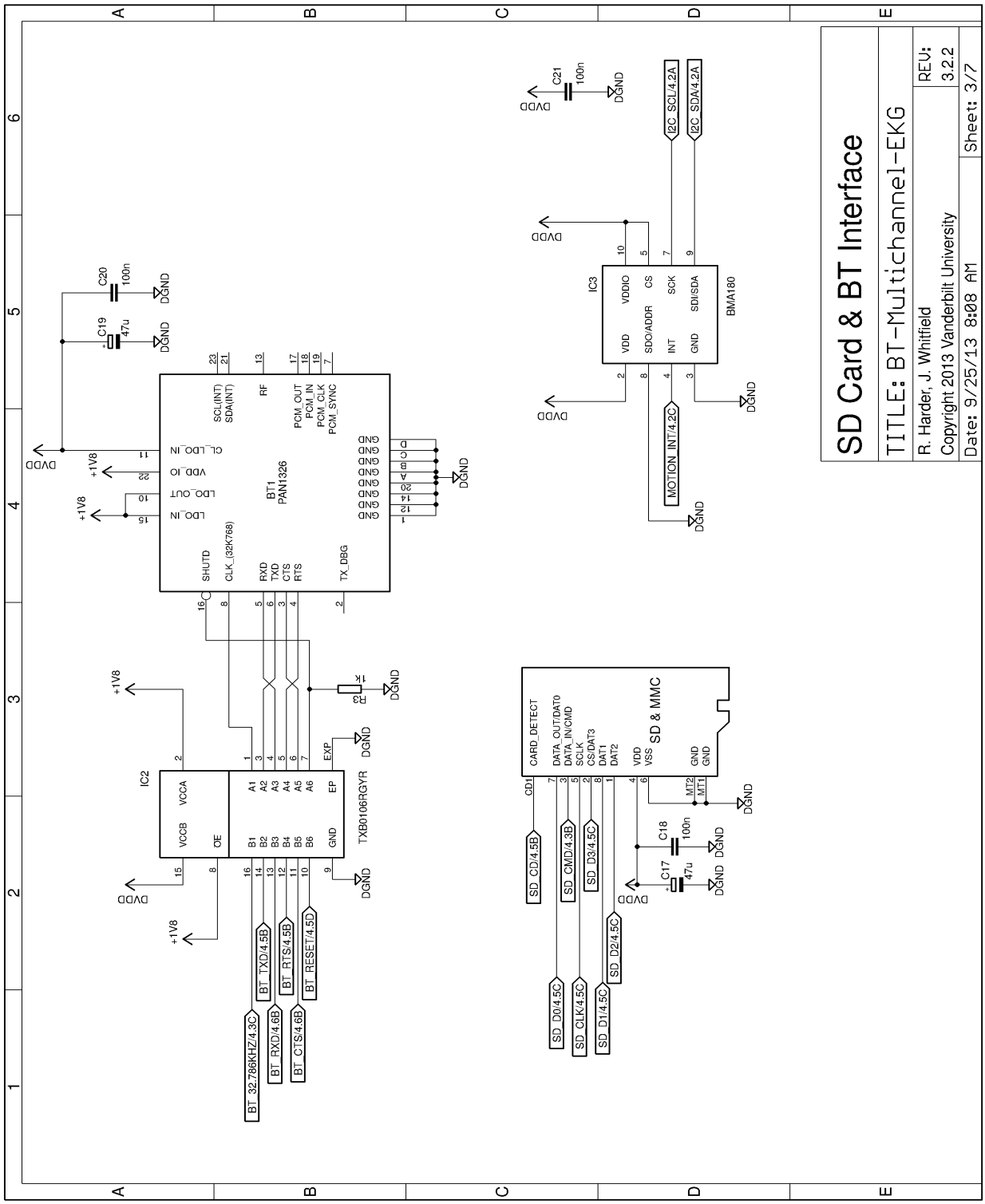
SD Card & BT Interface
TITLE: BT-Multichannel-EKG
R. Harder, J. Whitfield
Copyright 2013 Vanderbilt University
REV: 3.2.2
Date: 9/25/13 8:08 AM
Sheet: 3/7
BT1 PAN1326
IC2 TXB0106RGYR
IC3 BMA180
SD & MMC
C19 47u
C20 100n
C21 100n
C17 47u
C18 100n
R2
R3
DVDD
+1V8
DGND
BT_32.786KHZ/4.3C
BT_RXD/4.6B
BT_CTS/4.6B
BT_TXD/4.5B
BT_RTS/4.5B
BT_RESET/4.5D
SD_D0/4.5C
SD_CLK/4.5C
SD_D1/4.5C
SD_D2/4.5C
SD_D3/4.5C
SD_CMD/4.3B
SD_CD/4.5B
I2C_SCL/4.2A
I2C_SDA/4.2A
MOTION_INT/4.2C

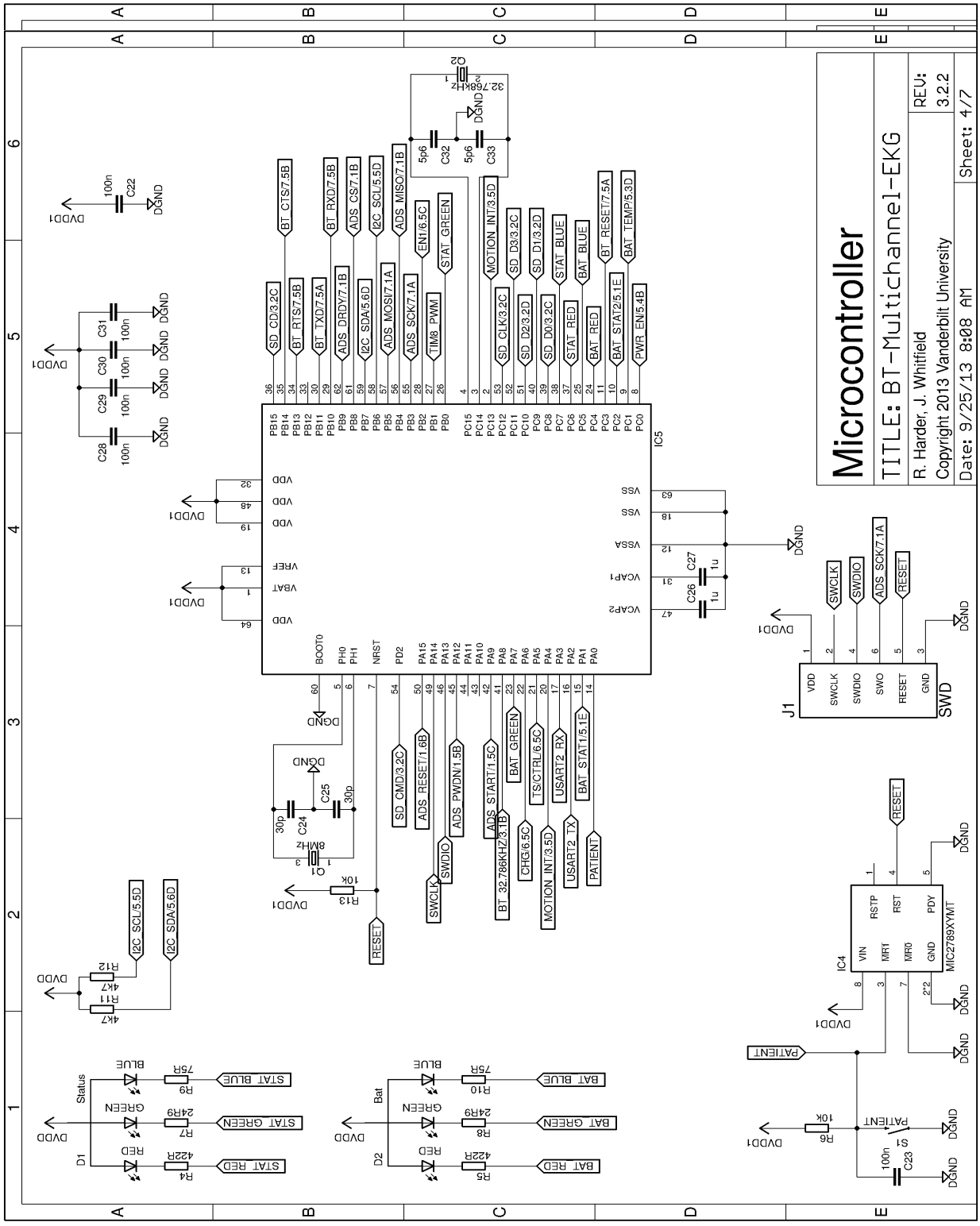
Microcontroller
TITLE: BT-Multichannel-EKG
R. Harder, J. Whitfield
Copyright 2013 Vanderbilt University
REV: 3.2.2
Date: 9/25/13 8:08 AM
Sheet: 4/7
IC5
J1
SWD
IC4
MIC2789XYMT
Q1
Q2
Status
Bat
D1
D2

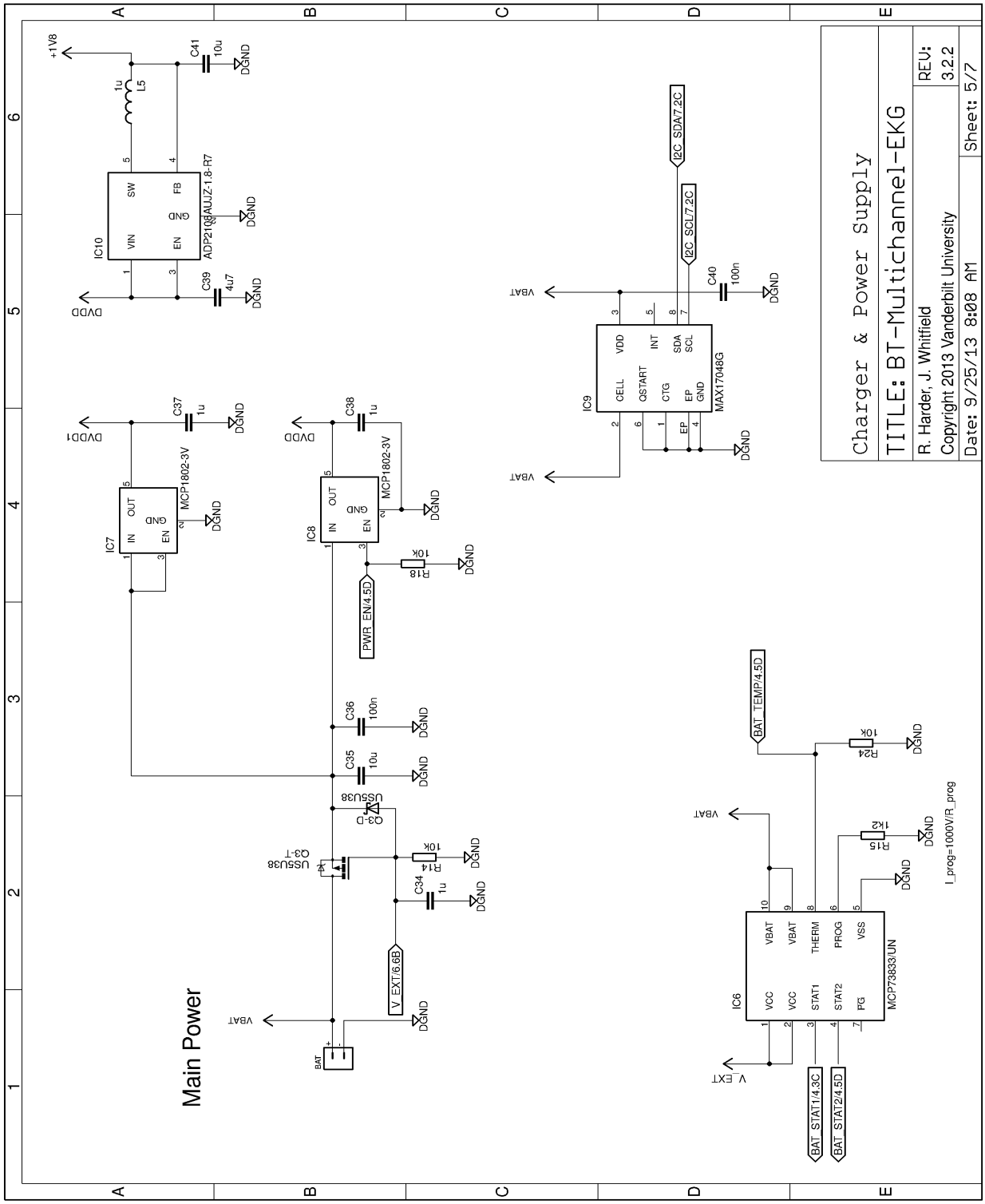
Charger & Power Supply
TITLE: BT-Multichannel-EKG
R. Harder, J. Whitfield
Copyright 2013 Vanderbilt University
REV: 3.2.2
Date: 9/25/13 8:08 AM
Sheet: 5/7
Main Power
+1V8
DVDD
DVDD1
VBAT
DGND
ADP2108AUJZ-1.8-R7
MCP1802-3V
MAX17048G
MCP73833/UN
I_prog=1000V/R_prog
PWR_EN/4.5D
V_EXT/6.6B
BAT_TEMP/4.5D
BAT_STAT1/4.3C
BAT_STAT2/4.5D
I2C_SDA/7.2C
I2C_SCL/7.2C

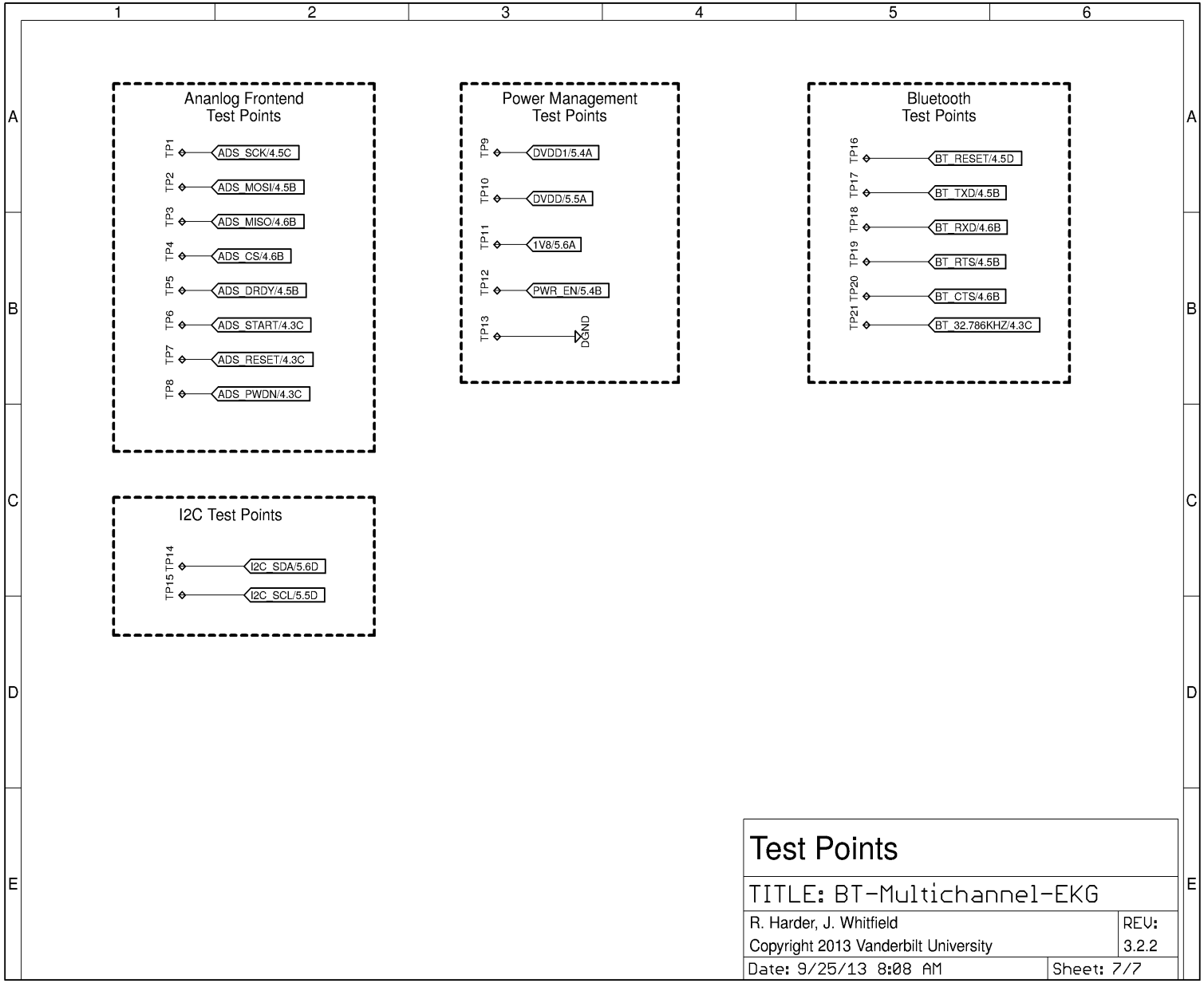
1
2
3
4
5
6
A
B
C
D
E
Ananlog Frontend
Test Points
TP1
ADS_SCK/4.5C
TP2
ADS_MOSI/4.5B
TP3
ADS_MISO/4.6B
TP4
ADS_CS/4.6B
TP5
ADS_DRDY/4.5B
TP6
ADS_START/4.3C
TP7
ADS_RESET/4.3C
TP8
ADS_PWDN/4.3C
Power Management
Test Points
TP9
DVDD1/5.4A
TP10
DVDD/5.5A
TP11
1V8/5.6A
TP12
PWR_EN/5.4B
TP13
DGND
Bluetooth
Test Points
TP16
BT_RESET/4.5D
TP17
BT_TXD/4.5B
TP18
BT_RXD/4.6B
TP19
BT_RTS/4.5B
TP20
BT_CTS/4.6B
TP21
BT_32.786KHZ/4.3C
I2C Test Points
TP14
I2C_SDA/5.6D
TP15
I2C_SCL/5.5D
Test Points
TITLE: BT-Multichannel-EKG
R. Harder, J. Whitfield
REV:
3.2.2
Copyright 2013 Vanderbilt University
Date: 9/25/13 8:08 AM
Sheet: 7/7

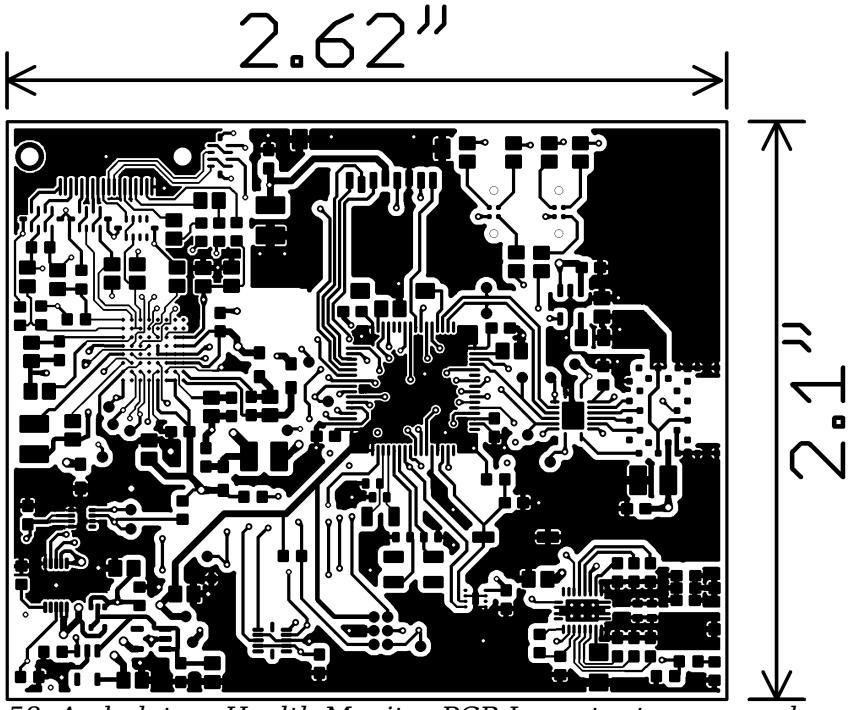

Figure 58: Ambulatory Health Monitor PCB Layout - top copper layer

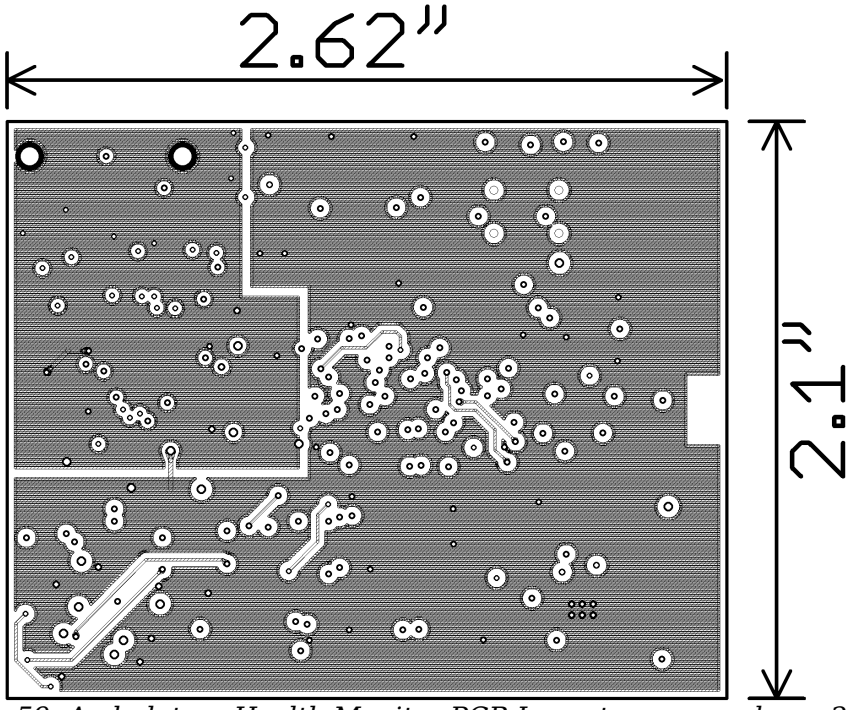

Figure 59: Ambulatory Health Monitor PCB Layout - copper layer 2

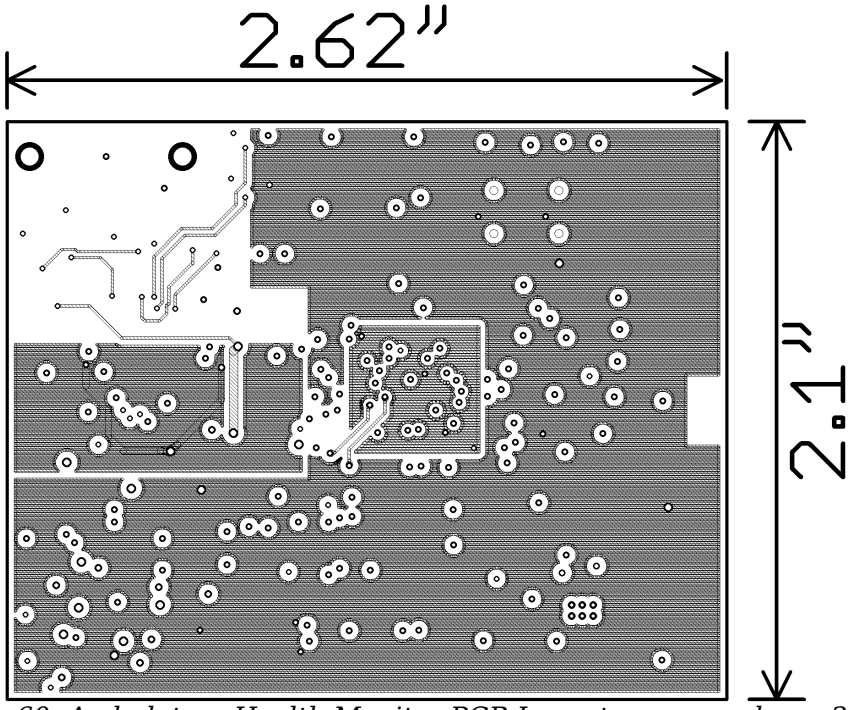

Figure 60: Ambulatory Health Monitor PCB Layout - copper layer 3

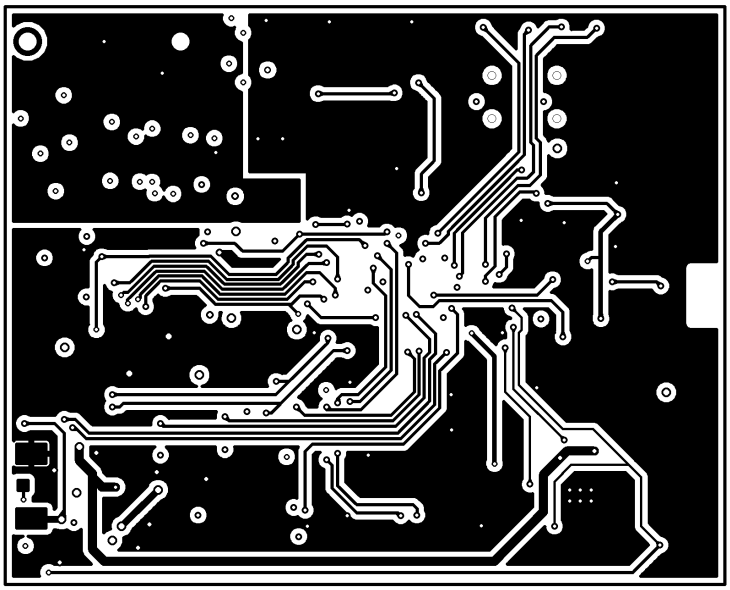

Figure 61: Ambulatory Health Monitor PCB Layout - bottom copper layer

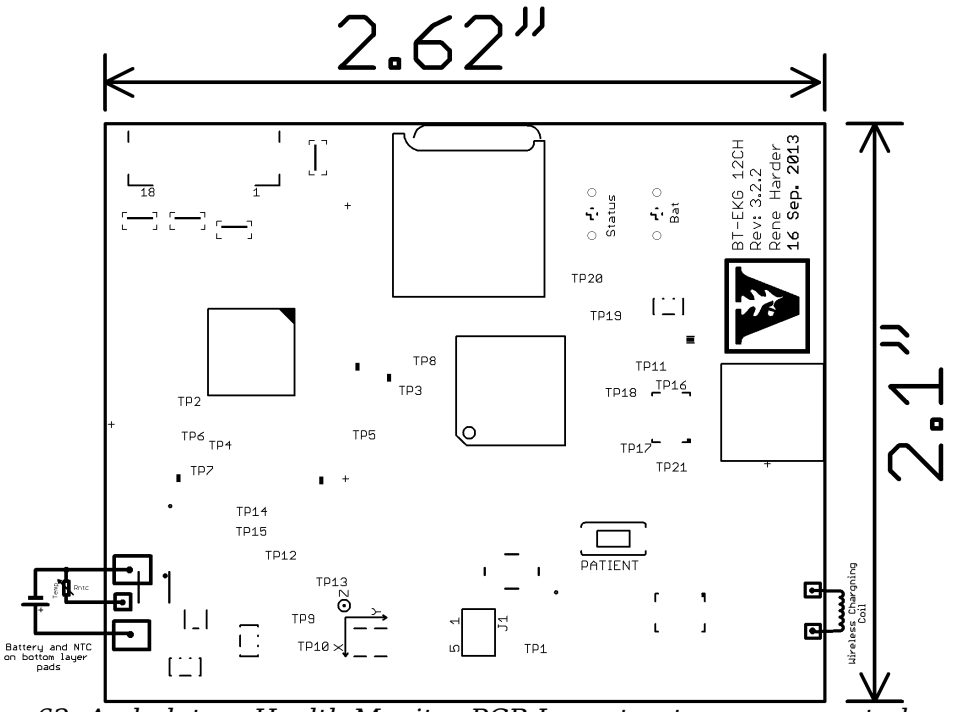

Figure 62: Ambulatory Health Monitor PCB Layout - top component placement

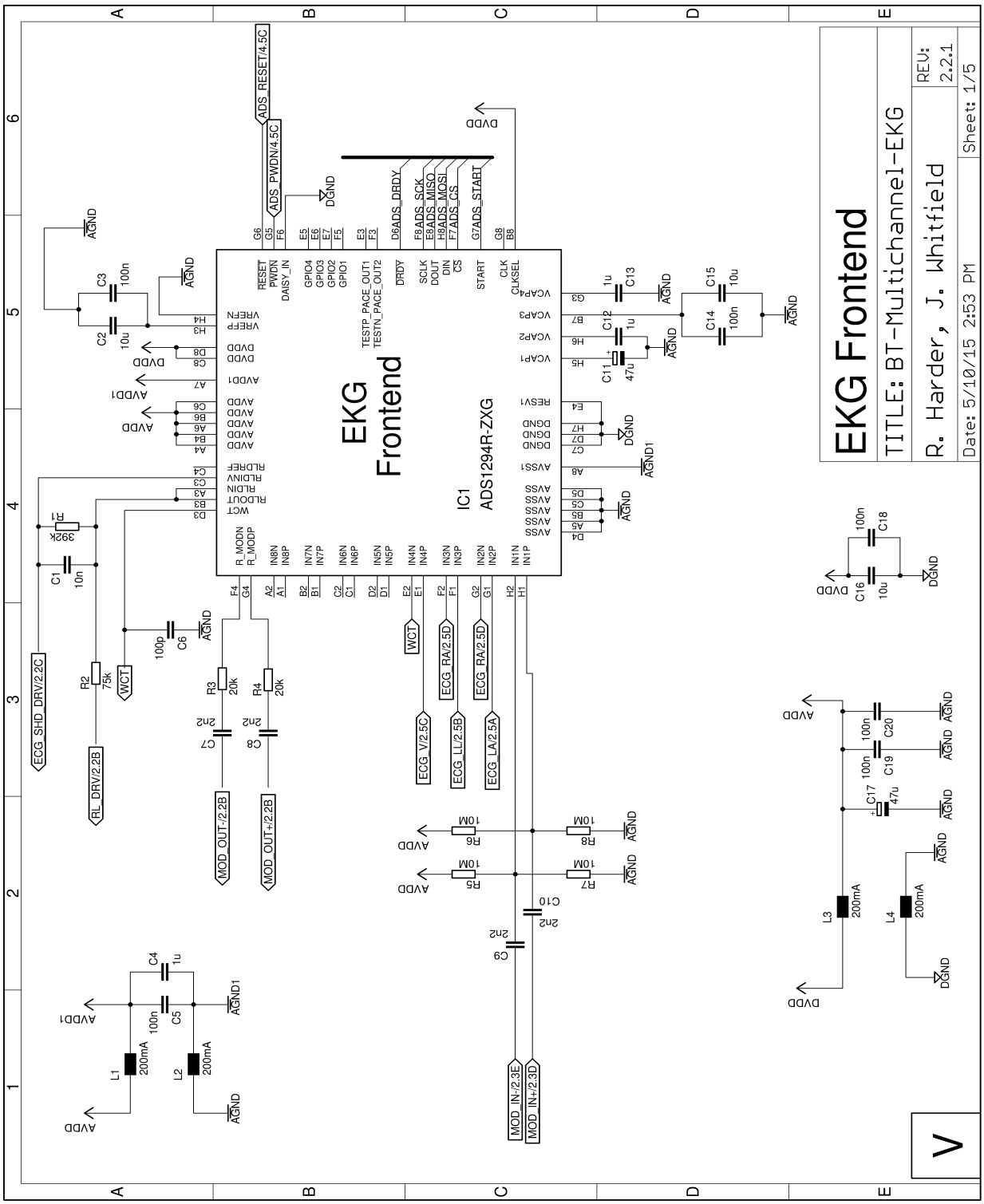
EKG Frontend
TITLE: BT-Multichannel-EKG
R. Harder, J. Whitfield
REV: 2.2.1
Date: 5/10/15 2:53 PM
Sheet: 1/5
IC1
ADS1294R-ZXG
ADS_RESET/4.5C
ADS_PWDN/4.5C
D6ADS_DRDY
F8ADS_SCK
E8ADS_MISO
H9ADS_MOSI
F7ADS_CS
G7ADS_START
ECG_SHD_DRV/2.2C
RL_DRV/2.2B
WCT
ECG_RA/2.5D
ECG_V/2.5C
ECG_LL/2.5B
ECG_LA/2.5A
MOD_OUT-/2.2B
MOD_OUT+/2.2B
MOD_IN-/2.3E
MOD_IN+/2.3D
AVDD
AVDD1
DVDD
AGND
AGND1
DGND

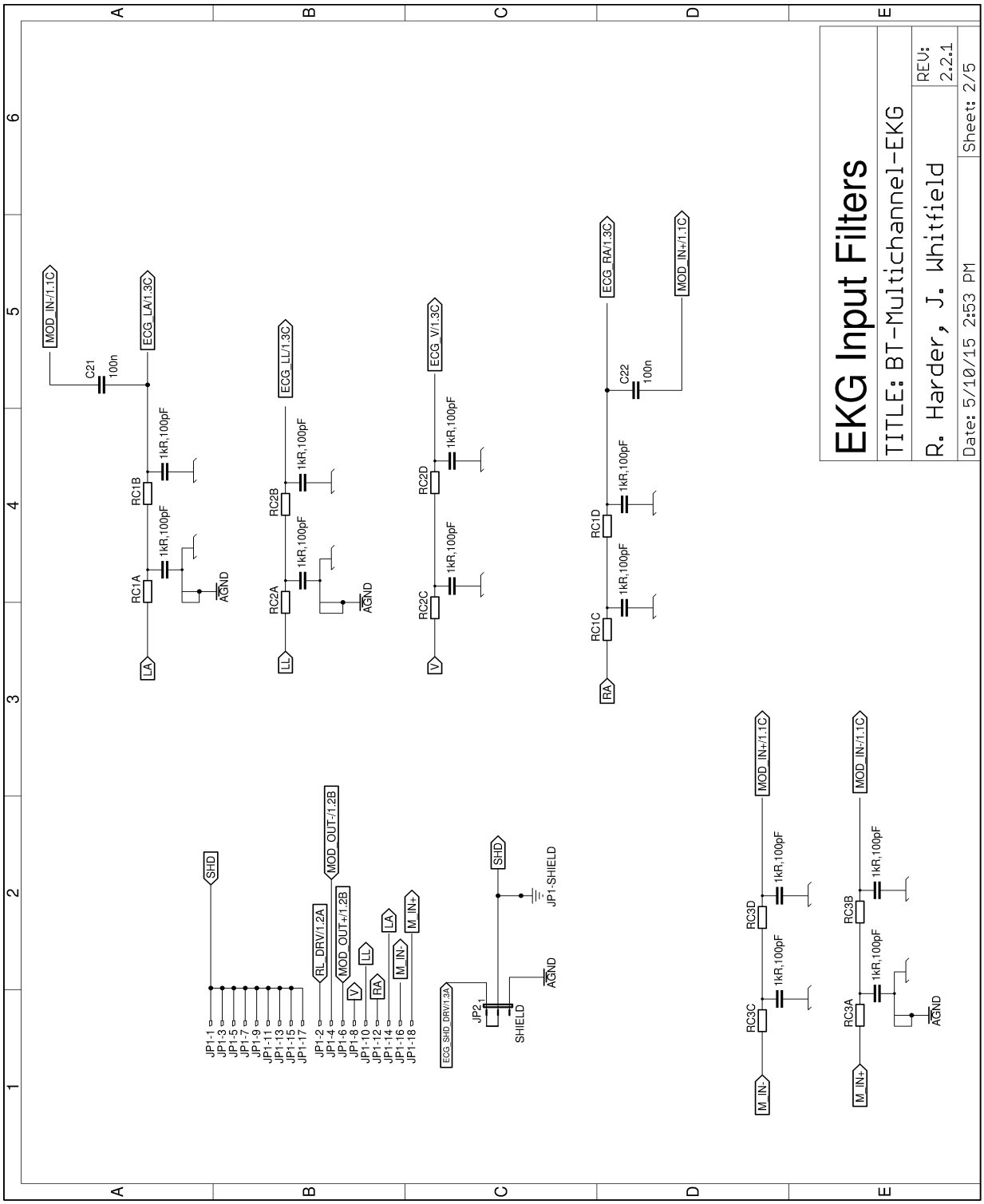
EKG Input Filters
TITLE: BT-Multichannel-EKG
R. Harder, J. Whitfield
REV: 2.2.1
Date: 5/10/15 2:53 PM
Sheet: 2/5
MOD_IN-/1.1C
C21
100n
ECG_LA/1.3C
RC1B
1kR,100pF
RC1A
1kR,100pF
AGND
LA
ECG_LL/1.3C
RC2B
1kR,100pF
RC2A
1kR,100pF
AGND
LL
ECG_V/1.3C
RC2D
1kR,100pF
RC2C
1kR,100pF
V
ECG_RA/1.3C
C22
100n
MOD_IN+/1.1C
RC1D
1kR,100pF
RC1C
1kR,100pF
RA
SHD
RL_DRV/1.2A
MOD_OUT-/1.2B
MOD_OUT+/1.2B
V
LL
RA
LA
M_IN-
M_IN+
JP1-1
JP1-3
JP1-5
JP1-7
JP1-9
JP1-11
JP1-13
JP1-15
JP1-17
JP1-2
JP1-4
JP1-6
JP1-8
JP1-10
JP1-12
JP1-14
JP1-16
JP1-18
ECG_SHD_DRV/1.3A
JP2
SHIELD
SHD
JP1-SHIELD
AGND
MOD_IN+/1.1C
RC3D
1kR,100pF
RC3C
1kR,100pF
M_IN-
MOD_IN-/1.1C
RC3B
1kR,100pF
RC3A
1kR,100pF
AGND
M_IN+

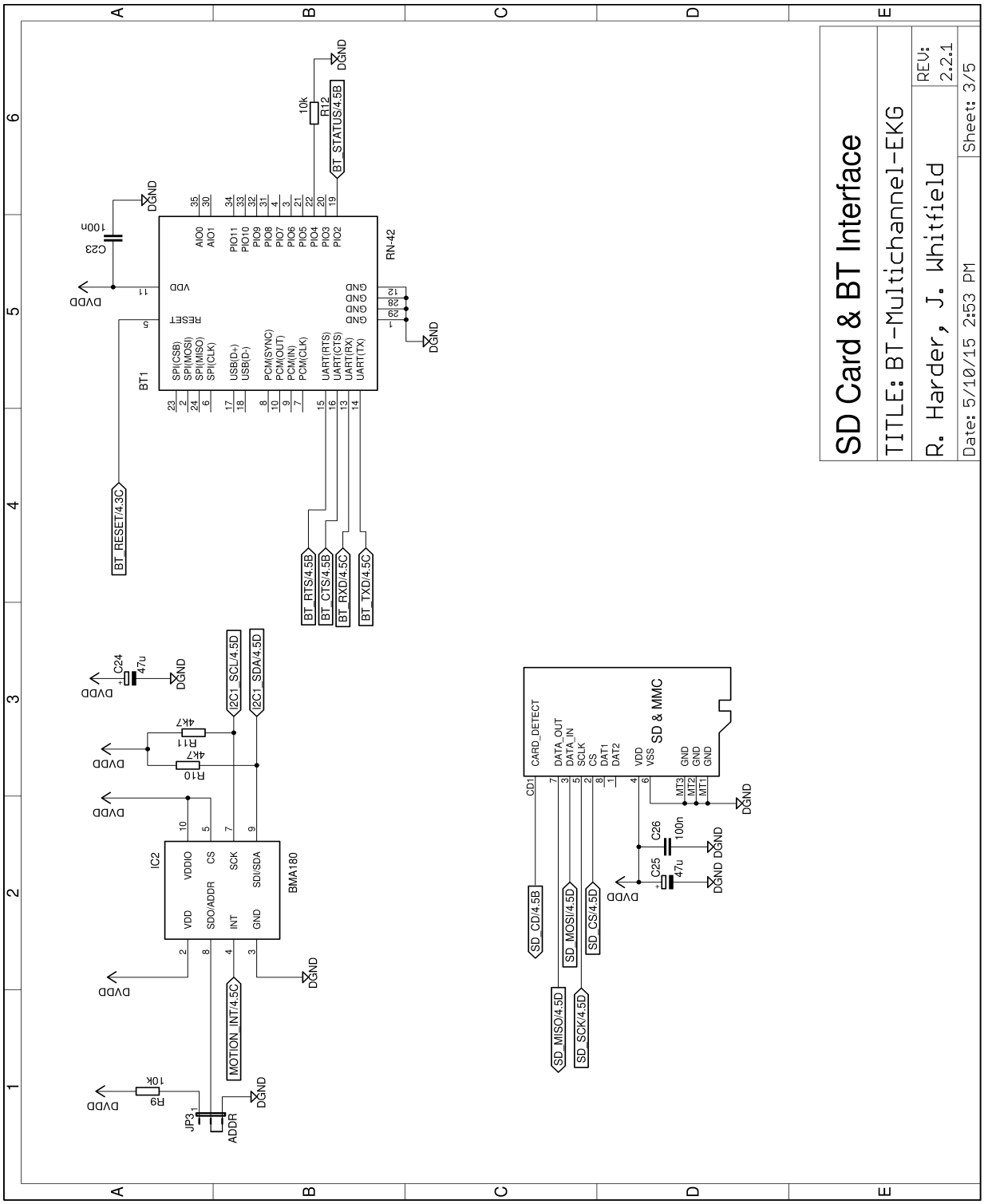
SD Card & BT Interface
TITLE: BT-Multichannel-EKG
R. Harder, J. Whitfield
REV: 2.2.1
Date: 5/10/15 2:53 PM
Sheet: 3/5
RN-42
BT1
BT_RESET/4.3C
BT_STATUS/4.5B
BT_RTS/4.5B
BT_CTS/4.5B
BT_RXD/4.5C
BT_TXD/4.5C
SD & MMC
SD_CD/4.5B
SD_MOSI/4.5D
SD_MISO/4.5D
SD_SCK/4.5D
SD_CS/4.5D
IC2
BMA180
I2C1_SCL/4.5D
I2C1_SDA/4.5D
MOTION_INT/4.5C
ADDR
DVDD
DGND

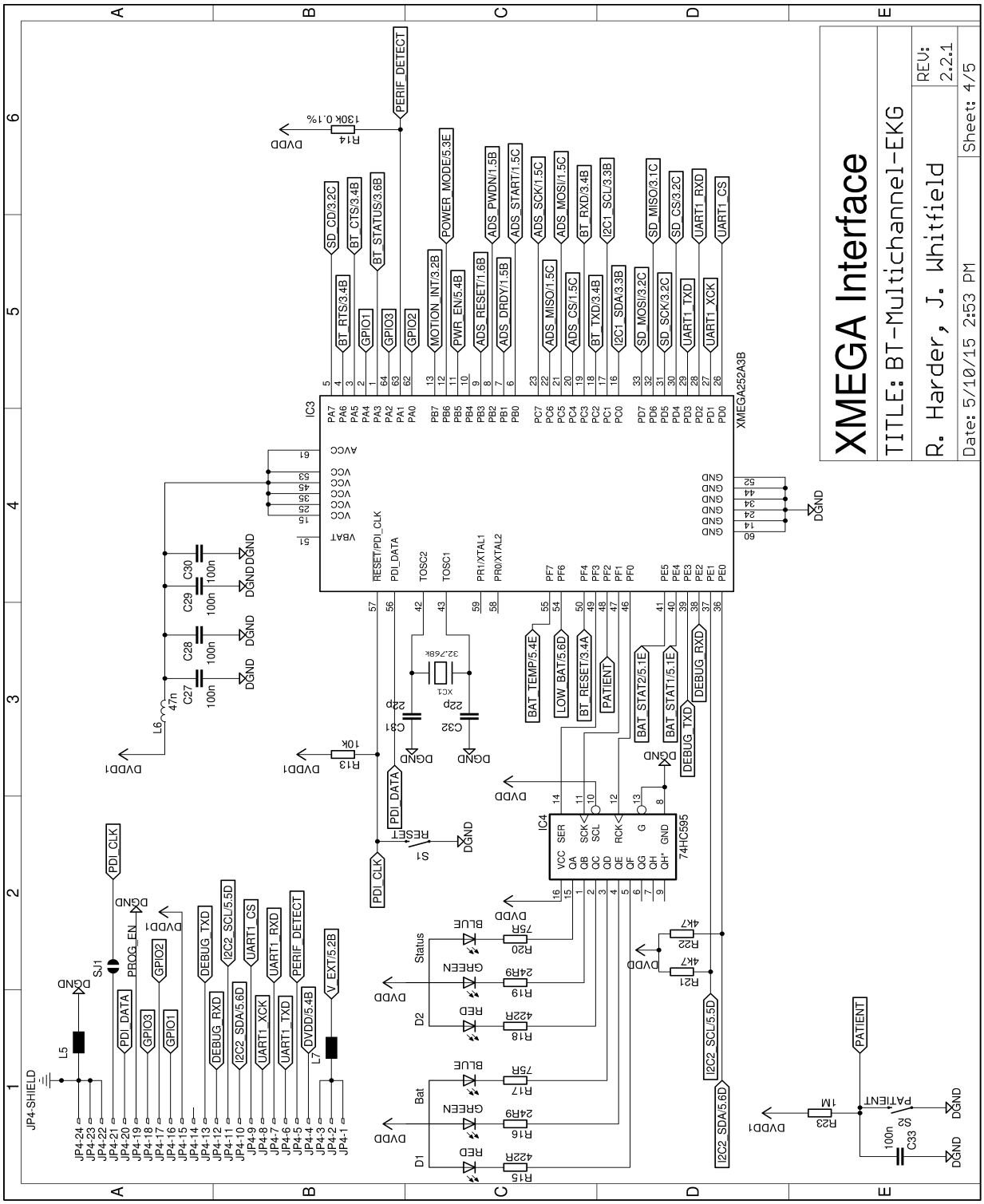
XMEGA Interface
TITLE: BT-Multichannel-EKG
R. Harder, J. Whitfield
REV: 2.2.1
Date: 5/10/15 2:53 PM
Sheet: 4/5
XMEGA252A3B
74HC595
PERIF_DETECT
POWER_MODE/5.3E
BT_STATUS/3.6B
BT_CTS/3.4B
BT_RTS/3.4B
SD_CD/3.2C
MOTION_INT/3.2B
PWR_EN/5.4B
ADS_RESET/1.6B
ADS_DRDY/1.5B
ADS_PWDN/1.5B
ADS_START/1.5C
ADS_SCK/1.5C
ADS_MISO/1.5C
ADS_MOSI/1.5C
ADS_CS/1.5C
BT_RXD/3.4B
BT_TXD/3.4B
I2C1_SCL/3.3B
I2C1_SDA/3.3B
SD_MISO/3.1C
SD_MOSI/3.2C
SD_SCK/3.2C
SD_CS/3.2C
UART1_RXD
UART1_TXD
UART1_XCK
UART1_CS
BAT_TEMP/5.4E
LOW_BAT/5.6D
BT_RESET/3.4A
PATIENT
BAT_STAT2/5.1E
BAT_STAT1/5.1E
DEBUG_RXD
DEBUG_TXD
PDI_DATA
PDI_CLK
RESET
I2C2_SDA/5.6D
I2C2_SCL/5.5D
DEBUG_TXD
DEBUG_RXD
UART1_CS
UART1_RXD
UART1_TXD
UART1_XCK
PERIF_DETECT
DVDD/5.4B
V_EXT/5.2B
PROG_EN
GPIO2
GPIO3
GPIO1
JP4-SHIELD
Status
Bat
D1
D2
RED
GREEN
BLUE
DVDD
DVDD1
DGND
130K 0.1%
10K
4K7
75R
422R
249R
47n
100n
22p
32.768K
1M

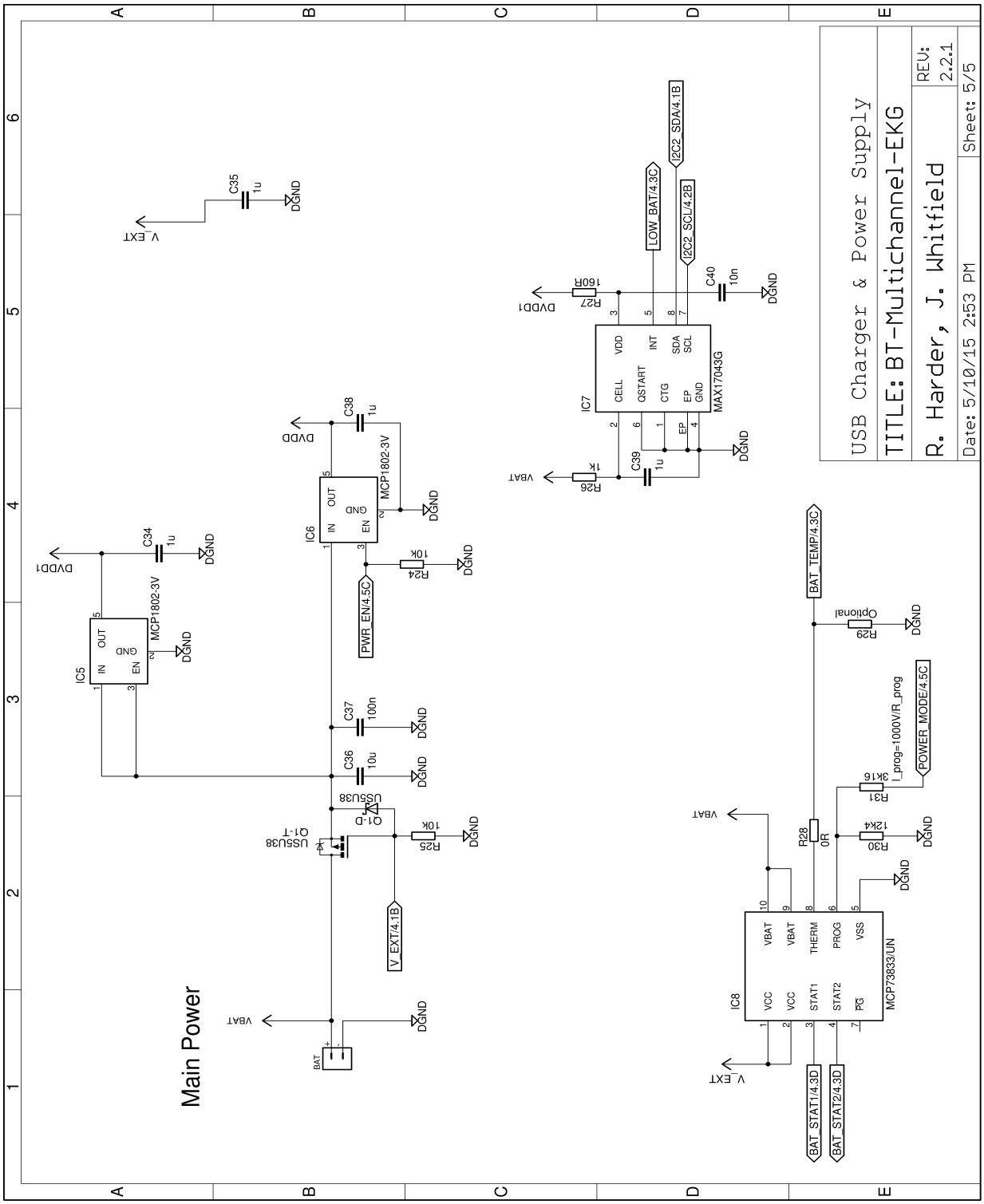
USB Charger & Power Supply
TITLE: BT-Multichannel-EKG
R. Harder, J. Whitfield
REV: 2.2.1
Date: 5/10/15 2:53 PM
Sheet: 5/5
Main Power
C35 1u
V_EXT
DGND
C38 1u
DVDD
C34 1u
DVDD1
IC6 MCP1802-3V
IC5 MCP1802-3V
IN OUT GND EN
R24 10K
PWR_EN/4.5C
C37 100n
C36 10u
Q1-T USSU38
Q1-B USSU38
R25 10K
V_EXT/4.1B
VBAT
BAT
IC7 MAX17043G
CELL VDD QSTART INT CTG SDA EP SCL GND
R27 160R
C40 10n
C39 1u
R26 1K
LOW_BAT/4.3C
I2C2_SDA/4.1B
I2C2_SCL/4.2B
IC8 MCP73833/UN
VCC VBAT THERM PROG VSS STAT1 STAT2 PG
BAT_TEMP/4.3C
R29 Optional
R28 0R
R31 3K16
I_prog=1000V/R_prog
POWER_MODE/4.5C
R30 12K4
BAT_STAT1/4.3D
BAT_STAT2/4.3D

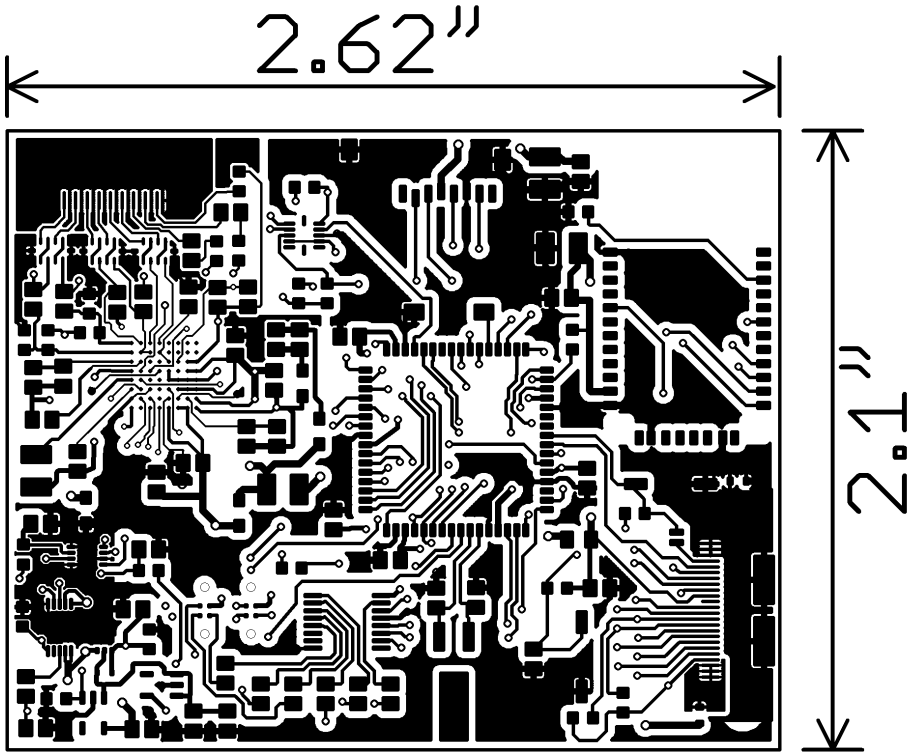

Figure 63: Ambulatory Health Monitor PCB Layout Rev. 2.2.1 - top copper layer

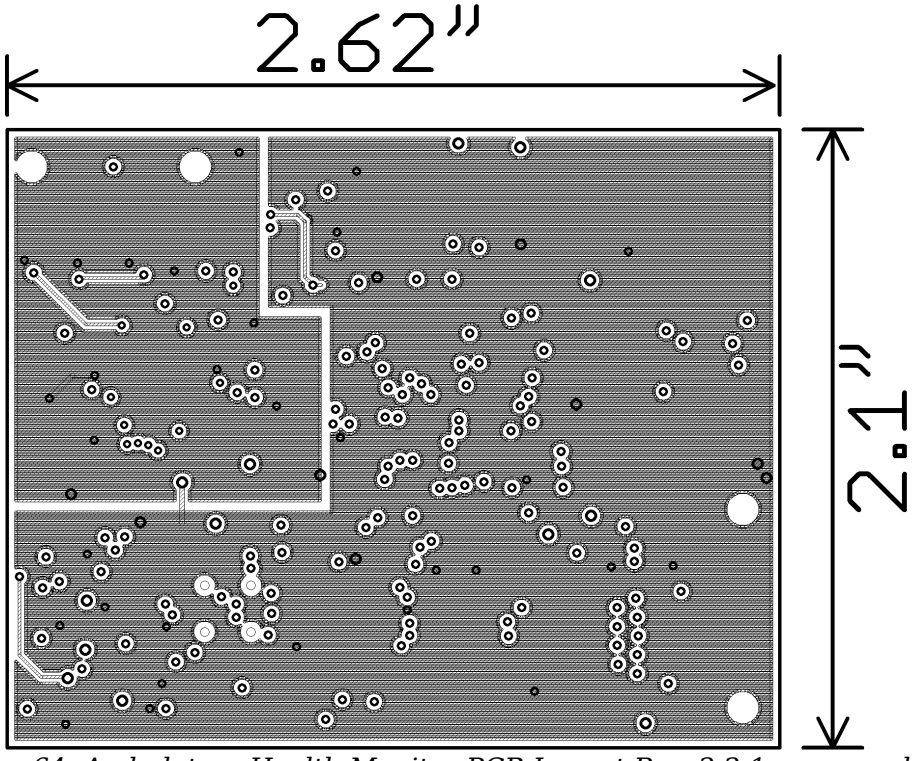

Figure 64: Ambulatory Health Monitor PCB Layout Rev. 2.2.1 - copper layer 2

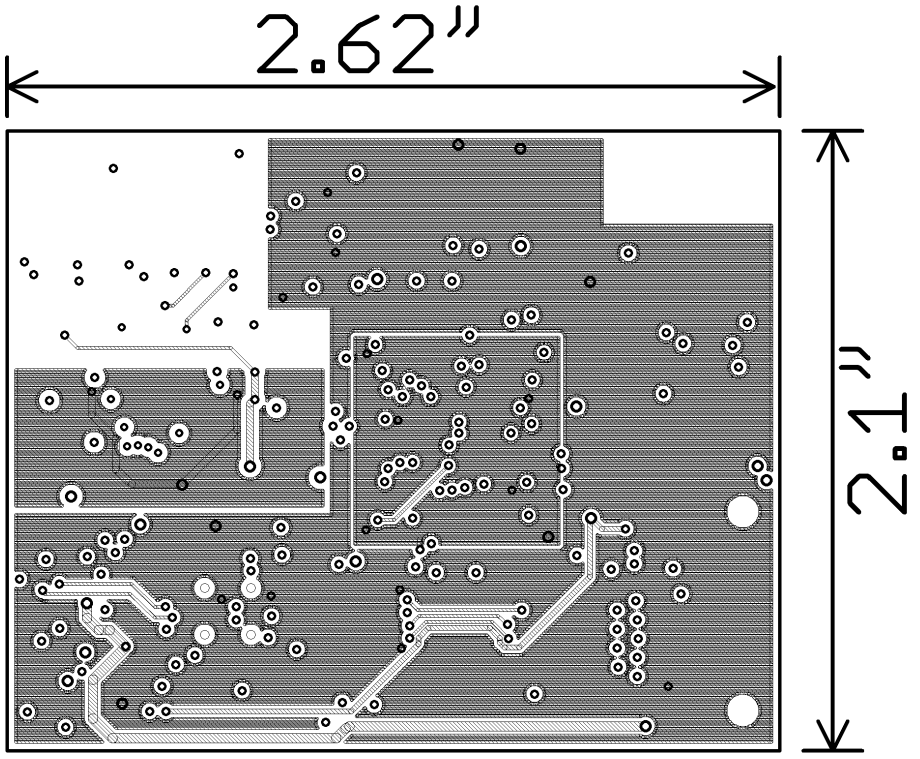

Figure 65: Ambulatory Health Monitor PCB Layout Rev. 2.2.1 - copper layer 3

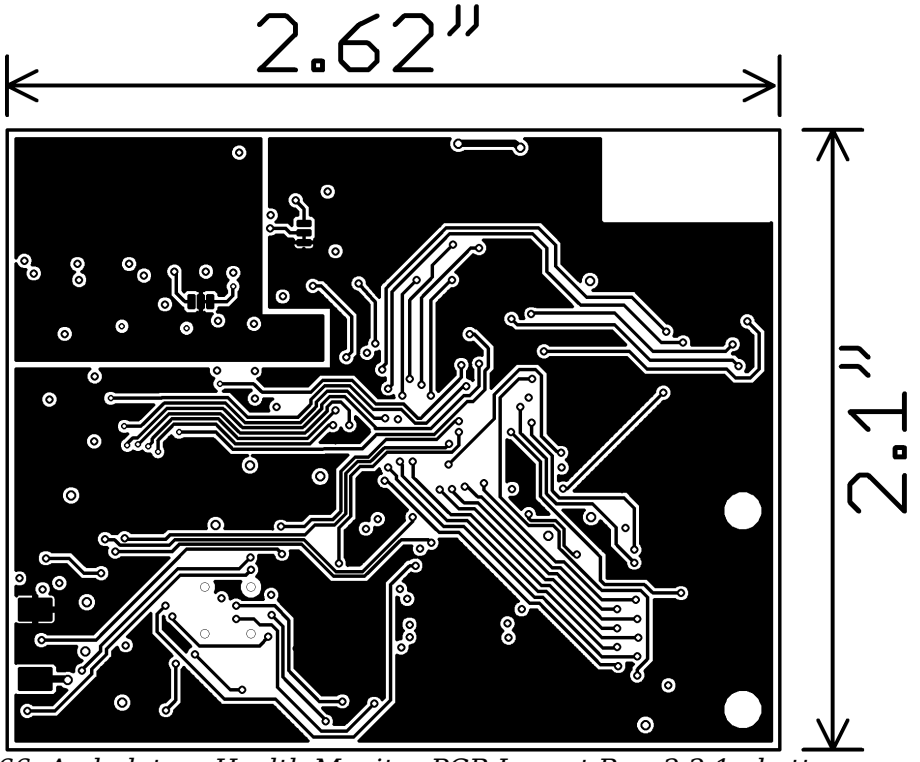

Figure 66: Ambulatory Health Monitor PCB Layout Rev. 2.2.1 - bottom copper layer

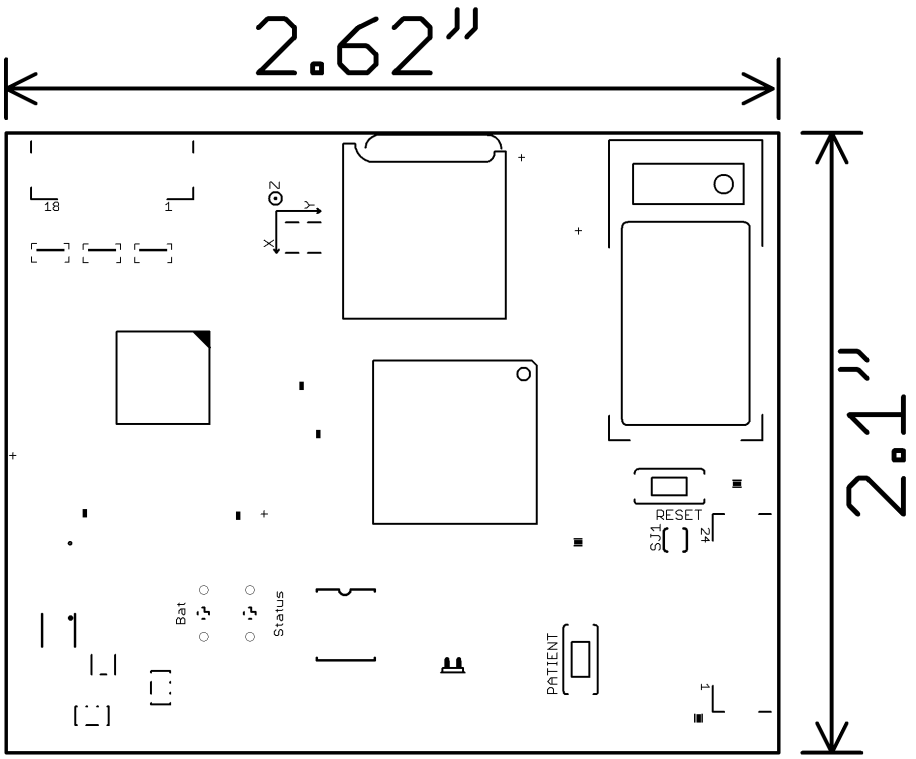

Figure 67: Ambulatory Health Monitor PCB Layout Rev. 2.2.1 - top component placement.

A.2 Multi-frequency Impedance Spectrometer

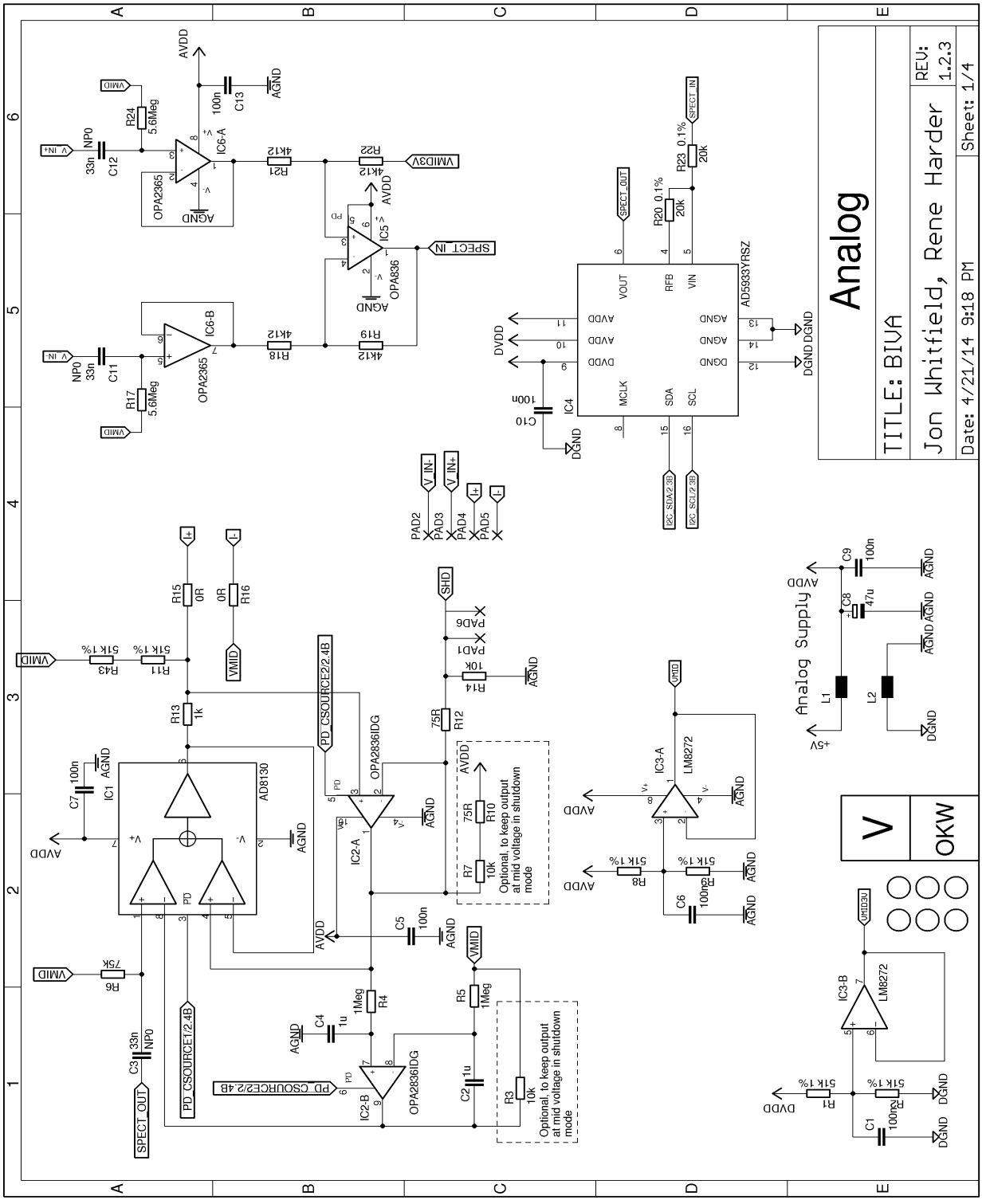

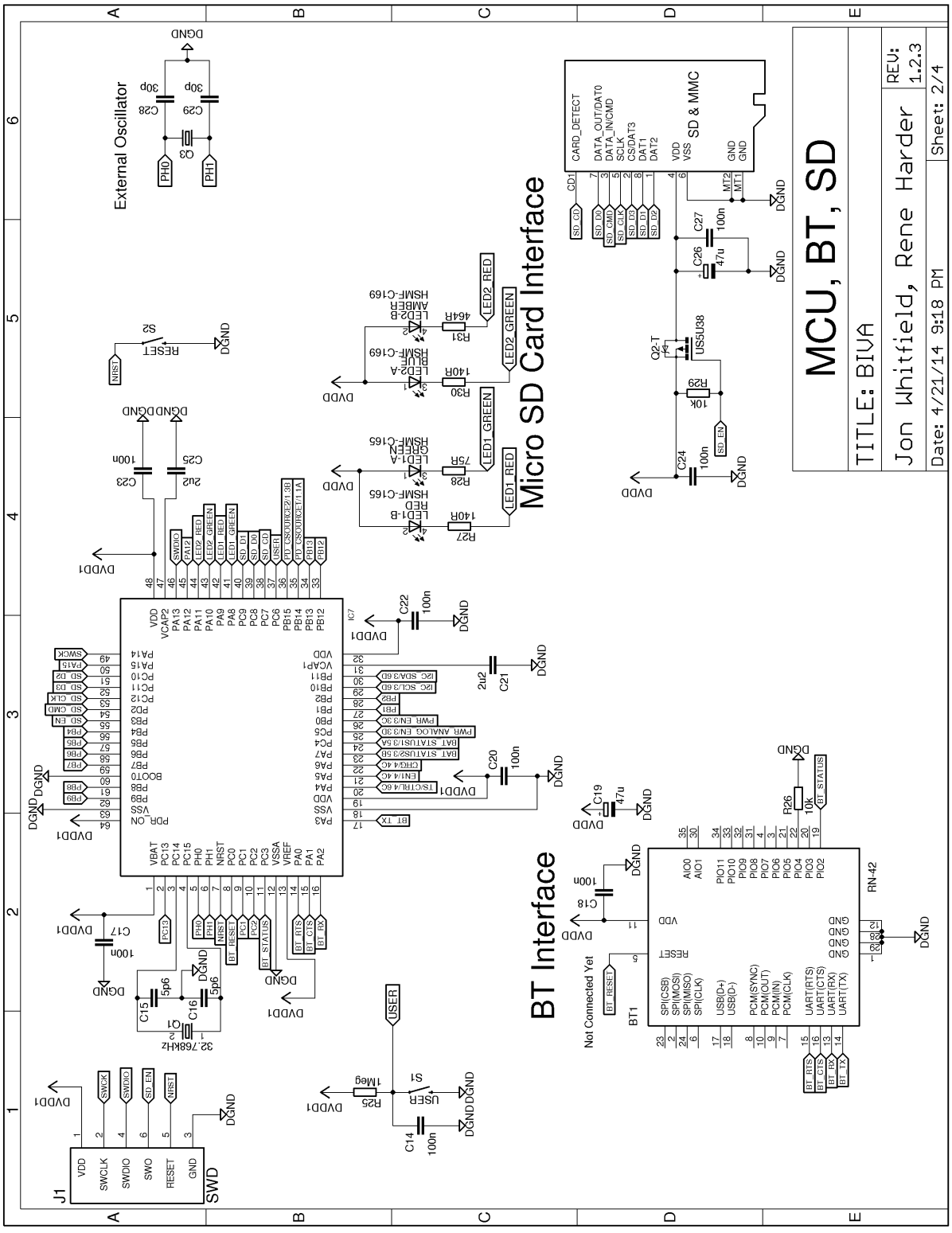
MCU, BT, SD
TITLE: BIVA
Jon Whitfield, Rene Harder
REV: 1.2.3
Date: 4/21/14 9:18 PM
Sheet: 2/4
Micro SD Card Interface
BT Interface
External Oscillator
SD & MMC
RN-42
Not Connected Yet

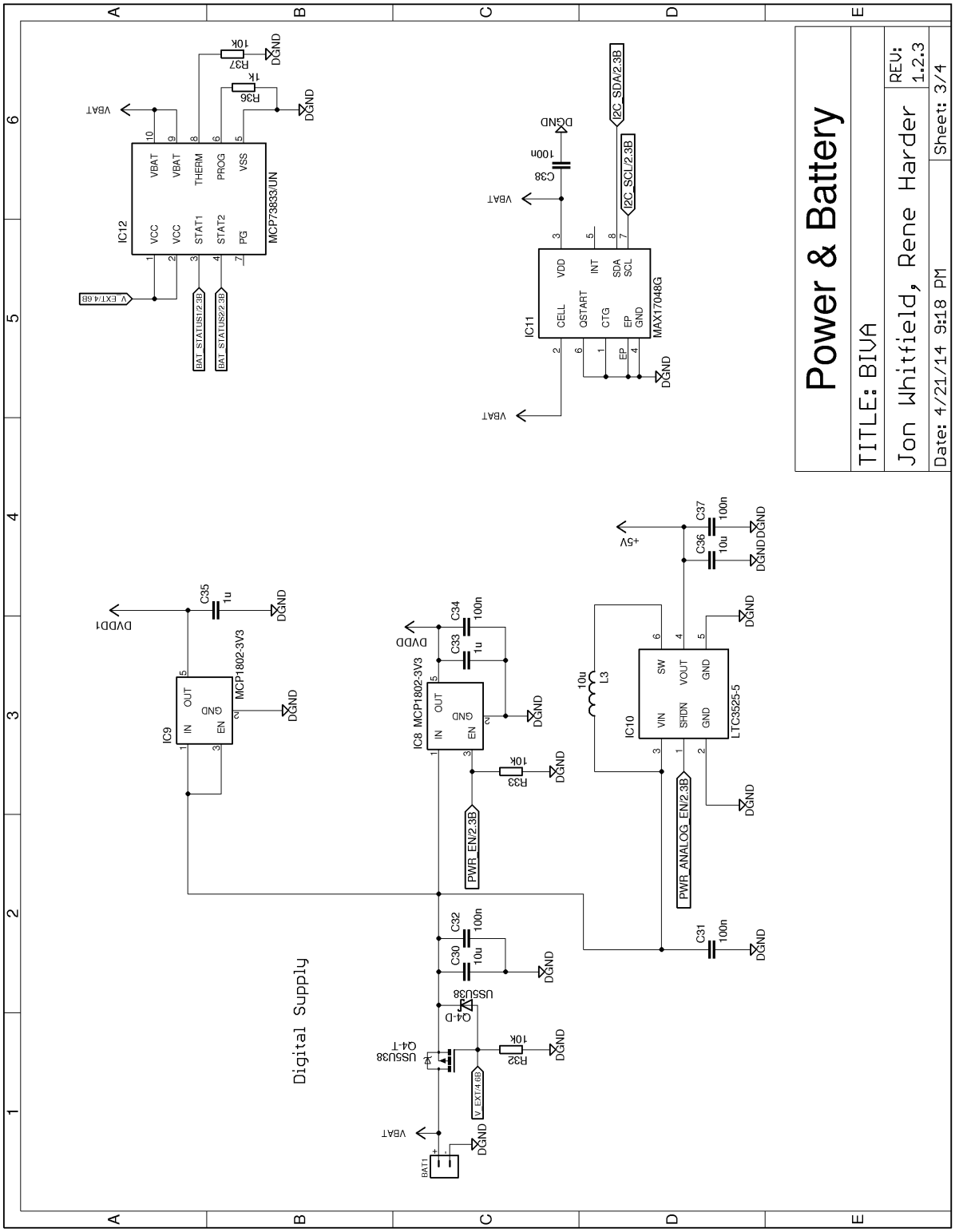
Power & Battery
TITLE: BIVA
Jon Whitfield, Rene Harder
REV: 1.2.3
Date: 4/21/14 9:18 PM
Sheet: 3/4
Digital Supply
IC12
MCP73833/UN
VBAT
VBAT
THERM
PROG
VSS
VCC
VCC
STAT1
STAT2
PG
R37
10K
R36
1K
DGND
V_EXT/4.6B
BAT_STATUS1/2.3B
BAT_STATUS2/2.3B
IC11
MAX17048G
VDD
INT
CELL
QSTART
CTG
SDA
SCL
EP
GND
C38
100n
I2C_SDA/2.3B
I2C_SCL/2.3B
DGND
IC9
MCP1802-3V3
IN
OUT
GND
EN
C35
1u
DVDD1
IC8
MCP1802-3V3
C34
100n
C33
1u
DVDD
R33
10K
PWR_EN/2.3B
IC10
LTC3525-5
VIN
SW
VOUT
GND
SHDN
L3
10u
+5V
C37
100n
C36
10u
C31
100n
PWR_ANALOG_EN/2.3B
C32
100n
C30
10u
US5U38
Q4-D
Q4-T
R32
10K
V_EXT/4.6B
BAT1

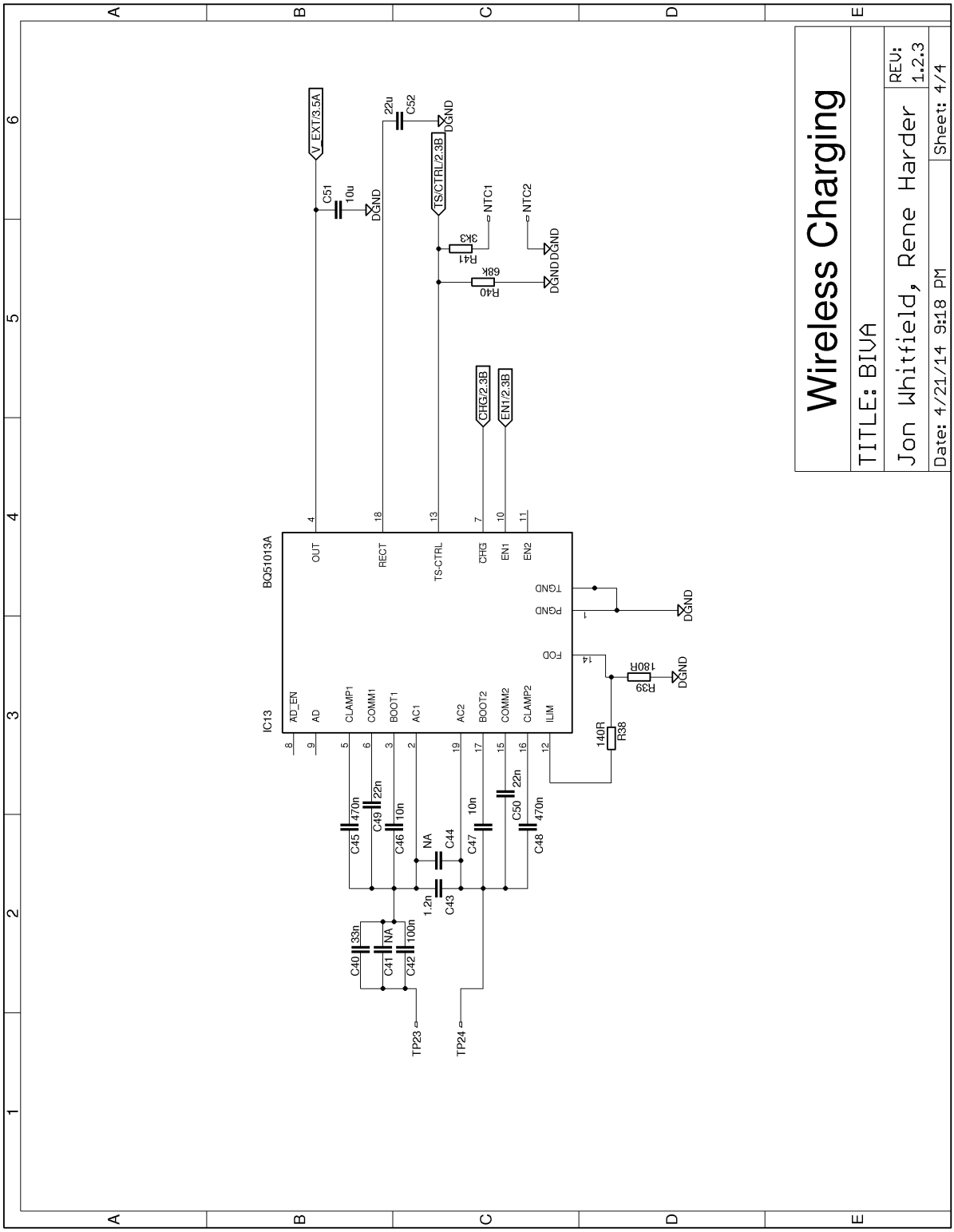
Wireless Charging
TITLE: BIVA
Jon Whitfield, Rene Harder
REV: 1.2.3
Date: 4/21/14 9:18 PM
Sheet: 4/4
IC13
BQ51013A
V_EXT/3.5A
C51
10u
DGND
22u
C52
TS/CTRL/2.3B
R41
3k3
NTC1
R40
68k
NTC2
CHG/2.3B
EN1/2.3B
OUT
RECT
TS-CTRL
CHG
EN1
EN2
TGND
PGND
FOD
AD_EN
AD
CLAMP1
COMM1
BOOT1
AC1
AC2
BOOT2
COMM2
CLAMP2
ILIM
180R
R39
140R
R38
C45
470n
C49
22n
C46
10n
NA
C44
C47
10n
C50
22n
C48
470n
1.2n
C43
C40
33n
C41
NA
C42
100n
TP23
TP24

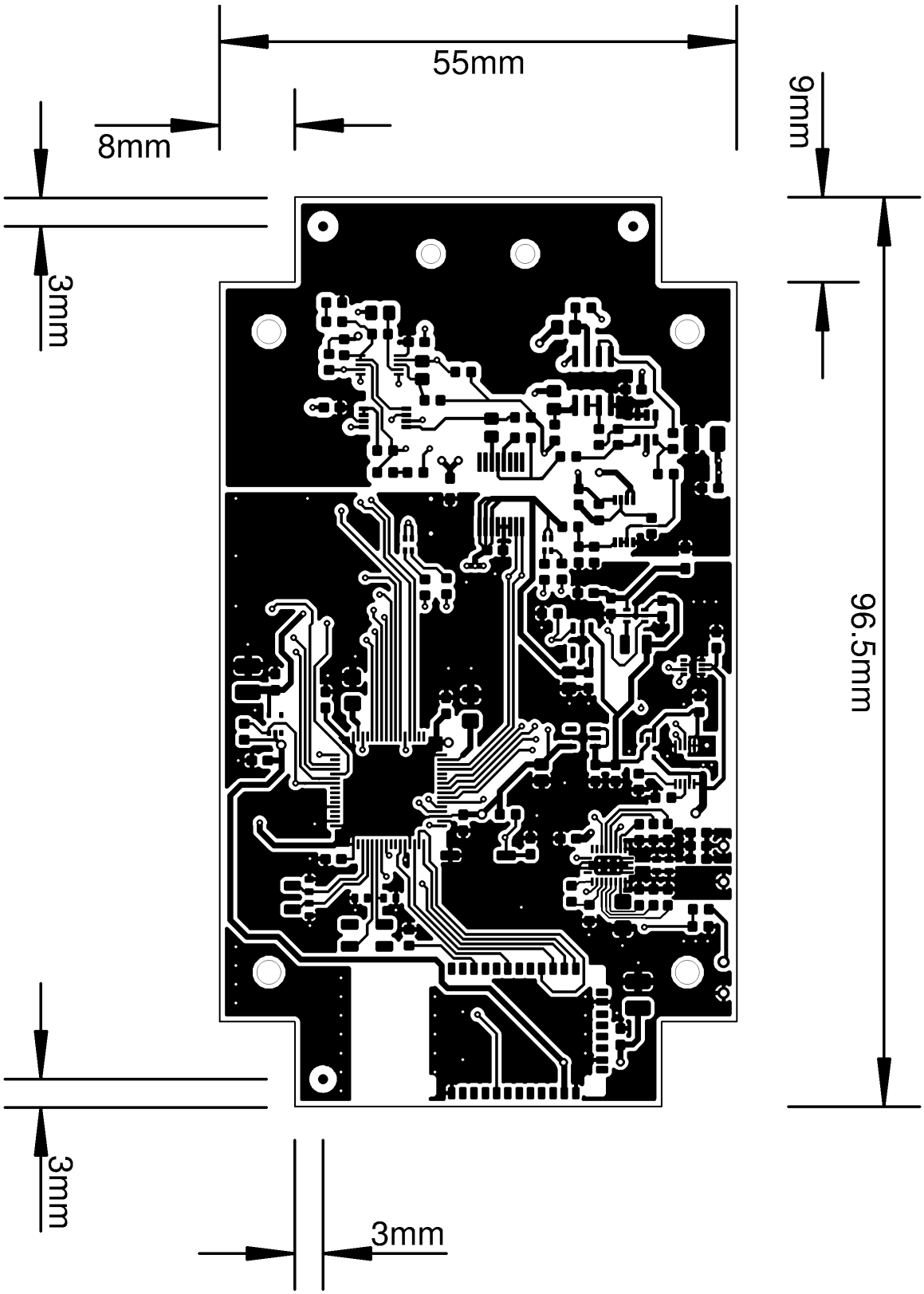

Figure 68: Multi-frequency Impedance Spectrometer PCB layout - top copper layer

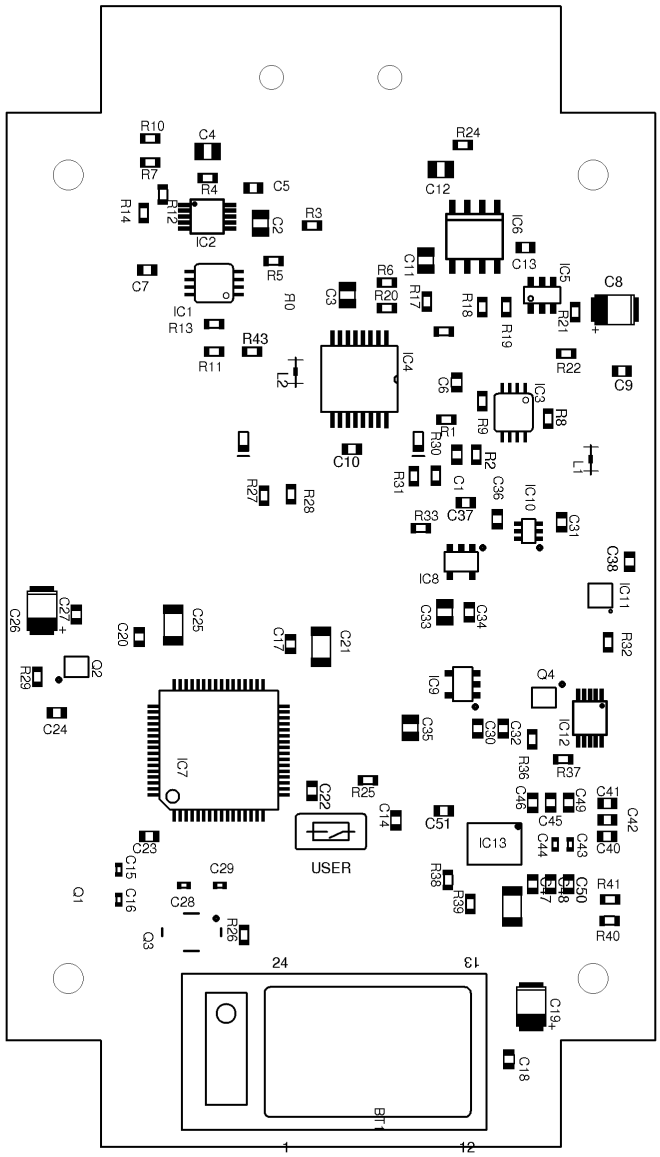

Figure 69: Multi-frequency Impedance Spectrometer PCB layout - top component placement

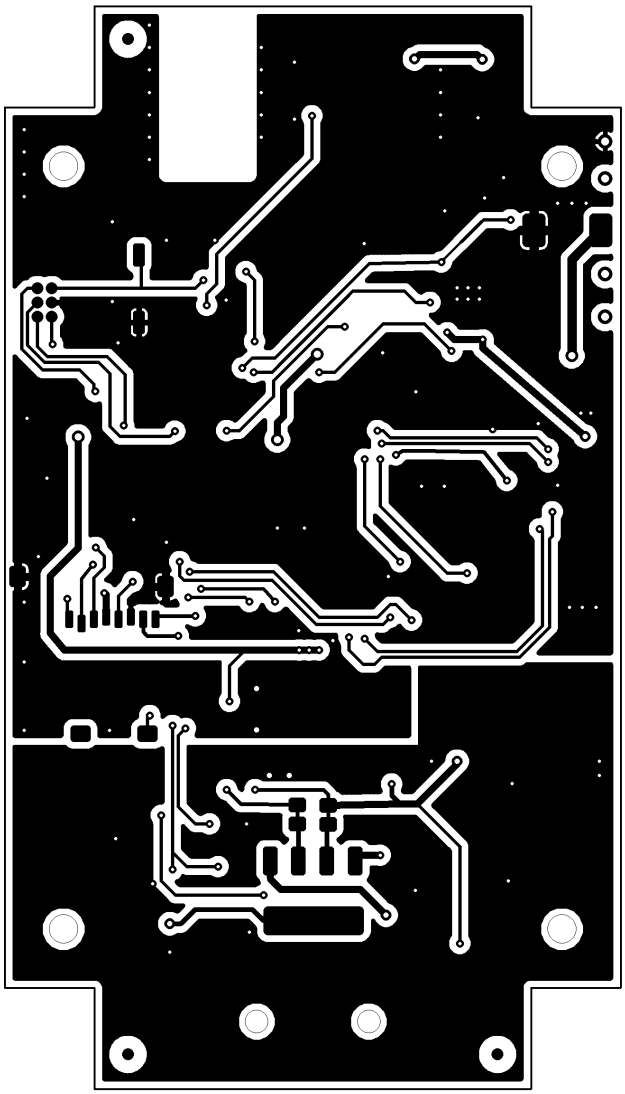

Figure 70: Multi-frequency Impedance Spectrometer PCB layout - bottom copper layer.

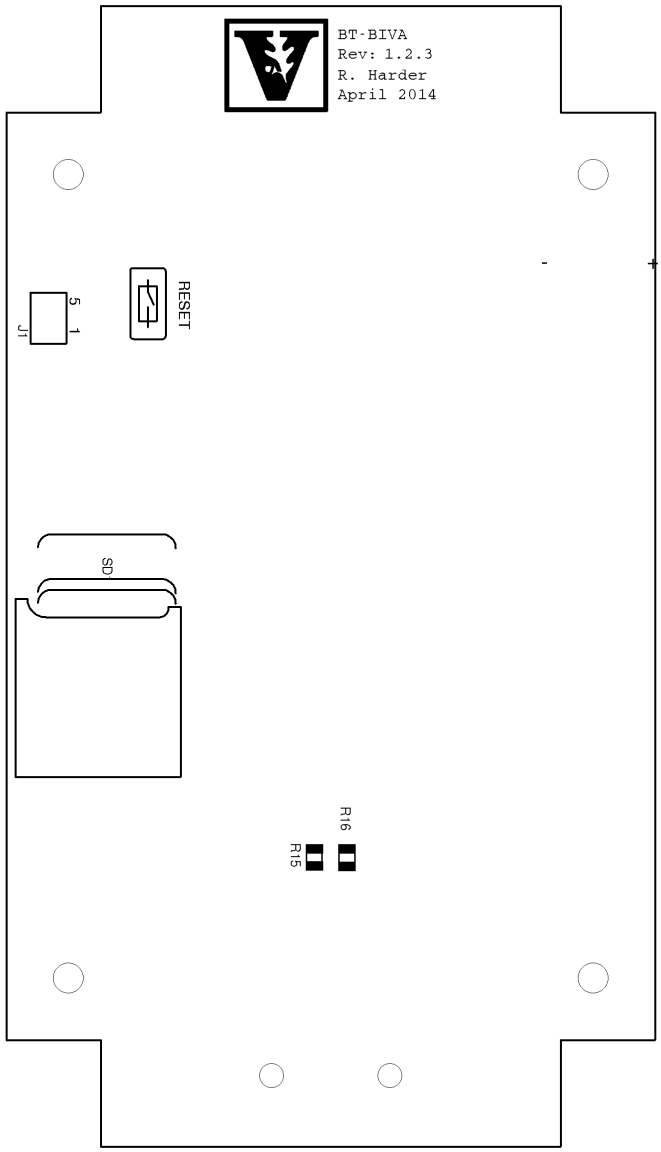

Figure 71: Multi-frequency Impedance Spectrometer PCB layout - bottom component placement.

A.3 Wireless 12-lead ECG Monitor

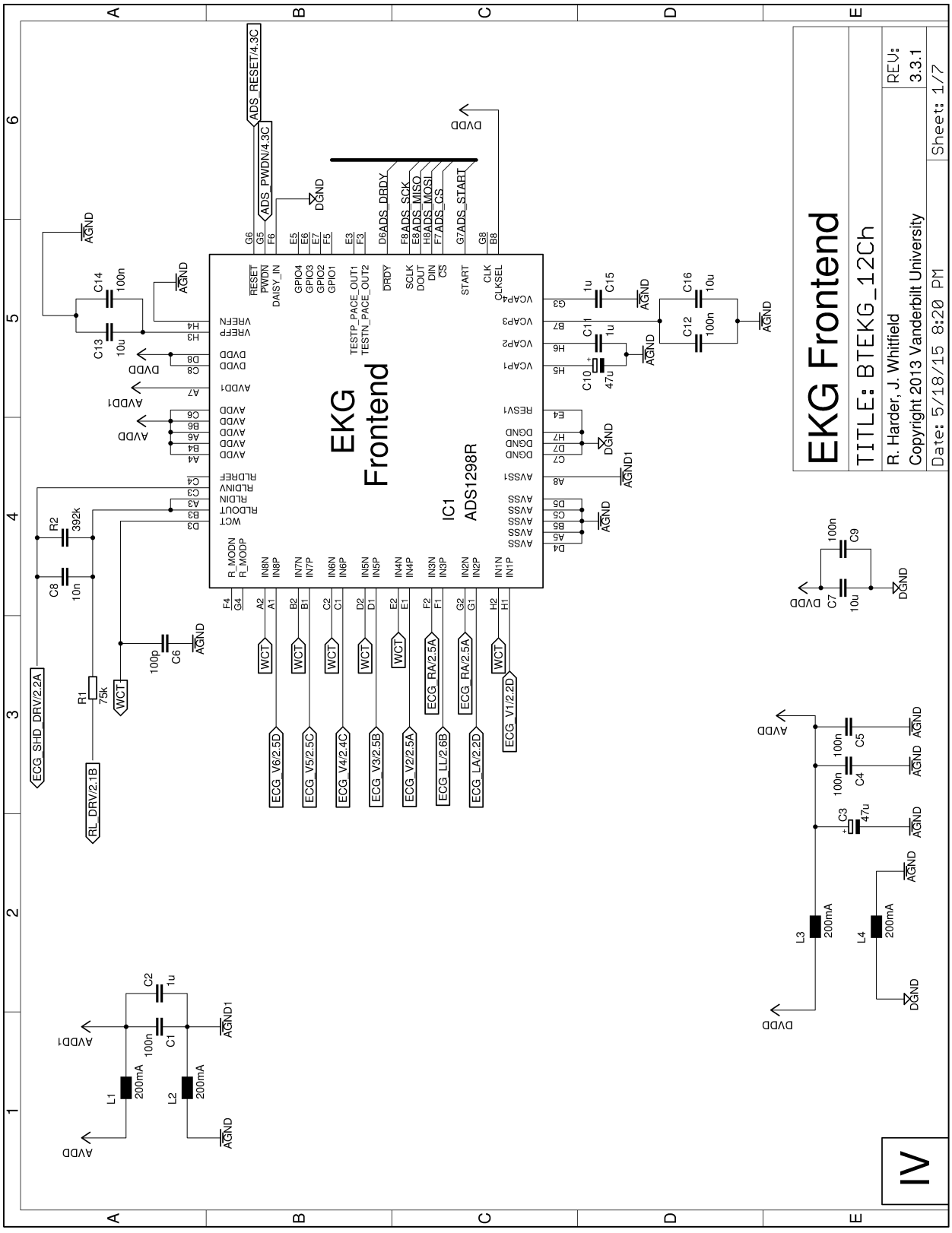

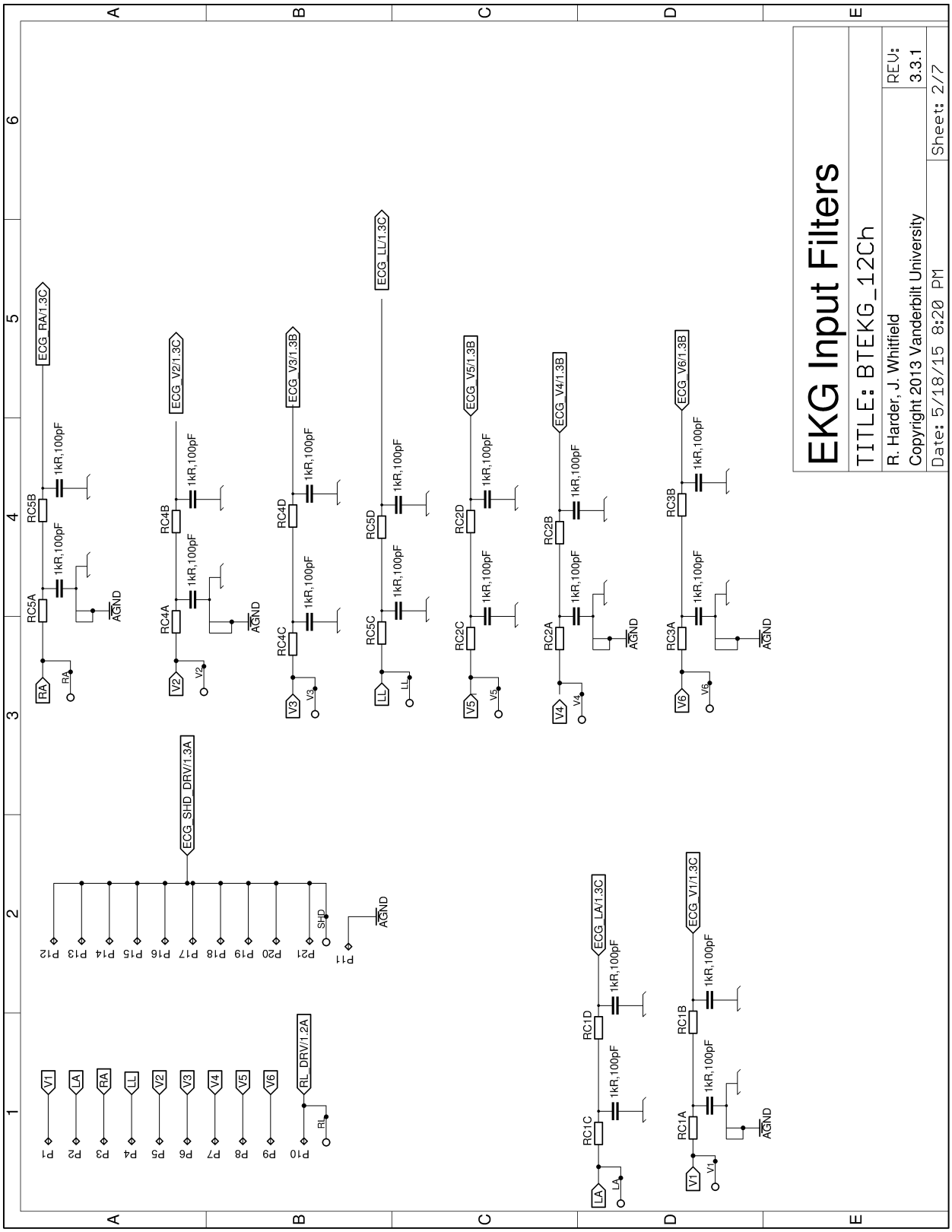
EKG Input Filters
TITLE: BTEKG_12Ch
R. Harder, J. Whitfield
Copyright 2013 Vanderbilt University
REV: 3.3.1
Date: 5/18/15 8:20 PM
Sheet: 2/7
ECG_RA/1.3C
ECG_V2/1.3C
ECG_V3/1.3B
ECG_LL/1.3C
ECG_V5/1.3B
ECG_V4/1.3B
ECG_V6/1.3B
ECG_LA/1.3C
ECG_V1/1.3C
ECG_SHD_DRV/1.3A
RL_DRV/1.2A
1kR,100pF
AGND

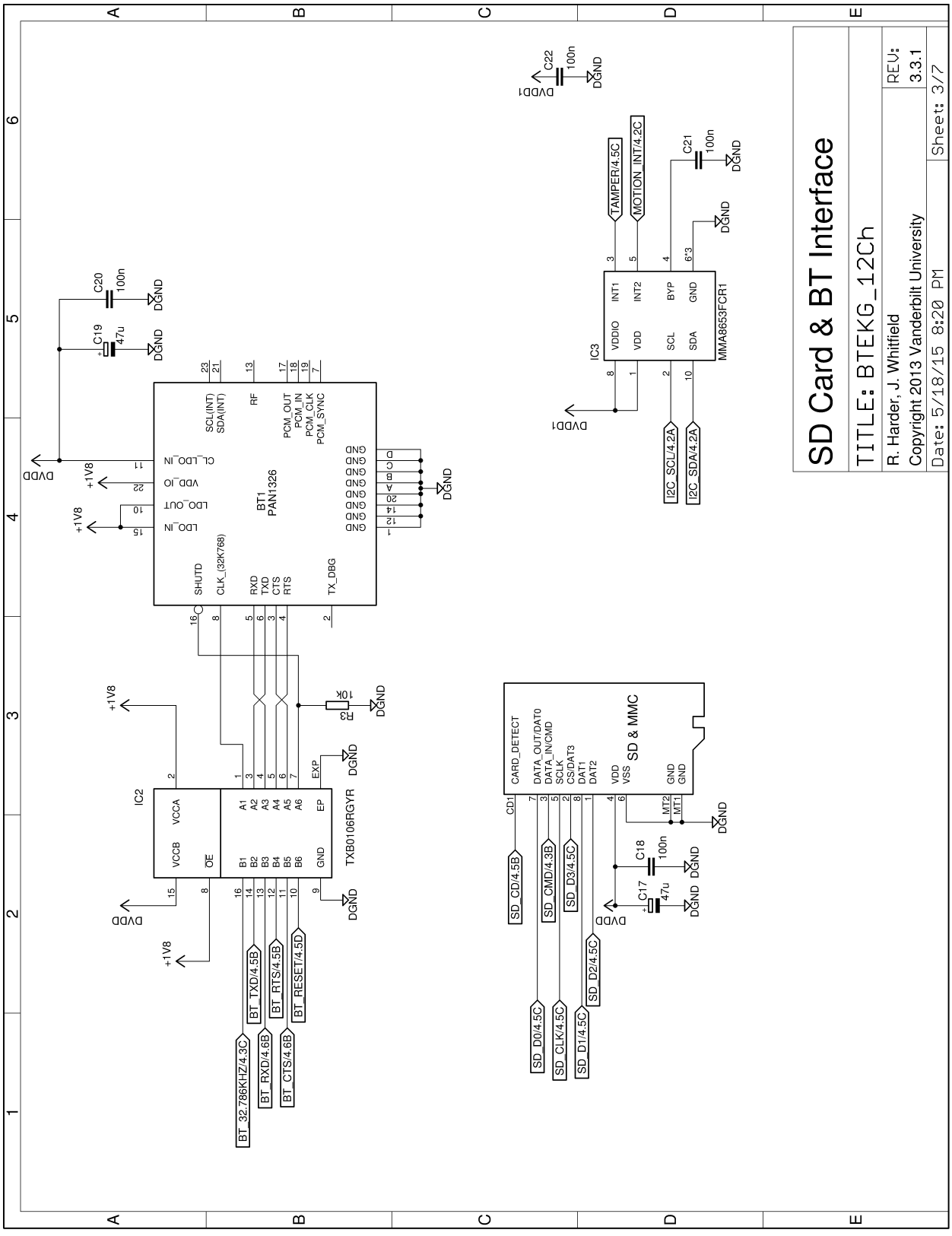
SD Card & BT Interface
TITLE: BTEKG_12Ch
R. Harder, J. Whitfield
Copyright 2013 Vanderbilt University
REV: 3.3.1
Date: 5/18/15 8:20 PM
Sheet: 3/7
BT1
PAN1326
IC2
TXB0106RGYR
IC3
MMA8653FCR1
SD & MMC
BT_32.786KHZ/4.3C
BT_TXD/4.5B
BT_RTS/4.5B
BT_RESET/4.5D
BT_RXD/4.6B
BT_CTS/4.6B
SD_CD/4.5B
SD_D0/4.5C
SD_CMD/4.3B
SD_CLK/4.5C
SD_D3/4.5C
SD_D1/4.5C
SD_D2/4.5C
I2C_SCL/4.2A
I2C_SDA/4.2A
TAMPER/4.5C
MOTION_INT/4.2C
+1V8
DVDD
DVDD1
DGND
C17 47u
C18 100n
C19 47u
C20 100n
C21 100n
C22 100n
R3 10K

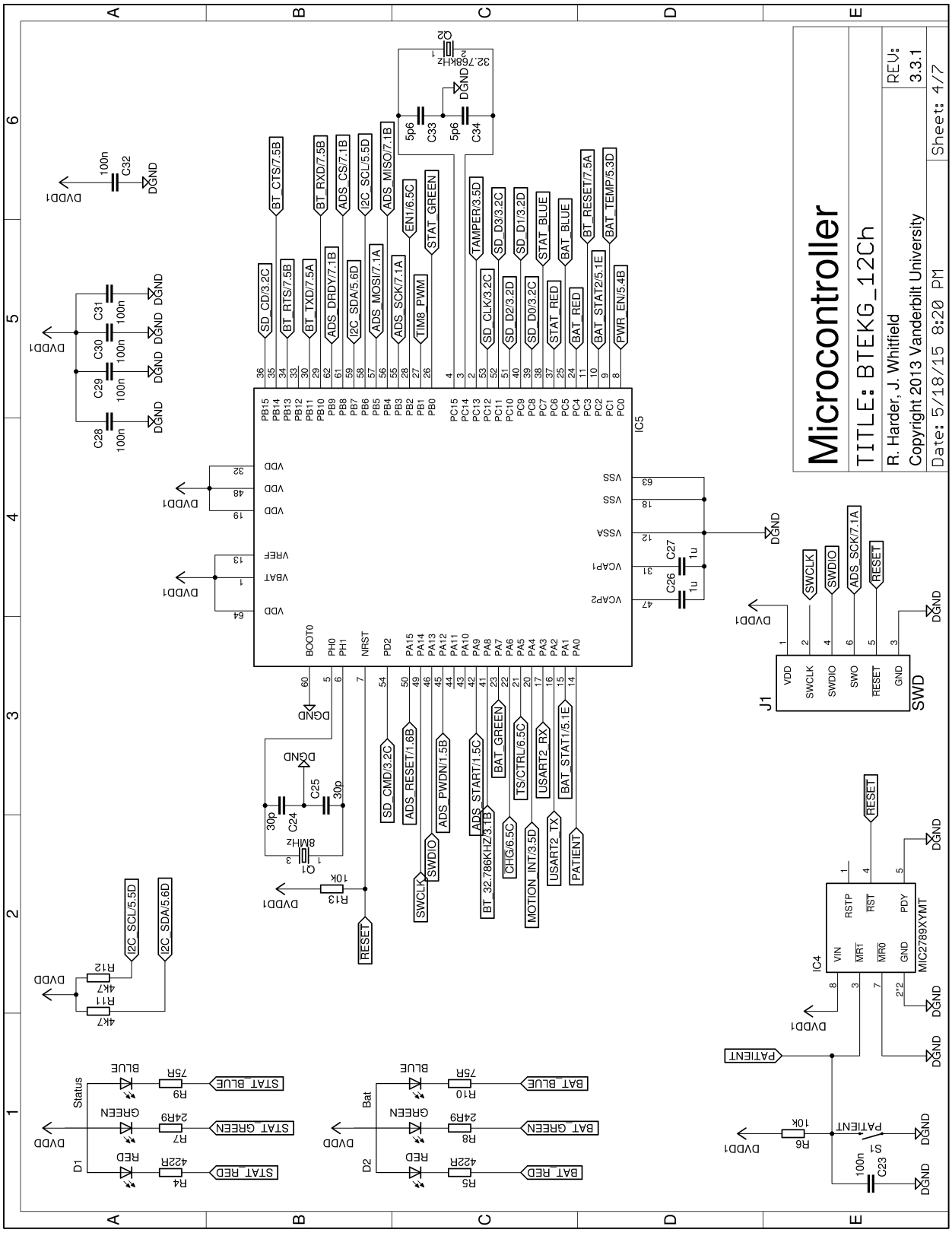
Microcontroller
TITLE: BTEKG_12Ch
R. Harder, J. Whitfield
Copyright 2013 Vanderbilt University
REV: 3.3.1
Date: 5/18/15 8:20 PM
Sheet: 4/7
IC5
J1
SWD
IC4
MIC2789XYMT
Q1
8MHz
Q2
32.768KHz
Status
Bat
D1
D2

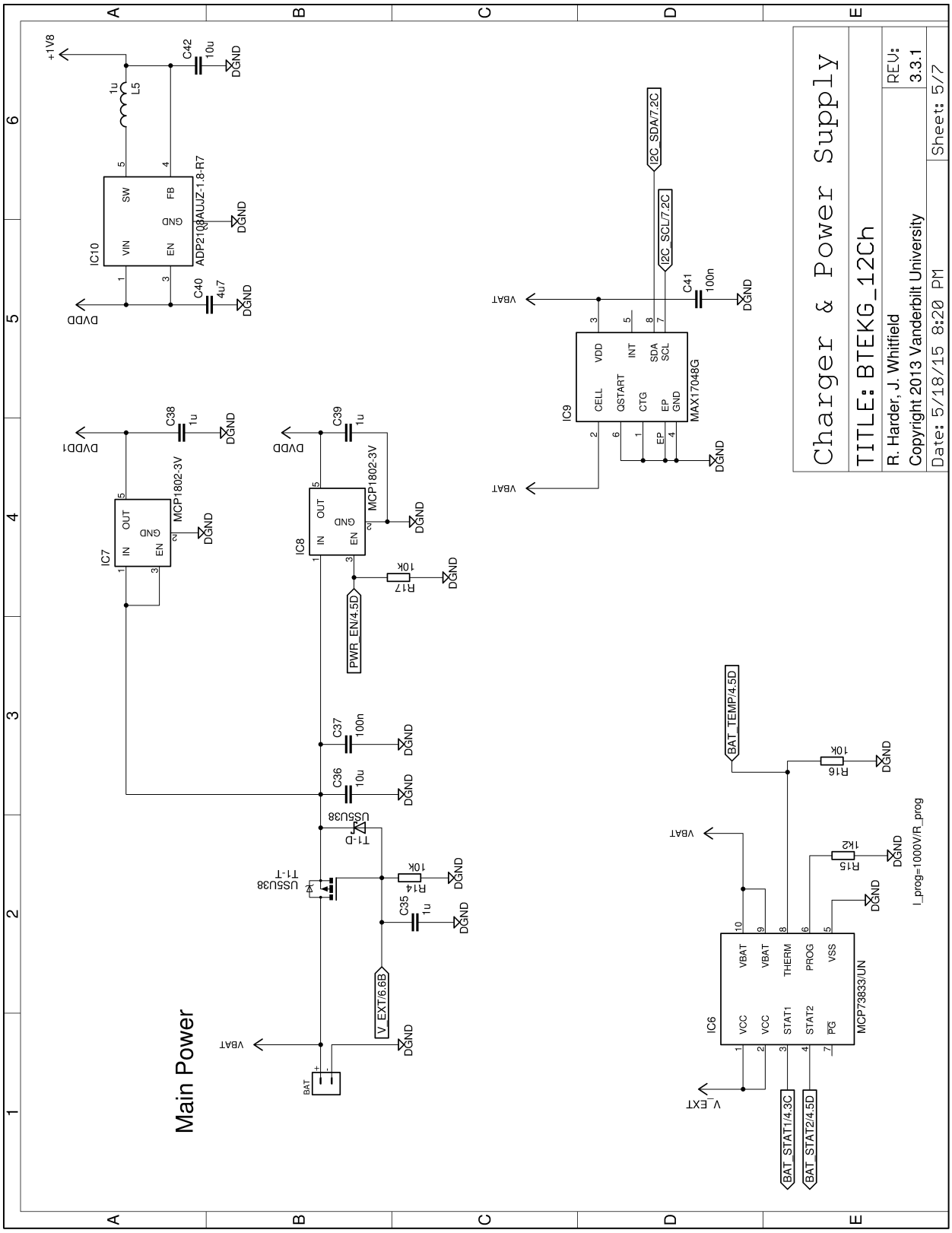
Charger & Power Supply
TITLE: BTEKG_12Ch
R. Harder, J. Whitfield
REV: 3.3.1
Copyright 2013 Vanderbilt University
Date: 5/18/15 8:20 PM
Sheet: 5/7
Main Power
+1V8
DVDD
DVDD1
VBAT
V_EXT
DGND
IC10
ADP2108AUJZ-1.8-R7
IC7
MCP1802-3V
IC8
MCP1802-3V
IC9
MAX17048G
IC6
MCP73833/UN
L5
1u
C42
10u
C40
4u7
C38
1u
C39
1u
C41
100n
C37
100n
C36
10u
C35
1u
R17
10K
R14
10K
R16
10K
R15
1K2
PWR_EN/4.5D
V_EXT/6.6B
BAT_TEMP/4.5D
BAT_STAT1/4.3C
BAT_STAT2/4.5D
I2C_SDA/7.2C
I2C_SCL/7.2C
T1-D
T1-T
US5U38
BAT
I_prog=1000V/R_prog

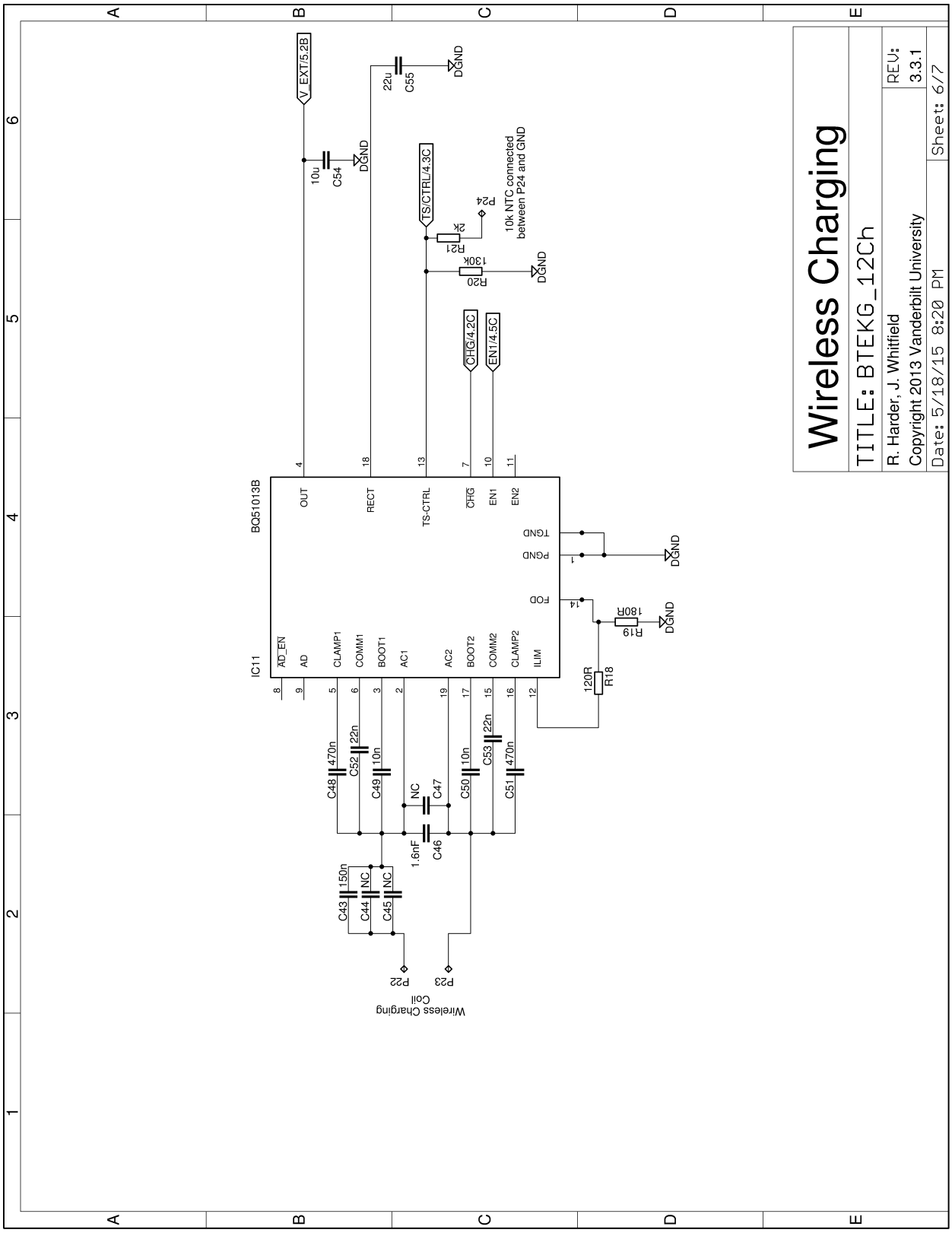
Wireless Charging
TITLE: BTEKG_12Ch
R. Harder, J. Whitfield
Copyright 2013 Vanderbilt University
REV: 3.3.1
Date: 5/18/15 8:20 PM
Sheet: 6/7
V_EXT/5.2B
10u
C54
DGND
22u
C55
TS/CTRL/4.3C
R21
2K
P24
10k NTC connected between P24 and GND
R20
130K
CHG/4.2C
EN1/4.5C
IC11
BQ51013B
OUT
RECT
TS-CTRL
CHG
EN1
EN2
TGND
PGND
FOD
ILIM
AD_EN
AD
CLAMP1
COMM1
BOOT1
AC1
AC2
BOOT2
COMM2
CLAMP2
R19
180R
R18
120R
C48 470n
C52 22n
C49 10n
C43 150n
C44 NC
C45 NC
NC
C47
1.6nF
C46
C50 10n
C53 22n
C51 470n
P22
P23
Wireless Charging Coil

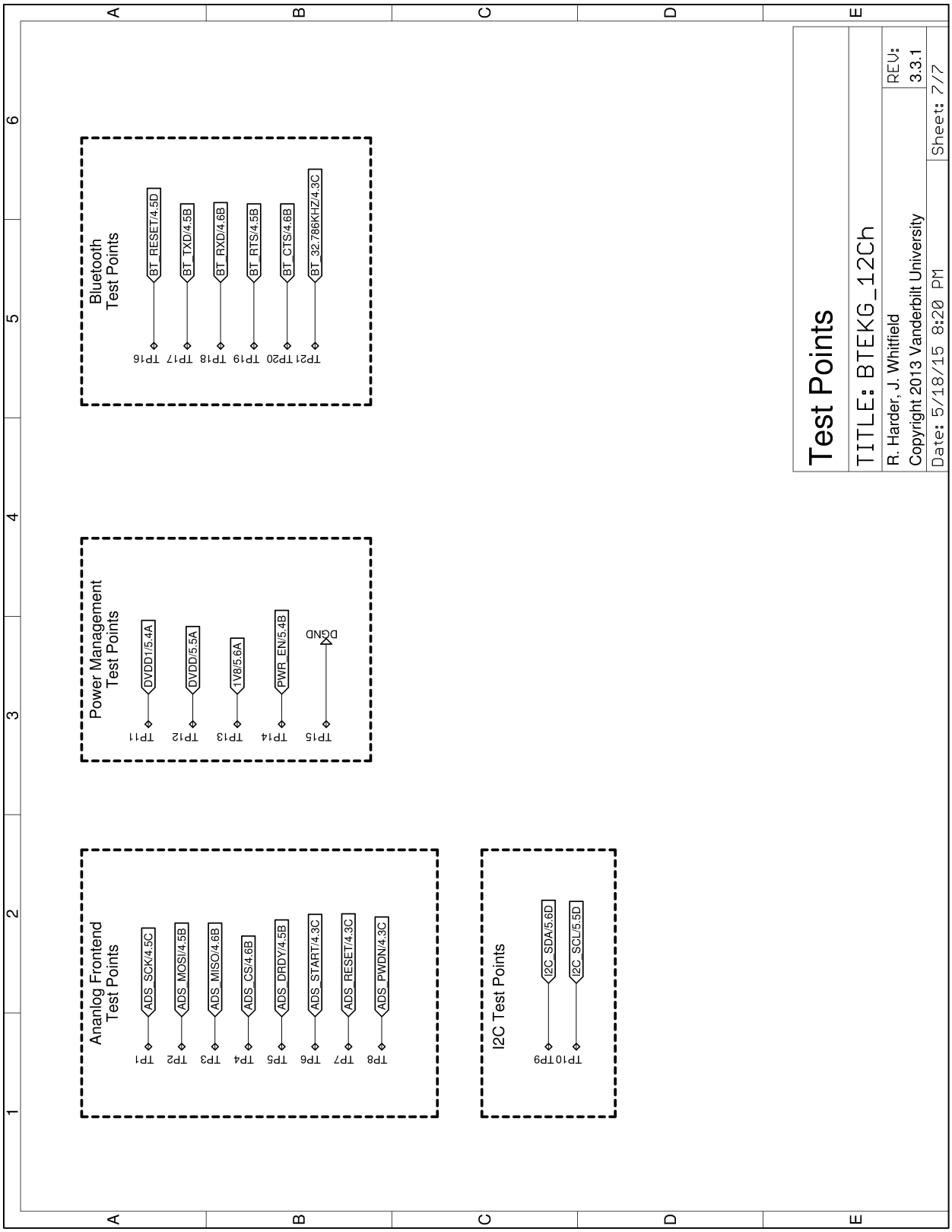
Test Points
TITLE: BTEKG_12Ch
R. Harder, J. Whitfield
Copyright 2013 Vanderbilt University
REV: 3.3.1
Date: 5/18/15 8:20 PM
Sheet: 7/7
Bluetooth Test Points
BT_RESET/4.5D
BT_TXD/4.5B
BT_RXD/4.6B
BT_RTS/4.5B
BT_CTS/4.6B
BT_32.786KHZ/4.3C
TP16 TP17 TP18 TP19 TP20 TP21
Power Management Test Points
DVDD1/5.4A
DVDD/5.5A
1V8/5.6A
PWR_EN/5.4B
DGND
TP11 TP12 TP13 TP14 TP15
Ananlog Frontend Test Points
ADS_SCK/4.5C
ADS_MOSI/4.5B
ADS_MISO/4.6B
ADS_CS/4.6B
ADS_DRDY/4.5B
ADS_START/4.3C
ADS_RESET/4.3C
ADS_PWDN/4.3C
TP1 TP2 TP3 TP4 TP5 TP6 TP7 TP8
I2C Test Points
I2C_SDA/5.6D
I2C_SCL/5.5D
TP9 TP10

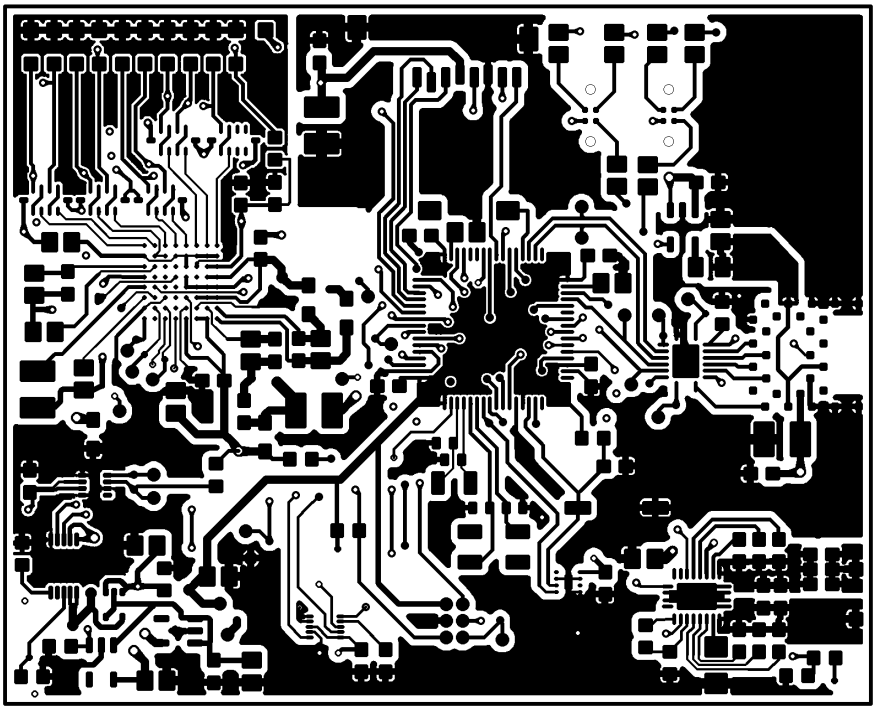

Figure 72: Wireless 12-lead ECG Monitor PCB Layout - top copper layer.

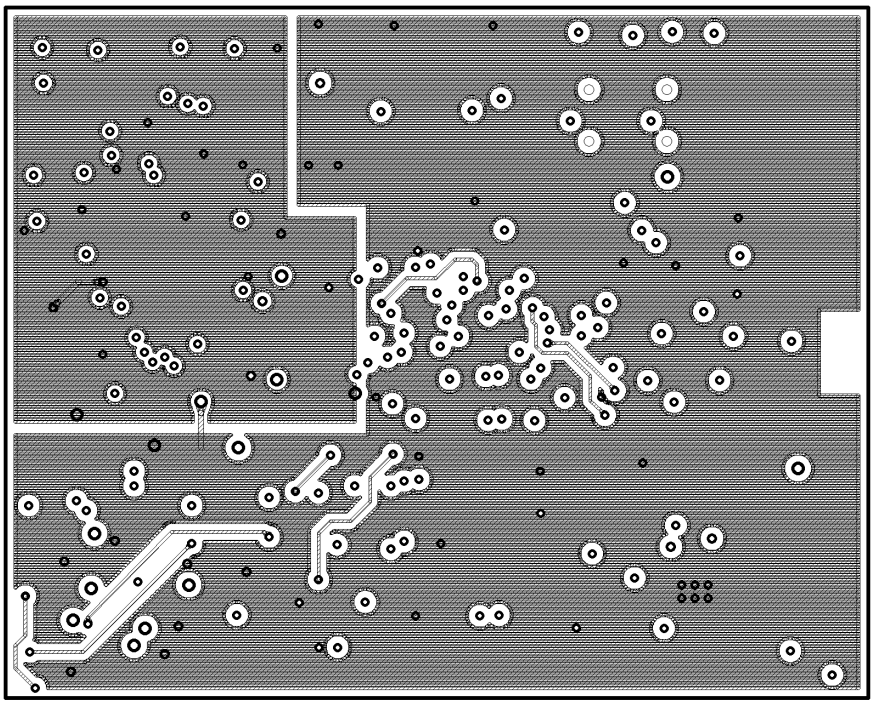

Figure 73: Wireless 12-lead ECG Monitor PCB Layout - copper layer 2.

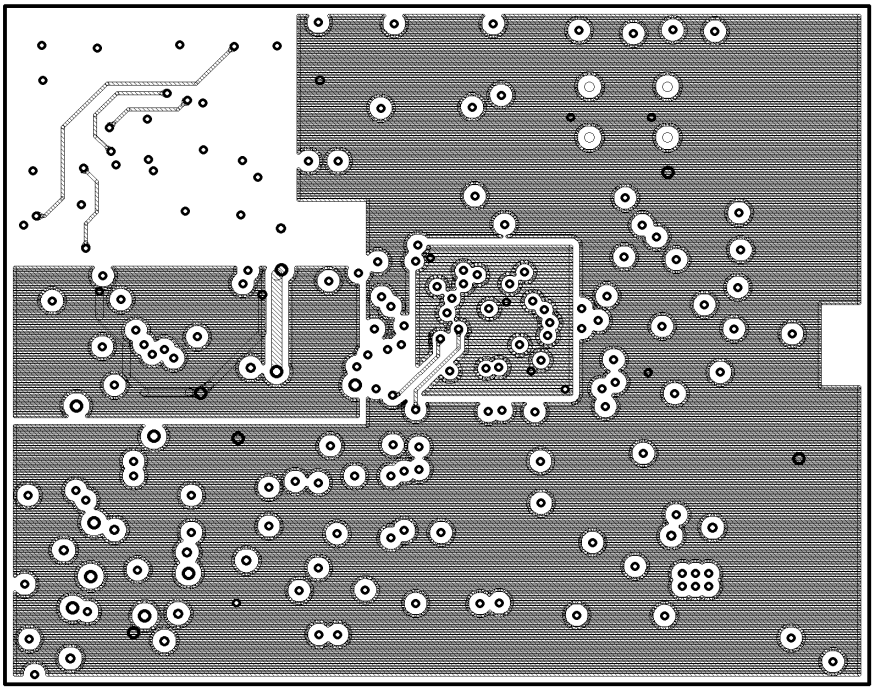

Figure 74: Wireless 12-lead ECG Monitor PCB Layout - copper layer 3.

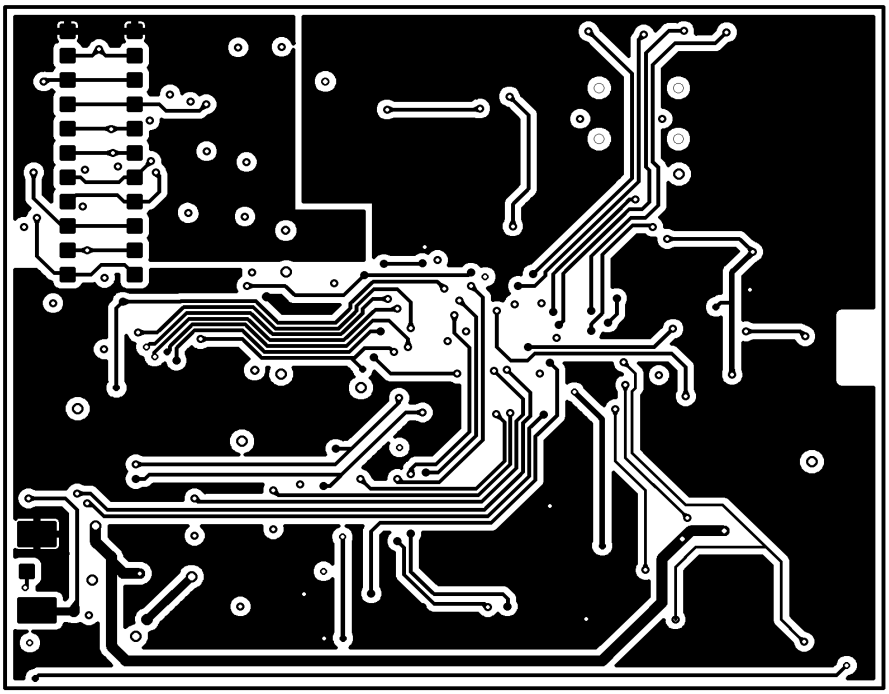

Figure 75: Wireless 12-lead ECG Monitor PCB Layout - bottom copper layer.

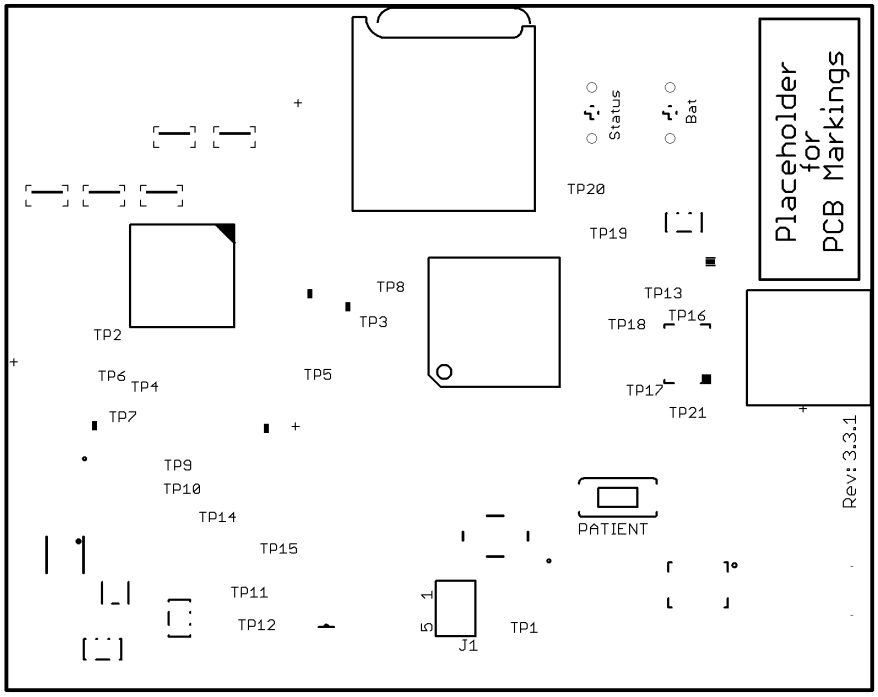

Figure 76: Wireless 12-lead ECG Monitor PCB Layout - top component placement.

VANDERBILT Bioelectrical Impedance Vector Analyzer

This is an investigational device produced the Smart Healthcare Team at the Biomedical, Electrical Engineering, and Medicine departments and at Vanderbilt University by Franz Baudenbacher, André Diedrich, René Harder and Jonathan Whitfield.

Contact Information
René Harder: rene.harder@vanderbilt.edu
Franz Baudenbacher: franz.baudenbacher@vanderbilt.edu
Jonathan Whitfield: jonathan.s.whitfield@vanderbilt.edu
André Diedrich: andre.diedrich@vanderbilt.edu

This project is funded by the Bill Gates Foundation and Vanderbilt University

INTRODUCTION

This device uses alternating current to measure the complex impedance of the body. This allows for the determination of body composition and gives insight into the patient's nutrition.

The electrodes should be placed as shown in the diagram below:

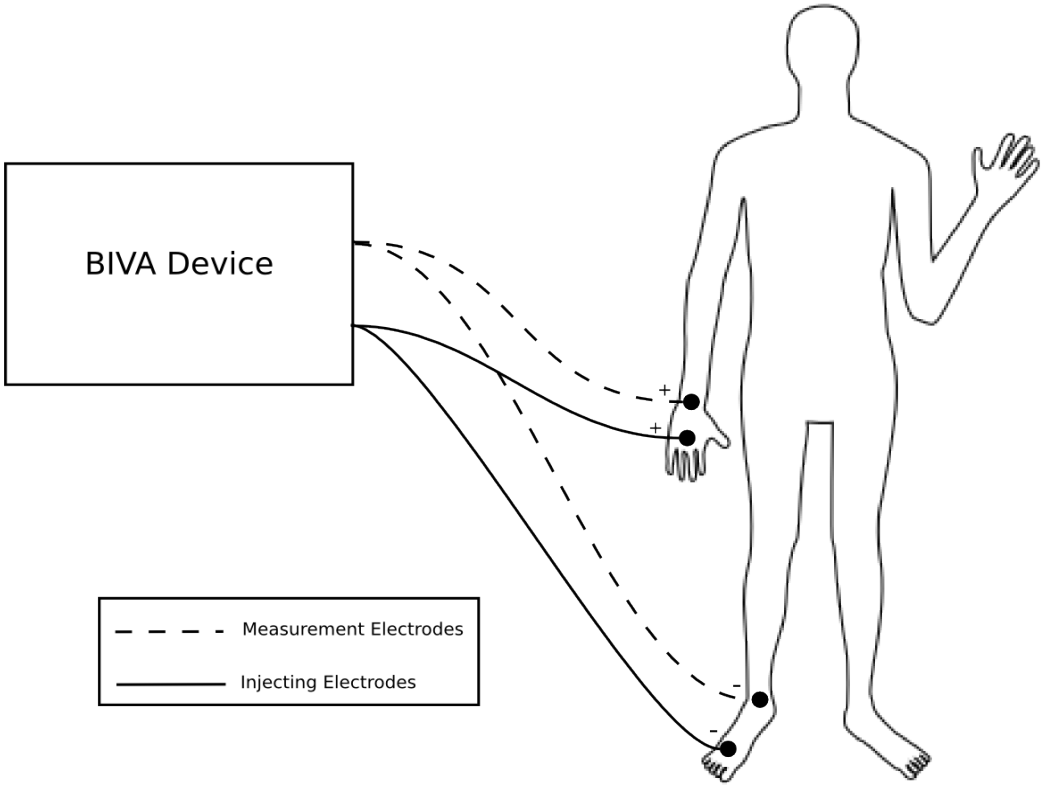

The injecting electrodes are marked with a '+' and '-' and should be placed distally to the measurement electrodes that are marked with a solid black dot and smaller '+' and '-' to signify which injecting electrode they should be paired with.

Injecting Electrodes

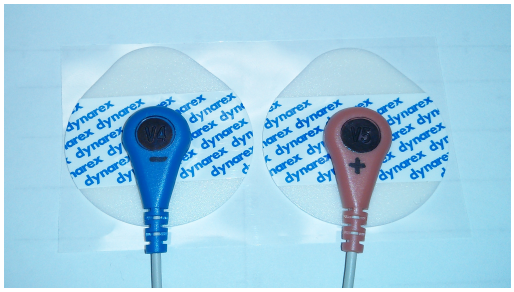

Measurement Electrodes

STARTING THE APP

Ensure that the BIVA device is powered on and look for this icon in the application menu or on the main screen.

Select the icon and the app should open to the main screen:

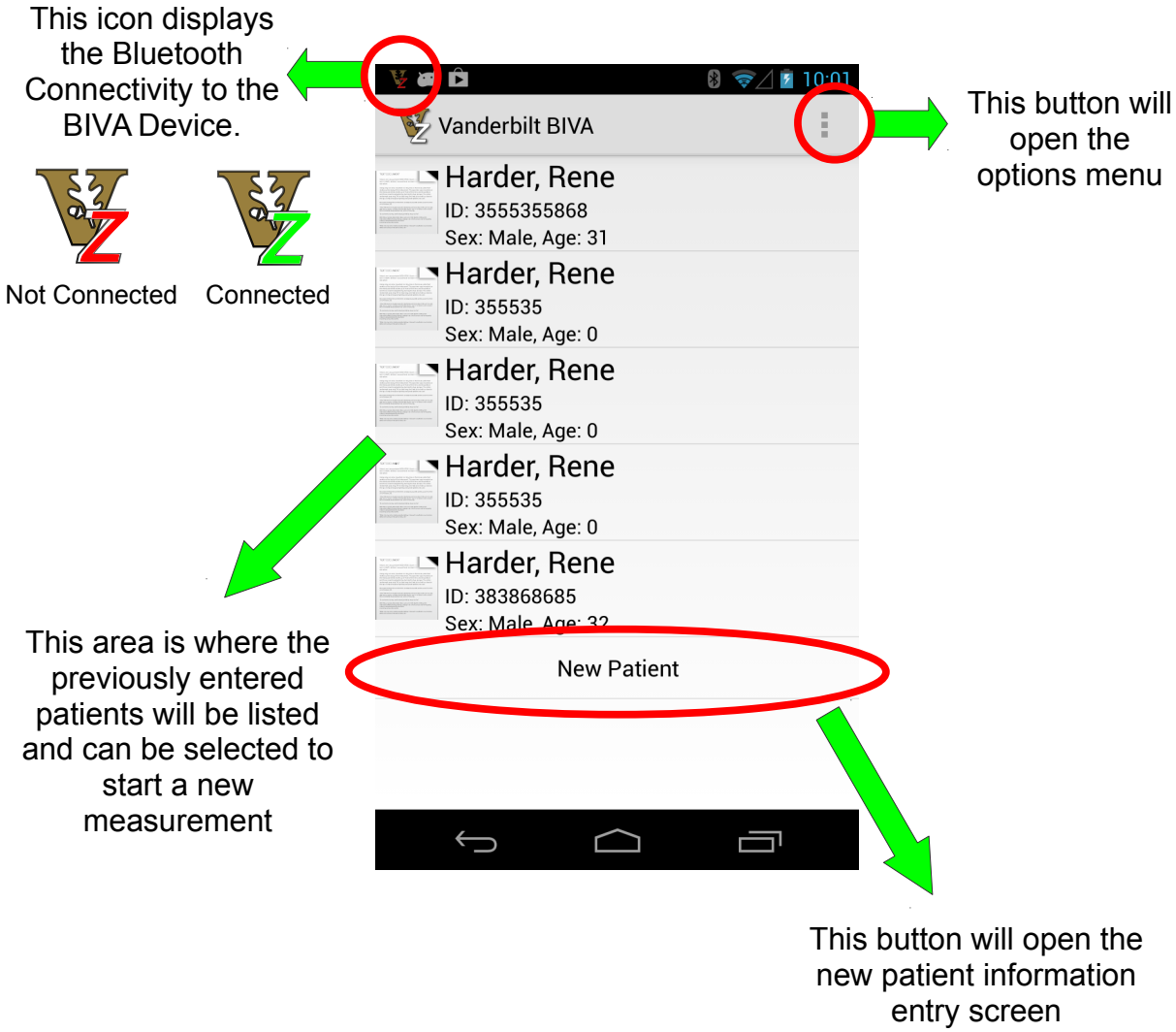

CONNECTING TO THE BIVA DEVICE

If the app is started after the BIVA device is powered on, the app should automatically handle the Bluetooth connection.

When a connection is established, the 'Z' in the status bar will change from red to green and the 'Enter New Patient' button will appear on the bottom of the screen.

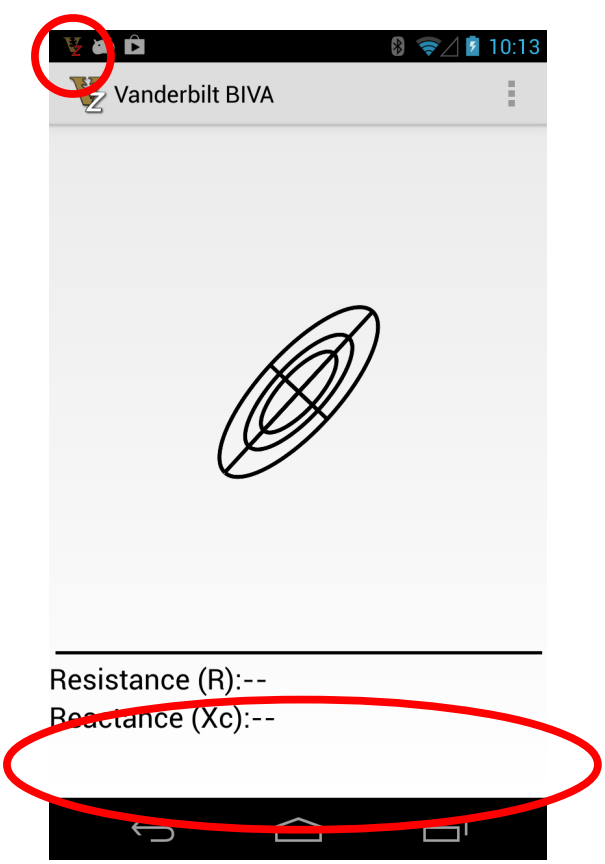

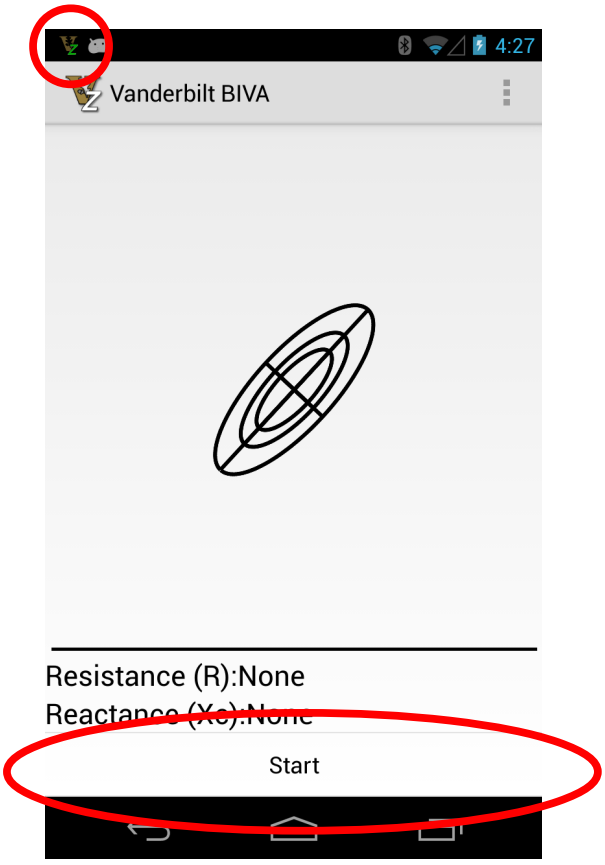

If the app has not been started after the device has powered up, then the user can manually initiate the connection process by opening the options menu and selecting the 'Connect a device' option.

If the device is still not connecting refer to the troubleshooting section.

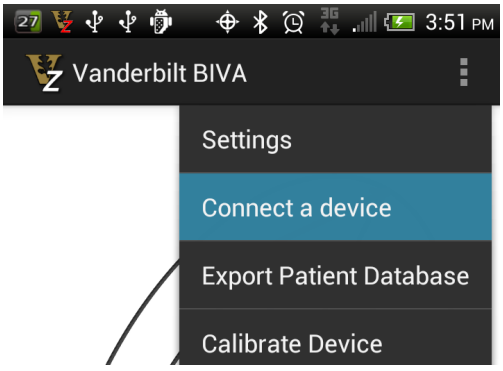

STARTING A MEASUREMENT

Ensure that the BIVA device is powered on and that there is an active Bluetooth connection between the BIVA device and the BIVA app.

If the patient exists in the phone's local database then select them from the list shown on start up. If the patient is not listed press the new patient button to start entering patient information:

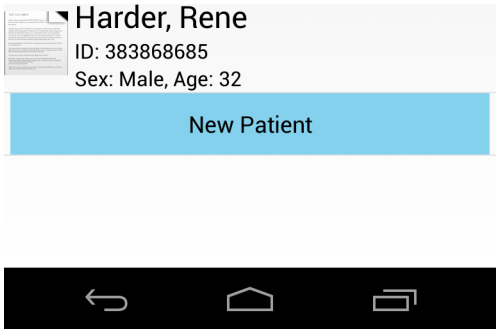

Pressing this button will open the list of previous patients. Upon the first running of the application this view should look like this:

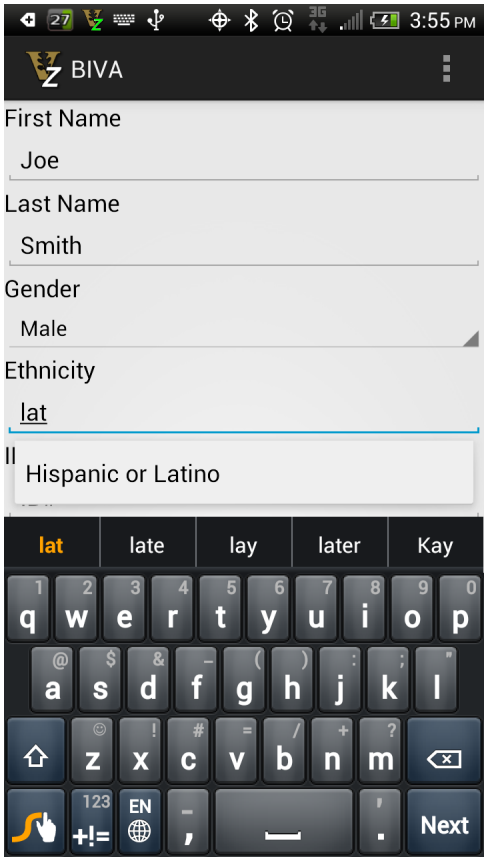

STARTING A MEASUREMENT CONTINUED

Ensure that all fields are filled and select the 'Save' button on the bottom of the screen. The patient you just entered should appear on top of the patient list:

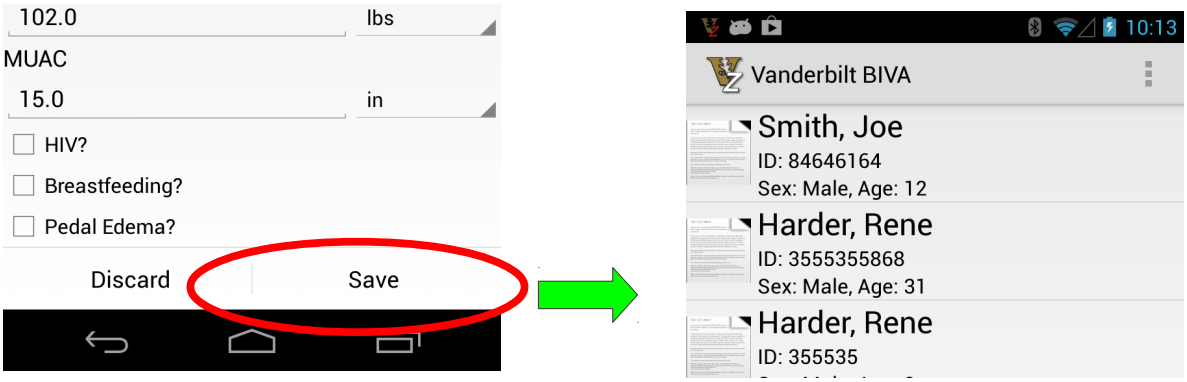

Selecting the current patient from the patient list will return you to the main screen, but now the 'Enter New Patient' button should read 'Start' and the patient's previous measurements (if any) should be displayed as vectors on their corresponding reference population tolerance ellipses:

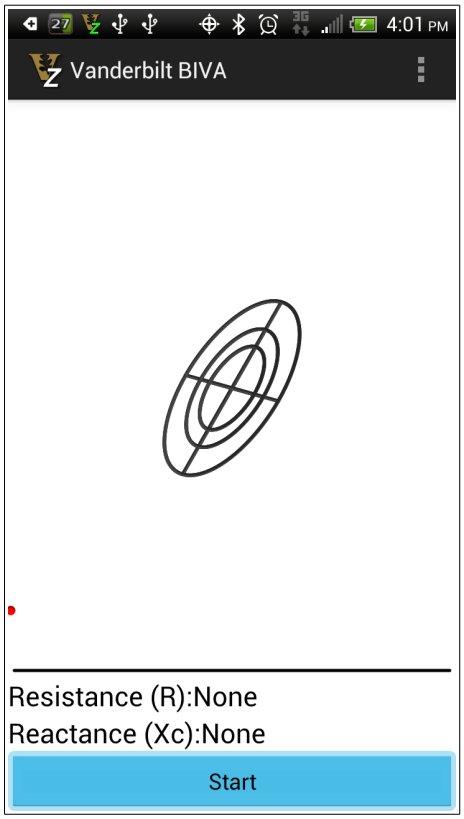

STARTING A MEASUREMENT CONTINUED

A progress bar will open on the screen for the duration of the measurement:

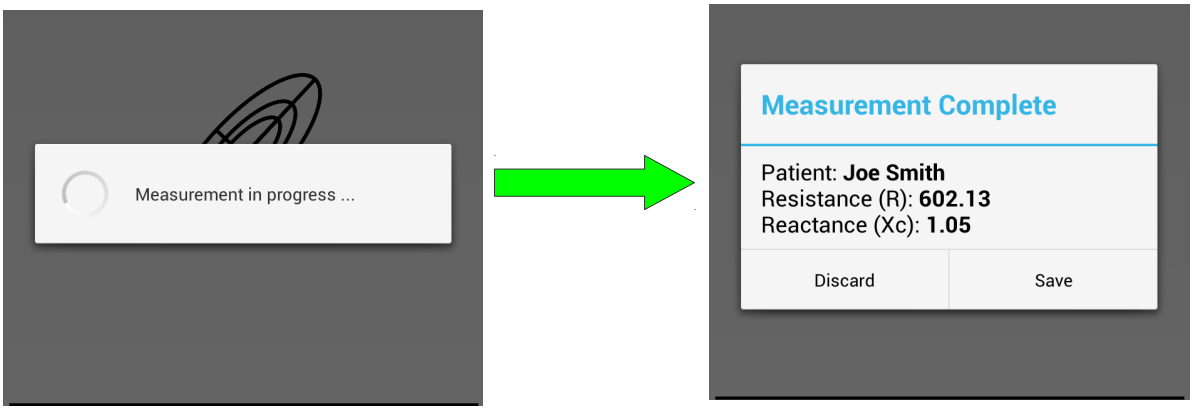

The BIVA device will return the resistance and reactance values at 50kHz and the app will display them above the 'Start' button. Pressing the 'Save' button will plot the current point on the tolerance ellipse (as well as any previous data).

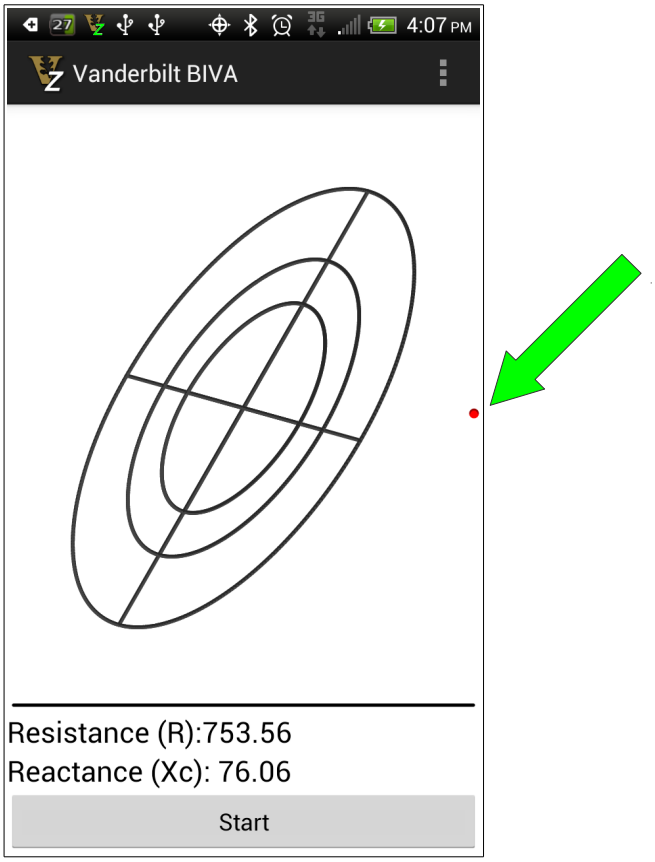

STARTING A MEASUREMENT CONTINUED

Subsequent measurements will be plotted on the tolerance ellipses. The current vector will be drawn in red, with all previous vectors drawn in blue:

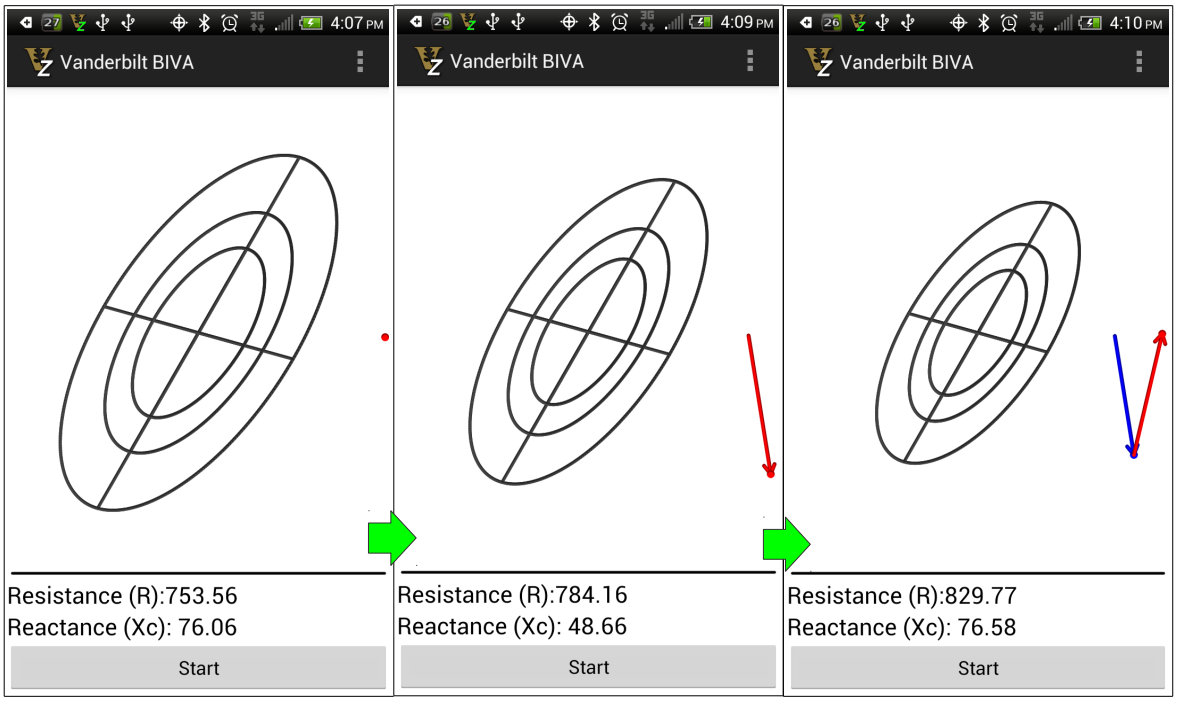

CALIBRATING THE DEVICE

Ensure the the BIVA device is connected to the calibration standard and select the 'Calibrate Device' option from the options menu in the app:

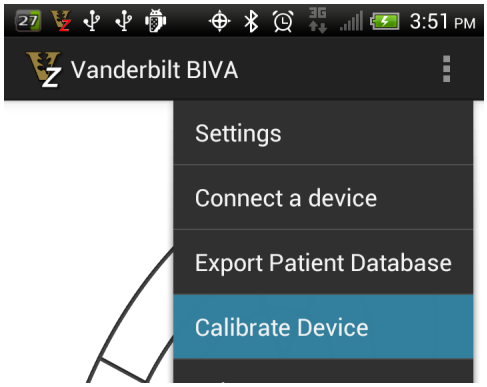

This will open a warning to remind the user to ensure correct calibration standard connection before continuing with the calibration. Selecting 'Continue' will start the calibration. Calibration progress can be monitored in the progress bar that will open on the screen:

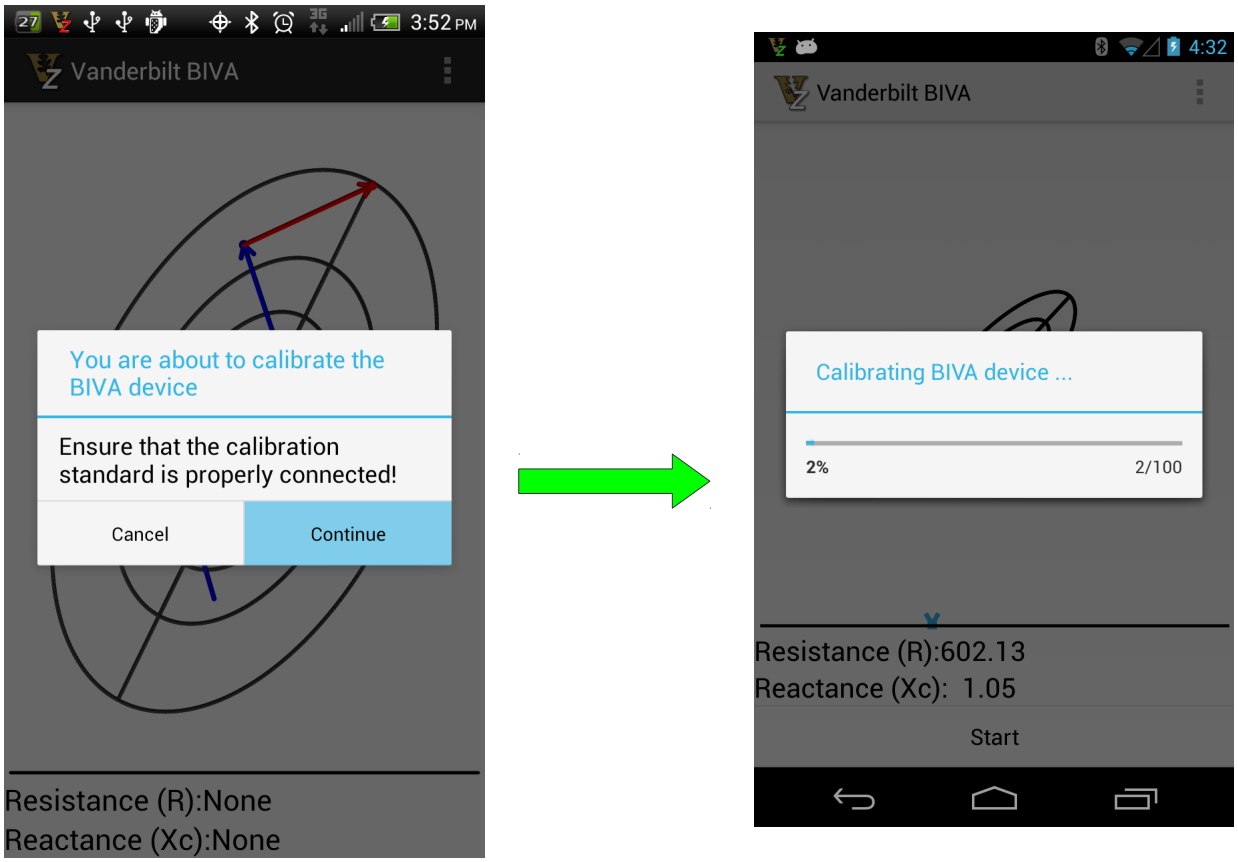

REVIEWING PATIENT INFORMATION

Swiping the BIVA plot screen to the left will open the patient visit information:

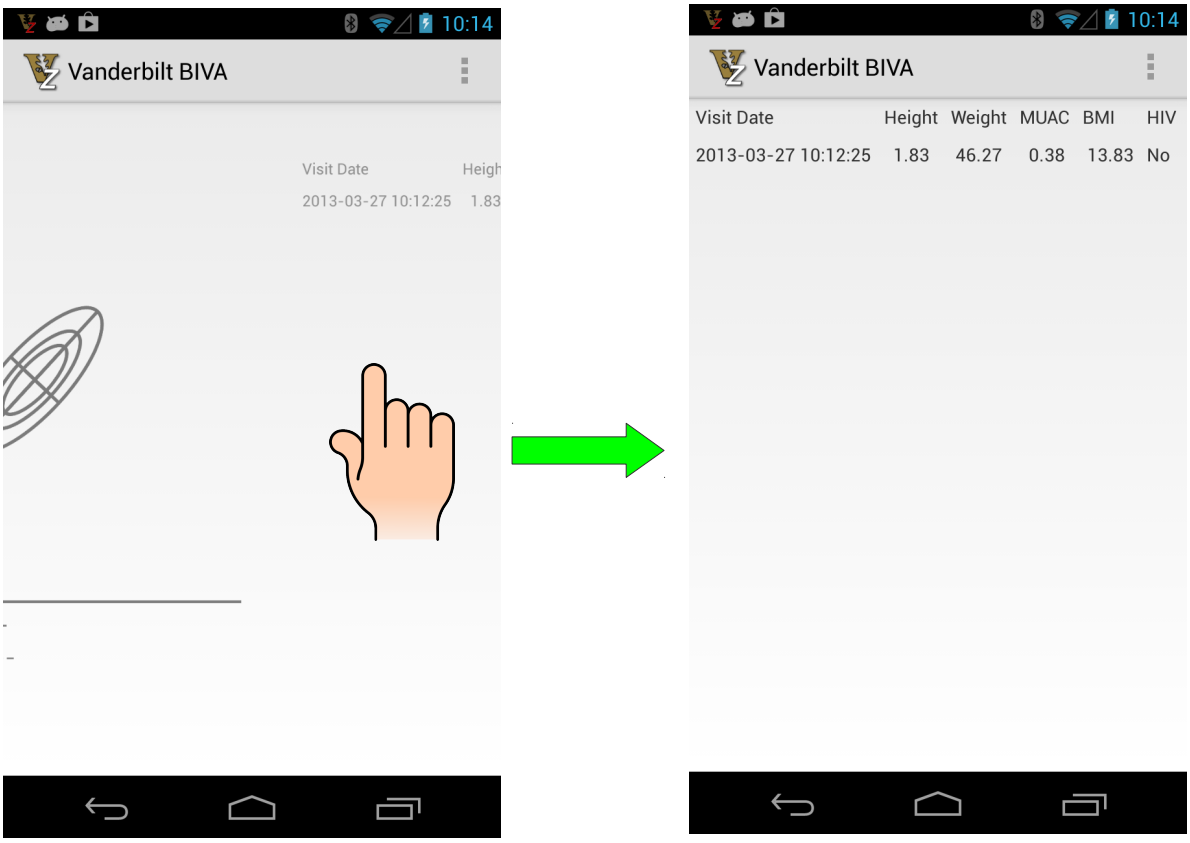

This screen displays height, weight, MUAC, BMI and other criteria from the patients previous visits (including the current information entered).

REVIEWING PATIENT INFORMATION

Swiping the patient visit information screen to the left will open the patient measurement table:

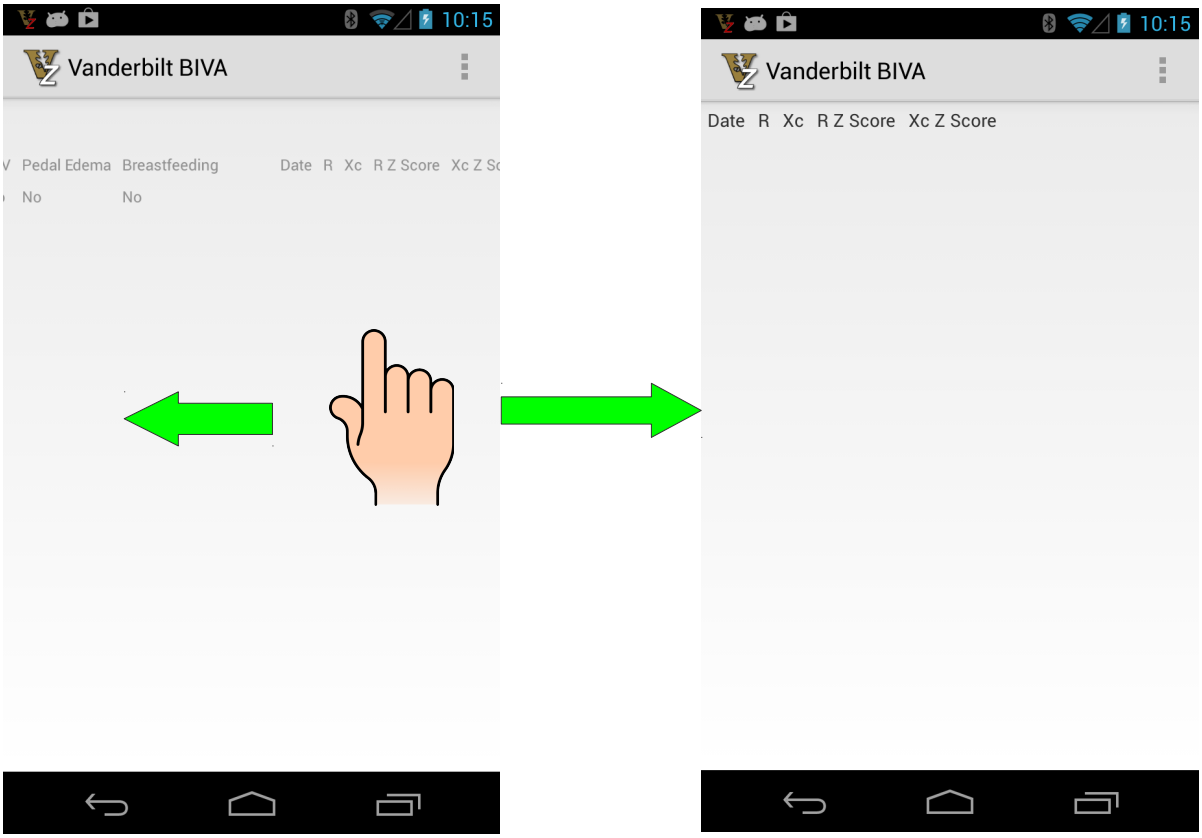

This table will show all of the previous measurements made sorted from oldest to newest for quick comparison

REVIEWING PATIENT INFORMATION

Swiping the BIVA plot to the right will open the patient visit update screen

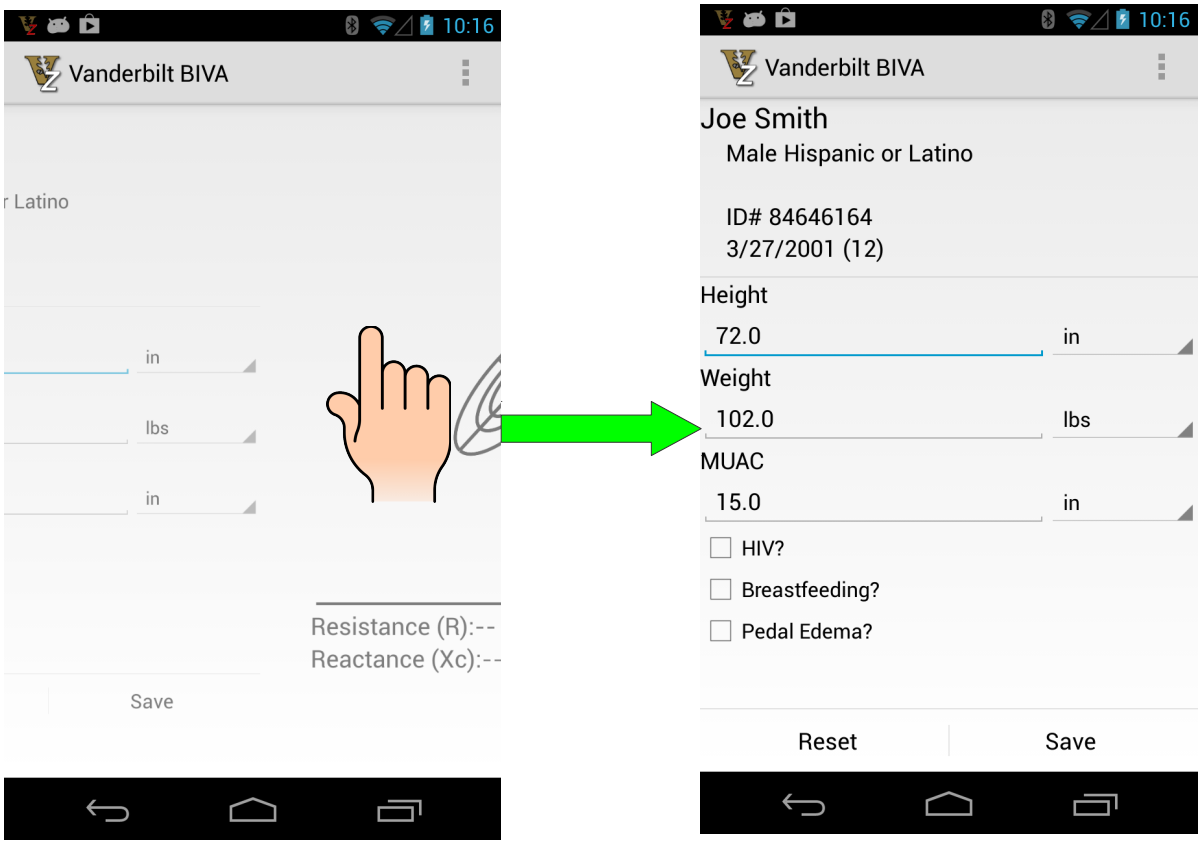

On this screen you can update the patient's height, weight, MUAC and other criteria. The patient's previous measurements are saved and can be viewed to review patient progress in the patient visit information screen.

To save the updated information ensure that you press the 'Save' button on the bottom of the screen. This dialog will appear when the data has been successfully saved:

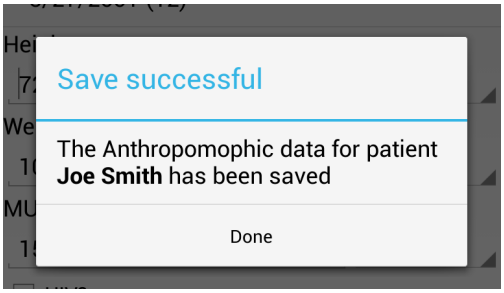

TROUBLESHOOTING

ISSUE:

Cannot establish Bluetooth connection between app and BIVA device.

SOLUTION:

Turn off the BIVA device by holding the button down until the lights turn off and exit the app by selecting 'Close Program' in the options menu. Power the device on by holding the button down until the lights start flashing rapidly. Wait until the light begin to flash slowly, this means the device is ready to connect. Restart the application and attempt to connect again.

If the above procedure fails, the app might not be configured properly. To remedy this, start the app and select 'Settings' from the options menu:

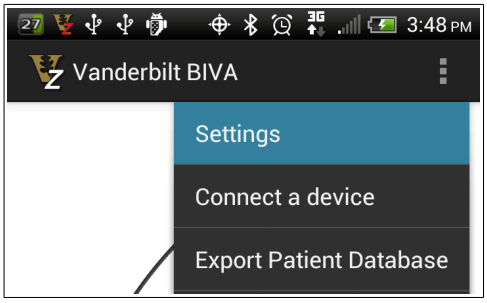

Select 'Bluetooth Address' from the menu and then select 'BIVA001' from the device list:

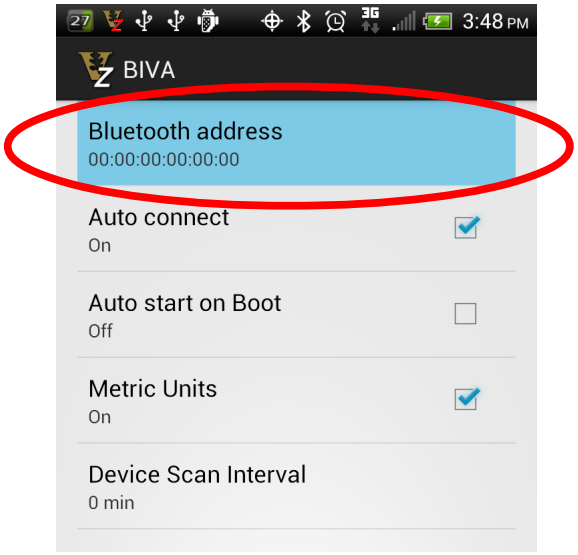

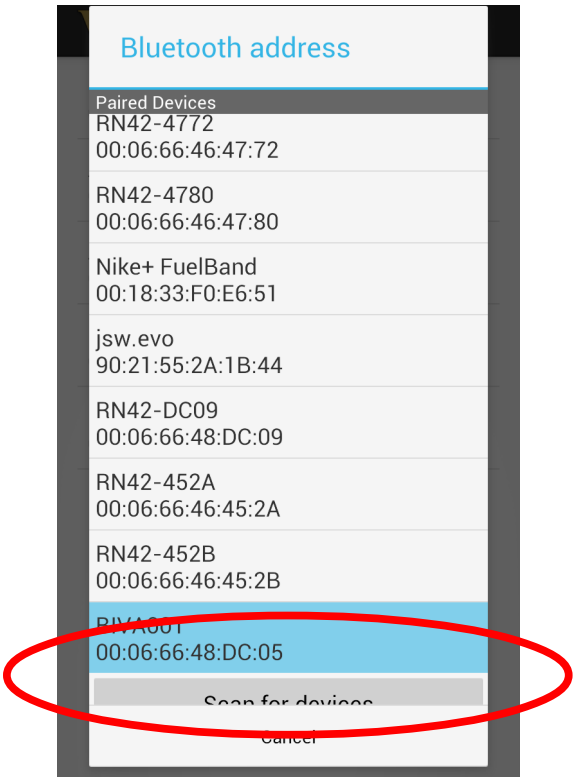

TROUBLESHOOTING

The 'Bluetooth Address' should now reflect the choice you selected from the device list.

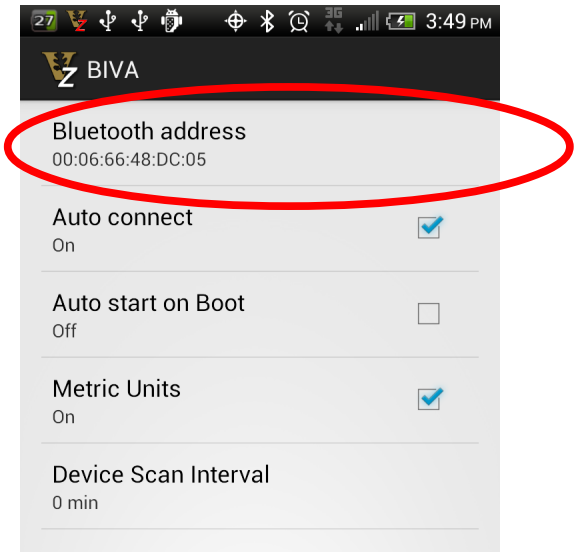

Now exit the menu to the main screen and select 'Connect Device' from the options menu and the device should connect.

If all of the above procedures fail the BIVA device's battery are most likely too low to establish a Bluetooth connection and needs to be charged before further use.

SPECIFICATIONS

Parameter	Min	Typical	Max	Unit
Battery Voltage	3.0	3.7	4.2	V
Digital Supply Dropout Voltage		3.4		V
Output Voltage	141	283	1414	mV RMS
Output Current	141	283	1414	µA RMS
Supply Current	1	20	100	mA

DEVICE BLOCK DIAGRAM

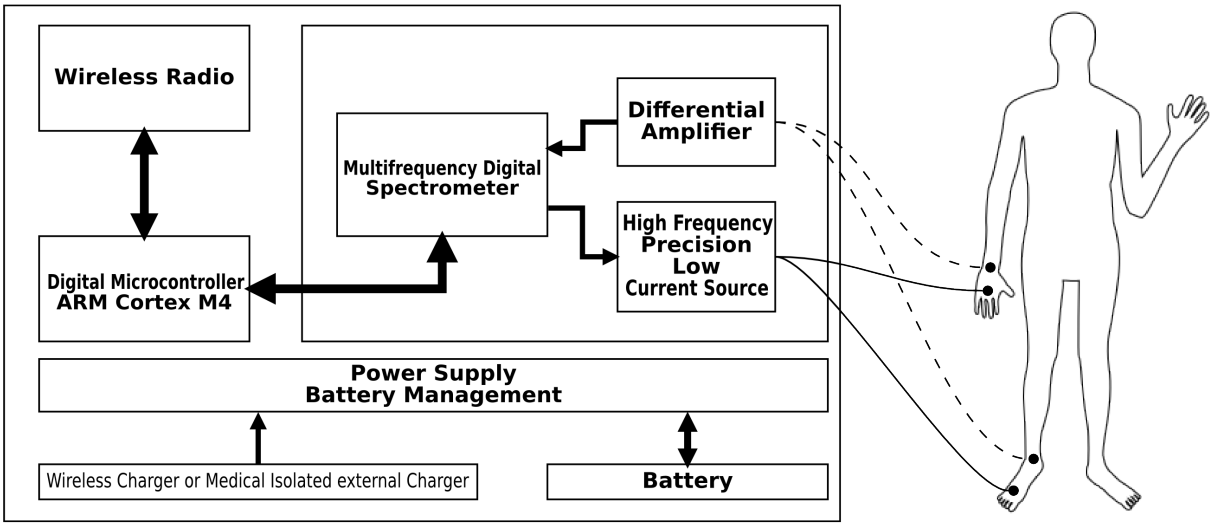

C. Vanderbilt ECG Dispatch System

C.1 System Summary

Figure 77 shows a brief system overview of the Vanderbilt ECG Dispatch Service (Webservice; MDDS)

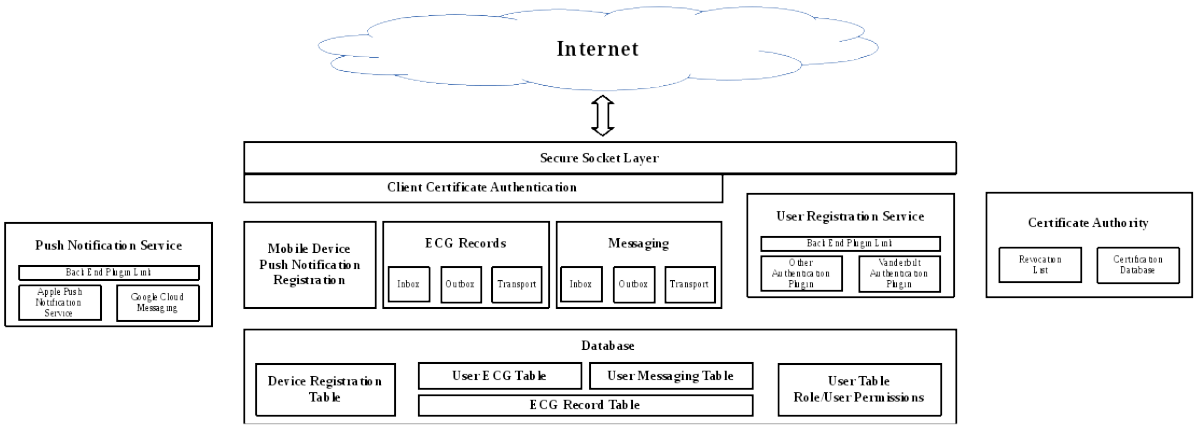

Figure 77: Block diagram of Vanderbilt ECG Dispatch System or MDDS

Secure Socket Layer (SSL)

Every communication with the webservice is encrypted using SSL technology. Currently only TLS 1.0 is supported. After initial user registration the webservice authenticates user access based on SSL client certificate authentication. Therefore the webservice validated the client certificate with the Certification Authority and against Revocation Lists for every request.

Certification Authority (CA)

The CA interacts with the SSL Socket Layer and User Registration Service. The CA generates user client certificates and private keys (2048 bit) upon first login/registration. It maintains a database of every created certificate as well as a revocation list.

User Registration Service (URS)

For every device to use the service a user has to be authenticated and verified upon first login. The webservice requires at least three different user inputs (userid, password, organization). The URS chooses the appropriate authentication plugin based on the supplied organization input field. Once the user has been validated the URS requests the users client certificate and private key from the CA. If none exists a new on will be created. The webservice forwards this information to the user for further use of the webservice. Currently the certificate/private key is stored encrypted (user selected pin code) on the mobile device.

Messaging

The Messaging module provides the user with an Inbox for received personal messages as well as an Outbox for send messages. The Transport performs the delivery of messages to selected recipients when a message is send or forwarded. Every message is stored in the database encrypted with the users public key to ensure only the user is able to retrieve the plain text message. Furthermore each message is signed by the sender with his private key to ensure authenticity. Additionally a message can be linked to a specific ECG using a reference field and the unique ECG record identifier.

ECG Records

The ECG Record Module provides the user with an Inbox for received ECG records as well as an Outbox for send ECG records. The Transport performs the delivery of ECG records to the selected recipients when ECG is send or forwarded. The Inbox and Outbox tables hold only a reference to the ECG records stored in the ECG file table. This ensures that a user can only access the ECG he has received/send.

Mobile Device Push Notification Registration (PNR)

The when a user want's to be notified about changes to his account (new ECG/Message, status changes etc.) he can register his device for Push Notifications (PN) based on mobile device app settings. This module will create/delete a database record for the user upon registration/dereregistration and if certain events occur will be notified about those changes. During the registration process the PNR requires that the notification service provider is selected. (For now only Google Cloud Messaging and Apple Push Notification Service implemented)

Push Notification Service (PNS)

If the user has registered a device for PNs he will receive notifications on certain events. Depending on the registration setting for his device the PNS will use the appropriate plugin to deliver the notifications. For GCM the notifications a fully encrypted with the users public key. Furthermore the message will be signed by the server with a specific signing key (public server key provided to the user upon push notification registration) For APN due to message size limitations no encryption is used. The push notification does not contain any personal information therefore encryption is not an absolute necessity.

Usage Scenarios

User registration/ User Login

Before a user can use the webservice he needs to be authenticated by the webservice. The application running on the RMD requests valid login credentials and organization from the user. The application then forwards this information through a SSL secured channel to the webservice. For establishing the SSL connection the application is shipped with the certification authorities root certificate. This root certificate builds the trust anchor for the secure connection.

Once the webservice has received the user input (userid, password, organization) it selects the appropriate authentication plugin based on the organization input field and a predefined organization lookup table. The authentication plugin verifies and authenticates the user based on organization predefined procedures. After authentication/validation of the user the URS checks if the user is already associated with a valid client certificate in the user table. If no entry is found the CA is contacted and a new client certificate based on the information returned by the authentication plugin is created. Mandatory information returned by the authentication plugin for a new user entry and client certificate: First Name, Last Name, Unique User ID, Common Name, Display Name, Organization, Organization department, State, Country, Affiliation.

Once a valid user entry exists in the user table the webservice returns the client certificate (certificate and private key) to the user. On failure or if user could not be authenticated an error is returned and the login procedure is aborted.

On successful login the application on the mobile device requests a PIN code from the user which will then be used to encrypt the users private key on the mobile device. To increase difficulty of a brute force attacks on the users encrypted private key and key stretching algorithm (PBKDF2 with HMAC_SHA1) is applied to the PIN code.

For further communication with the webservice the application on the mobile device will request the users PIN code before unlocking the users client certificate and private key. Which then is used to establish a secure connection with the webservice. The webservice verifies and identifies the user based on his supplied

client certificate. If the user closes the application or the screen lock turns on, the in memory existing decrypted client certificate is destroyed and the user is ask for his PIN code upon reopening the application.

ECG File Transfer

- Transfer from MD to LMD
    - When the user presses the 'Capture' button on the LMD application the MD begins streaming the ECG file to the LMD. The file is recorded at 500Hz and is stored in a proprietary binary file format.
- Preview on LMD
    - When the file transfer is complete, the binary file is temporarily stored on the phone, parsed and displayed on the LMD in a standard static 12 lead format. The user then can choose to send or discard the ECG. When the user chooses to send the ECG, a list of eligible receiving users is downloaded from the server and populates an auto-complete list. As the user types in an address this list is used to provide suggested auto-completions based on the user's input. Using the selected receiving address the temporary ECG file the file is transmitted to the server. Upon closing the preview view or if the user chooses to discard the ECG, the temporary ECG file is discarded.
- Transfer from LMD to Server
    - To send an ECG file the LMD must have an active internet connection. The LMD provides the server with the sending address, ECG file, and 'file' action using the send.php script. The server will respond with a boolean 'success' (i.e. 'true' on success and 'false' on failure) field and a human readable error only upon failure. On success the ECG file will be stored on the ECG record table with a link to the file in the sending user's outbox and the receiving user's inbox. This arrangement ensures that the only ECGs a user has access to are intended for their viewing and no ECG files are duplicated to save on storage.
- Transfer from Server to receiving RMD
    - Notifications

        - When the user has a new (unread) ECG in their inbox/outbox they will receive a push notification on the RMD on which they have saved their credentials. The notification will contain the information about the unread ECG.
        - When there is a status update, a push notification will be sent to make sure the user's local inbox/outbox is updated with the most recent status of the read/unread ECG file.
    - Load inbox/outbox
        - The RMD will request the entire inbox or outbox using the corresponding inbox.php or outbox.php and the 'getall' action. The server returns the entire list of read and unread ECG's which is used to populate a list view in the IH application.
    - Download File
        - When a user selects an ECG to view, the RMD supplies the server with the 'get_file' action along with the ECG's inbox/outbox ID and the file format of the ECG being transmitted. 'raw' will supply the RMD with the proprietary binary file format, and 'json' will supply a JSON encoded string containing the ECG data. If the information supplied by the RMD to the server is correct, the server will initiate a file transfer to the RMD. Upon receiving the ECG, the RMD parses the file and displays the information in a standard 12 lead format. Once the application on the RMD displays a new ECG record it contacts the webservice and changes the status of this ECG record to 'read'. The server sends out a PN to all registered devices of this user to notify about this status change.

Messaging

Once the user has send or received an ECG record. He is able to start a conversation with the sender.

To initiate a conversation he can select the chat icon right next to an ECG in the inbox or outbox. Once the icon is selected a messaging dialog opens and the user can type the message he wants to send. Once he presses the send button the application contacts the server which transports the message to the designated recipient. During transfer to the webservice the application on the mobile device supplies the ECG record identifier as a reference to the webservice. The webservice stores this reference with the message. Therefore each message can be associated with a specific ECG.

Before the message is transmitted to the server the application generates a signature based on the transmitting users private key. (RSA with SHA1 algorithm). The server verifies the message signature and the existence of the recipient. Once verified the webservice accepts the message and stores the message in the senders outbox. The plain text message is encrypted using the senders private key before stored in the database. Furthermore the webservice resolves the recipient if a transport address is used and stores the message in the recipients inbox. The plain text message is encrypted using the recipients public key before stored into the database.

The webservice sends a PN to the all the recipients to inform about the new message in their inbox. Once the application on the recipients mobile device receives the PN it downloads the users message inbox and notifies the user visually and acoustically. If the recipient has the current conversion dialog open the new message is decrypted and displayed in the dialog. At no time is the message stored unencrypted on the mobile device it is decrypted on the fly in the conversation dialog view.

Vanderbilt ECG Dispatch System

API Documentation

Rev. 0.1.14

Jan 9, 2015

Table of Contents

Document History

Version	Date	Author	Description
0.1.14	9. Jan. 2015	Rene Harder	Added CC parameter to send email Added additional outputs to directory
0.1.13	16. Jul. 2014	Rene Harder	Made signature for send message optional Added plain text format to mbox
0.1.12	30. Sep. 2013	Rene Harder	Fixed typo in error response Added change_status of Message
0.1.11	17. Sep. 2013	Rene Harder	Fixed typos Added reference input field to Message Box→Receiving Messages/Send Mesages Added isDiagnose flag to Send→ send Message
0.1.10	18. Aug. 2013	Rene Harder	Removed note in Send→Forward File Added send PDF via email Added alternative output PDF Added notes where push notification are send
0.1.9	7.Aug.2013	Jonathan Whitfield	Added Forward file to document. Added User directory to documentation Appendix moved one chapter up
0.1.8	1.Aug.2013	Rene Harder	Added optional reference to send message Added chapter Addressing
0.1.7	2. Jul. 2013	Rene Harder	Added document history. Added message related chapters Added Appendix and Encryption Method
0.1.6	30. Jun. 2013	Rene Harder	added alternative output formats (JSON variants)
0.1.5	28. Jun. 2013	Rene Harder	Initial version

User Login & Registration

The login and registrations script do not require client certificate authentication. However they do require a secured http connection.

HTTP Response Codes: 403, The script set's the response code to “403 Forbidden” if the scripts is accessed through an insecure connection or any of the required input parameters is missing

Request Methods: GET & POST

Login

URL: https://IP-ADDRESS/VandyECG/login.php

Input Parameters:

Name	Type	Description
uid	String	The users login id (e.g. VUnetID)
password	String	The users password
org	String	The organization's identifier (e.g.VANDY)

Output Parameters:

Format: JSON encoded String

Name	Type	Description
success	Boolean	True if login was successful, false on error
cert	String [on success only]	Contains the users base64 encoded client certificate
key	String [on success only]	Contains the users private key, Key is base64 encoded and encrypted with user's password
pkcs12	String[on success only]	Contains user client certificate and key, base64 encoded and protected with users password in PKCS12 container
error	String[on error only]	A human readable error message

Registration

URL: https://IP-ADDRESS/VandyECG/register.php

Request Methods: GET & POST

Note: The registration script is still incomplete and more input parameters will be added later. For now only Vanderbilt is supported, input/output is basically identical to the login script.

Input Parameters:

Name	Type	Description
uid	String	The users login id (e.g. VUnetID)
password	String	The users password
org	String	The organization's identifier (e.g.VANDY)

Output Parameters:

Format: JSON encoded String

Name	Type	Description
success	Boolean	True if registration was successful, false on error
cert	String [on success only]	Contains the users base64 encoded client certificate
key	String [on success only]	Contains the users private key, Key is base64 encoded and encrypted with user's password
pkcs12	String [on success only]	Contains user client certificate and key, base64 encoded and protected with users password in PKCS12 container
error	String [on error only]	A human readable error message

Push Notification Registration

User client certificate authentication is required.

Request Methods: GET & POST

Response Codes: 403 on insecure connection, missing input parameters or invalid client certificate

Device Registration

Register a device to receive push notifications on new or updated events

URL: https://IP-ADDRESS/VandyECG/eds/push_registration.php

Input Parameters:

Name	Type	Description
device_id	String	Unique device identifier
token	String	The device token from the push provider
service	String (google | apple)	The push provider. For now only google is implemented Apple will be in the next couple of weeks

Output Parameters:

Format: JSON encoded String

Name	Type	Description
success	Boolean	True if registration was successful, false on error
signaturekey	String [on success only]	The server's base64 encoded public signing key. Used to verify origin and integrity of pushed message
error	String [on error only]	A human readable error message

Device Unregistration

Disables a device push notification. The device will no longer be notified about events.

URL: https://IP-ADDRESS/VandyECG/eds/push_unregistration.php

Input Parameters:

Name	Type	Description
device_id	String	Unique device identifier
token	String	The device token from the push provider

Output Parameters:

Format: JSON encoded String

Name	Type	Description
success	Boolean	True if unregistration was successful, false on error
error	String [on error only]	A human readable error message

Files Inbox and Outbox

User client certificate authentication is required

Request Methods: GET & POST

Response Codes: 403 on insecure connection, missing input parameters or invalid client certificate

Inbox

To manage users inbox. The inbox contains received files for a user

URL: https://IP-ADDRESS/VandyECG/eds/inbox.php

Input Parameters:

Name	Type	Description
action	String	The action to perform
boxid	String [action specific]	The box identifier as reported by action getall
status	String [action specific]	The status the inbox entry gets marked as (“new” or “read”)
format	String [action specific]	The format of the output (raw, json, deflate_json, bzip_json …) for file download only.

Retrieve entire inbox

action: getall

Required inputs: action

Output Parameters:

Format: JSON encoded String

Name		Type	Description
success		Boolean	True if action was successful, false on error
inbox		Array	User inbox entries as an array each row represents one entry
inbox[i].	id	String	The unique inbox id (also refereed to as boxid)
	filetype	String	The file type of the attached file (“ecg” the only supported type for now)
	fileid	String	A unique file identifier
	sender	String	The address of the sender
	recipient	String	The address of the recipient (usually the user)
	transports	String Array	Array of transport addresses which redirected the message/file. The oldest transport is the last on in the array
	status	String	The status of the inbox entry (“new” or “read”)
	send_time	Integer	Unix timestamp in milliseconds when the file was send
timestamp		Integer	Unix timestamp when the inbox ouput was generated
error		String [on error only]	A human readable error message

Change status of entry

action: change_status

Required inputs: action, boxid, status

Note: If user has registered a device for push notification a notification is send about this event

Output Parameters:

Format: JSON encoded String

Name	Type	Description
success	Boolean	True if status change was successful, false on error
status	String	The new status of the inbox entry (“new” or “read”)
error	String [on error only]	A human readable error message

Delete an entry

action: delete

Required inputs: action, boxid

Note: If user has registered a device for push notification a notification is send about this event

Output Parameters:

Format: JSON encoded String

Name	Type	Description
success	Boolean	True if deleting was successful, false on error
error	String [on error only]	A human readable error message

Retrieve File

To download a file from the inbox. If no format is specified it defaults to the proprietary raw format

Proprietary Raw Format

action: get_file

Required inputs: action, boxid, format

format: raw

Output Parameters:

On success a File Transfer is initiated. Content Type: application/octet-stream

On error the HTTP response code is set to 404 Not Found and the following output is generated

Format: JSON encoded String

Name	Type	Description
success	Boolean	Always false
error	String [on error only]	A human readable error message

JSON Encoded Data

action: get_file

Required inputs: action, boxid, format

format: json

Output Parameters:

On success the data is put in a JSON encoded string as described in the table below

Format: JSON encoded String

Name	Type	Description
stream_labels	Array	List containing the labels of each stream (STREAM_LABEL), Each output can containing multiple streams. (e.g. ECG, info ...)
STREAM_LABEL_n	Object	Stream content of stream n
header	Object	The header information of the stream
num_channels	Integer	Number of channels in this stream
id	Integer	Stream identifier as stored in the raw file
sampling_rate	Integer	The sampling rate of the data, if 0 or negative the time vector should be considered
channel_names	Array	List containing the name of each channel
units	Array	List containing the unit (e.g mV) for each channel
channels[i]	Array	Array containing the channel data channel[0] first channel channel[1] second channel up to channel[num_channels-1]
time	Array	The time vector, should only be considered of sampling_rate<=0

On error the HTTP response code is set to 404 Not Found and the following output is generated

Format: JSON encoded String

Name	Type	Description
success	Boolean	Always false
error	String [on error only]	A human readable error message

JSON Encoded Data (Deflate compression)

action: get_file

Required inputs: action, boxid, format

format: deflate_json

Output Parameters:

On success a File Transfer is initiated. Content Type: application/octet-stream. The content of the file is the deflate (RFC 1951) compressed JSON encoded data as described in section .

On error the HTTP response code is set to 404 Not Found and the following output is generated

Format: JSON encoded String

Name	Type	Description
success	Boolean	Always false
error	String [on error only]	A human readable error message

JSON Encoded Data (Bzip2 compression)

action: get_file

Required inputs: action, boxid, format

format: bzip_json

Output Parameters:

On success a File Transfer is initiated. Content Type: application/octet-stream. The content of the file is the bzip2 compressed JSON encoded data as described in section .

On error the HTTP response code is set to 404 Not Found and the following output is generated

Format: JSON encoded String

Name	Type	Description
success	Boolean	Always false
error	String [on error only]	A human readable error message

PDF

Converts a file associated with an inbox entry into a PDF document.

action: get_file

Required inputs: action, boxid, format

Format: pdf

Output Parameters:

On success a File Transfer is initiated. Content Type: application/pdf.

On error the HTTP response code is set to 404 Not Found and the following output is generated

Format: JSON encoded String

Name	Type	Description
success	Boolean	Always false
error	String [on error only]	A human readable error message

Outbox

To manage users outbox. The outbox contains the send files for a user

URL: https://IP-ADDRESS/VandyECG/eds/outbox.php

Input Parameters:

Name	Type	Description
action	String	The action to perform
boxid	String [action specific]	The box identifier as reported by action getall
status	String [action specific]	The status the inbox entry gets marked as (“new” or “read”)
format	String [action specific]	The format of the output (raw, json, deflate_json, bzip_json …) for file download only.

Retrieve entire outbox

action: getall

Required inputs: action

Output Parameters:

Format: JSON encoded String

Name		Type	Description
success		Boolean	True if action was successful, false on error
outbox		Array	User outbox entries as an array each row represents one entry
outbox[i].	id	String	The unique outbox id (also refereed to as boxid)
	filetype	String	The file type of the attached file (“ecg” the only supported type for now)
	fileid	String	A unique file identifier
	sender	String	The address of the sender (usually the user)
	recipient	String	The address of the recipient (if transport was used the first transport is listed as the recipient)
	transports	String Array	Array of transport addresses which redirected the message/file. The oldest transport is the last on in the array
	status	String	The status of the outbox entry (“new”, “read” or “failed”), By default the status is set to “read” when file was send and “failed” on error
	send_time	Integer	Unix timestamp in milliseconds when the file was send
timestamp		Integer	Unix timestamp when the outbox ouput was generated
error		String [on error only]	A human readable error message

Change status of entry

action: change_status

Required inputs: action, boxid, status

Note: If user has registered a device for push notification a notification is send about this event

Output Parameters:

Format: JSON encoded String

Name	Type	Description
success	Boolean	True if status change was successful, false on error
status	String	The new status of the outbox entry (“new”, “read” or “failed”)
error	String [on error only]	A human readable error message

Delete an entry

action: delete

Required inputs: action, boxid

Note: If user has registered a device for push notification a notification is send about this event.

Output Parameters:

Format: JSON encoded String

Name	Type	Description
success	Boolean	True if deleting was successful, false on error
error	String [on error only]	A human readable error message

Retrieve File

To download a file from the outbox. If no format is specified it defaults to the proprietary raw format.

Proprietary Raw Format

action: get_file

Required inputs: action, boxid

Format: raw

Output Parameters:

On success a File Transfer is initiated. Content Type: application/octet-stream

On error the HTTP response code is set to 404 Not Found and the following output is generated

Format: JSON encoded String and HTTP response code 404 or 403

Name	Type	Description
success	Boolean	Always false
error	String [on error only]	A human readable error message

JSON Encoded Data

action: get_file

Required inputs: action, boxid, format

Format: json

Output Parameters:

On success the data is put in a JSON encoded string as described in the table below

Format: JSON encoded String

Name	Type	Description
stream_labels	Array	List containing the labels of each stream (STREAM_LABEL), Each output can containing multiple streams. (e.g. ECG, info ...)
STREAM_LABEL_n	Object	Stream content of stream n
header	Object	The header information of the stream
num_channels	Integer	Number of channels in this stream
id	Integer	Stream identifier as stored in the raw file
sampling_rate	Integer	The sampling rate of the data, if 0 or negative the time vector should be considered
channel_names	Array	List containing the name of each channel
units	Array	List containing the unit (e.g mV) for each channel
channels[i]	Array	Array containing the channel data channel[0] first channel channel[1] second channel up to channel[num_channels-1]
time	Array	The time vector, should only be considered of sampling_rate<=0

On error the HTTP response code is set to 404 Not Found and the following output is generated

Format: JSON encoded String

Name	Type	Description
success	Boolean	Always false
error	String [on error only]	A human readable error message

JSON Encoded Data (Deflate compression)

action: get_file

Required inputs: action, boxid, format

Format: deflate_json

Output Parameters:

On success a File Transfer is initiated. Content Type: application/octet-stream. The content of the file is the deflate (RFC 1951) compressed JSON encoded data as described in section .

On error the HTTP response code is set to 404 Not Found and the following output is generated

Format: JSON encoded String

Name	Type	Description
success	Boolean	Always false
error	String [on error only]	A human readable error message

JSON Encoded Data (Bzip2 compression)

action: get_file

Required inputs: action, boxid, format

Format: bzip_json

Output Parameters:

On success a File Transfer is initiated. Content Type: application/octet-stream. The content of the file is the bzip2 compressed JSON encoded data as described in section .

On error the HTTP response code is set to 404 Not Found and the following output is generated

Format: JSON encoded String

Name	Type	Description
success	Boolean	Always false
error	String [on error only]	A human readable error message

PDF

Converts a file associated with an outbox entry into a PDF document.

action: get_file

Required inputs: action, boxid, format

Format: pdf

Output Parameters:

On success a File Transfer is initiated. Content Type: application/pdf.

On error the HTTP response code is set to 404 Not Found and the following output is generated

Format: JSON encoded String

Name	Type	Description
success	Boolean	Always false
error	String [on error only]	A human readable error message

Message Box

To request received or send private messages

Request Methods: GET & POST

Response Codes: 403 on insecure connection, missing input parameters or invalid client certificate

Receiving Messages (Inbox)

To get messages intended for a user.

URL: https://IP-ADDRESS/VandyECG/eds/mbox.php

Input Parameters:

Name	Type	Description
action	String	The action to perform
type	String	The type of the action for received messages type=inbox
format	String [“plain” or “encrypted”]	The format a message text is presented either encrypted or plain text
msgid	String [action specific]	The message identifier as reported by action getall etc. To request multiple messages use a comma separated list of msgids
status	String [action specific]	The message status. “new”, “read” or “failed”
search	String [action specific]	The search string, only used for action=find.
reference	String [optional]	Specify a specific reference. The output will be limited to messages with this reference string set.

Retrieve all Messages

This will output all messages in the users inbox

action: getall

Required inputs: action

Optional inputs: reference

Output Parameters:

Format: JSON encoded String

Name		Type	Description
success		Boolean	True, if action was successful, false on error
inbox		Array	User inbox entries as an array each row represents one entry
inbox[i].	id	String	The unique inbox id (also refereed to as msgid)
	message	String	Base64 encoded plain text or encrypted message using users public key. See Appendix -Encryption Method
	signature	String	The signature of the sender, See Appendix -Signing Method
	sender	String	The address of the sender
	recipient	String	The address of the recipient (usually the user)
	transports	String Array	Array of transport addresses which redirected the message. The oldest transport is the last on in the array
	status	String	The status of the inbox message entry (“new” or “read”)
	reference	String	An application settable reference to group messages (e.g. thread reference)
	send_time	Integer	Unix timestamp in milliseconds when the message was send
	recv_time	Integer	Unix timestamp in milliseconds when the message was received. It is 0 until the message is marked from new -> read. (the first time only)
timestamp		Integer	Unix timestamp when the output was generated
error		String [on error only]	A human readable error message

Get all new Messages

This will output all new messages in the users message inbox

action: getnew

Required inputs: action

Optional inputs: reference

Output Parameters:

Format: JSON encoded String

Name		Type	Description
success		Boolean	True if action was successful, false on error
inbox		Array	User inbox entries as an array each row represents one entry
inbox[i].	id	String	The unique inbox id (also refereed to as msgid)
	message	String	Base64 encoded plain text or encrypted message using users public key. See Appendix -Encryption Method
	signature	String	The signature of the sender, See Appendix -Signing Method
	sender	String	The address of the sender
	recipient	String	The address of the recipient (usually the user)
	transports	String Array	Array of transport addresses which redirected the message. The oldest transport is the last on in the array
	status	String	The status of the inbox message entry, (should be “new “only)
	reference	String	An application settable reference to group messages (e.g. thread reference)
	send_time	Integer	Unix timestamp in milliseconds when the message was send
	recv_time	Integer	Unix timestamp in milliseconds when the message was received. It is 0 until the message is marked from new -> read. (the first time only)
timestamp		Integer	Unix timestamp when the output was generated
error		String [on error only]	A human readable error message

Get specific messages

This will output one or multiple specific messages in the users message inbox

action: get

Required inputs: action, msgid

The msgid can be a single message id or a comma separated list of multiple msgids

Optional inputs: reference

Output Parameters:

Format: JSON encoded String

Name		Type	Description
success		Boolean	True if action was successful, false on error
inbox		Array	User inbox entries as an array each row represents one entry
inbox[i].	id	String	The unique inbox id (also refereed to as msgid)
	message	String	Base64 encoded plain text or encrypted message using users public key. See Appendix -Encryption Method
	signature	String	The signature of the sender, See Appendix -Signing Method
	sender	String	The address of the sender
	recipient	String	The address of the recipient (usually the user)
	transports	String Array	Array of transport addresses which redirected the message. The oldest transport is the last on in the array
	status	String	The status of the inbox message entry, (“new“ or “read”)
	reference	String	An application settable reference to group messages (e.g. thread reference)
	send_time	Integer	Unix timestamp in milliseconds when the message was send
	recv_time	Integer	Unix timestamp in milliseconds when the message was received. It is 0 until the message is marked from new -> read. (the first time only)
timestamp		Integer	Unix timestamp when the output was generated
error		String [on error only]	A human readable error message

Change Status of Message

action: change_status

Required inputs: action, msgid, status

Note: If user has registered a device for push notification a notification is send about this event

Output Parameters:

Format: JSON encoded String

Name	Type	Description
success	Boolean	True if status change was successful, false on error
status	String	The new status of the inbox message (“new” or “read”)
error	String [on error only]	A human readable error message

Sent Messages (Outbox)

To get messages the user has or tried to send

URL: https://IP-ADDRESS/VandyECG/eds/mbox.php

Input Parameters:

Name	Type	Description
action	String	The action to perform
type	String	The type of the action for sent messages type=outbox
format	String [“plain” or “encrypted”]	The format a message text is presented either encrypted or plain text
msgid	String [action specific]	The message identifier as reported by action getall etc. To request multiple messages use a comma separated list of msgids
status	String [action specific]	The message status. “new”, “read” or “failed”
search	String [action specific]	The search string, only used for action=find.
reference	String (optional)	Specify a specific reference. The output will be limited to messages with this reference string set.

Retrieve all Messages

This will output all messages in the users sent message box

action: getall

Required inputs: action, type

Optional inputs: reference

Output Parameters:

Format: JSON encoded String

Name		Type	Description
success		Boolean	True, if action was successful, false on error
outbox		Array	Users sent message entries as an array each row represents one entry
outbox[i].	id	String	The unique outbox id (also refereed to as msgid)
	message	String	Base64 encoded plain text or encrypted message using users public key. See Appendix -Encryption Method
	signature	String	The signature of the sender, See Appendix -Signing Method
	sender	String	The address of the sender
	recipient	String	The address of the recipient (if transport was used first transport also is recipient)
	transports	String Array	Array of transport addresses which redirected the message. The oldest transport is the last on in the array
	status	String	The status of the outbox message entry (“new”, “read” or “failed”)
	reference	String	An application settable reference to group messages (e.g. thread reference)
	send_time	Integer	Unix timestamp in milliseconds when the message was send
timestamp		Integer	Unix timestamp when the output was generated
error		String [on error only]	A human readable error message

Get all new Messages

This will output all new messages in the users message outbox

action: getnew

Required inputs: action, type=outbox

Optional inputs: reference

Output Parameters:

Format: JSON encoded String

Name		Type	Description
success		Boolean	True if action was successful, false on error
inbox		Array	User outbox entries as an array each row represents one entry
inbox[i].	id	String	The unique outbox id (also refereed to as msgid)
	message	String	Base64 encoded plain text or encrypted message using users public key. See Appendix -Encryption Method
	signature	String	The signature of the sender, See Appendix -Signing Method
	sender	String	The address of the sender
	recipient	String	The address of the recipient (usually the user)
	transports	String Array	Array of transport addresses which redirected the message. The oldest transport is the last on in the array
	status	String	The status of the outbox message entry, (should be “new “only)
	reference	String	An application settable reference to group messages (e.g. thread reference)
	send_time	Integer	Unix timestamp in milliseconds when the message was send
	recv_time	Integer	Unix timestamp in milliseconds when the message was received. It is 0 until the message is marked from new -> read. (the first time only)
timestamp		Integer	Unix timestamp when the output was generated
error		String [on error only]	A human readable error message

Get all read Messages

This will output all messages in the users message outbox which are marked read

action: getread

Required inputs: action, type=outbox

Optional inputs: reference

Output Parameters:

Format: JSON encoded String

Name		Type	Description
success		Boolean	True, if action was successful, false on error
outbox		Array	User's sent message entries as an array each row represents one entry
outbox[i].	id	String	The unique outbox id (also refereed to msgid)
	message	String	Base64 encoded plain text or encrypted message using users public key. See Appendix -Encryption Method
	signature	String	The signature of the sender, See Appendix -Signing Method
	sender	String	The address of the sender
	recipient	String	The address of the recipient (if transport was used first transport also is recipient)
	transports	String Array	Array of transport addresses which redirected the message. The oldest transport is the last on in the array
	status	String	The status of the outbox message entry, (should be “read “only)
	reference	String	An application settable reference to group messages (e.g. thread reference)
	send_time	Integer	Unix timestamp in milliseconds when the message was send
timestamp		Integer	Unix timestamp when the output was generated
error		String [on error only]	A human readable error message

Get all failed Messages

This will output all messages in the users message outbox which where not delivered to the recipient

action: getfailed

Required inputs: action,type=outbox

Optional inputs: reference

Output Parameters:

Format: JSON encoded String

Name		Type	Description
success		Boolean	True, if action was successful, false on error
outbox		Array	User's sent message entries as an array each row represents one entry
outbox[i].	id	String	The unique outbox id (also refereed to msgid)
	message	String	Base64 encoded plain text or encrypted message using users public key. See Appendix -Encryption Method
	signature	String	The signature of the sender, See Appendix -Signing Method
	sender	String	The address of the sender
	recipient	String	The address of the recipient (if transport was used first transport also is recipient)
	transports	String Array	Array of transport addresses which redirected the message. The oldest transport is the last on in the array
	status	String	The status of the outbox message entry, (should be “failed “only)
	reference	String	An application settable reference to group messages (e.g. thread reference)
	send_time	Integer	Unix timestamp in milliseconds when the message was send
timestamp		Integer	Unix timestamp when the output was generated
error		String [on error only]	A human readable error message

Get specific messages

This will output one or multiple specific messages in the users message outbox

action: get

Required inputs: action, msgid, type=outbox

The msgid can be a single message id or a comma separated list of multiple msgids

Optional inputs: reference

Output Parameters:

Format: JSON encoded String

Name		Type	Description
success		Boolean	True, if action was successful, false on error
outbox		Array	User's sent message entries as an array each row represents one entry
outbox[i].	id	String	The unique message id (also refereed to as msgid)
	message	String	Base64 encoded plain text or encrypted message using users public key. See Appendix -Encryption Method
	signature	String	The signature of the sender, See Appendix -Signing Method
	sender	String	The address of the sender
	recipient	String	The address of the recipient (if transport was used first transport also is recipient)
	transports	String Array	Array of transport addresses which redirected the message. The oldest transport is the last on in the array
	status	String	The status of the outbox message entry, (“new“, “read” or “failed”)
	reference	String	An application settable reference to group messages (e.g. thread reference)
	send_time	Integer	Unix timestamp in milliseconds when the message was send
timestamp		Integer	Unix timestamp when the output was generated
error		String [on error only]	A human readable error message

Change Status of Message

action: change_status

Required inputs: action, msgid, status, type=outbox

Note: If user has registered a device for push notification a notification is send about this event

Output Parameters:

Format: JSON encoded String

Name	Type	Description
success	Boolean	True if status change was successful, false on error
status	String	The new status of the outbox message (“new” or “read”)
error	String [on error only]	A human readable error message

Send

User client certificate authentication is required

Request Methods: GET & POST

Response Codes: 403 on insecure connection, missing input parameters or invalid client certificate

Send File

To send a File to a single user, multiple recipients are only supported using transports (at least for now, might change later)

URL: https://IP-ADDRESS/VandyECG/eds/send.php

Note: The file needs to be uploaded using POST request. The other parameters are accepted using GET.

Note: If the recipient has registered a device for push notification a notification is sent for this event.

Input Parameters:

Name	Type	Description
action	String (file)	The action to perform. For sending file action=”file”
to	String	The address of the recipient (e.g. john.doe@vanderbilt.edu)
data	File	The file to send

Output Parameters:

Format: JSON encoded String

Name	Type	Description
success	Boolean	True if file was send successfully, false on error
error	String [on error only]	A human readable error message

Send Message

To send a private message to a single recipient, multiple recipients are only supported using transports

URL: https://IP-ADDRESS/VandyECG/eds/send.php

Note: If the recipient has registered a device for push notification a notification is sent for this event.

Input Parameters:

Name	Type	Description
action	String (msg)	The action to perform. For sending message action=”msg”
to	String	The address of the recipient (e.g. john.doe@vanderbilt.edu)
message	String	Base64 encoded message text
signature	String (optional)	Base64 encoded signature of the message (signed with user's private key) Signature Algo: SHA1withRSA || `OPENSSL_ALGO_SHA1`
reference	String (optional)	An optional reference (e.g. thread) identifier, used to group messages
isDiagnose	Boolean (optional)	A flag to specify a message as a diagnose response from the physician. Used for internal statistics only

Output Parameters:

Format: JSON encoded String

Name	Type	Description
success	Boolean	True if file was send successfully, false on error
error	String [on error only]	A human readable error message

Forward File

To forward a File to a single user, multiple recipients are only supported using transports (at least for now, might change later)

URL: https://IP-ADDRESS/VandyECG/eds/send.php

Note: If the recipient has registered a device for push notification a notification is sent for this event.

Input Parameters:

Name	Type	Description
action	String (forward_file)	The action to perform. For sending file action=”forward_file”
to	String	The address of the recipient (e.g. john.doe@vanderbilt.edu)
boxid	String	The filebox ID of the file to be forwarded

Output Parameters:

Format: JSON encoded String

Name	Type	Description
success	Boolean	True if file was send successfully, false on error
error	String [on error only]	A human readable error message

Send Email (with attached PDF)

To send a file attached as PDF to a single user via email.

URL: https://IP-ADDRESS/VandyECG/eds/send.php

Input Parameters:

Name	Type	Description
action	String (email)	The action to perform. For sending pdf action=”email”
to	String	The email address of the recipient (e.g. john.doe@vanderbilt.edu)
boxid	String	The filebox ID of the file to be send as PDF
text	String (optional)	An optional text of the email body. If no text is specified the default “[USER] has send you an ECG.” will be used
confirm	Integer (optional)	Set to 1 if a read confirmation email is requested, 0 or not specified to disable
cc	Integer (option)	If set to 1 sender is added to the CC field of the email, will be ignored otherwise.

Output Parameters:

Format: JSON encoded String

Name	Type	Description
success	Boolean	True if PDF was send successfully, false on error
error	String [on error only]	A human readable error message

Directory

User Directory

User Directory

To pull a list of all registered users within the current user's organization.

URL: https://IP-ADDRESS/VandyECG/eds/directory.php

Note: The parameters are accepted using GET.

Input Parameters:

Name	Type	Description
action	String (user_list)	The action to perform. For user's directory action=”user_list”

Output Parameters:

Format: JSON encoded String

Name		Type	Description
success		Boolean	True if directory query was successful, false on error
error		String [on error only]	A human readable error message
user_list[i]	address	String	RFC822 compliant address (eg: “\”Doe, John H.\” <johndoe@email.com>”) for user in current user's organization
	firstname	String	The users first name (may be empty e.g. for forwarders)
	lastname	String	The users last name (may be empty e.g. for forwarders)
	city	String	The users city (may be empty e.g. for forwarders)
	state	String	The users state (may be empty e.g. for forwarders)
	org_unit	String	Registered user's organization unit (eg. Clinical Pharmacology, Biomedical Engineering, etc)
	cn	String	The common name for the registered user (eg. “John H. Doe”)
	org	String	The organization of the registered user
	affiliation	String	An array of organization specific affiliation codes

Appendix

Encryption Method

There are two different encryption methods used. If the unencrypted data is less that 245 bytes long, simple public/private key encryption is used (RSA with PKCS1 Padding)

If the encrypted data is longer, AES block encryption is used. The first 256 bytes (344 bytes base64 encoded) will contain the 256 bit long symmetric encryption key and 128 bit IV. This key and IV is encrypted using the users public/private key. (RSA with PKCS1 padding)

The remainder of the data then needs to be decoded using the result from the first encryption. (AES in CBC mode with Zero Byte Padding is used)

Signing Method

For the data a signature is generated using public or private key (depending on context, most time private key is used). The signature Algorithm is RSA with SHA1. The Signature should have a length of 256 bytes (344bytes base64 encoded).

Addressing

Every address described in this API documentation uses a RFC822 compliant addressing scheme.

Valid forms are. (Default used by server in **bold**)

- **Jon Doe <jon.doe@vanderbilt.edu>**
- “Doe, Joe” <jon.doe@vanderbilt.edu>
- jon.doe@vanderbilt.edu
- **<jon.doe@vanderbilt.edu>**

For addressing multiple users, users are comma or semicolon separated

- **Jon Doe <jon.doe@vanderbilt.edu>, Jane Doe <jane.doe@vanderbilt.edu>**
- Jon Doe <jon.doe@vanderbilt.edu>; Jane Doe <jane.doe@vanderbilt.edu>

Note: If display name contains either a comma or semicolon display name needs to be quoted.

D. Patents

The research in this dissertation resulted in 2 international patent filings, which are added to this appendix.

Patent Applications:

1. WO2014116968 A1 - Smart mobile health monitoring system and related methods .
2. WO2014071292 A1 - Compression device, system, and method for decreasing abdominal venous pooling.

D.1 Smart Mobile Health Monitoring System and Related Methods

(12) INTERNATIONAL APPLICATION PUBLISHED UNDER THE PATENT COOPERATION TREATY (PCT)

(19) World Intellectual Property Organization
International Bureau

(43) International Publication Date
31 July 2014 (31.07.2014)

WIPO | PCT

(10) International Publication Number
WO 2014/116968 A1

(51) International Patent Classification:
G06F 19/00 (2011.01)

(21) International Application Number:
PCT/US2014/012977

(22) International Filing Date:
24 January 2014 (24.01.2014)

(25) Filing Language: English

(26) Publication Language: English

(30) Priority Data:
61/756,717 25 January 2013 (25.01.2013) US

(71) Applicant: **VANDERBILT UNIVERSITY** [US/US]; 305 Kirkland Hall, 2201 West End Avenue, Nashville, Tennessee 37240 (US).

(72) Inventors: **BAUDENBACHER, Franz**; 182 North Berwick Lane, Franklin, Tennessee 37069 (US). **EAGLE, Susan**; 2510 Blair Blvd., Nashville, Tennessee 37212 (US). **HARDER, Rene**; 2129 Acklen Avenue, Apt. 12, Nashville, Tennessee 37212 (US). **WHITFIELD, Jonathan**; 707A Crescent Road, Nashville, Tennessee 37205 (US). **DIEDRICH, Andre**; 1121 Harpeth Mill Ct., Nashville, Tennessee 37221 (US). **PIETSCH, John B.**; 6528 Edinburgh Dr., Nashville, Tennessee 37221 (US). **MANDERS, Eric-Jan**; 1511 McLendon Ave. NE, Atlanta, Georgia 30307 (US).

(74) Agent: **WESORICK, Richard S.**; Tarolli, Sundheim, Covell & Tummino LLP, 1300 East Ninth Street, Suite 1700, Cleveland, Ohio 44114 (US).

(81) Designated States *(unless otherwise indicated, for every kind of national protection available)*: AE, AG, AL, AM, AO, AT, AU, AZ, BA, BB, BG, BH, BN, BR, BW, BY, BZ, CA, CH, CL, CN, CO, CR, CU, CZ, DE, DK, DM, DO, DZ, EC, EE, EG, ES, FI, GB, GD, GE, GH, GM, GT, HN, HR, HU, ID, IL, IN, IR, IS, JP, KE, KG, KN, KP, KR, KZ, LA, LC, LK, LR, LS, LT, LU, LY, MA, MD, ME, MG, MK, MN, MW, MX, MY, MZ, NA, NG, NI, NO, NZ, OM, PA, PE, PG, PH, PL, PT, QA, RO, RS, RU, RW, SA, SC, SD, SE, SG, SK, SL, SM, ST, SV, SY, TH, TJ, TM, TN, TR, TT, TZ, UA, UG, US, UZ, VC, VN, ZA, ZM, ZW.

(84) Designated States *(unless otherwise indicated, for every kind of regional protection available)*: ARIPO (BW, GH, GM, KE, LR, LS, MW, MZ, NA, RW, SD, SL, SZ, TZ, UG, ZM, ZW), Eurasian (AM, AZ, BY, KG, KZ, RU, TJ, TM), European (AL, AT, BE, BG, CH, CY, CZ, DE, DK, EE, ES, FI, FR, GB, GR, HR, HU, IE, IS, IT, LT, LU, LV, MC, MK, MT, NL, NO, PL, PT, RO, RS, SE, SI, SK, SM, TR), OAPI (BF, BJ, CF, CG, CI, CM, GA, GN, GQ, GW, KM, ML, MR, NE, SN, TD, TG).

Published:

— *with international search report (Art. 21(3))*

[Continued on next page]

(54) Title: SMART MOBILE HEALTH MONITORING SYSTEM AND RELATED METHODS

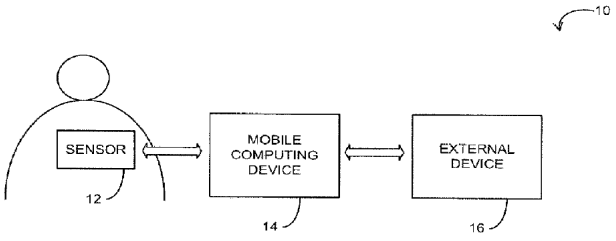

FIG. 1

(57) Abstract: One aspect of the present disclosure is a smart patient monitoring system. A sensor is coupled to a patient and configured to detect biometric data associated with the patient. A mobile computing device includes a memory that stores computer-executable instructions and a processor executes the computer-executable instructions. The mobile computing device receives the biometric data from the sensor; processes the biometric data to monitor a health status of the patient; and provides therapeutic feedback related to the health status.

WO 2014/116968 A1

— *before the expiration of the time limit for amending the claims and to be republished in the event of receipt of amendments (Rule 48.2(h))*

PATENT

SMART MOBILE HEALTH MONITORING SYSTEM AND RELATED METHODS

Related Applications

[0001] This application claims the benefit of U.S. Provisional Patent Application Serial No. 61/756,717, filed January 25, 2013, entitled "SMART PATIENT MONITORING SYSTEM." The entirety of the provisional application is hereby incorporated by reference for ali purposes.

Technical Field

[0002] The present disclosure relates generally to health monitoring, and more particularly to a smart mobile health monitoring system and related methods of use. Background

[0003] Traditional healthcare solutions focus on the treatment rather than the prevention of a disease. A steadily aging society with skyrocketing healthcare costs poses the need for a transformation from a reactive and hospital-driven healthcare system to a proactive, patient-centered and enabling healthcare system via medical equipment for home and ambulatory use. However, the medical equipment available for home and ambulatory use available today generally focuses on the pure acquisition of a single physiological parameter rather than multiple physiological parameters and treatment due to size, power and cost constraints.

Summary

[0004] In one aspect, the present disclosure includes mobile computing device. The mobile computing device includes a memory that stores computer-executable instructions and a processor that executes the computer-executable instructions. The execution of the computer- executable instructions enables the mobile computing device to receive biometric data detected by a sensor coupled to a body of a patient; process the biometric data to monitor a health status of the patient; and provide therapeutic feedback related to the current health status.

[0005] In another aspect, the present disclosure includes a system for smart mobile health monitoring that includes a sensor and a mobile computing device. The sensor is

coupled to a patient and configured to detect biometric data associated with the patient. The mobile computing device includes a memory that stores computer-executable instructions and a processor that executes the computer-executable instructions. The execution of the computer-executable instructions allows the mobile computing device to at least receive the biometric data from the sensor; process the biometric data to monitor at least one of diagnose a medical condition of the patient, or diagnose a disease of the patient; and provide therapeutic feedback related to the health status and at least one of an activity of the patient and a body position of the patient.

[0006] In a further aspect, the present disclosure includes a non- transitory computer-readabie device storing instructions executable by an associated processor to perform operations that facilitate smart mobile health monitoring. The operations inciude: receiving biometric data detected by a sensor coupled to a body of a patient; processing the biometric data to monitor a health status of the patient; providing therapeutic feedback related to the health status; and transmitting at least one of the biometric data, information related to the health status, and information related to the therapeutic feedback to an externa! device according to a wireless protocol. Brief Description of the Drawings

[0007] The foregoing and other features of the present disclosure will become apparent to those skilled in the art to which the present disclosure relates upon reading the following description with reference to the accompanying drawings, in which:

[0008] FIG. 1 is a schematic illustration of an example smart mobile health monitoring system in accordance with an aspect of the present disclosure;

[0009] FIG. 2 is a schematic illustration of an example sensor configuration that can be utilized within the system of F! G. 1 ;

[00103 FiG. 3 is a schematic illustration of an example mobile computing device configuration that can be utilized within the system of FIG. 1 ;

[0011] FIG. 4 is a schematic illustration of an example externa! device configuration that can be utilized within the system of F!G. 1 ; and

[0012] FiG 5 is schematic process flow diagram of an example method that facilitates health monitoring in accordance with an aspect of the present disclosure. Detailed Description

[0013] The present invention generally relates to smart mobile health monitoring. Applications of smart mobile health monitoring include, but are not limited to: monitoring a

health status while exercising, predicting and preventing falls, alerting emergency personnel of a change in health status, aiding in the diagnosis and management of patients with chronic conditions, and preventing and predicting medical events. The smart mobile health monitoring can be accomplished employing a sensor coupled to a patient and configured to detect biometric data (also referred to herein as "biomimetic data") associated with the patient and a mobile computing device can receive the biometric data from the sensor (e.g., via a wired connection and/or a wireless connection); process the biometric data to at least one of monitor a health status of the patient, diagnose a medical condition of the patient, or diagnose a disease of the patient; and provide therapeutic feedback related to the health status. The therapeutic feedback can also be related to an activity of the patient and/or a body position of the patient. The mobile computing device can include a wireless transmitter that can transmit the biometric data, information related to the health status, or information related to the therapeutic feedback to an external device according to a wireless protocol.

[0014] As used herein, the term "patient" can refer to any warmblooded organism including, but not limited to, human beings, pigs, rats, rnice, dogs, goats, sheep, horses, monkeys, apes, rabbits, cattle, etc. When used herein, the term "health status" generally refers to a

medical condition of a patient with respect to one or more properties represented by biometric data that can be detected by the sensor, The biometric data can inciude, but is not limited to: biopotential data, impedance data, biochemical data, temperature data, acoustical data, optical data, acceleration data, force data and pressure data,

[0015] The sensor can be auto-configurable and/or specialized for a particular patient. Examples of sensors that can be utilized within the smart sensor array include: biopotential sensors (e.g., to detect electrocardiogram (ECG), heart rate, etc.), impedance sensors (e.g., to detect hydration status, fluid shifts, respiration, cardiac output, etc.), acceleration sensors (e.g., to detect fall, activity, body position, etc.), pressure sensors (e.g., to detect diastolic blood pressure, mean blood pressure, systolic blood pressure, pulse pressure waveforms, etc.), and/or different types of sensors that can contribute to the smart health monitoring of the patient. The biopotential sensor can be a type of sensor that can detect electrocardiogram (ECG), skin potential (EDA), electroencephalogram (EEG), electromyogram (EMG), a heart rate, body impedance, a fluid status, a respiration, a cardiac output, a fall, an activity, a body position, a pulse wave form, blood oxygen levels, a respiratory CO2 value, a plethysmograph signal, venous/arterial biood pressure waveform, diastolic blood pressure, a systolic blood pressure, or another biopotential that can be used

in the monitoring of a health status, diagnosing a condition, and/or diagnosing a disease. The sensor is not limited to a single sensor; the sensor can include a plurality of individual sensors or electrodes. As an example, the sensor can be a configurable smart sensor array that can be coupled to the mobile computing device. The sensor can detect one or more parameters correlating to different medical conditions, including, but not limited to: arrhythmias, cardio vascular disease, myocardial infarction, heart failure, orthostatic hypotension, syncope, autism spectrum disorder, malnutrition, etc. The one or more parameters that are detected can indicate the health status of the patient.

[0016] The mobile computing device can communicate with the sensor and/or an external device according to a wireless protocol. Examples of mobile computing devices include, but are not limited to: smart phone devices, tablet computing devices, laptop computing device, personal media player devices, personal entertainment systems, or a device that includes at least a display, an input device, a wireless transceiver/hub, and a non-transitory computer readable medium storing executable instructions for a user interface, which can be used to display the biometric data, data derived from the biometric data, the information about the health status, or the information about the therapeutic feedback at the display and accept input from the user at the input device, as well as a processor configured to execute the

stored instructions. The wireless transmitter of the mobile computing device can be used to accomplish the mobile monitoring of one or more medical parameters of the patient while the patient has the capability of movement and/or motion. The wireless transmitter generally refers to a transmitter that does not require a wired connection to transmit the data. The wireless transmitter can employ wireless body area network technologies, such as: Bluetooth (BT), Bluetooth low energy (BLE), ZigBee, ANT+, WiFi, etc. The mobile computing device can be capable of securely transmitting information via an appropriate encryption algorithm.

[0017] The following paragraphs include definitions of exemplary terms used within this disclosure. Except where noted otherwise, variants of all terms, including singular forms, plural forms, and other forms, fall within each exemplary term meaning. Except where noted otherwise, capitalized and non-capitalized forms of all terms fall within each meaning.

[0018] It will be understood that, although the terms "first," "second," etc. may be used herein to describe various elements, these elements should not be limited by these terms. These terms are only used to distinguish one element from another. Thus, a "first" element discussed below could also be termed a "second" element without departing from the teachings of the present disclosure.

The sequence of operations (or steps) is not limited to the order presented in the claims or figures unless specifically indicated otherwise.

[0019] In the context of the present disclosure, the singular forms "a," "an" and "the" can include the plural forms as well, unless the context clearly indicates otherwise. It will be further understood that the terms "comprises" and/or "comprising," as used herein, can specify the presence of stated features, steps, operations, elements, and/or components, but do not preclude the presence or addition of one or more other features, steps, operations, elements, components, and/or groups thereof. As used herein, the term "and/or" can include any and all combinations of one or more of the associated listed items. "Or," as used herein, except where noted otherwise, is inclusive, rather than exclusive. In other words, "or' is used to describe a list of alternative things in which one may choose one option or any combination of alternative options. For example, "A or B" means "A or B or both" and "A, B, or C" means "A, B, or C, in any combination or permutation." if "or" is used to indicate an exclusive choice of alternatives or if there is any limitation on combinations of alternatives, the list of alternatives specifically indicates that choices are exclusive or that certain combinations are not included. For example, "A or B, but not both" is used to indicate use of an exclusive "or" condition. Similarly, "A, B, or C, but no

combinations" and "A, B, or C, but not the combination of A, B, and C" are examples where certain combinations of alternatives are not included in the choices associated with the list.

[0020] The present disclosure includes reference to block diagrams and/or flowchart illustrations of methods, apparatus (systems) and/or computer program products according to certain aspects of the disclosure. It is understood that each block of the block diagrams and/or flowchart illustrations, and combinations of blocks in the block diagrams and/or flowchart illustrations, can be implemented by computer program instructions. These computer program instructions may be provided to a processor of a general purpose computer, special purpose computer, and/or other programmable data processing apparatus to produce a machine, such that the instructions, which execute via the processor of the computer and/or other programmable data processing apparatus, create means for implementing the functions/acts specified in the block diagrams and/or flowchart block or blocks.

[0021] These computer program instructions may also be stored in a computer-readabie memory that can direct a computer or other programmable data processing apparatus to function in a particular manner, such that the instructions stored in the computer-readabie

memory produce an article of manufacture including instructions, which implement the function/act specified in the block diagrams and/or flowchart block or blocks.

[0022] The computer program instructions may also be loaded onto a computer or other programmable data processing apparatus to cause a series of operational steps to be performed on the computer or other programmable apparatus to produce a computer-implemented process such that the instructions that execute on the computer or other programmable apparatus provide steps for implementing the functions/acts specified in the block diagrams and/or flowchart block or blocks.

[0023] Accordingly, the present disclosure may be embodied in hardware and/or in software (including firmware, resident software, microcode, etc.). Furthermore, aspects of the present disclosure may take the form of a computer program product on a computer-usable or computer- readable storage medium having computer-usable or computer-readable program code embodied in the medium for use by or in connection with an instruction execution system. A computer-usable or computer-readable medium may be any non-transitory medium that can contain or store the program for use by or in connection with the instruction or execution of a system, apparatus, or device.

[0024] The computer-usable or computer-readable medium may be, for example but not limited to, an electronic, magnetic, optical, electromagnetic, infrared, or semiconductor system, apparatus or device. More specific examples (a no n -exhaustive list) of the computer-readable medium can include the following: a portable computer diskette; a random access memory; a read-only memory; an erasable programmable read-only memory (or Flash memory); and a portable compact disc read-only memory.

[0025] "Operative communication," as used herein includes, but is not limited to, a communicative relationship between devices, logic, or circuits, including wired and wireless relationships. Direct and indirect electrical, electromagneiic, and optical connections are examples of connections that facilitate operative communications. Two devices are in operative communication if an action from one causes an effect in the other, regardless of whether the action is modified by some other device. For example, two devices in operable communication may be separated by one or more of the following: i) amplifiers, ii) filters, iii) transformers, iv) optical isolators, v) digital or analog buffers, vi) analog integrators, vii) other electronic circuitry, viii) fiber optic transceivers, ix) Bluetooth communications links, x) IEEE 802.1 1 communications links, xi) satellite communication links, xii) gateways, repeaters, routers, and hubs, xiii) wired or wireless networks, xiv) mobile communications towers,

and xv) other wired or wireless communication links. Operative communication may be facilitated by and exist between devices using, for example, the internet or service provider networks. As another example, an electromagnetic sensor is in operative communication with a signal if it receives electromagnetic radiation from the signal. As a final example, two devices not directly connected to each other, but both capable of interfacing with a third device, e.g., a central processing unit (CPU), are in operative communication.

[0026] "Processor," as used herein includes, but is not limited to, one or more of virtually any number of processor systems or stand-alone processors, such as microprocessors, microcontrollers, central processing units (CPUs), distributed processors, paired processors, and digital signal processors (DSPs), in any combination. The processor may be associated with various other circuits that support operation of the processor, such as random access memory (RAM), read-only memory (ROM), programmable read-only memory (PROM), erasable programmable read-only memory (EPROM), clocks, decoders, memory controllers, or interrupt controllers, etc. These support circuits may be interna! or external to the processor or its associated electronic packaging. The support circuits are in operative communication with the processor. The support circuits are not necessarily shown separate from the processor in block diagrams or other drawings. [0027] "Software,"

as used herein includes a set of computer readable or executable instructions stored on a non-transitory computer readable medium that can be executed to cause a computer or another electronic device to perform functions, actions, or behave in a desired manner. The instructions may be embodied in various forms such as routines, algorithms, modules or programs including separate applications or code from dynamically linked libraries. Software may also be implemented in various forms such as a stand-alone program, a function call, a servlet, an applet, instructions stored in a memory, part of an operating system, or other types of executable instructions. It will be appreciated by one of ordinary skill in the art that the form of software is dependent on, for example, requirements of a desired application, the environment it runs on, or the desires of a designer/programmer or the like. Software may be embodied as an "application."

[0028] Referring now to FIG. 1 , illustrated is a schematic illustration of an example smart mobile health monitoring system 0 in accordance with an aspect of the present disclosure. The smart mobile health monitoring system includes a sensor 12 associated with (e.g., coupled to, in proximity with, attached to, etc.) a patient in a manner that allows the sensor to detect biometric data from the patient. The sensor 12 is coupled to a mobile computing device 14 via a wired connection or a wireless connection (employing a wireless protocol) for

transmission of the biometric data from the sensor to the mobile computing device. The mobile computing device 14 can receive the biometric data from the sensor 12 and process the biometric data to monitor a health status of the patient, diagnose a medical condition of the patient, and/or diagnose a disease of the patient. Additionally, the mobile computing device 14 can provide therapeutic feedback related to the health status of the patient. The therapeutic feedback can also be related to an activity of the patient and/or a body position of the patient

[0029] The mobile computing device 14 can provide the therapeutic feedback to the patient (e.g., by a display, an alarm, a speech, or another type of alert). In response to the therapeutic feedback, the mobile computing device 4 can receive speech input or other type of input {e.g., from the patient and/or a person administering treatment to the patient). The input can include, but is not limited to, information about an activity, symptoms, status, a medication, a body position and/pr food consumption. As an example, the mobile computing device 14 can alert an external device 16 to take an action (e.g. , initiate a treatment procedure and/or a preventive procedure) in response to the speech input. However, the speech input is not required for the external device 16 to take the action.

[0030] The mobile computing device 14 can be coupled to the external device 16 (e.g., via a wired connection or a wireless connection employing a wireless protocol) to transmit the biometric data, information regarding the health status, or information regarding the therapeutic feedback to the external device. In response, the externa! device 16 can provide an input to the mobile computing device 14 and/or the sensor 12 that can include a query, processed data, an instruction to adjust at least one of the health status and the therapeutic feedback for diagnostic purposes, and/or an instruction to change patient treatment regiments.

[0031] The external device 6 can be a therapeutic device configured to deliver a therapeutic treatment to the patient based on the information received from the mobile computing device 14. The external device 16 can access or include a secured external data store that can be accessible to a physician, other authorized medical personnel or caregiver associated with the patient. The external device 16 can include an expert system that can, for example, determine a procedure that can be used on the patient based on the information received from the mobile computing device 14.

[0032] FIG. 2 shows a schematic diagram of a sensor 12 that can be utilized within the smart mobile heath monitoring system. Although a single sensor is illustrated, the sensor 12 can be understood to include a

plurality of sensors, each receiving inputs that contribute to the biometric parameter. The sensor 12 can be remotely configured, dynamically configured, and/or adapted for a specific physiological state, a condition, and/or a specific disease to provide optimized feedback and/or diagnostic capabilities. The sensor 12 can include a detector 22 that can detect the biometric parameter, a data processor 24 that can process the detected biometric parameter (e.g., transform the biometric parameter into signal and/or a data type that can be received by the mobile computing device), and a transmitter 26 that can transmit the processed biometric parameter to the mobile computing device (e.g., via a wired and/or a wireless interface with the mobile computing device). The detector 22, the data processor 24, and the transmitter 26 can be referred to coliectively as "the components of the sensor".

[0033] One or more of the components of the sensor can be implemented by computer program instructions that can be stored in memory 20, a non-transitory computer-readable memory (e.g., an electronic, magnetic, optical, electromagnetic, infrared, or semiconductor system, apparatus or device) and provided to a processor 8 (e.g., microprocessor, and/or other programmable data processing apparatus). The processor 8 can execute the instructions such that the sensor can implement the functions of one or more of the components of the sensor. In an example, the memory 20 can be based on a

memory card (e.g., a SD card) and the processor 18 can be based on a microcontroller (e.g., an Atmel xMega microcontroller). The sensor 2 can include a power source (e.g., one or more batteries or the like) that can power one or more of the components of the sensor.

[0034] FIG. 3 shows a schematic diagram of the mobile computing device 14 that can be utilized within the smart mobile heath monitoring system. The mobile computing device 14 can include a receiver 32 that can receive the biometric data (or a signai that includes the biometric data) from the sensor (e.g., transmitted across a wired connection or a wireless connection). The mobile computing device 14 can also include a signal processor 34 that can process the biometric data (or the signal including the biometric data) and determine a health status of the patient based on the biometric data. Based on the biometric data and/or the health status, a therapeutic feedback determination unit 36 can provide therapeutic feedback related to the health status. The therapeutic feedback (the biometric data and/or the health status) can be presented to a user on a display 39 of the mobile computing device 14. The mobile computing device 14 also includes a wireless transmitter that can transmit the biometric data, information regarding the health status, and/or information regarding the therapeutic feedback to an external device. The receiver 32, the signal processor 34, the therapeutic feedback determination unit 36, the wireless

transmitter 38 and the display 39 can be referred to collectively as "the components of the mobile computing device."

[0035] One or more of the components of the mobile computing device can be implemented by computer program instructions that can be stored in memory 30, a non-transitory computer-readable memory (e.g., an electronic, magnetic, optical, electromagnetic, infrared, or semiconductor system, apparatus or device) and provided to a processor 28 (e.g., microprocessor, and/or other programmable data processing apparatus). The processor 28 can execute the instructions such that the mobile computing device can implement the functions of one or more of the components of the mobile computing device.

[0036] The mobile computing device 14 can include a global positioning system (GPS) that can determine the location of the patient. The location can be transmitted to the external device 16 in connection with the biometric data, the information related to the health status, and/or the information related to the therapeutic feedback. The mobile computing device 4 can choose an externa! device 16 {or devices) to receive the biometric data, the information related to the health status, and/or the information related to the therapeutic feedback based on the location. For example, when a patient is experiencing a medical emergency, the mobile

computing device 14 can send the biometric data, the information related to the health status, and/or the information related to the therapeutic feedback to an external device 16 (e.g., associated with a first responder or a hospital) in closest proximity to the location.

[0037] FIG. 4 shows a schematic diagram of an external device that can receive the biometric data, data derived from the biometric data, the information about the health status of the patient and/or the information about the therapeutic feedback from the mobile computing device. The external device can include a receiver 44 that can receive the biometric data, data derived from the biometric data, the data derived from the biometric data, the information about the health status of the patient and/or the information about the therapeutic feedback from the mobile computing device in a wireless transmission. Upon receiving the wireless transmission, a treatment planning unit 46 can determine a treatment for the patient based on the received biometric data, data derived from the biometric data, information about the health status of the patient and/or information about the therapeutic feedback from the mobile computing device. The treatment plan can be displayed on a display 48 and/or executed by a treatment unit. The biometric data, the data derived from the biometric data, the information about the health status of the patient, the information about the

therapeutic feedback from the mobile computing device and/or the treatment plan can be stored in a secure data store (e.g., external to the external device 16 or interna! to memory 42) that is accessible to a physician, caregiver and/or other authorized medical personnel associated with the patient. The receiver 44, the treatment planning unit 46, and the display 48 can be referred to collectively as "the components of the externa! device."

[0038] One or more of the components of the external device can be implemented by computer program instructions that can be stored in memory 42, a non-transitory computer-readable memory (e.g., an electronic, magnetic, optical, electromagnetic, infrared, or semiconductor system, apparatus or device) and provided to a processor 40 (e.g., microprocessor, and/or other programmable data processing apparatus). The processor 40 can execute the instructions such that the external device can implement the functions of one or more of the components of the externa! device.

[0039] The external device 16 can be coupled to one or more additional devices to implement the treatment plan. Examples of additional devices include, but are not limited to: defibrillators, sphygmomanometers, accelerometers, pulse oximeters, blood pressure measurement systems, drug, blood or fluid infusion devices, and respirators. The additional devices can

communicate wirelessly with the mobile computing device 14 to provide additional biometric parameters and treatment/responses for the patient. The external device 16 (e.g., associated with a physician, caregiver, hospital, an expert system, or the like) can use this data from the additional devices to monitor the treatment plan and/or to initiate a new treatment plan. The mobile computing device 14 can be electrically shielded from the actions of the additional devices. Additionaliy, any wired connection to the sensor 2 and/or the additional devices can also be electrically shielded. The sensor 12 and/or the mobile device 14 can be operated by an internal battery (e.g., the battery can be chargeable via a radio frequency (RF) charging circuit or another type of non-contact charging circuit).

[0040] As an example, the smart mobile health monitoring system 10 of FIG. 1 can be wireless with a miniature, cost-effective, and/or wearable sensor 12. The smart mobile health monitoring system 10 can be personalized to meet clinical and/or personal needs of the patient (e.g., the sensor 2 can be configured with times to sense the biometric parameter). In one example, the smart mobile health monitor can be a smart ECG device that can record an ECG. The sensor 12 can be a twelve-lead ECG (e.g., the leads can be electrically shielded) that can send the biometric data to a mobile computing device 14 associated with a paramedic or other first responder or on-scene caregiver, which can transmit the

data from the emergency setting to the external device 16 to display the ECG data in a manner familiar to a physician (e.g., on a dynamic twelve-lead ECG grid that scales dynamically with a zoom level of the ECG with a dynamically adjustable grid density). [0041] The external device 16 can be associated with the nearest hospital with a qualified interventional cardiology team and/or a physician associated with the patient to initiate pre-hospital thrombolytic therapy and/or fast track the treatment of patients with myocardial infarct and reduce the time between diagnosis and treatment. Immediate transmission of a paramedic performed recording to a qualified infarct team allows for effective triage of patients with ST-elevation myocardial infarction (STEIvll), reduces the time to balloon angioplasty, and have the potential to minimize the degree of myocardial damage and loss.

[0042] The external device 16 can include a tracking application that estimates or allows the physician to estimate the location and arrival time of patient at hospital to allow for advanced planning of any potential intervention. The patient's care in transit to the hospital can be supervised effectively by the physician, and any necessary medical interventions can be provided immediately or upon the patient's arrival at the hospital, increasing the likelihood of a positive medical outcome. The external device 16 can also allows the physician to provide instant therapeutic feedback (e.g., selected

among predefined message templates) to the paramedic or other first responder after reviewing the ECG data to manage the patient's care en route to the hospital.

[0043] This smart mobile health monitoring system 10 (also referred to as a smart ECG device) can overcome current obstacles, including current non-universal ECG transmission and costly alterations of hospital infrastructure in order to receive ECGs. The miniature, battery operated, wireless Smart ECG device communicates with smart phones, allowing the ECG to be recorded transmitted to the nearest hospital with interventional cardiology abilities by pressing a single button. A mobile device application allows a physician to retrieve the ECG data from an online service of the hospital and display the ECG data on a physician familiar standard grid. Instant therapeutic feedback can be provided to the paramedics via a secure messaging system embedded into a user interface of the mobile device application. The form factor of the ECG device is small and fits easily into the pocket of a doctor or paramedic's coat. The system is designed to be compatible with existing data infrastructure, and can be directly integrated in existing patient database systems.

[0044] The smart mobile health monitoring system 10 of FIG. 1 can be used to monitor autonomic function during sleep in autistic patients. For example, the sensor 12 can be used to measure activity, electrodermal activity, and

polysomnography of the autistic patient to study the heart rate of autistic patients during sleep. Information related to the heart rate during sleep can be sent to mobile computing device 14 and then aggregated at an external device 16 associated with a medical study.

[0045] The smart mobile health monitoring system 10 of FIG. 1 can also be used to detect and predict syncope by sensing biometric parameters associated with a patient and analyzing the biometric parameters on the mobile computing device 14. The external device 16 can be used to perform an action to prevent the syncope upon receiving a signal from the mobile computing device 14. For example, when indicated by the health status exceeding a threshold indicating that syncope may occur, communicating to an external electrical stimulator to provide electrical stimuli to the patient to prevent the syncope. The smart mobile health monitoring system 10 can also be used to detect and monitor malnutrition levels in children (e.g., through an application on the mobile computing device 14 and/or the external device 16 in connection with one or more impedance sensors).

[0046] For example, the malnutrition of children in developing countries or rural locations within developed countries can be managed by sensing and processing an impedance parameter (e.g., based on a bioelectricai impedance algorithm) and sending the parameter and/or

the processed parameter to an externa! device (e.g., associated with a hospital, doctor, researcher, or the like within the developed country and/or within a developed country). The bioelectricai impedance analysis (BIA) can rely on change in impedance of electrical current traveling through the body and an analytical approach based on this measurement. Bioelectricai Impedance Vector analysis is an example of the analytical approach that uses a graphical technique to determine body composition by plotting changes in total body water and cell membrane functionality. Coupling BIVA and decision support and longitudinal record keeping can further guide a nutritional intervention and facilitates tracking a patient through an episode of care.

[0047] In view of the foregoing structural and functional features described above, a method in accordance with various aspects of the present invention will be better appreciated with reference to FIG. 5, While, for purposes of simplicity of explanation, the method of FIG. 5 is shown and described as executing serially, it is to be understood and appreciated that the present invention is not iimited by the illustrated order, as some aspects could, in accordance with the present invention, occur in different orders and/or concurrently with other aspects from that shown and described herein. Moreover, not all illustrated features may be required to implement a methodology in accordance with an aspect of the present invention. It will be appreciated that some

or all of each of these methods can be implemented as machine-executable instructions stored on a non-transitory computer readable device (e.g., memory 20, 30 and/or 42). The instructions can be executed by a processor (e.g., processor 18, 28 and/or 40) to facilitate the performance of operations of the method.

[0048] FIG. 5 illustrates an example of a method that facilitates health monitoring. At 52, biometric data (e.g., related to an ECG, a heart rate, a hydration status, fluid shift, a respiration, a cardiac output, a fail, an activity, a body position, a diastolic blood pressure, mean blood pressure, a systolic blood pressure, etc.) can be received (e.g., at mobile computing device 14 across a wired or a wireless connection employing a wireless protocol, such as: a Bluetooth protocol, a Bluetooth low energy protocol, a ZigBee protocol, an ANT+ protocol, a WiFi protocol, etc.) from a sensor (e.g., sensor 12) coupled to a patient's body. At 54, the biometric data is processed (e.g., by the mobile computing device 4) to determine a health status of the patient. At 56, therapeutic feedback (e.g., to the patient and/or to an external device) related to the health status can be provided (e.g., by the mobile computing device 14).

[0049] From the above description, those skilled in the art will perceive improvements, changes and modifications. Such improvements, changes, and modifications are within the skill of one in the art and are intended to be

covered by the appended claims. All references cited herein and listed above are incorporated by reference in their entireties as needed and as discussed herein.

The following is claimed:

1. A mobile computing device comprising:

a memory that stores computer-executable instructions; and a processor that executes the computer-executable instructions to at least:

receive biometric data detected by a sensor coupled to a body of a patient;

process the biometric data to monitor a health status of the patient; and

provide therapeutic feedback related to a current health status of the monitored health status.

2. The mobile computing device of ciaim 1 , wherein the biometric data comprises at least one of biopotential data, impedance data, biochemical data, temperature data, acoustical data, optica! data, acceleration data, force data and pressure data,

3. The mobile computing device of claim 1 , wherein the processor executes the computer-executable instructions to transmit information regarding the health status to an external device.

4. The mobile computing device of claim 3, wherein the external device comprises a therapeutic device configured to follow at least one of a treatment procedure and a preventive procedure for the patient determined based on the health status.

5. The mobile computing device of claim 3, wherein the external device comprises a secured external data store accessible to a physician associated with the patient, a caregiver associated with the patient, or a healthcare expert system.

6. The mobile computing device of claim 1 , wherein the processor executes the computer-executable instructions to store at least one of the biometric data, information related to the health status, and information related to the therapeutic feedback in a data store, wherein the data store is at least one of internal to the mobile computing device or external to the mobile computing device.

7. The mobile computing device of claim 6, wherein the processor executes the computer-executable instructions to:

receive an input from the patient related to at least one of an activity, symptoms, status, a medication, a body position and a food consumption; and store information related to the input in the data store.

8. A system for smart mobile health monitoring, comprising: a sensor coupled to a patient and configured to detect biometric data associated with the patient; and a mobile computing device, comprising:

a memory that stores computer-executable instructions; and a processor that executes the computer-executable instructions to at least:

receive the biometric data from the sensor;

process the biometric data to at least one of monitor a health status of the patient, diagnose a medical condition of the patient, or diagnose a disease of the patient; and

provide therapeutic feedback related to the health status and at least one of an activity of the patient and a body position of the patient.

9. The system of claim 8, wherein the processor executes the computer-executable instructions to transmit at least one of the biometric data, data derived from the biometric data, information about the health status, and information about the therapeutic feedback to an external device via a wireless protocol.

10. The system of claim 9, wherein the wireless protocol comprises a Biuetooth protocol, a Bluetooth low energy protocol, a ZigBee protocol, an ANT+ protocol, and a WiFi protocol.

11. The system of claim 9, wherein the external device is a therapeutic device configured to deliver a therapeutic treatment to the patient based on the at least one of the biometric data, information about the health status, and information about the therapeutic feedback.

12. The system of claim 8, wherein the mobile computing device is configured to display at least one of the biometric data, data derived from the biometric data, information about the health status, and information about the therapeutic feedback.

13. The system of claim 8, wherein the sensor is coupled to the mobile computing device according to a wired connection comprising a plurality of electrodes implemented in a platform that, upon placement at an appropriate location on the patient, is configured to maintain each of the set of electrodes in an anatomically correct position without placement of individual leads.

14. The system of claim 8, wherein the sensor is at least one of remotely configured, dynamically configured, and adapted for a specific physiological state, a condition, or a specific disease to provide optimized feedback and diagnostic capabilities.

15. The system of claim 8, wherein the mobile computing device configures a global positioning system (GPS) device configured to determine a first location of the mobile computing device; and wherein the processor executes the computer-executable instructions to select an external device to receive a transmission at least one of the biometric data, information about the health status, and information about the therapeutic feedback to a remote device based on the first location of the mobile device and a second location of the external device.

16. The system of claim 8, wherein the processor executes the computer-executable instructions to, when indicated by the health status exceeding a threshold, communicating with an external electrical stimulator to provide at least one of electrical, chemical, and drug induced stimuli to the patient. 7. A non-transitory computer-readable device storing instructions executable by an associated processor to perform operations that facilitate smart mobile health monitoring, the operations comprising:

receiving biometric data detected by a sensor coupled to a body of a patient;

processing the biometric data to determine a health status of the patient;

providing therapeutic feedback related to the health status; and transmitting at least one of the biometric data, information related to the health status, and information related to the therapeutic feedback to an external device according to a wireless protocol.

18. The non-transitory computer-readable device of claim 7, wherein the operations further comprise receiving an input from the external device comprising at least one of a query, processed data, an instruction to adjust at least one of the health status and the therapeutic feedback for diagnostic purposes, and an instruction to change patient treatment regiments.

19. The non-transitory computer-readable device of claim 17, wherein the external device is configured to provide a therapeutic procedure to the patient based on at least one of the biometric data, information related to the health status, and information related to the therapeutic feedback

20. The non-transitory computer-readable device of claim 17, wherein the biometric data is related to at least one of an electrocardiogram (ECG), skin potential (EDA), electroencephalogram (EEG), electromyogram (EMG), a heart rate, body impedance, a fluid status, a respiration, a cardiac output, a fall, an activity, a body position, a pulse wave form, blood oxygen levels, a plethysmograph signal, venous/arterial blood pressure waveform, diastolic blood pressure, and a systolic blood pressure.

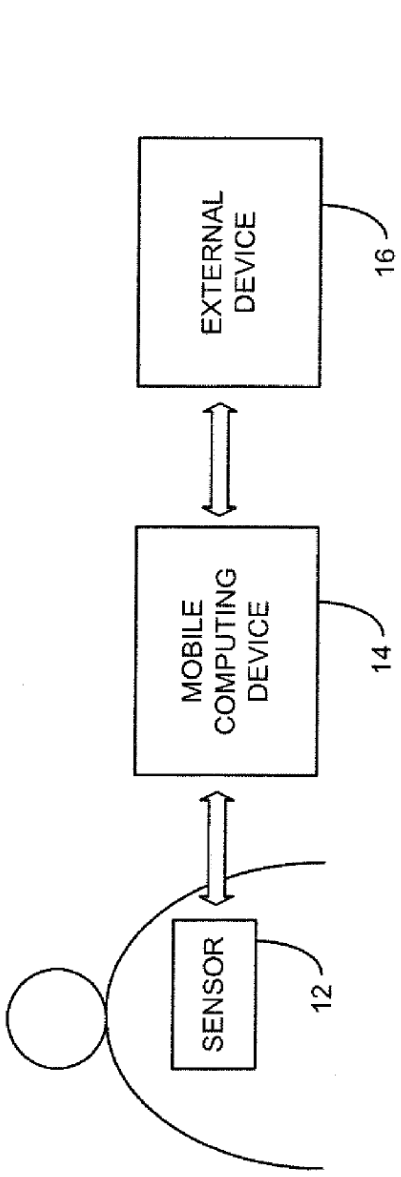

FIG. 1

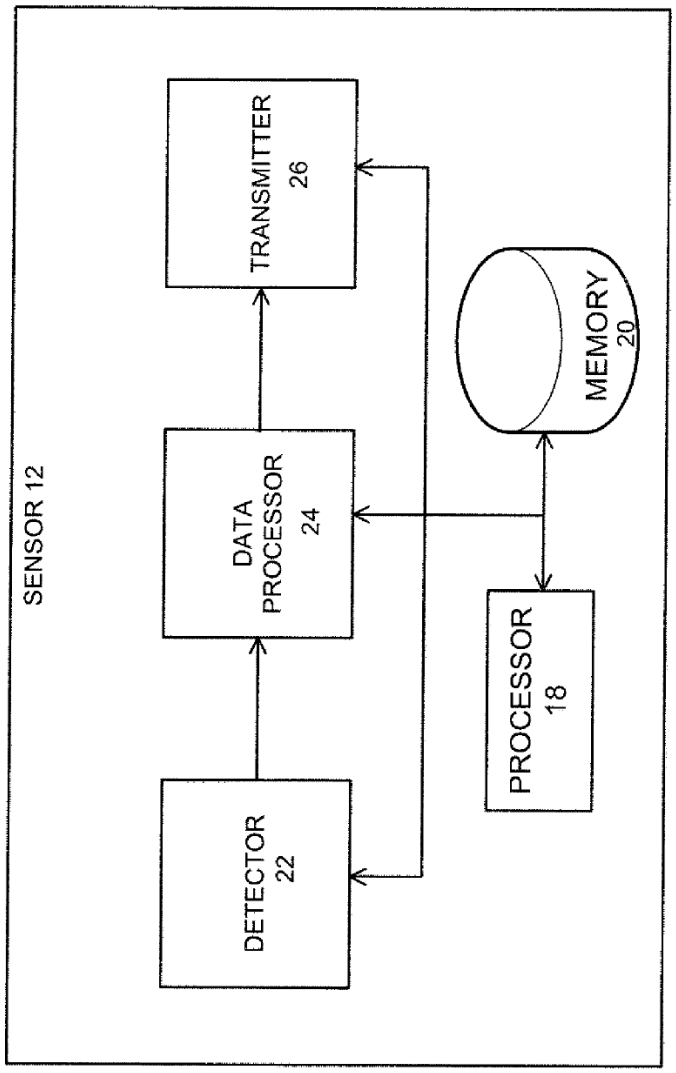
SENSOR 12
TRANSMITTER 26
MEMORY 20
DATA PROCESSOR 24
PROCESSOR 18
DETECTOR 22

FIG. 2

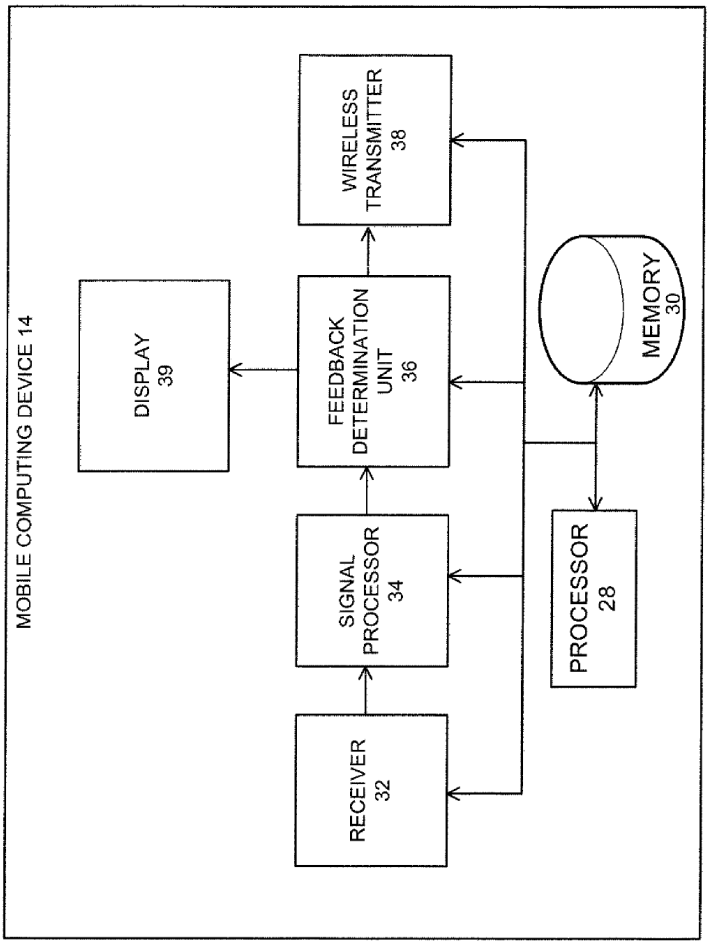
MOBILE COMPUTING DEVICE 14
WIRELESS TRANSMITTER 38
DISPLAY 39
FEEDBACK DETERMINATION UNIT 36
MEMORY 30
SIGNAL PROCESSOR 34
PROCESSOR 28
RECEIVER 32

FIG. 3

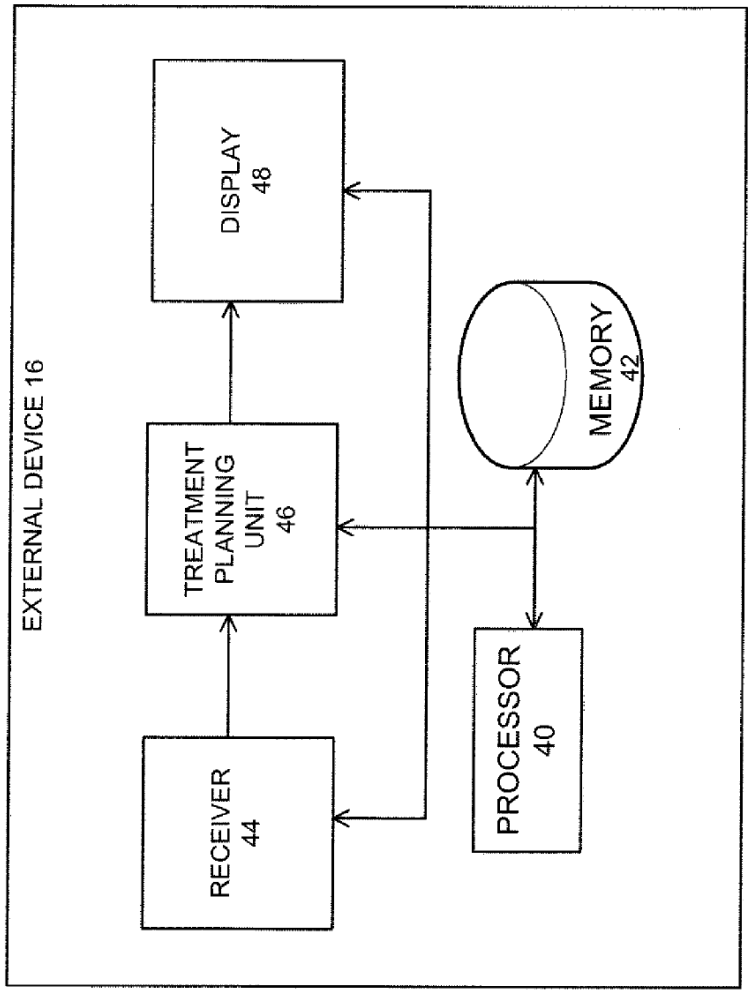
EXTERNAL DEVICE 16
DISPLAY 48
MEMORY 42
TREATMENT PLANNING UNIT 46
PROCESSOR 40
RECEIVER 44

FIG. 4

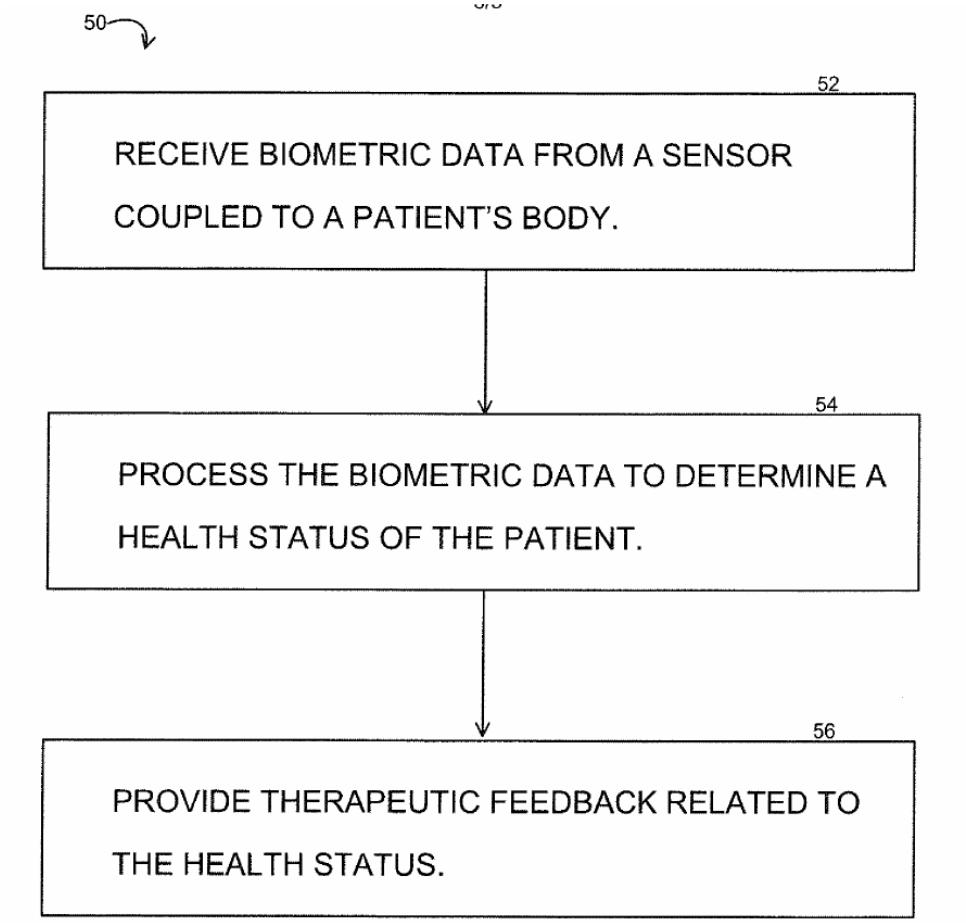
50
52
RECEIVE BIOMETRIC DATA FROM A SENSOR COUPLED TO A PATIENT'S BODY.
54
PROCESS THE BIOMETRIC DATA TO DETERMINE A HEALTH STATUS OF THE PATIENT.
56
PROVIDE THERAPEUTIC FEEDBACK RELATED TO THE HEALTH STATUS.

FIG. 5

D.2 Compression Device, System and Method for Decreasing Abdominal Venous Pooling

(12) INTERNATIONAL APPLICATION PUBLISHED UNDER THE PATENT COOPERATION TREATY (PCT)

(19) World Intellectual Property Organization
International Bureau

(43) International Publication Date
8 May 2014 (08.05.2014)

WIPO | PCT

(10) International Publication Number
WO 2014/071292 A1

(51) International Patent Classification:
A61B 17/135 (2006.01) *A61H 11/00* (2006.01)
A61F 5/34 (2006.01)

(21) International Application Number:
PCT/US2013/068270

(22) International Filing Date:
4 November 2013 (04.11.2013)

(25) Filing Language: English

(26) Publication Language: English

(30) Priority Data:
61/721,781 2 November 2012 (02.11.2012) US

(71) Applicant: **VANDERBILT UNIVERSITY** [US/US]; 305 Kirkland Hall, 2201 West End Avenue, Nashville, Tennessee 37240 (US).

(72) Inventors: **BAUDENBACHER, Franz**; 182 North Berwick Lane, Franklin, Tennessee 37069 (US). **BIAGGIONI, Italo**; 2873 Sugar Tree Road, Nashville, Tennessee 37215 (US). **HARDER, Rene**; 2129 Acklen Avenue, Apt. 12, Nashville, Tennessee 37212 (US). **DIEDRICH, Andre**; 1121 Harpeth Mill Court, Nashville, Tennessee 37221 (US). **OKAMOTO, Luis**; 915 18th Avenue South, Apt. 302, Nashville, Tennessee 37212 (US).

(74) Agent: **WESORICK, Richard S.**; Tarolli, Sundheim, Covell & Tummino LLP, 1300 East Ninth Street, Suite 1700, Cleveland, Ohio 44114 (US).

(81) Designated States *(unless otherwise indicated, for every kind of national protection available)*: AE, AG, AL, AM, AO, AT, AU, AZ, BA, BB, BG, BH, BN, BR, BW, BY, BZ, CA, CH, CL, CN, CO, CR, CU, CZ, DE, DK, DM, DO, DZ, EC, EE, EG, ES, FI, GB, GD, GE, GH, GM, GT, HN, HR, HU, ID, IL, IN, IR, IS, JP, KE, KG, KN, KP, KR, KZ, LA, LC, LK, LR, LS, LT, LU, LY, MA, MD, ME, MG, MK, MN, MW, MX, MY, MZ, NA, NG, NI, NO, NZ, OM, PA, PE, PG, PH, PL, PT, QA, RO, RS, RU, RW, SA, SC, SD, SE, SG, SK, SL, SM, ST, SV, SY, TH, TJ, TM, TN, TR, TT, TZ, UA, UG, US, UZ, VC, VN, ZA, ZM, ZW.

(84) Designated States *(unless otherwise indicated, for every kind of regional protection available)*: ARIPO (BW, GH, GM, KE, LR, LS, MW, MZ, NA, RW, SD, SL, SZ, TZ, UG, ZM, ZW), Eurasian (AM, AZ, BY, KG, KZ, RU, TJ, TM), European (AL, AT, BE, BG, CH, CY, CZ, DE, DK, EE, ES, FI, FR, GB, GR, HR, HU, IE, IS, IT, LT, LU, LV, MC, MK, MT, NL, NO, PL, PT, RO, RS, SE, SI, SK, SM, TR), OAPI (BF, BJ, CF, CG, CI, CM, GA, GN, GQ, GW, KM, ML, MR, NE, SN, TD, TG).

Published:

— *with international search report (Art. 21(3))*

(54) Title: COMPRESSION DEVICE, SYSTEM, AND METHOD FOR DECREASING ABDOMINAL VENOUS POOLING

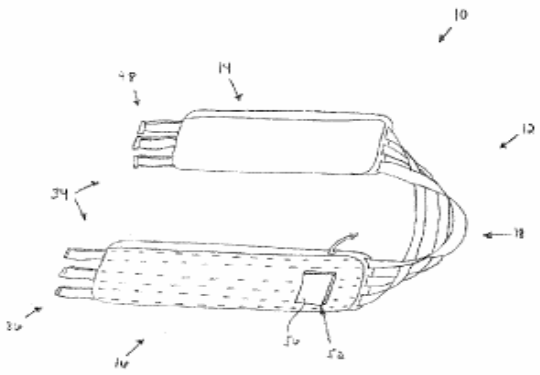

(57) Abstract: A compression device can include an adjustable belt, an inflation bladder, and a control module. The adjustable belt can be sized to fit circumferentially around a subject's abdomen. The inflatable bladder and the control module can be secured to the belt. The control module can include a housing that encloses at least one of a pump, a pressure relief valve, and a controller. The pump and the pressure relief valve can be in fluid communication with the bladder. The pump can be configured to inflate the bladder to a pre-determined pressure and apply a compressive pressure to the subject's abdomen. The pressure relief valve can be configured to decrease the pressure within the bladder. The controller can be configured to automatically adjust the compressive pressure in response to a change in the subject's posture. The controller can be in electrical communication with the pump and the pressure relief valve.

WO 2014/071292 A1

COMPRESSION DEVICE. SYSTEM. AND METHOD FOR DECREASING ABDOMINAL VENOUS POOLING

RELATED APPLICATION

[0001] This application claims the benefit of U.S. Provisional Patent Application Serial No. 61/721,781, filed November 2, 2012, the entirety of which is hereby incorporated by reference for all purposes.

TECHNICAL FIELD

[0002] The present disclosure relates generally to medical devices and methods and, more particularly, to compression devices, systems, and methods for decreasing abdominal venous pooling in a subject..

BACKGROUND

[0003] Orthostatic hypotension (OH) is the most disabling manifestation of autonomic failure and many other medical conditions, including diabetes. Orthostatic hypotension can also be seen as a consequence of medications and even aging. For example, drugs that increase vascular resistance (e.g., midodrine) and/or

plasma volume (e.g., fludrocortisone) are first-line therapy. Such drugs, however, may worsen supine hypertension and may be contraindicated in patients with significant cardiovascular disease (e.g., congestive heart failure). More importantly, these approaches to treatment do not target the main reason blood pressure (BP) falls on standing, which is gravity-related venous pooling that reduces venous return and cardiac output. Most of this venous pooling occurs in the splanchnic circulation.

[0004] Abdominal compression is a safe and effective approach to improve standing BP. Thus, it is considered the standard of care in the non-phannacologic treatment of neurogenic OH. This recommendation, however, is based on acute studies (i.e., less than two hours). And there are no controlled trials that have proven the continued efficacy of this approach, much less patient acceptance. Indeed, evidence suggests that this approach is not effective in most patients mostly due to decreased efficacy and low compliance. The limitations with currently available devices, such as elastic abdominal binders are explained by the fact that it is difficult for patients to apply pressure at an effective compression level (e.g., 20-40 mm Hg). Not only does this reduce efficacy of currently available compression devices, but such devices are also uncomfortable to wear for prolonged periods of time if kept at effective compression levels.

SUMMARY

[0005] The present disclosure relates generally to medical devices and methods and, more particularly, to compression devices, systems, and methods for decreasing abdominal venous pooling in a subject.

[0006] One aspect of the present disclosure relates to a compression device. The compression device can comprise an adjustable belt, an inflatable bladder, and a control module. The adjustable belt can be sized to fit circumferentially around the abdomen of a subject. The inflatable bladder can be secured to the belt. The control module can be secured to the belt and include a housing that encloses one or more of a pump, at least one pressure relief valve, and a controller. The pump can be in fluid communication with the bladder. The pump can be configured to inflate the bladder to a pre-determined pressure and thereby apply a compressive pressure to the abdomen of the subject. The at least one pressure relief valve can be in fluid communication with the bladder. The at least one pressure relief valve can be configured to decrease the pressure within the bladder. The controller can be configured to automatically adjust the compressive pressure in response to a change in the posture of the subject. The controller can be in electrical communication with the pump and the at least one pressure relief valve.

[0007] Another aspect of the present disclosure relates to a system for decreasing abdominal venous pooling in a subject. The system can comprise a compression device and a handheld electronic device. The compression device can comprise an adjustable belt, an inflatable bladder, and a control module. The adjustable belt can be sized to fit circumferentially around the abdomen of a subject. The inflatable bladder can be secured to the belt. The control module can be secured to the belt and include a housing that encloses one or more of a pump, at least one pressure relief valve, and a controller. The pump can be in fluid communication with the bladder. The pump can be configured to inflate the bladder to a pre-determined pressure and thereby apply a compressive pressure to the abdomen of the subject. The at least one pressure relief valve can be in fluid communication with the bladder. The at least one pressure relief valve can be configured to decrease the pressure within the bladder. The controller can be configured to automatically adjust the compressive pressure in response to a change in the posture of the subject. The controller can be in electrical communication with the pump and the at least one pressure relief valve. The handheld electronic device can be in wireless communication with the controller.

[0008] Another aspect of the present disclosure relates to a method for decreasing abdominal venous pooling in a subject. The method can comprise automatically

applying a compressive pressure to the abdomen of the subject in response to a change in the posture of the subject

BRIEF DESCRIPTION OF THE DRAWINGS

[0009] The foregoing and other features of the present disclosure will become apparent to those skilled in the art to which the present disclosure relates upon reading the following description with reference to the accompanying drawings, in which:

[0010] Fig. 1 is a perspective view showing a compression device for decreasing abdominal venous pooling constructed in accordance with one aspect of the present disclosure;

[0011] Fig. 2A is a schematic illustration showing an inner surface of the compression device in Fig. 1 ;

[0012] Fig. 2B is a schematic illustration showing an outer surface of the compression device in Fig. 1;

[0013] Fig. 2C is a schematic illustration showing a top view of the compression device in Fig. 1;

[0014] Fig. 3 A is a perspective view showing an abdominal (ventral) portion of the compression device in Fig. 1 with a control module directly secured thereto;

[0015] Fig. 3B is a perspective view showing the abdominal (ventral) portion of the compression device in Fig. 3 A with the control module connected thereto via a cable;

[0016] Fig. 4 is a schematic illustration showing one configuration of the control module in Figs. 3A-B;

[0017] Fig. 5A is a schematic illustration showing a subject transitioning between supine, sitting, and upright postures with an accelerometer attached to a thigh of the subject;

[0018] Fig. 5B is a schematic illustration showing a subject transitioning between supine, sitting, and upright postures with an accelerometer attached to the waist of the subject;

[0019] Fig. 6A is a process flow diagram illustrating one example of a pressurization/depressurization protocol for use with the accelerometer shown in Fig. 5 A;

[0020] Fig. 6B is a process flow diagram illustrating one example of a pressurization/depressurization protocol for use with the accelerometer shown in Fig. SB;

[0021] Fig. 7 is a schematic illustration showing a system for decreasing abdominal venous pooling constructed in accordance with another aspect of the present disclosure;

[0022] Fig. 8 is a schematic illustration showing one configuration of a control module for use with the system in Fig. 7; and

[0023] Fig. 9 is a process flow diagram illustrating a method for decreasing abdominal venous pooling in a subject according to another aspect of the present disclosure.

DETAILED DESCRIPTION

[0024] Definitions

[0025] Unless defined otherwise, all technical and scientific terms used herein have the same meaning as is commonly understood by one of skill in the art to which the present disclosure pertains.

[0026] In the context of the present disclosure, the singular forms "a," "an" and "the" can include the plural forms as well, unless the context clearly indicates otherwise. It will be further understood that the terms "comprises" and/or "comprising," as used herein, can specify the presence of stated features, steps, operations, elements, and/or components, but do not preclude the presence or addition of one or more other features, steps, operations, elements, components, and/or groups thereof.

[0027] As used herein, the term "and/or" can include any and all combinations of one or more of the associated listed items.

[0028] As used herein, phrases such as "between X and Y" and "between about X and Y" can be interpreted to include X and Y.

[0029] As used herein, phrases such as "between about X and Y" can mean "between about X and about Y".

[0030] As used herein, phrases such as "from about X to Y" can mean "from about X to about Y".

[0031] It will be understood that when an element is referred to as being "on," "attached" to, "connected" to, "coupled" with, "contacting," etc., another element, it can be directly on, attached to, connected to, coupled with or contacting the other element or intervening elements may also be present. In contrast, when an element is referred to as being, for example, "directly on," "directly attached" to, "directly connected" to, "directly coupled" with or "directly contacting" another element, there are no intervening elements present. It will also be appreciated by those of skill in the art that references to a structure or feature that is disposed "adjacent" another feature may have portions that overlap or underlie the adjacent feature.

[0032] Spatially relative terms, such as "under " "below," "lower," "over," "upper" and the like, may be used herein for ease of description to describe one element or feature's relationship to another element(s) or feature(s) as illustrated in the figures. It will be understood that the spatially relative terms can encompass different orientations of the apparatus in use or operation in addition to the orientation depicted in the figures. For example, if the apparatus in the figures is inverted, elements described as "under" or "beneath" other elements or features would then be oriented "over" the other elements or features.

[0033] It will be understood that, although the terms "first," "second," etc. may be used herein to describe various elements, these elements should not be limited by these terms. These terms are only used to distinguish one element from another. Thus, a "first" element discussed below could also be termed a "second" element without departing from the teachings of the present disclosure. The sequence of operations (or steps) is not limited to the order presented in the claims or figures unless specifically indicated otherwise.

[0034] As used herein, the term "subject" can be used interchangeably with the term "patient" and refer to any warm-blooded organism including, but not limited to,

human beings, pigs, rats, mice, dogs, goats, sheep, horses, monkeys, apes, farm animals, livestock, rabbits, cattle, etc.

[0035] As used herein, the term "electrical communication" can refer to the ability of a generated electric field to be transferred to, or have an effect on, one or more components, structures, or elements of the present disclosure. In some instances, the generated electric field can be directly transferred to a component, structure or element {e.g., via a wire or lead). In other instances, the generated electric field can be wirelessly transferred to a component, structure or element.

[0036] As used herein, the term "orthostatic intolerance" can refer to the development of a set of characteristic symptoms while standing or sitting upright that include, but are not limited to, lightheadedness, palpitations, nausea, breathing or swallowing difficulties, headache, visual disturbances, pallor, sweating, tremors, fatigue, altered mentation and syncope. In some instances, such symptoms can be accompanied by postural tachycardia and elevated plasma norepinephrine.

[0037] Overview

[0038] The present disclosure relates generally to medical devices and methods and, more particularly, to compression devices, systems, and methods for decreasing abdominal venous pooling in a subject. As

illustrated in Fig. 1 , one aspect of the present disclosure can include a compression device for decreasing abdominal venous pooling in a subject. Conditions associated with orthostatic intolerance, such as orthostatic hypotension are significant medical problems caused by gravity-induced venous pooling with decreased venous return. Besides certain pharmacological agents, abdominal binders are considered to be the standard of care in the treatment of orthostatic hypotension. For several reasons, however, such devices are not optimal. For example, it is difficult for patients to apply pressure at an effective compression level (e.g., about 20-40 mm Hg). Additionally, even if an effective compression level is obtained, such devices are uncomfortable to wear for prolonged periods of time if pressure is maintained about the patient's abdomen during all forms of posture (i.e., standing, sitting and supine).

[0039] Advantageously, the present disclosure provides devices, systems, and methods that automatically adjust the effective compression level applied to a patient's abdomen to decrease venous pooling and thereby reduce orthostatic hypotension and improve upright blood pressure and orthostatic intolerance. As discussed in more detail below, the devices, systems, and methods of the present disclosure automatically adjust the amount of compression applied to a patient's abdomen based on the posture of the patient. This allows for

normal physiologic changes in intra-abdominal pressure during routine activities, such as coughing, deep breathing, bending over, etc. Since effective compression is only applied when a patient is at risk of experiencing venous pooling (e.g., when standing or transitioning to standing), the present disclosure advantageously increase comfort when the patient is sitting or in a supine position. Other advantages of the present disclosure, which will be apparent to one skilled in the art, are discussed below.

[0040] Compression Devices

[0041] One aspect of the present disclosure can include a compression device. In some instances, the compression device can include an adjustable belt, an inflatable bladder secured to the belt, and a control module that is also secured to the belt. Unlike conventional abdominal binders, which are often bulky and cumbersome, the compression device of the present disclosure is shaped and dimensioned for easy application to (and removal from) a subject. For example, the compression device can have a low profile, streamlined construction that allows it to be worn under garments (e.g., a shirt or dress) without creating an unsightly or noticeable bulge around a patient's midsection. The compression device is also constructed of flexible and lightweight materials that make it economical and easy to transport when not in use. The simple construction of the compression

device also makes it an effective, low-cost option for effectively treating conditions associated with orthostatic intolerance, such as orthostatic hypotension.

[0042] Adjustable Belt

[0043] In another aspect, the adjustable belt of the compression device can be sized and dimensioned to fit circumferentially around the abdomen of a subject. Generally speaking, the adjustable belt can have a length, width, and thickness appropriate to facilitate snug placement of the belt around the abdomen of a subject. In one example, the length of the belt can be sufficient to wrap around an adult subject. The width of the belt should not be so wide as to constrain expansion of the thorax of the subject. In some instances, the dimensions of the belt can be tailored based on the known size (girth) of the subject. In other instances, the belt can have a one-size-fits-all configuration. In further instances, the belt can have one of a series of standard dimensions. The adjustable belt can additionally or optionally include an adjustment mechanism that enables a subject to selectively adjust the length of the belt Non-limiting examples of adjustment mechanisms can include Velcro® straps, zippers, hook and loop fasteners, etc. The belt can be ventilated and/or padded. The belt can be made of one or combination of flexible (e.g., elastic), semi-rigid and/or rigid materials, such as nylon, neoprene, polyester, etc.

[0044] In another aspect, at least one radially inflatable bladder can be secured to the adjustable belt. In some instances, an inflatable bladder can be integrated within the belt so that the inflatable bladder is completely enveloped by the material comprising the belt. In such instances, the belt can include a pre-formed pocket configured to receive the inflatable bladder. In other instances, the inflatable bladder can be secured to an inner surface of the adjustable belt so that the inflatable bladder is disposed between the belt and the abdomen of the subject when in use. The inflatable bladder can be arranged about the belt so that inflation of the inflatable bladder imparts compressive pressure to all or only a portion of the subject's abdomen. For example, the inflatable bladder may be located about a first portion of the adjustable belt so that inflation of the bladder results in application of compressive pressure to only the ventral abdomen of the subject. The size of the inflatable bladder can be varied to accommodate a desired volume of air (e.g., about 2L). The inflatable bladder can be made of one or a combination of materials, such as rubber, polyurethane-coated nylon fabric, etc.

[0045] Figs. 1 and 2A-C illustrate one example of a compression device 10 according to the present disclosure. Referring to Fig. 1 L ews compression device 10 can include an adjustable belt 12 having a two-panel design, which provides a better custom fit for different body sizes. The

belt 12 can include oppositely disposed dorsal and ventral portions (or panels) 14 and 16. The dorsal portion 14 can be configured to apply compressive pressure to only the lower back of a subject, while the ventral portion 16 can be configured to apply compressive pressure to only the abdomen of the subject. The dorsal and ventral portions 14 and 16 are joined together by one or more straps 18. The straps 18 allow better air circulation about the sides of the subject. The straps 18 also allow for better adjustment and fitting of the belt 12 to the abdomen and waist of the subject.

[0046] The ventral portion 16 (Figs. 2A-C) has a generally rectangular configuration defined by a length L_v and a width W_v. In one example, the length L_v can be about equal to, or greater than, the width W_v. The ventral portion 16 can include oppositely disposed first and second major surfaces 20 and 22, as well as oppositely disposed first and second ends 24 and 26. The ventral portion 16 can also include a valve stem 28, which is in communication with an inflatable bladder 30 and/or a pump 32 (Fig. 4). The first end 24 (Figs. 2A-C) of the ventral portion 16 is connected to the straps 18 by stitching, for example. The second end 26 of the ventral portion 16 includes an attachment mechanism 34, which is configured so that a subject can selectively connect the ventral portion to the dorsal portion 14 and thereby

secure the compression device 10 about the subject's waist. As shown in Figs. 2A-C, the attachment mechanism 34 can include three straps 36 extending from the second end 26 of the ventral portion 16. A distal end 38 of each strap 36 can include a male mating member (not shown in detail), which is configured to mate with a female mating member (not shown in detail) (e.g., via a buckle or snap-fit mechanism). It will be appreciated that the length of each strap 36 may be adjustable to accommodate various waist sizes. The attachment mechanism 34 provides not only a quick and easy means for securing and removing the compression device, but also a simple way to adjust the total length of the belt 12 and ensure a snug fit between the subject's waist and the compression device.

[0047] As shown in Figs. 2A-B, a radially expandable inflatable bladder 30 can be secured to the ventral portion 16. In some instances, the inflatable bladder 30 can be disposed within the ventral portion 16. For example, the inflatable bladder 30 can be disposed within a pre-formed pocket (not shown) of the ventral portion 16 such that the material comprising the ventral portion completely envelops the inflatable bladder. In other instances, the inflatable bladder 30 can be secured to the second major surface 22 of the ventral portion 16. In such instances, an adhesive material (e.g., Velcro® strips) can be used to affix the inflatable bladder 30 to the second major surface 22. The shape and dimensions

of the inflatable bladder 30 can be varied as needed to apply adequate compressive pressure to the abdomen of the subject. For instance, the inflatable bladder 30 can have a rectangular configuration with a length and width that are less than the length $L_>$ and width W_v of the ventral portion 16. The inflatable bladder 30 can be made of rubber, for example, and have an inflated volume of about 2L.

[0048] The dorsal portion 14 of the adjustable belt 12 has a generally rectangular configuration defined by a length L_d and a width $W_{d.}$ In one example, the length L_d can be about equal to, or greater than, the width W_d. The length L_d and/or width W_d of the dorsal portion 14 can be less than, equal to, or greater than the length Ly and/or width W_v of the ventral portion 16. The dorsal portion 14 can include oppositely disposed first and second major surfaces 40 and 42, as well as oppositely disposed first and second ends 44 and 46. The first end 44 of the dorsal portion 14 can be connected to the straps 18 by stitching, for example. The second end 46 of the dorsal portion 14 can comprise the attachment mechanism 34. As shown in Figs. 2A-C, the attachment mechanism 34 can further include three straps 48 extending from the second end 46 of the dorsal portion 14. A distal end 50 of each strap 48 can include a female mating member, which is configured to mate with the male mating member of the ventral portion 16 (e.g. , via

a buckle or snap-fit mechanism). It will be appreciated that the length of each strap 48 may be adjustable to accommodate various waist sizes. Advantageously, the attachment mechanism 34 is located along a lateral aspect of the subject's waist, which makes the attachment mechanism easily reachable and removes the inconvenience associated with conventional attachment mechanisms (e.g., buckles), which are often located on the back.

[0049] As shown in Fig. 1 , the straps 18 can extend longitudinally across the ventral portion 16. In some instances, each of the straps can extend through a separate channel (not shown) that is embedded within the ventral portion. In other instances, each of the straps can extend across the first major surface of the ventral portion. In such instances, each of the straps can extend through one or more loops (not shown) that hold and maintain the position of each strap while also allowing each strap to slide therethrough. The presence of the straps across the ventral portion prevents the ventral portion, and in particular the first major surface, from bulging upon inflation of the inflatable bladder. A rigid or semi-rigid material can be used to form the first major surface of the ventral portion, which also prevents bulging thereof after inflation of the bladder. The second major surface of the ventral portion can be formed from an elastic material capable of stretching, which allows optimal pressure transfer between the inflatable bladder

and the abdomen of a subject. It will be appreciated that the straps, 18, 36, and 48 can the same (e.g., a single strap) or different (e.g., each strap comprised of three separate straps).

[0050] Control Module

[0051] Another aspect of the present disclosure can include a control module 52 (Figs. 3A-B) secured to the compression belt 10. As discussed in more detail below, the control module 52 can house the hardware and software components needed for operation of the compression device 10. The control module 52 can be secured to compression belt 10 in a variety of ways. As shown in Fig. 3 A, the control module 52 can be directly connected to the first major surface 20 of the ventral portion 16 (e.g., by an adhesive, stitches, clips, pins, etc.). Alternatively, the control module 52 can be connected to the compression belt 10 via a flexible cable 54 (Fig. 3B). In this configuration, a subject can more easily access and handle the control module 54 and, if desired, store the control module in a garment pocket, fanny pack, etc.

[0052] The control module 54 can include a housing 56 that encloses one or more hardware and/or software components, such as a pump 32 (Fig. 4), a pressure relief valve 58, and a controller that comprises a processor 60 and a memory device 62. Other hardware and/or software components that may be contained

within the housing 56 are discussed below. The housing 56 can include any type of container configured to enclose the hardware and/or software component(s) of the present disclosure. In one example, the housing 56 can have a box-shaped configuration and include a hinge (not shown) that allows opposing portions of the housing to be opened and closed. When closed, an interior surface (not shown) of the housing 56 can define an interior space mat is sized and dimensioned to accommodate one or more of the hardware and/or software components. Also when closed, the housing 56 can be hermetically sealed so as to prevent moisture from entering the interior space and contacting the hardware and/or software components. The housing 56 can be made of a durable and lightweight material, such as a hardened plastic {e.g., PVC). The housing 56 can also have a streamlined, ergonomic shape to facilitate ease of patient handling and to minimize its presence when the compression device 10 is worn under a garment.

[0053] In addition to the pump 32, pressure relief valve(s) 58, and the controller, additional hardware components that may be enclosed or contained within the housing 56 can include a pressure sensor 64 or pressure transducer, an accelerometer 66, a power switch (not shown), a voltage converter (not shown), a charger (not shown), a visual status indicator (e.g., LEDs) 68, and a power source (e.g., a lithium-ion rechargeable battery) (not shown), as

well as other components that one skilled in the art would appreciate are needed for operation of the control module 52 (e.g., drivers, connectors, etc.). One configuration of such hardware components is shown in Fig. 4. The hardware components can be disposed on a commercially available microcontroller board (not shown), which is optionally integrated with a daughter shield (not shown). Hardware components can be in electrical communication with one another via a series of wire connectors (not shown). Control module architecture can be configured to allow multiple communication protocols (e.g., SPI, US ART, I^2C, etc.). In one example, information and command flow (e.g., processor controls) can be programmed and controlled via serial USART and USB interface. In some instances, the processor 60 can control the valve(s) 58 and pump 32 through standard IO ports (e.g., GPIOs). Accelerometer and pressure sensor data can be acquired via 12C Bus.

[0054] In another aspect, the pump 32 can be in fluid communication with the inflatable bladder 30. For example, flexible tubing (not shown) may be used to connect the pump 32 to the inflatable bladder 30. As discussed in more detail below, the pump 32 can be operated to inflate the bladder 30 to a pre-determined pressure (e.g., about 20-50 mm Hg) and thereby apply compressive pressure to the abdomen of a subject. In one example, the pump 32 can include a miniature

diaphragm pump, such as the T2-04 pump available from Parker Hannifin, Inc. (Hollis, NH). The T2-04 pump is a twin head pump with a single set of ports and a double diaphragm design. The T2-04 can provide flow rates of up to 7.5 LPM, and is configured to have a low power draw.

[0055] In another aspect, the control module 52 can include one or more pressure relief valves 58. The pressure relief valve(s) 58 can be in fluid communication with the inflatable bladder 30. As discussed in more detail below, the pressure relief valve(s) 58 can be operated and controlled to decrease pressure within the inflatable bladder 30 (e.g., when a subject transitions between a standing-sitting or standing-supine posture). One example of a suitable pressure relief valve 58 can include the X- VALVE (Parker Hannifin, Inc., Hollis, NH), which is a miniature pneumatic solenoid valve capable of supporting a large range of pressure options (e.g., 6 psi, 30 psi and 100 psi).

[0056] In another aspect, the control module 52 can include at least one pressure sensor 64 or pressure transducer located within the housing 56. The pressure sensor(s) 64 can be configured to detect the pressure within the inflatable bladder 30, which may then be relayed to the controller. In one example, a suitable pressure sensor 64 can include an ASDX Series pressure transducer, which is commercially available from Honeywell, Inc.

(Morristown, NJ). ASDX Series pressure transducers are fully calibrated and temperature-compensated for sensor offset, sensitivity, temperature effects, and non-linearity using an on-board ASIC. ASDX Series pressure transducers can operate at low voltages, and are capable of sensing a range of pressure (e.g., from 10 psi to 100 psi).

[0057] In another aspect, one or more external accelerometers 66 can be connected to the control module 52 via a direct electrical linkage (e.g., a cable or wire) or a wireless electrical linkage. Each accelerometer 66 is capable of detecting a change in the posture of a subject, which can then be relayed to the controller. The accelerometer 66 can be securely affixed to a portion of a subject's body, such as a thigh (Fig. SA). In this configuration, the accelerometer 66 can comprise a 2-axis accelerometer capable of detecting a sitting-standing transition and/or standing-sitting transition. When fixed on a thigh, for example, a 2-axis accelerometer can sense upright posture in the x-y axis. When the accelerometer 66 is in the horizontal position, a signal indicative of the subject's posture can be relayed to the pump 32, which then triggers deflation of the inflatable bladder 30. When the subject stands up, a different signal can be sent from the accelerometer 66 to the pump 32, which is activated to inflate the inflatable bladder 30. In one example, the accelerometer

66 can include an ACTIVPAL accelerometer, which is commercially available from PAL Technologies Ltd. (Glasgow, UK).

[0058] In another aspect, one or more accelerometers 66 can be contained within the control module 52. Each accelerometer 66 is capable of detecting a change in the posture of a subject, which can then be relayed to the controller. In one example, the accelerometer 66 can comprise a 3-axis accelerometer capable of detecting motion in x-y-z planes. Advantageously, locating a 3-axis accelerometer within the control module can not only improve patient satisfaction and compliance (e.g., by removing the need to place an accelerometer 66 on the thigh of a subject), but also provide the ability to differentiate supine from seated postures.

[0059] In another aspect, the controller can include a processor 60 and a memory device 62. In some instances, the memory device 62 can include solid state memory that does not need to have its content periodically refreshed (e.g., memory which retains its state even in the event of a power loss to the memory). In one example, the memory device 62 can include non-volatile memory, such as read-only memory (ROM) (e.g., programmable ROM and erasable programmable ROM) and flash memory. The processor 60 can be configured to execute commands associated with the memory device 62. The processor 60 can include a microprocessor, for example,

configured to perform arithmetic or logic operations using logic circuitry that responds to and processes commands in the memory device 62. In some instances, the processor 60 can include any conventional, general purpose single- or multi-chip microprocessor (or any one of a number of microcontrollers or other devices) that process commands. In other instances, the processor 60 can be any conventional special purpose microprocessor, such as a digital signal processor or a graphics processor. It will be appreciated that the processor 60 can additionally or optionally include conventional address lines, conventional data lines, and one or more conventional control lines.

[0060] In another aspect, the memory device 62 can be programmed to include a predefined pressurization/depressurization protocol (or algorithm) for automatically adjusting the compressive pressure in response to a change in the posture of the subject {e.g., as detected by an accelerometer 66). As discussed below, the implemented pressurization/depressurization protocol can depend upon the type and/or location of the accelerometer 66. The pressurization/depressurization protocol illustrated in Fig. 6A, for example, can be implemented when the accelerometer 66 is a 2-axis accelerometer located external to the control module 52 {e.g., on the thigh of the subject). In this case, the pressurization/depressurization protocol illustrated in Fig. 6A is based on the detected acceleration of the

subject's thigh. Thus, when seated, the upright vector on the accelerometer 66 is perpendicular to the gravitational vector, and the corresponding acceleration is 0 g. When standing, the upright vector on the accelerometer 66 is parallel to the gravitational vector, and the acceleration is -1 g.

[0061] In another aspect, the pressurization/depressurization protocol (or algorithm) illustrated in Fig. 6B can be implemented when the accelerometer 66 is a 3-axis accelerometer located within the control module 52. In some instances, the pressurization/depressurization protocol shown in Fig. 6B uses multi-factorial inputs and state logic to detect supine, sitting, and standing positions. The decision tree shown in Fig. 6B can depend on trunk angle, total power in the accelerometer signal, and derived speed and distance. For example, supine posture can be detected using the orientation of the subject's torso when no movement or low amplitude movements are present Walking can be detected by high and rhythmic activities. To determine if a subject is sitting or standing, the transition between sitting and standing can be detected. This can be done by detecting the onset of movement, integration of the accelerometer data to calculate the velocity signal, and further integration of the velocity signal to estimate the distance of vertical movement.

[0062] Systems

[0063] Another aspect of the present disclosure can include a system 70 (Fig. 7) for decreasing abdominal venous pooling in a subject. As shown in Fig. 7, the system 70 can include a compression device 10 having a controller associated therewith, and a handheld electronic device 72 in wireless communication with the controller. Other components of the system 70 are described below. In some instances, the compression device 10 can be identically or similarly constructed as the compression device shown in Fig. 1 and described above. For example, the compression device 10 of the system 70 can generally comprise an adjustable belt 12, an inflatable bladder 30 secured to the belt, and a control module 52 that is also secured to the belt. The control module 52 can further include a pump 32 in fluid communication with the inflatable bladder 30, at least one pressure relief valve 58 in fluid communication with the bladder, and a controller configured to automatically adjust a compressive pressure applied to the abdomen of a subject during operation of the system 70. As discussed below, the system 70 of the present disclosure advantageously provides a "smart" wireless compression device 10 capable of detecting posture and activity to automatically trigger inflation and deflation during upright and sitting or supine postures (respectively).

[0064] As shown in Fig. 7, the handheld electronic device 72 can be in wireless communication with the compression device 10 and, in particular, the controller of the

compression device. To enable wireless communication with the handheld electronic device 72, the control module 52 can be similarly or identically constructed as the control module shown in Fig. 4 and described above. For example, in addition to the hardware components described for the control module 52 in Fig. 4, the control module can further include a wireless interface 74 (Fig. 8) that enables communication between the controller and the handheld wireless device 72. In one example, the wireless interface 74 can be a Bluetooth interface. To permit activity detection (e.g., resting, walking, etc.), it will be appreciated that the system 70 can include a first accelerometer 66 located in the control module 52 (e.g., to detect posture), and one or more additional accelerometers (not shown) secured to a body part (other than the torso) of the subject (e.g., a thigh, arm, etc.). Although not shown, it will also be appreciated that the system 70 can include additional sensors capable of detecting a physiological parameter of interest. For example, the system 70 can include a sensor that provides blood pressure information to the subject and/or a health care provider 76 (Fig. 7), thereby improving control of the compressive pressure applied to the subject.

[0065] The handheld electronic device 72 can include any electronic device that is typically operated while being held in one or both hands of a subject. Cellular phones, PDAs, tablets, media players, and GPS units are

examples of handheld portable electronic devices. In one example, the handheld electronic device 72 can include a GPS-enabled smartphone. In such instances, the smartphone can include an intuitive, patient-friendly interface that is: (1) speech-activated and graphic-guided; (2) capable of automatically logging activity behavior and, when needed, functioning as a notification or alert system to a health care provider 76; and (3) linked to a secured patient database 78 and/or healthcare provider expert system. For example, the smartphone can be configured to query patient status and initiate status alerts to a health care provider 76 or EMS personnel with GPS location, voice, and data communications. In some instances, the smartphone interface is configured for real-time digital signal processing, which can provide immediate alarm, feedback, and remote data provision to a healthcare provider 76. For instance, patient activity can be processed and analyzed for posture and daily pattern. If the patient falls or there is a change in the patient's behavior (e.g., the patient does not get out of bed at the usual time), the smartphone interface will notify the healthcare provider 76 (e.g., via SMS and/or Internet). The same smartphone interface can additionally or optionally be used to provide patient instructions and/or for input of personalized settings. In other instances, the secured patient database 78 can provide immediate access to current patient data and generate automated reports to optimize treatment plans, adherence to

medical regimens, and aid in the management of patients with chronic medical conditions. Advantageously, the real-time wireless feedback and alarm function allows the healthcare provider 76 to manage patients more effectively, adjust individual treatment parameters (e.g., blood pressure), and reduce the risk of stroke (e.g., during supine hypertension) or falls (e.g., caused by orthostatic hypotension).

[0066] Methods

[0067] Another aspect of the present disclosure can include a method 80 (Fig. 9) for decreasing abdominal venous pooling in a subject. The method 80 can be used to treat one or a combination of conditions characterized by orthostatic intolerance. The terms "treat" or "treating" can refer to therapeutically regulating, preventing, improving, alleviating the symptoms of, reversing and/or reducing the effects of a condition characterized by orthostatic intolerance. Examples of conditions treatable by the method 80 can include, but are limited to, orthostatic hypotension, post-dialytic orthostatic hypotension, syncope, orthostatic tachycardia, delayed orthostatic hypotension, post-spaceflight orthostatic intolerance, spinal cord injury, and postural tachycardia syndrome.

[0068] Generally speaking, the method 80 can comprise automatically applying a compressive pressure to the abdomen of a subject in response to a change in the

posture of the subject. More particularly, and as shown in Fig. 9, the method 80 can include the following steps: providing a compression device (Step 82); securing the compression device to the subject (Step 84); optionally adjusting the compression device (Step 86); optionally pairing the compression device with a handheld wireless device (Step 88); and activating the compression device (Step 90). As discussed below, the method 80 automatically adjusts the amount of compression applied to a patient's abdomen based on the posture of the patient. This allows for normal physiologic changes in intra-abdominal pressure during routine activities, such as coughing, deep breathing, bending over, etc. Since effective compression is only applied when a patient is at an increased risk of abdominal venous pooling {e.g., when standing or transitioning to a standing position), the method 80 advantageously increases patient comfort when the patient is sitting or in a supine position.

[0069] At Step 82 of the method 80, a compression device 10 is provided. In some instances, the compression device 10 can be identically or similarly constructed as the compression device shown in Fig. 1 and described above. It will be appreciated that the particular construction of the compression device 10 can depend on a variety of factors, including the size and/or age of the subject, the general health of the subject, the familiarity of the subject with wireless technologies, the

particular condition with which the subject is afflicted, etc. Once an appropriate compression device 10 has been selected, the compression device can be secured or fitted to the subject (Step 84). This can be done, for example, by first positioning the belt 12 about the waist of the subject so that the ventral and dorsal portions 16 and 14 of the belt are directly adjacent the subject's belly button and lower back, respectively. Next, the buckles comprising the attachment mechanism 34 can be snap-fit together so that the compression device 10 is circumferentially fitted around the subject's waist. The compression device 10 should be snugly positioned about the subject's waist so mat movement (e.g., walking, sitting, standing, etc.) does not displace the ventral and dorsal portions 16 and 14 of the belt 12. Therefore, if needed, the fit of the belt 12 about the patient's waist can be adjusted using the attachment mechanism 34 (Step 86).

[0070] At Step 88, the compression device 10 can be optionally paired with a wireless, handheld electronic device 72, such as a GPS-enabled smartphone. In such instances, it will be appreciated that the compression device 10 can be configured as part of a system 70 (described above).

[0071] With the compression device 10 secured to the subject, the compression device can be activated at Step 90. As the subject transitions between different positions or postures over the course of a day (or night), the

accelerometer(s) 66 can detect accelerations) (e.g., on three axises) and then send corresponding signals to the controller, which translates the signals to either "sitting", "standing" or "supine". If the detected acceleration indicates that the subject is standing, or moving from a sitting position to a standing position, the controller automatically signals the pump 32 to inflate the bladder 30 to a pre-detennined pressure threshold (e.g., about 20-50 mm Hg). Consequently, compressive pressure is applied to the abdomen of the subject, which decreases venous pooling. The compressive pressure can be sustained at the pre-determined pressure throughout the transition period and/or for the time that the subject is standing. If the pressure within the inflatable bladder 30 is above the predetermined threshold, pumping stops and the pressure relief valve(s) 58 is/are activated to release an appropriate amount of pressure. If the detected acceleration indicates that the subject is sitting, supine, or transitioning from an upright to a sitting or supine position, the controller automatically causes the pressure relief valve(s) 58 to open and thereby deflate the bladder 30. Where the compression device 10 is wirelessly paired with a handheld electronic device 72, it will be appreciated that one or more of the operations associated with the system 70 (described above) may be performed prior to, contemporaneous with, or after operation of the compression device. By automatically applying and regulating compressive pressure in

subjects suffering from orthostatic intolerance, the method 80 advantageously improves upright blood pressure and reduces medical problems caused by gravity-induced venous pooling.

[0072] From the above description of the present disclosure, those skilled in the art will perceive improvements, changes and modifications. Such improvements, changes, and modifications are within the skill of those in the art and are intended to be covered by the appended claims. All patents, patent applications, and publication cited herein are incorporated by reference in their entirety.

The following is claimed:

1. A compression device comprising:

an adjustable belt sized to fit circumferentially around the abdomen of a subject;

an inflatable bladder secured to the belt; and

a control module secured to the belt, the control module including a housing that encloses one or more of the following:

a pump in fluid communication with the bladder and configured to inflate the bladder to a pre-determined pressure and thereby apply a compressive pressure to the abdomen of the subject;

at least one pressure relief valve in fluid communication with the bladder and configured to decrease the pressure within the bladder, and

a controller configured to automatically adjust the compressive pressure in response to a change in the posture of the subject, the controller being in electrical communication with the pump and the at least one pressure relief valve.

2. The device of claim 1 , the bladder further including:

a dorsal portion configured to apply compressive pressure to only the lower back of the subject; and

a ventral portion that is oppositely disposed from the dorsal portion and configured to apply compressive pressure to only the abdomen of the subject

3. The device of claim 1, the controller further including:

a memory device; and

a processor configured execute commands in the memory device.

4. The device of claim 3, further including:

an accelerometer located within the housing and configured to detect the change in the posture of the subject; and

at least one pressure sensor located within the housing and configured to detect the pressure within the bladder;

wherein each of the accelerometer and the at least one pressure sensor is in electrical communication with the controller.

5. The device of claim 4, wherein the accelerometer is a 3 -axis accelerometer.

6. The device of claim 1 , wherein the controller causes the pressure in the bladder to increase to the pre-deterrained pressure in response to a sitting-standing transition.

7. The device of claim 1, wherein the controller causes the pressure in the bladder to decrease in response to a standing-sitting or standing-supine transition.

8. The device of claim 3, wherein the memory device includes a predefined pressurization/depressurization protocol for automatically adjusting the compressive pressure in response to the change in the posture of the subject.

9. The device of claim 1 , whereby application of the compressive pressure constrains the abdomen of the subject and reduces pooling of venous blood within the internal organs of the subject.

10. A system for decreasing abdominal venous pooling in a subject, the system comprising:

a compression device including:

an adjustable belt sized to fit circumferentially around the abdomen of a subject;

an inflatable bladder secured to the belt; and

a control module secured to the belt, the control module including a housing that encloses one or more of the following:

a pump in fluid communication with the bladder and configured to inflate the bladder to a pre-determined pressure and thereby apply a

compressive pressure to the abdomen of the subject;

at least one pressure relief valve in fluid communication with the bladder and configured to decrease the pressure within the bladder; and

a controller configured to automatically adjust the compressive pressure in response to a change in the posture of the subject, the controller being in electrical communication with the pump and the at least one pressure relief valve; and

a handheld electronic device in wireless communication with the controller.

11. The system of claim 10, wherein the controller further includes a wireless interface for communicating with the handheld electronic device.

12. The system of claim 10, wherein the handheld electronic device is a smart phone.

13. The system of claim 10, further including an accelerometer that is secured to a thigh of the subject and in wireless communication with the controller.

14. The system of claim 10, wherein the controller includes a processor for executing commands stored in a memory device, the processor activating the pump to increase pressure within the bladder to the predetermined pressure when a sitting-standing transition is detected by a pressure sensor; and activating the at least one pressure relief valve to decrease pressure within the bladder when a standing-sitting or standing-supine transition is detected by the pressure sensor; wherein the activating steps are based on a pressurization/depressurization protocol stored in the memory device.

15. A method for decreasing abdominal venous pooling in a subject comprising automatically applying a compressive pressure to

the abdomen of the subject in response to a change in the posture of the subject.

16. The method of claim 15, wherein the compressive pressure is applied to the abdomen by inflating a compressive device worn by the subject about the abdomen.

17. The method of claim 16, wherein the compressive pressure is automatically adjusted by a pump controlled by a controller.

18. The method of claim 17, wherein the controller adjusts the compressive pressure in accordance with a predefined pressurization/depressurization protocol.

19. The method of claim 18, further comprising:

activating the pump to increase pressure within the bladder when a sitting-standing transition is detected by a pressure sensor associated with the compressive device; and

activating at least one pressure relief valve associated with the compressive device to decrease the pressure within the bladder when a standing-sitting or standing-supine transition is detected by the pressure sensor.

20. The method of claim 15, wherein the subject is suffering from a condition characterized by orthostatic intolerance selected from the group consisting of orthostatic hypotension, post-dialytic orthostatic hypotension, syncope, orthostatic tachycardia, delayed orthostatic hypotension, post-spaceflight orthostatic intolerance, spinal cord injury, and postural tachycardia syndrome.

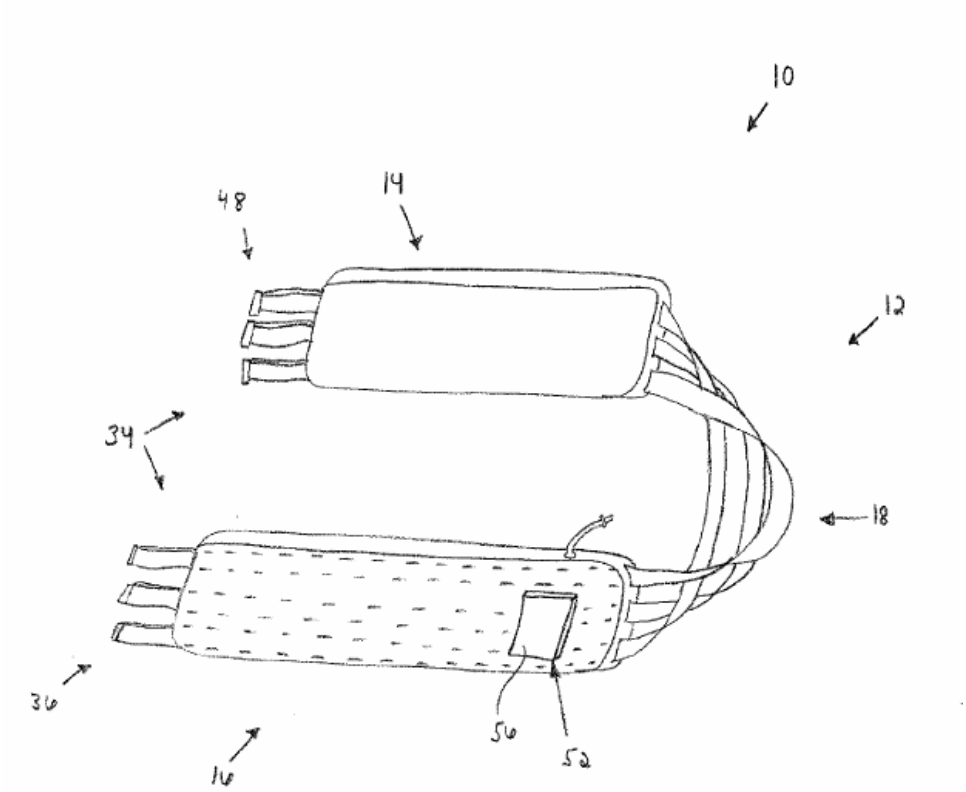

Fig. 1

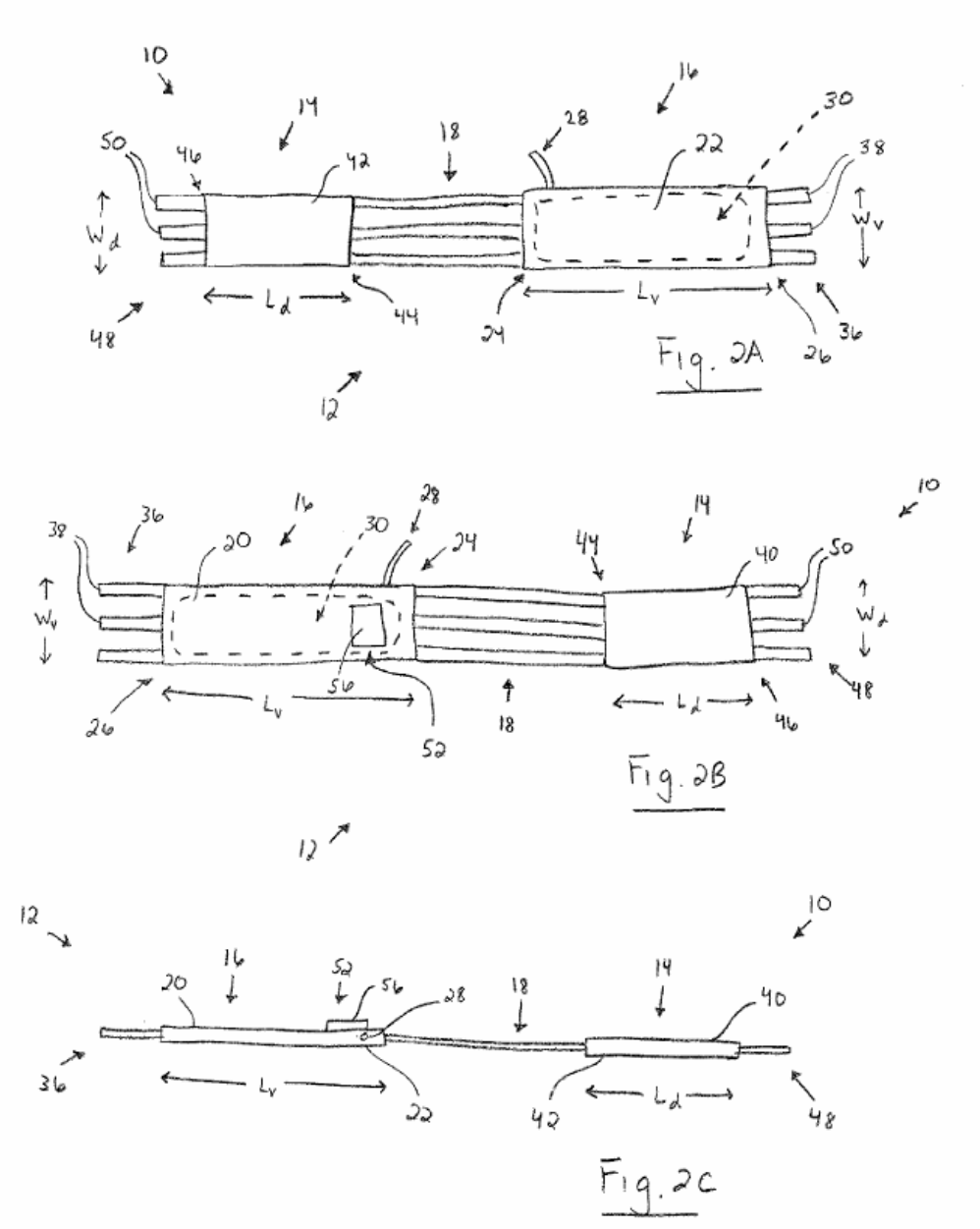

Fig. 2A

Fig. 2B

Fig. 2C

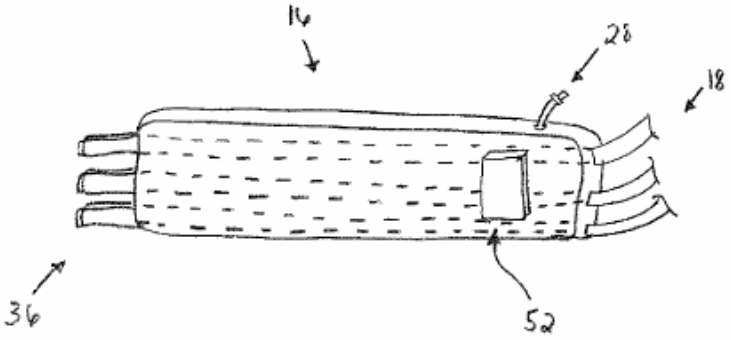

Fig. 3A

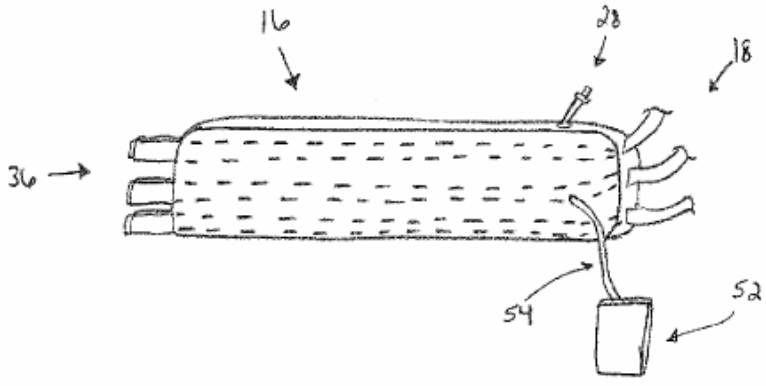

Fig. 3B

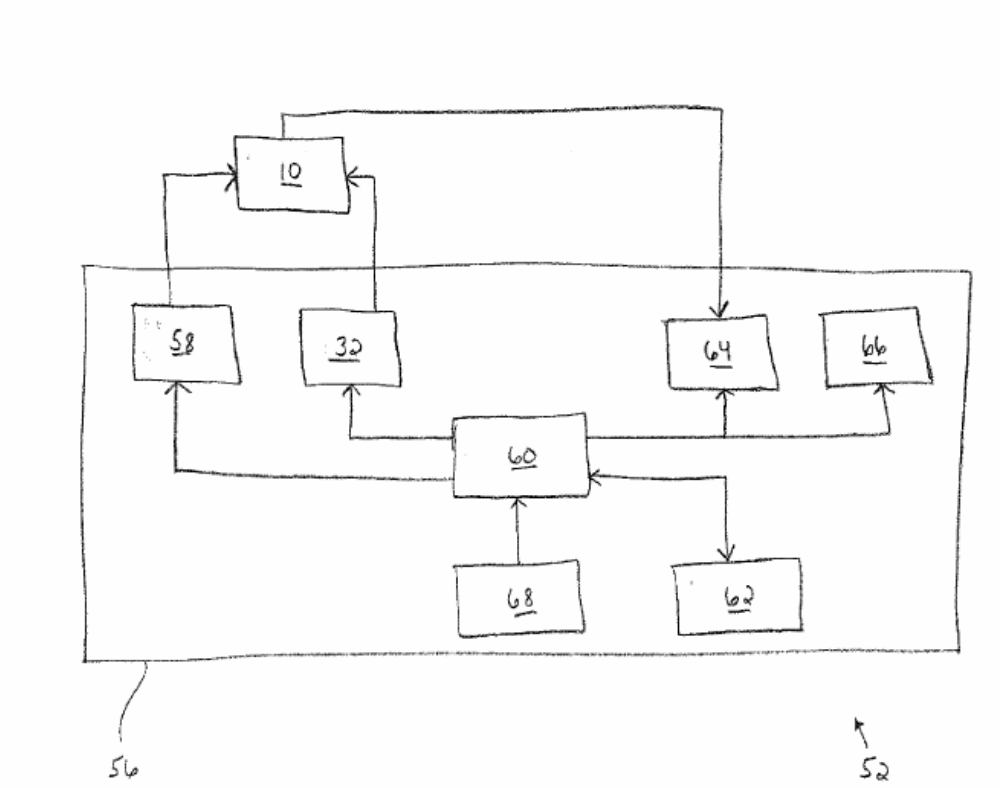

Fig. 4

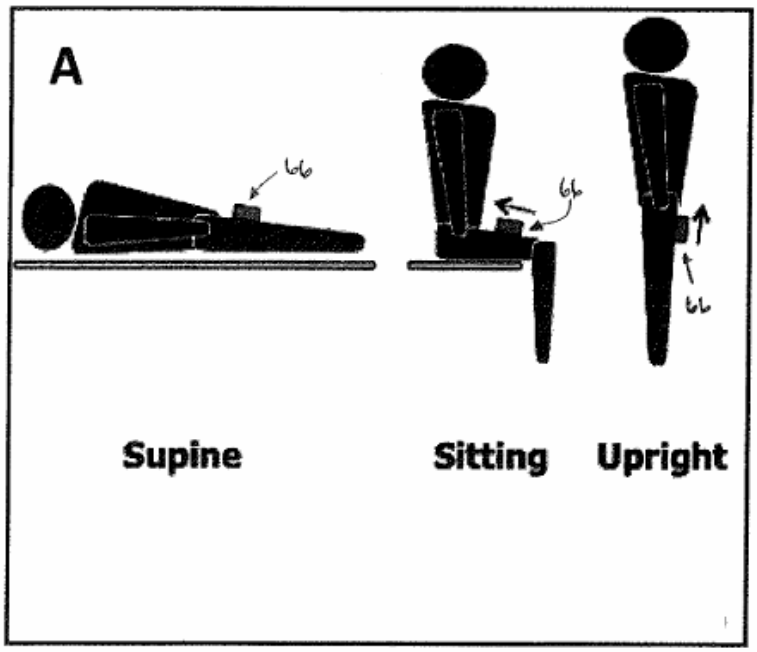

Fig. 5A

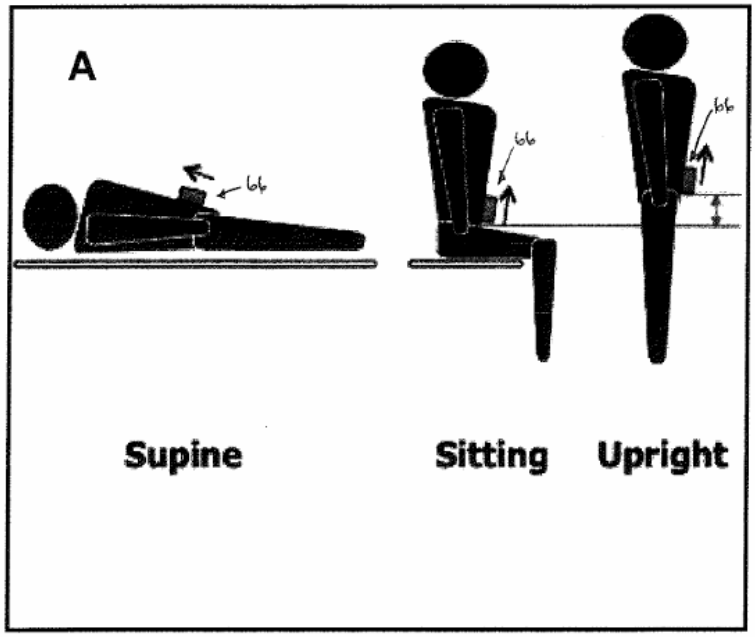

Fig. 5B

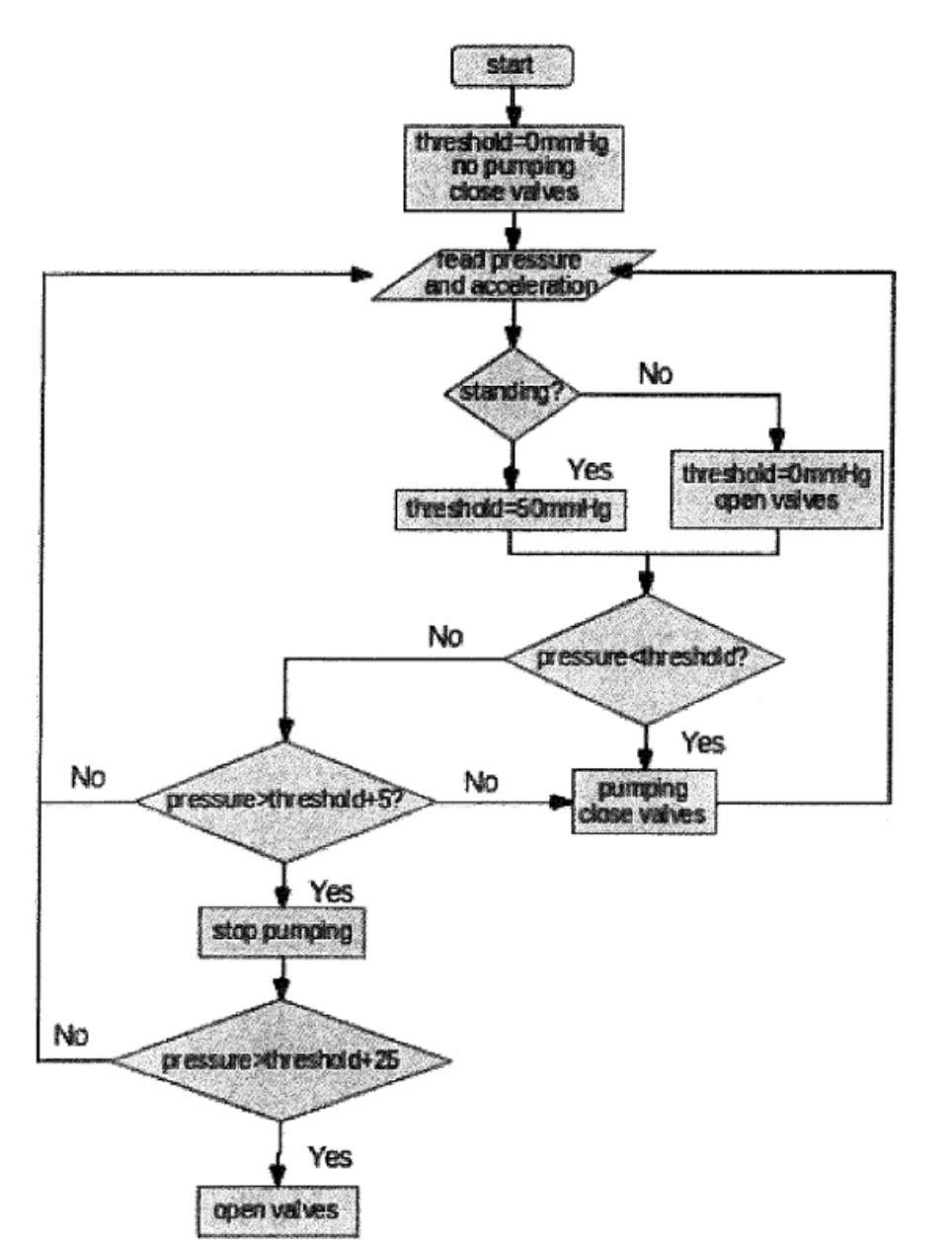
start
threshold=0mmHg
no pumping
close valves
read pressure
and acceleration
standing?
No
Yes
threshold=50mmHg
threshold=0mmHg
open valves
No
pressure<threshold?
Yes
No
pressure>threshold+5?
No
pumping
close valves
Yes
stop pumping
No
pressure>threshold+25
Yes
open valves

Fig. 6A

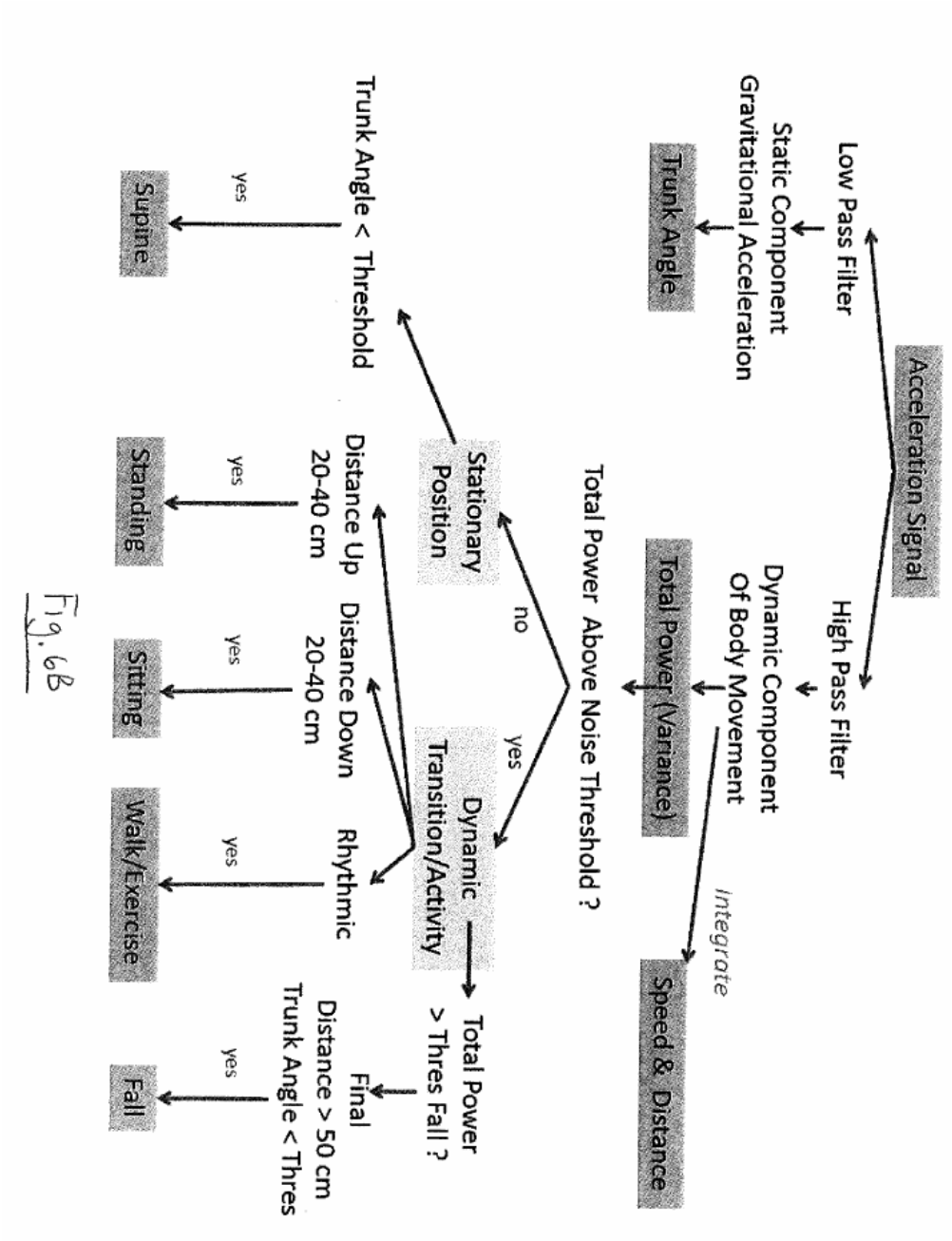
Acceleration Signal
Low Pass Filter
High Pass Filter
Static Component Gravitational Acceleration
Dynamic Component Of Body Movement
Trunk Angle
Total Power (Variance)
integrate
Speed & Distance
Total Power Above Noise Threshold ?
no
yes
Stationary Position
Dynamic Transition/Activity
Trunk Angle < Threshold
Distance Up 20-40 cm
Distance Down 20-40 cm
Rhythmic
Total Power > Thres Fall ?
Final Distance > 50 cm
Trunk Angle < Thres
yes
Supine
Standing
Sitting
Walk/Exercise
Fall

Fig. 6B

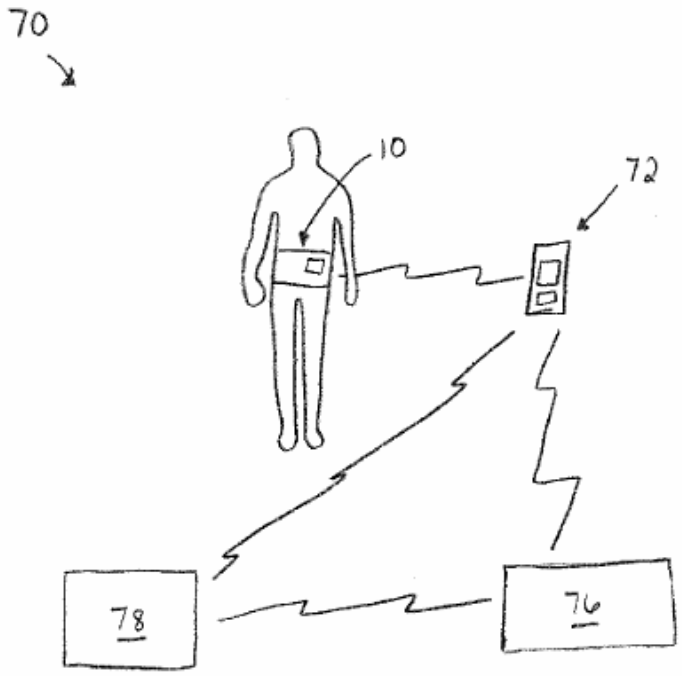

Fig. 7

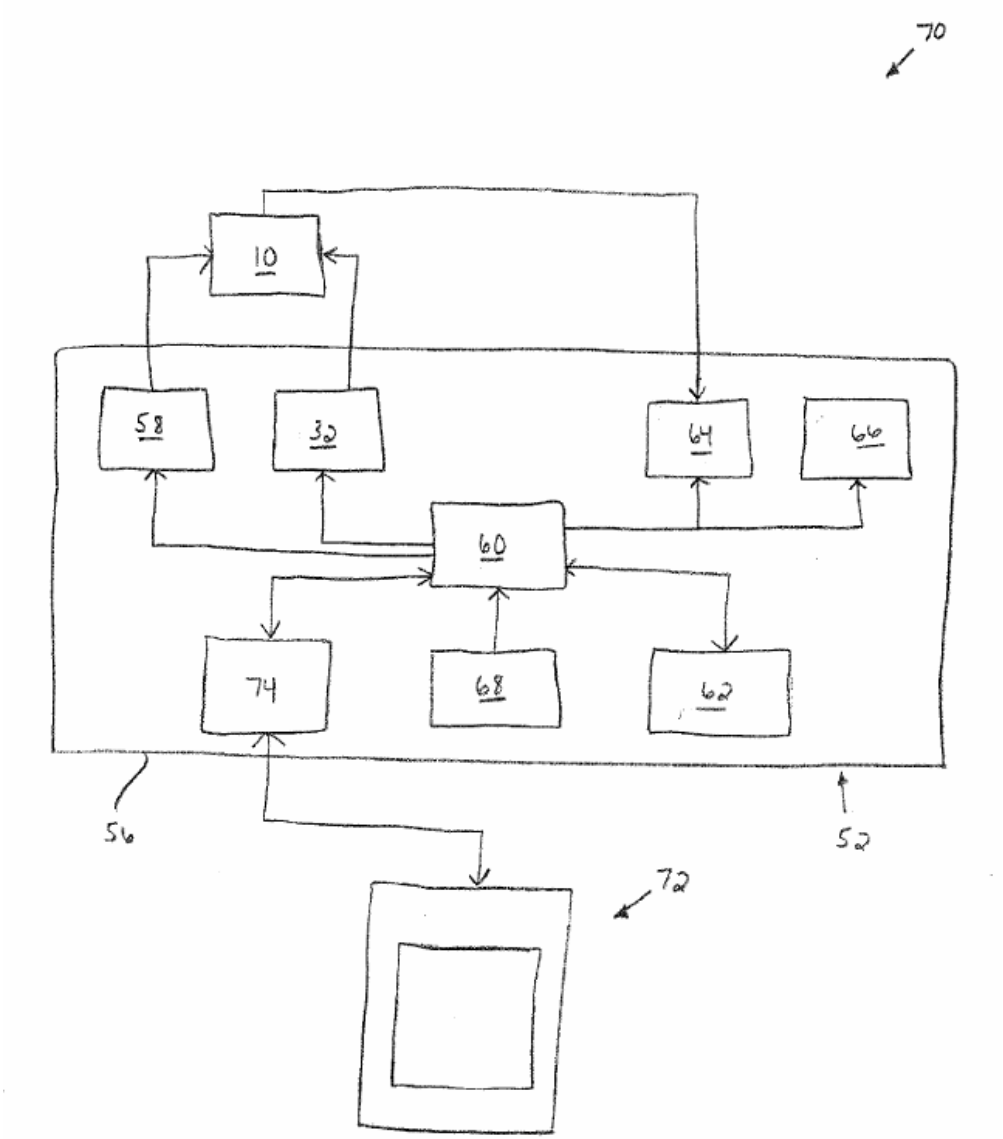

Fig. 8

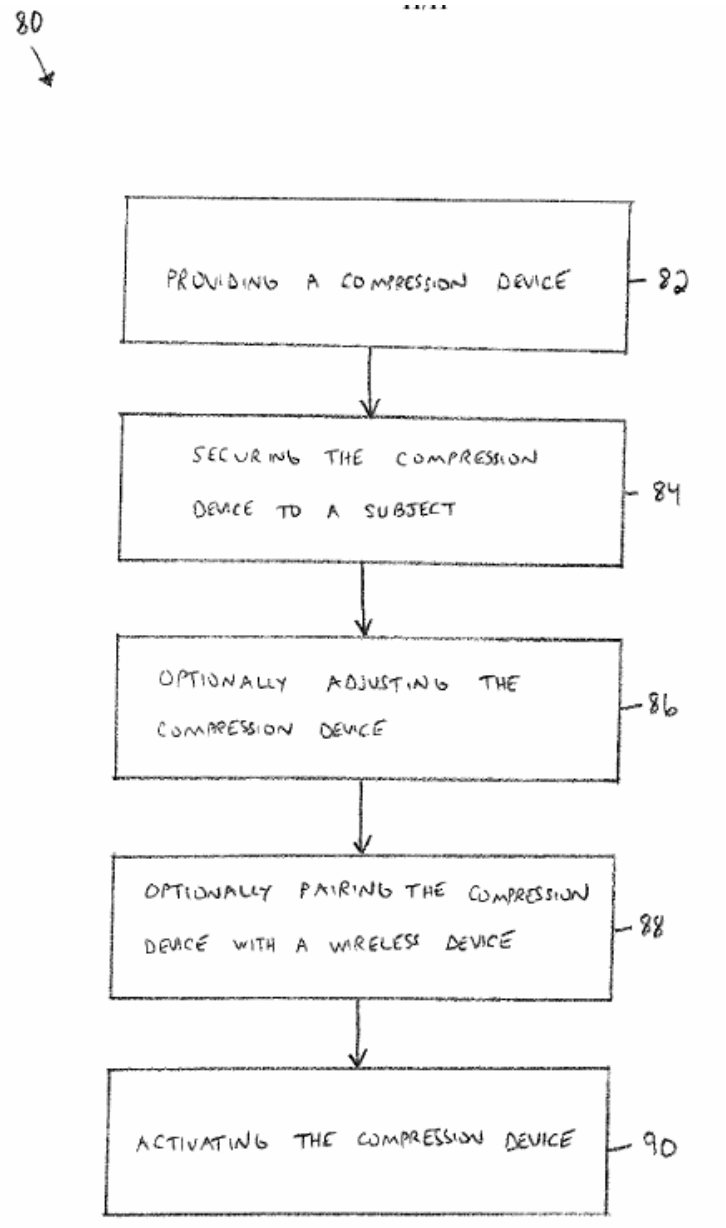
80
PROVIDING A COMPRESSION DEVICE
82
SECURING THE COMPRESSION DEVICE TO A SUBJECT
84
OPTIONALLY ADJUSTING THE COMPRESSION DEVICE
86
OPTIONALLY PAIRING THE COMPRESSION DEVICE WITH A WIRELESS DEVICE
88
ACTIVATING THE COMPRESSION DEVICE
90

Fig. 9